

Cancer cell biology / edited by Takeo Nagayo, Wataru Mori.

Contributors

Nagayo, Takeo, 1921-
Mori, Wataru.
Nihon Gan Gakkai.

Publication/Creation

Tokyo : Japan Scientific Societies Press, [1980]

Persistent URL

<https://wellcomecollection.org/works/dg2hr9xj>

License and attribution

You have permission to make copies of this work under a Creative Commons, Attribution, Non-commercial license.

Non-commercial use includes private study, academic research, teaching, and other activities that are not primarily intended for, or directed towards, commercial advantage or private monetary compensation. See the Legal Code for further information.

Image source should be attributed as specified in the full catalogue record. If no source is given the image should be attributed to Wellcome Collection.



Wellcome Collection
183 Euston Road
London NW1 2BE UK
T +44 (0)20 7611 8722
E library@wellcomecollection.org
<https://wellcomecollection.org>

GANN Monograph on Cancer Research No. 25

Monograph on Cancer Research No.25

CANCER CELL BIOLOGY

JAPANESE CANCER ASSOCIATION

JAPAN SCIENTIFIC SOCIETIES PRESS, Tokyo

Japanese Cancer Association

GANN, Japanese Journal of Cancer Research

This journal, GANN, is an official organ of the Japanese Cancer Association, and is published bimonthly. GANN was founded in 1907 by the late Dr. Katsusaburo Yamagiwa for the advancement of research in cancer, and is believed to be one of the oldest periodicals in the world devoted to the publication of results in the field of cancer research. The word "GANN" means "cancer" in Japanese. The hieroglyphic character "GANN" depicted on the front cover expresses "a disease that forms knotty protrusions like rocks." GANN, the Japanese Journal of Cancer Research, solicits manuscripts describing original observations in laboratory as well as in clinical research on all aspects of cancer. Manuscripts for publication in GANN should be submitted exclusively to GANN and should consist of work which has not been published elsewhere.

Annual subscription rate vol.72 (6 issues) 1981 ¥13,500 \$45.00

ISSN 0016-450X

IMMUNOLOGICAL XENOGENIZATION OF TUMOR CELLS

GANN Monograph on Cancer Research 23

Edited by HIROSHI KOBAYASHI

"Xenogenization" is now a general term used to describe all attempts at making a tumor cell antigenically foreign to the host (Greek: Xenos=foreign), for which either an acquisition of new foreign antigen, or an increase in the antigenicity of formerly existing TSA, or both is required. This monograph documents the presentation given at the International Workshop of the same title held at the Park Hotel in Sapporo, Japan, on June 6-8, 1978, and covers the following five major topics: Xenogenization with virus; Xenogenization with chemicals and enzymes; Recognition of cell surface antigens undergoing xenogenization; Xenogenization by cell hybridization; Application of xenogenization to human cancer.

320pp. (7×10) 1979 ¥8,000 \$49.50

PROGRESS IN CANCER BIOCHEMISTRY

In Memory of Dr. Waro Nakahara

GANN Monograph on Cancer Research 24

Edited by TAKASHI SUGIMURA, HIDEYA ENDO, TETSUO ONO, and HARUO SUGANO

The purpose of this volume is to review the progress of cancer research in Japan, especially in biochemistry, including subjects such as carcinogenesis of 4-nitroquinoline 1-oxide and "Toxohormone," a liver catalase-depressing factor, which Dr. Nakahara himself initiated. This monograph includes papers subgrouped into the following four major topics: Historical Survey of Cancer Research in Japan; Carcinogenesis (4-nitroquinoline 1-oxide, naturally occurring carcinogens, xeroderma pigmentosum); Treatment of Cancer (immunotherapy, cyclophosphamide, enzyme, inhibitors); Cancer Phenotypes (carcinoembryonic proteins, phenotypic induction, toxohormone, isozymes, tRNA, differentiation); and Japanese cancer researchers who have been under the direct and indirect influence of Dr. Nakahara are invited to contribute their papers.

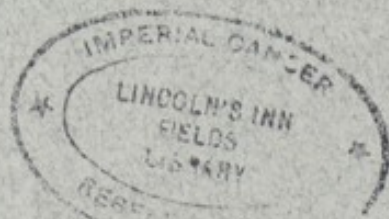
300pp. (7×10) 1979 ¥8,500 \$49.50

ISBN 4-7622-0250-2

GANN Monograph on Cancer Research No.25

CANCER CELL BIOLOGY

To control the dreaded disease of cancer, it is obvious that basic research in such fields as biochemistry, molecular biology, immunology, cell kinetics and genetics, etc., must play an essential and pioneering role; but it is also true that unless the results obtained through these investigations are incorporated into several aspects of medical science, the ultimate goal of controlling cancer cannot be realized and the basic research must be subordinate to pure biological science. This monograph is a record of a symposium held in Nagoya, Japan, November 26-27, 1979 under the sponsorship of the Japanese Cancer Association, with 16 participating speakers. The symposium was intended to further cooperation between workers in biology and medicine and was composed of four sessions dealing with: 1) Membrane studies of cancer cells; 2) Cell kinetics of normal and neoplastic tissues; 3) Analysis of the morphology and function of precancerous changes; and 4) Cell genetics of diseases of high-risk groups. Each of these topics is of the utmost importance to future study of cancer control.



IMPERIAL
CANCER RESEARCH
FUND

3



LIBRARY

Author: NAGAYO (T.) & MORI (W.) editors

Title: Cancer cell biology

Acc. No.	Class Mark	Date	Volume
004533	QZ 202	1981	



CANCER CELL BIOLOGY

The book is a comprehensive text on the biology of cancer cells. It covers the basic principles of cell biology, the history of cancer research, and the molecular biology of cancer. The book is written in a clear and concise style, making it accessible to students and researchers alike. It is a valuable resource for anyone interested in the biology of cancer.

The book is divided into several sections. The first section covers the basic principles of cell biology, including cell structure, function, and the cell cycle. The second section covers the history of cancer research, from the early days of cancer as a mysterious disease to the modern understanding of cancer as a genetic disease. The third section covers the molecular biology of cancer, including the role of genes, proteins, and signaling pathways in cancer development. The fourth section covers the clinical aspects of cancer, including diagnosis, treatment, and prevention.

The book is a comprehensive text on the biology of cancer cells. It covers the basic principles of cell biology, the history of cancer research, and the molecular biology of cancer. The book is written in a clear and concise style, making it accessible to students and researchers alike. It is a valuable resource for anyone interested in the biology of cancer.

The book is a comprehensive text on the biology of cancer cells. It covers the basic principles of cell biology, the history of cancer research, and the molecular biology of cancer. The book is written in a clear and concise style, making it accessible to students and researchers alike. It is a valuable resource for anyone interested in the biology of cancer.

GANN Monograph on Cancer Research

The series of GANN Monograph on Cancer Research was initiated in 1966 by the late Dr. Tomizo Yoshida (1903-73) for the purpose of publishing proceedings of international conferences and symposia on cancer and allied research fields, and papers on specific subjects of importance in cancer research.

The decision to publish a monograph is made by the Editorial Board of the Japanese Cancer Association, with the final approval of the Board of Directors. It is hoped that the series will serve as an important source of information in cancer research.

Japanese Cancer Association

The publication of this monograph owes much to the financial support given by the late Professor Kazushige Higuchi of Jikei University.

Editorial Board of the Japanese Cancer Association

Genshichiro Fujii	Yoshiyuki Hashimoto	Kokichi Kikuchi
Tomoyuki Kitagawa	Wataru Mori	Tadashige Murakami
Chikayoshi Nagata	Susumu Nishimura	Yasuaki Nishizuka
Kazuo Nitta	Tetsuo Ono	Tamenori Onoé
Haruo Sato	Hiroto Shimojo	Toyozo Terasima
Kumao Toyoshima	Shigeru Tsuiki	Shigeru Tsukagoshi
Tadashi Utakoji	Kazumasa Yamada	Tadashi Yamamoto

Editor-in-Chief

Tadashi Yamamoto

In Charge of Monographs

Tetsuo Ono

JAPANESE CANCER ASSOCIATION

GANN Monograph on Cancer Research No.25

CANCER CELL BIOLOGY

Edited by TAKEO NAGAYO
WATARU MORI



JAPAN SCIENTIFIC SOCIETIES PRESS, Tokyo

© JAPAN SCIENTIFIC SOCIETIES PRESS, 1981

ISBN 4-7622-0250-2

Printed in Japan

All rights reserved. No part of this publication may be reproduced or transmitted in any form or by any means, electronic or mechanical, including photocopy, recording, or any information storage and retrieval system, without permission in writing from the publisher.

December 1980

7456927

WELLCOME INSTITUTE LIBRARY	
Coll.	WelMCmec
Coll.	
No.	67

Published by :

JAPAN SCIENTIFIC SOCIETIES PRESS

2-10 Hongo, 6-chome, Bunkyo-ku, Tokyo 113, Japan

Sole distributor for the outside Japan :

BUSINESS CENTER FOR ACADEMIC SOCIETIES JAPAN

20-6 Mukogaoka, 1-chome, Bunkyo-ku, Tokyo 113, Japan

PREFACE

To control the dreaded disease of cancer, it is obvious that basic research in such fields as biochemistry, molecular biology, immunology, cell kinetics and genetics, etc., must play an essential and pioneering role; but it is also true that unless the results obtained through these investigations are incorporated into several aspects of medical science, the ultimate goal of controlling cancer cannot be realized and the basic research must be subordinate to pure biological science.

This monograph is a record of a symposium held in Nagoya, Japan, November 26-27, 1979 under the sponsorship of the Japanese Cancer Association, with 16 participating speakers. As can be seen in the table of contents, the symposium was intended to further cooperation between workers in biology and medicine and was composed of four sessions dealing with: 1) Membrane studies of cancer cells; 2) Cell kinetics of normal and neoplastic tissues; 3) Analysis of the morphology and function of precancerous changes; and 4) Cell genetics of diseases of high-risk groups. Each of these topics is of the utmost importance to future study of cancer control. We sincerely hope that this monograph will serve as a milestone on the way to our ultimate goal.

October 1980

Takeo NAGAYO
Wataru MORI

CONTENTS

Preface	v
---------------	---

MEMBRANE STUDIES OF CANCER CELLS

Identification of Cell-to-cell Adhesion Molecules of Chinese Hamster Fibroblasts	3
Masatoshi TAKEICHI	
A Cell Surface-associated Adhesive Glycoprotein from Cancer Cell.....	
Yasuji ISHIMARU, Ryoichi KURANO, and Hideo HAYASHI	9
Isolation of Growth Inhibitory Factor from Cell Surface of Cultured Chick Embryo Fibroblasts	29
Yoshihito YAOI and Kimiko MOTOHASHI	
Change in Surface Mucopolysaccharides during the Differentiation and Transformation of Blood Cells	
Chikako SATO, Kiyohide KOJIMA, Takahiko MIYAZAWA, Kimiko NISHIZAWA, Minoru OKAYAMA, and Kayoko OGURI	41

CELL KINETICS OF NORMAL AND NEOPLASTIC TISSUES

Stroma as a Rate Limiting Factor for Growth of Tumors <i>in Vivo</i>	57
Setsuya FUJITA	
Computer Analysis of Decycling Processes	
Manabu TAKAHASHI and Michiyoshi MASUDA	67
Primordial Germ Cell Proliferation and Its Relation to Teratocarcinogenesis in Mice	79
Takehiko NOGUCHI	
Cell Kinetics of Duodenal Cancer Induced by N-ethyl-N'-nitro-N-nitrosoguanidine in C3H/He Mice	
Masao ITO, Seiji YAMADA, Mutsushi MATSUYAMA, and Takeo NAGAYO	89

ANALYSIS OF MORPHOLOGY AND FUNCTION OF PRECANCEROUS CHANGES

Histochemical Investigation of Precancerous Lesions Induced by 3'-Me-DAB in Rat Liver	103
Michio MORI, Tohru KAKU, Kimimaro DEMPO, Masaaki SATOH, Aiko KANEKO, and Tamenori ONOÉ	
Characteristics of Cultured Fibroblasts of Skin from Patients with Adenomatosis Coli and Peutz-Jeghers' Syndrome	
Michiko MIYAKI, Noriko AKAMATSU, Utako HIRONO, Kazutoshi SUZUKI, Makoto ROKUTANDA, Tetsuo ONO, Masao S. SASAKI, Akira TONOMURA, and Joji UTSUNOMIYA	115

Adenomatous Hyperplasia in Liver Cirrhosis: An Approach from a Micro-angiographical Point of View.....	Kenichi SASAKI	127
Analytical Study of Precancerous Lesions in Rat Stomach Mucosa Induced by N-methyl-N'-nitro-N-nitrosoguanidine	Oichiro KOBORI	141

CELL GENETICS OF DISEASES OF HIGH-RISK GROUPS

Recent Advances in Somatic Cell Genetics: A Chronological Review	Kazuhiko R. UTSUMI	153
Intersubspecies Hybrid of Mouse as a Tool for Studying Genetic System Governing Tumor Development	Kazuo MORIWAKI, Toshihiko SHIROISHI, Nobumoto MIYASHITA Naotoshi KANDA, and Hirotami IMAI	165
Sister Chromatid Exchange and DNA Repair in Bloom's Syndrome and Human Malignant Diseases	Yukimasa SHIRAISHI	177
Androgenetic Origin of Hydatidiform Moles: Its Bearing on Carcinogenesis ...	Tadashi KAJII	189
Subject Index		195

IDENTIFICATION OF CELL-TO-CELL ADHESION MOLECULES OF CHINESE HAMSTER FIBROBLASTS

MEMBRANE STUDIES OF CANCER CELLS

1941. *Journal of Biological Chemistry*, 134, 1-10.

1942. *Journal of Biological Chemistry*, 141, 1-10.

1943. *Journal of Biological Chemistry*, 151, 1-10.

1944. *Journal of Biological Chemistry*, 159, 1-10.

1945. *Journal of Biological Chemistry*, 167, 1-10.

1946. *Journal of Biological Chemistry*, 173, 1-10.

1947. *Journal of Biological Chemistry*, 181, 1-10.

1948. *Journal of Biological Chemistry*, 189, 1-10.

1949. *Journal of Biological Chemistry*, 197, 1-10.

1950. *Journal of Biological Chemistry*, 205, 1-10.

IDENTIFICATION OF CELL-TO-CELL ADHESION MOLECULES OF CHINESE HAMSTER FIBROBLASTS

Masatoshi TAKEICHI

*Department of Biophysics, Faculty of Science, Kyoto University**

Molecules involved in the aggregation of Chinese hamster V79 cells were investigated. These cells were provided with two kinds of sites for their mutual adhesion, a Ca^{2+} -dependent site (CDS) and a Ca^{2+} -independent site (CIDS). These sites are composed of cell surface molecules with different immunological specificity. The junctional structures formed with the CIDS were only simple appositions of plasma membranes, while some specialized junctions, such as gap and intermediate junctions, were formed in aggregates with the CDS. A cell surface glycoprotein was identified as the functional molecule of the CIDS, which was detected only in a particular cell type in some heterogeneous cell populations. A molecule which may be functional in the CDS was also found by electrophoretic analysis of radioiodinated cell surface proteins. The roles of these cell adhesion sites in intercellular recognition are discussed.

Animal tissues are dissociated into single cells by treatment with proteases or chelating reagents. The dissociated cells then reaggregate into cell masses if cultured in suspended conditions, and sometimes reconstruct the original tissue architecture in the aggregates (9). This experimental system of cell dissociation and reaggregation has been extensively used for the analysis of mechanisms of cell adhesion and sorting out (3).

Cells of many established lines are also cohesive to each other, and form aggregates when cultured in suspension just as do cells derived from tissues. The use of cell lines is of great advantage in the study of cell adhesion, since a large number of homogeneous cells can be readily obtained when necessary. In addition, the cells can be maintained in better condition than tissue-derived cells during *in vitro* experiments, guaranteeing the reproducibility of results. We have investigated the mechanism of cell-cell adhesion, using V79 cells, a Chinese hamster cell line derived from lung tissue (12), and have attempted to identify the molecules involved in the adhesion of these cells. The results of these experiments will be described and discussed in connection with the cellular recognition mechanisms.

Dual Mechanism for Aggregation of V79 Cells

V79 cells in a monolayer can be dissociated into single cells by a variety of dif-

* Kitashirakawa, Sakyo-ku, Kyoto 606, Japan (竹市雅俊).

TABLE I. Aggregating Properties of V79 Cells Dissociated with Different Treatments

Dissociation treatment ^a	Abbreviated cell name	Aggregation		Presumed adhesion sites preserved
		With Ca ²⁺	Without Ca ²⁺	
EDTA	E-cells	+++	++	CDS, CIDS
Trypsin-Ca ²⁺	TC-cells	+++	—	CDS
Light trypsin-EDTA	LTE-cells	+++	+++	CIDS
Trypsin-EDTA	TE-cells	—	—	None

^a EDTA, 1 mM EDTA; trypsin-Ca²⁺, 0.01% trypsin with 1 mM Ca²⁺; light trypsin-EDTA, 0.0001% trypsin with 1 mM EDTA; trypsin-EDTA, 0.01% trypsin with 1 mM EDTA.

ferent treatments. Cells dissociated with such different treatments, however, show different respective aggregating properties, as summarized in Table I. For example, cells dissociated with 0.01% crystallized trypsin containing Ca²⁺ (0.1 to 1 mM) (TC-cells) aggregate only in the presence of Ca²⁺, while cells dissociated with 0.0001% crystallized trypsin containing 1 mM EDTA (LTE-cells) aggregate independently of the presence of Ca²⁺ (5, 9).

Some considerable evidence has been obtained that demonstrates that V79 cells are provided with two different kinds of sites for their mutual adhesion. One is a Ca²⁺-dependent site (CDS) which requires Ca²⁺ and levels of physiological temperature for the action. This site is very sensitive to trypsin, being inactivated with 0.0001% trypsin. However, it becomes resistant to trypsin in the presence of Ca²⁺. TC-cells, therefore, retain active CDS, while LTE-cells do not. Another is a Ca²⁺-independent site (CIDS) which requires neither Ca²⁺ nor physiological temperature. A relatively higher concentration of trypsin (0.01%) is needed to inactivate this site. Ca²⁺ shows no protective effect on the inactivation of the CIDS with trypsin. Thus, LTE-cells are provided with the CIDS alone, and TC-cells are provided with the CDS alone. As expected from the above characterization of the CDS and CIDS, cells dissociated with 0.01% trypsin containing EDTA (TE-cells) lose both sites so that they are completely non-adhesive to each other. Cells dissociated with EDTA alone preserve both sites.

Independent Action of CDS and CIDS

The CDS and CIDS probably consist of entirely independent molecular systems, as suggested from the following experimental results.

When cells with the CDS alone (TC-cells) and cells with the CIDS alone (LTE-cells), were mixed and incubated, they aggregated independently and never formed chimeric aggregates (6). This result clearly demonstrates that the CDS and CIDS do not share common cell surface molecules.

Further evidence for the discrimination between the CDS and CIDS was obtained by the following immunological experiment. An antibody acting against the surface of V79 cells was prepared by injecting intact cells dissociated with EDTA into rabbits. Urushihara *et al.* (9) demonstrated that Fab fragments of this antibody (anti-E-V79) strongly inhibit the aggregation of LTE-cells, but not that of TC-cells. This result suggests that the CDS and CIDS are composed of cell surface components with different immunological specificity.

Functional Difference between CDS and CIDS

Atsumi and Takeichi (2) compared the morphological difference between aggregates formed by the CDS and CIDS, respectively. LTE-cells (with CIDS alone) were associated into loose aggregates, in which individual cells remained rounded. TC-cells (with CDS alone) aggregated more tightly, adhering to neighboring cells from a wide contact area.

At an ultrastructural level, the cells in LTE-cell aggregates were connected to one another by simple appositions of plasma membranes. No other junctional structures were observed. The simple appositions of plasma membranes were also the only junctional structures in TC-cell aggregates at the early stage of their aggregation (15 min). However, after 30 to 60 min of TC-cell aggregation, two specialized junctions, gap and intermediate junctions, were noted.

These results suggest that the CDS and CIDS bind cells by quite different means. The adhesion of cells to the CIDS seems to depend on a purely biochemical reaction between cell surface components, such as the reaction between antigen and antibody or lectin and its receptor, since none of these reactions requires physiological temperature. On the other hand, the fact that CDS action is temperature dependent suggests that the CDS must involve some cellular active processes including movement of the cell surface. Moreover, the finding that gap and intermediate junctions are observed only in TC-cell aggregates suggests that the adhesion of cells to the CDS is a prerequisite for the formation of these specialized junctions.

Identification of Molecules in CIDS

The CIDS is inactivated by treating cells with 0.01% trypsin. Urushihara *et al.* (9) found that some proteinous substance is released from the cells by this treatment. This substance showed an activity neutralizing the inhibitory effect of anti-E-V79 Fab on LTE-cell aggregation. This active substance was purified by gel filtration, and its molecular weight was found to be approximately 80,000.

An antibody against this purified substance was raised, and the effect of Fab fragments of this antibody on the aggregation of V79 cells was tested. The Fab was found to inhibit the aggregation of LTE-cells but not that of TC-cells. It was therefore postulated that this trypsin-released substance is a fragment of the CIDS molecule. The next step was an attempt to identify the original intact molecule from which the fragment was derived. The above mentioned antibody will be called hereafter the anti-trypsin released fragment of the CIDS (anti-TRF).

Surface proteins of LTE-cells were first labeled with ^{125}I by the lactoperoxidase-catalyzed iodination method, and then solubilized with detergents. Anti-TRF was added into this ^{125}I -labeled cell lysate and the immunoprecipitate formed was analyzed by SDS-electrophoresis. It was found that only one component among a number of radioiodinated cell surface components is immunoprecipitated by anti-TRF (10). This component, the molecular weight of which is about 125,000, was also labeled with ^3H -fucose and ^3H -glucosamine, suggesting that it is a glycoprotein. The monospecificity of the anti-TRF was determined by two-dimensional electrophoresis of the immunoprecipitate collected from the lysate of cells metabolically labeled with

³⁵S-methionine. Staining of the cells with immunofluorescent antibodies showed that antigens to anti-TRF are distributed over the cell surfaces.

The inhibition of LTE-cell aggregation by anti-TRF was not complete: Some aggregation of cells occurred at the Fab saturated concentration. This result suggested that the CIDS is composed of multiple types of molecules. Urushihara and Takeichi (10) found that a hyaluronidase derived from *Streptomyces hyalurolyticus* also partially inhibits the aggregation of LTE-cells. When the anti-TRF was added to LTE-cells with the hyaluronidase, the aggregation of cells became totally inhibited. Perhaps some hyaluronidase-sensitive substance present on the cell surface is functional for the CIDS, independent of the 125K component system.

Identification of Molecules in CDS

Surface proteins, labeled with ¹²⁵I, of cells both with the CDS (TC-cells) and without the CDS (TE-cells) were compared by SDS-electrophoresis (5). When radioiodination was carried out in a normal balanced salt solution containing Ca²⁺, no difference in the electrophoretic pattern of radio-iodinated proteins was detected between TC- and TE-cells. However, when cells were radio-iodinated in the absence of Ca²⁺, one component with a molecular weight of 150,000 was found in the TC-cells alone.

We can assume that the molecules functional for the CDS have some reactivity with Ca²⁺. The phenomenon that the CDS becomes resistant to trypsin in the presence of Ca²⁺ may be due to a conformational change in the functional molecules after their reaction with Ca²⁺. By the same mechanism, the accessibility of lactoperoxidase to the CDS may be altered by Ca²⁺, resulting in failure to catalyze the radio-iodination of the CDS molecules in the presence of Ca²⁺. For these reasons, it may be that the 150K component is one of functional molecules in the CDS.

Cell Type Specificity of Adhesion Sites

The aggregating property of several other cells was examined as before with the V79 cells. Cells of various established lines were provided with both the Ca²⁺-dependent and the Ca²⁺-independent sites, like the V79 cells. These included not only cells such as BHK, polyoma-transformed BHK (4, 11) and retinoblastoma Y79 cells (8), but also embryonic tissue cells such as chicken embryonic neural retinal cells (9). These two kinds of sites, therefore, seem to be commonly present in a wide variety of cell types. Many epithelial cells, however, may be provided with other kinds of sites, as these cells cannot be dissociated by the methods used for V79 cells nor do they share the same aggregating property as the V79 cells (unpublished observation).

The cell-type specificity of these adhesion sites was examined by observing a heterotypic cell aggregation in mixtures of two different cell types (6). With combinations of V79 and chick neural retina cells, and with V79 and retinoblastoma Y79 cells (6, 8), the two types of cells when mixed formed chimeric aggregates. This occurred when both cell types being prepared featured the same kind of cell-cell adhesion sites, either the CDS or the CIDS. Particularly, cells with the CDS adhered to different cell-types nonselectively. Cells with the CIDS alone, however, showed some cell type specificity in aggregation. These cells tended to segregate from different cell types in

their chimeric aggregates, indicating that cells are more adhesive to the same cell type when aggregated with the CIDS.

The cell type specificity of the CIDS was demonstrated more clearly by immunofluorescent antibodies. When hepatic cells derived from newborn Chinese hamsters cultured *in vitro* were treated with immunofluorescent anti-TRF, only fibroblastic cells, but not parenchymal cells, showed staining with this antibody. This result suggested that the antigens to anti-TRF are present only in some particular cell types, probably the fibroblastic type (10).

Some types of cells are deficient in both the CDS and CIDS. For example, Ehrlich ascites tumor cells are essentially nonadhesive to each other. Aoyama *et al.* (1) studied control mechanisms of CDS and CIDS synthesis using hybrid cell lines between V79 and Ehrlich ascites cells. All the hybrid cells obtained by fusion with Sendai virus showed less adhesiveness than parent V79 cells; particularly, the activity of the CIDS was greatly reduced as compared with that of the CDS in the hybrid cells. The authors, therefore, concluded that chromosomes derived from Ehrlich ascites cells suppress the synthesis or activity of adhesion sites of V79 cells, and the expression of genes for the CIDS is more unstable.

All these results described above suggest that the CDS and CIDS have different specificity in binding cells. The CDS binds different cell types nonselectively, while the CIDS may be involved in the recognition of intercellular adhesion. Cooperative action of these cell adhesion sites may be important for the formation of complex structures of tissues or organs in animal development. The loss of the organized action of these adhesion sites perhaps results in abnormal behavior of cells as seen in malignant cells.

REFERENCES

1. Aoyama, H., Okada, T. S., and Takeichi, M. Analysis of the cell adhesion mechanism using somatic cell hybrids: I. Aggregation of hybrid cells between adhesive V79 and non-adhesive Ehrlich's ascites tumor cells. *J. Cell Sci.*, **43**, 391-406 (1980).
2. Atsumi, T. and Takeichi, M. Cell association pattern in aggregates controlled by multiple cell-cell adhesion mechanisms. *Dev. Growth Differ.*, **22**, 133-142 (1980).
3. Curtis, A.S.G. "The Cell Surface: Its Molecular Role in Morphogenesis" (1967). Academic Press, New York.
4. Ozaki, H., Okada, T. S., and Yasuda, K. Does colchicine affect aggregation of normal and transformed BHK cells differently? *Dev. Growth Differ.*, **20**, 55-59 (1978).
5. Takeichi, M. Functional correlation between cell adhesive properties and some cell surface proteins. *J. Cell Biol.*, **75**, 464-474 (1977).
6. Takeichi, M., Ozaki, H. S., Tokunaga, K., and Okada, T. S. Experimental manipulation of cell surface to affect cellular recognition mechanisms. *Dev. Biol.*, **70**, 195-205 (1979).
7. Trinkaus, J. P. "Cells into Organs. The Forces That Shape the Embryo" (1969). Prentice-Hall, New Jersey.
8. Uéda, K., Takeichi, M., and Okada, T. S. Differences in the mechanisms of cell-cell and cell-substrate adhesion revealed in a human retinoblastoma cell line. *Cell Struct. Funct.*, **5**, 188-190 (1980).
9. Urushihara, H., Ozaki, H. S., and Takeichi, M. Immunological detection of cell surface components related with aggregation of Chinese hamster and chick embryonic cells. *Dev. Biol.*, **70**, 206-216 (1979).

10. Urushihara, H. and Takeichi, M. Cell-cell adhesion molecule: Identification of a glycoprotein relevant to the Ca^{2+} -independent aggregation of Chinese hamster fibroblasts. *Cell*, **20**, 363-371 (1980).
11. Urushihara, H., Ueda, M. J., Okada, T. S., and Takeichi, M. Calcium-dependent and -independent adhesion of normal and transformed BHK cells. *Cell Struct. Funct.*, **2**, 289-296 (1977).
12. Yu, C. K. and Sinclair, W. K. Homogeneity and stability of chromosomes of Chinese hamster cells *in vitro*. *Can. J. Genet. Cytol.*, **6**, 109-116 (1964).

A CELL SURFACE-ASSOCIATED ADHESIVE GLYCOPROTEIN FROM CANCER CELL

Yasuji ISHIMARU, Ryoichi KURANO, and Hideo HAYASHI

*Department of Pathology, Kumamoto University Medical School**

A cell surface-associated adhesive glycoprotein is separated from rat ascites hepatoma AH136B cells (forming cell islands *in vivo*) and then highly purified by chromatography. This substance is stable for heat or acid and its molecular weight is about 70,000 when examined by polyacrylamide gel electrophoresis in the presence of sodium dodecyl sulfate. The adhesive potency of the substance is inhibited specifically by D-mannose or α -methyl-D-mannoside. Its activity is concerned with the protein portion of the molecule, not with the carbohydrate portion, because this factor is sensitive to trypsin but resistant to periodate. This type of adhesive factor cannot be separated from rat ascites hepatoma AH109A and Yoshida sarcoma (YS) cells (present as single cells *in vivo*).

Exogenous application of this adhesive factor to the rat ascites hepatoma cells described above induces not only aggregation but also adhesiveness of the cells characterized by well-defined junctional complexes including tight junctions, desmosomes and intermediate junctions. When examined with the ^{125}I -labeled factor, the numbers of the binding sites per cell of the factor are calculated to be 6×10^5 .

This adhesive factor is synthesized by AH136B cells but not by AH109A and YS cells, as shown in the use of ^{125}I -labeled antibody against the factor. Its synthesis begins to rise rapidly and reaches its peak in 24 hr cultivation, *i.e.*, a 10-fold increase. Cell surface localization of the synthesized factor is shown by the indirect immunofluorescence test. The intensity and distribution of immunofluorescence increase in parallel to the duration of cell cultivation.

AH136B cells, recovered at 24 hr cultivation after dissociation, adhere to each other, finally resulting in the development of junctional complexes, provided they were cultured at a reasonably high cell density (2×10^6 cells/ml) possibly capable of inducing cell contact. Thus, it seems reasonable that the cell surface-associated adhesive glycoprotein from rat ascites hepatoma cells may play a key role in cell adhesiveness and island formation.

On the other hand, a serum-associated adhesive glycoprotein is separated from tumor cells that is stable for heat with a molecular weight of more than 100,000. This factor is not specific for tumor cells and was also separated from normal rat serum. However, the cell surface-associated factor is separated from tumor-bearing rat serum but not from normal rat serum. This serum factor can aggregate tumor cells but cannot develop junctional complexes.

* Honjo 2-2-1, Kumamoto 860, Japan (石丸靖二, 蔵野良一, 林 秀男).

As is well known, intercellular adhesion is of fundamental importance in the physiology of multicellular organisms, but our knowledge of the molecular mechanisms of this phenomenon is still limited.

Recently, evidence indicating that this phenomenon may be mediated by specific binding between cell surface-associated molecules in a receptor-ligand type of interaction has been accumulated. The first successful demonstration of a specific adhesive substance was in marine sponges (17). The substance was released from sponge cells, which were dissociated mechanically in Ca^{2+} - and Mg^{2+} -free sea water and then purified (4, 15); it was a proteoglycan with a molecular weight of 2×10^6 daltons. The tissue-specific adhesive component was separated from conditioned medium of embryonic chick neural retina cells and then purified (30, 31); it was a glycoprotein with a molecular weight of approximately 50,000 daltons (11). Cell-aggregating protein with tissue-specific effects has also been obtained from embryonic mouse cerebrum, optic tectum and spinal cord (7, 13) and embryonic chick liver (29).

As is well known, the histopathology of malignant tumor cells (of epithelial cell origin) indicates that the cells termed the well-differentiated type exhibit a tendency for cell-to-cell adhesion in varying degrees, while the cells, termed poorly differentiated type or undifferentiated type show a tendency to proliferate as single cells, indicating the loss of cellular recognition. Electron microscopically, the adhesion of well-differentiated tumor cells is characterized by the development of junctional complexes to different extents and with different distributions. Accordingly, it is of special importance to confirm whether any adhesive substance(s), which is associated with cellular adhesion, exists in the well-differentiated tumor cells but not in the undifferentiated tumor cells. In other words, the presence of such an adhesive substance(s) may be concerned in the problem of tumor cell differentiation.

As is well known, rat ascites hepatoma cell lines, established by Yoshida and his associates, exhibited subpopulations of cells with different growth capabilities, adhesive capacities, and antigenicities. Among the strains, the island-forming strains (called the well-differentiated type) such as AH136B and AH7974 cells can be favorably utilized for separation of the putative adhesive factor. Tasaki and Hayashi (45, 46) have successfully separated a previously undescribed adhesive substance from those tumor cells and then Kudo *et al.* (25, 26) have purified it, as described below. In contrast, the cells of rat ascites hepatoma AH109A and Yoshida sarcoma (YS) strains (called the poorly-differentiated or undifferentiated type) are present as single cells *in vivo* and lack the ability to synthesize the adhesive substance. The purpose of the present article is to define the scope of the biological significance and biochemical properties of this adhesive substance, although many problems (such as the adhesive selectivity of this substance) remain to be solved.

Adhesiveness of Tumor Cells

Prior to separation of a putative adhesive factor from tumor cells, favorable types of tumor cells, which are characterized by a constant development of junctional complexes including tight junctions, desmosomes and intermediate junctions must be chosen for the purpose; and the electron microscopic features of cell adhesiveness must be established.

Rat ascites hepatoma AH136B cell islands (37) were composed of approximately 30–40 cells; the external shape of the cell islands was usually round or oval and individual cells showed close contact. The close contact in the apical portion of the cell islands was, as a rule, characterized by tight junctions, while that in the inner portion consisted largely of simple apposition and interdigitation of plasma membranes, and partly of intermediate junctions and desmosomes. The mean number of tight junctions, desmosomes and intermediate junctions in the cell islands, when counted for 150 nuclei in cross-sections by the method of Overton (39), was approximately 100, 24, and 28, respectively (19) (Photo 1). On the other hand, rat ascites hepatoma AH7974 cell islands (37) were composed of approximately 5–10 cells; the external shape of the cell islands was rather irregular, and the individual cells were in relatively loose contact. The close contact in the apical portion of the cell islands was also characterized by tight junctions. Although the contact area in the inner portion was smaller, the area exhibited many intermediate junctions and desmosomes, while simple apposition was apparently less frequent. The mean number of tight junctions, desmosomes and intermediate junctions was approximately 100, 80, and 64, respectively (19), suggesting that these cells are more convenient than AH136B cells for analyzing the detailed structural changes in desmosomes and intermediate junctions. In contrast, rat ascites hepatoma AH109A and YS cells (38) were floating as single cells in the ascitic fluids, presenting an advantage in comparison with island-forming tumor cells.

The regular distribution and constant presence of such tight junctions, resembling those described by Farquhar and Palade (6), in the apical portion of the cell islands suggest that they may form continuous belts around the adherent cells by which the interior circumstance of the cell islands may be favorably maintained; the junctions have been known to function as a complete barrier to the passage of fluids along cell surfaces (42). The desmosomes, resembling those described by Farquhar and Palade (6), have been thought to play a part in maintaining cell adhesion and tension (42).

The above island-forming tumor cells, when subcutaneously transplanted, also developed cell islands resembling those floating in the ascitic fluids. On the other hand, the above free tumor cells, when subcutaneously transplanted, mostly proliferated as single cells. Although some cells formed an island-like structure, the cell contact in the structure consisted of only simple apposition with no intermediate junctions, desmosomes or tight junctions.

Discovery of Adhesive Factor from Cancer Cells

On the basis of the observations mentioned above, separation of the adhesive factor which is involved in the aggregation and adhesiveness of tumor cells was performed as follows:

1. Separation of adhesive factor

The activity of the adhesive factor was, as a rule, shown by an induction of tumor cell aggregation (27, 45, 46). The same volumes (1 ml) of the test sample and of rat ascites hepatoma cell suspension were mixed in a Falcon tube and incubated at 37° in a roller tube culture apparatus with one rotation/8 min. At various time intervals after incubation, cell aggregation in both gross and microscopic features was recorded. The

TABLE I. Procedures of Separation and Purification of Adhesive Factors

Rat ascites hepatoma cells forming island	
— Suspended in Hanks' balanced salt solution free of Ca^{2+} and Mg^{2+}	
— Subjected 50 gentle pipettings	
— Allowed to stand for 3 hr at 4°	
Cell-free supernatant fluid	
— Eluted in 0.02 M phosphate buffer plus 0.3 M NaCl (pH 6.8) on DEAE-Sephadex A-50	
— Eluted in Hanks' balanced salt solution (pH 7.3) on Bio-gel A-5m; second fraction used	
Adhesive fraction	
— Eluted on immunoadsorbent column with rabbit antibody (IgG fraction) against rat serum	
Cell surface-associated adhesive factor (unabsorbed factor)	Serum-associated adhesive factor (absorbed factor)
— Absorbed on immunoadsorbent column with rabbit antibody (IgG fraction) against unabsorbed factor, separated from tumor-bearing rat serum	— Eluted at pH 2.4 with 1.0 M acetic acid
— Eluted at pH 2.4 with 1.0 M acetic acid	Partially purified factor
Highly purified factor ^a	

^a Approximately 220 μg of the factor can be obtained from cell-free supernatant fluid (containing 40.0 mg protein from 1.5×10^7 AH136B cells).

grading of the induced cell aggregation was achieved by counting the aggregating cells and freely floating cells, respectively, in the fluids after 30 min of incubation (27). AH109A and YS cells were used immediately after collection from the ascitic fluids, because these cells were mostly present as single cells in the ascitic fluids. On the other hand, AH136B and AH7974 cells were used immediately after dissociation, because these cells were present as island-forming cells in the ascitic fluids.

The active substance was released from AH136B cells or AH7974 cells, which were suspended in Hanks' balanced salt solution (free of Ca^{2+} and Mg^{2+}), gently pipetted and then allowed to stand for 3 hr in the cold. The substance in the cell-free supernatant fluids was partially purified by chromatography with a DEAE-Sephadex and Biogel A-5m (27, 45, 46) (Table I). This substance was noncytotoxic and clearly effective for aggregation of rat ascites hepatoma cells mentioned above as well as SV40-transformed cells, but not for liver cells from normal rats. Cell aggregation at a similar grading was induced by dissociated AH136B cells (5×10^5 cells/ml), AH109A cells (1.5×10^6 cells/ml) or YS cells (1.5×10^6 cells/ml); aggregation became visible after 10 min of incubation with the substance at 37° (but not at 4°). After 30 min incubation, the cell aggregates, which became larger and fused together, settled to the bottom of the Falcon tubes. No such induction of cell aggregation was revealed in the absence of the substance. The action of this substance was much more potent than that of Jack bean concanavalin A (Con A) when assayed for aggregation of SV40-transformed cells (27).

It is important to note that this active substance could be separated from the island-forming hepatoma cells under very mild conditions as noted above, in which the cells

were not treated with a proteolytic enzyme such as trypsin. The cells after releasing the adhesive substance were still alive when examined by toluidine blue staining. Such mild procedures have been successfully described for the separation of an aggregation promoting substance from sponge cells (4, 15, 17, 33). In the separation, the cells were mechanically dissociated and then suspended in Ca^{2+} - and Mg^{2+} -free sea water. Accordingly, it seemed reasonable that the active substance separated from tumor cells was not an artificial product that appeared during the separation.

2. *Induction of cancer cell adhesiveness by the factor*

It is of special interest that the tumor cells, aggregated in 30 min or 2 hr incubation with the adhesive factor, could be easily dissociated by pipetting, while those incubated for 12 or 24 hr with the factor mostly could not be dissociated by pipetting, indicating a distinct difference in the development of binding structures in the aggregated cells. Such a difference in the binding manner was clearly explained by the use of aggregated AH109A and YS cells, which required no previous dissociation before aggregation.

a) *Cell contact at 2 hr incubation with the factor:* The most common sort of aggregated cell contact observed at this stage was simple apposition of plasma membranes. Apposed plasma membranes were separated by a space of 20–30 nm showing no electron density, resembling those observed in the island-forming tumor cells. At this stage of cell contact, intermediate junctions were very rarely found, and no desmosomes or tight junctions were observable (20, 23).

b) *Cell contact at 12 hr incubation with the factor:* The cell contact became closer and more distinct at this stage; a distinct increase in intermediate junctions was noticed. The junctions consisted of 2 outer leaflets disposed in a parallel fashion and separated by an intercellular space of 10–15 nm exhibiting low electron density, resembling those observed on the island-forming tumor cells (Photo 2A). In the cytoplasm subjacent to the inner leaflets, moderate electron density was revealed (20, 23). The desmosome- and tight junction-like structures were found in the limited surface regions of close cell contact. The desmosome-like structure consisted of 2 outer leaflets running in a parallel fashion and separated by an intercellular space of approximately 20 nm containing a central disc of electron-dense materials. In the cytoplasm subjacent to each inner leaflet, electron-dense laminar plaques running parallel to the inner leaflets were observed. A few tonofilaments were frequently found in the cytoplasm, but they were unrelated to the laminar plaques. Such structures seemed to correspond to that of desmosomes in the process of development (Photo 2B). Tight junctions, corresponding to the focal tight junctions described by Stachelin (42), were revealed less frequently at this stage; they were characterized by a narrow gap of less than 4 nm in distance which was formed by close approximation and punctate fusion of outer leaflets.

c) *Cell contact at 24 hr incubation with the factor:* At this stage of incubation, cell contact became closer and more characteristic. The cell surface regions showing close contact clearly increased (Photo 3); the cell contact was characterized by an increase in desmosomes and tight junctions. Well-fined desmosomes observed at this stage were characterized by one distinct laminar plaque accompanied by prominent tonofilaments (Photo 4A) (20, 23). Tight junctions showed a tendency to develop in the apical portion of the cell aggregates, but some also developed in the inner portion of the aggregates

(Photo 4B). In the above-mentioned cell islands, however, tight junctions could not be found in the inner portion. Such a difference in the distribution of tight junctions can be explained as described below.

The development by this adhesive factor of tight junctions, desmosomes and intermediate junctions was strongly inhibited in the presence of actinomycin D during 24 hr of cultivation (23). The failure to develop junctional complexes was associated with the inhibition of RNA synthesis by actinomycin D (40), exclusively resulting in the failure to synthesize the proteins required for the development of junctional complexes.

Separation of Cell Surface- and Serum-associated Adhesive Factors

1. Immunological comparison

In view of the biological significance of the adhesive factor noted above, further characterization of the substance was required. Since AH136B cells floating in the ascitic fluids were clearly coated with serum proteins, exuded by the mechanisms of increased vascular permeability after intraperitoneal inoculation of the cells (36), the adhesive preparation noted above was found to contain a considerable quantity of serum proteins (25). For removing the serum proteins, the adhesive preparation was eluted through an immunoadsorbent column coupled with anti-rat serum antibody (Table I) (25). As a result, the preparation was revealed to be a mixture of at least two types of adhesive factors with different antigenic determinants; one, which is clearly more potent for induction of tumor cell aggregation, is not absorbed by the antibody, *i.e.*, the unabsorbed factor and the other, which is apparently less active, is absorbed by the antibody, *i.e.*, the absorbed factor.

In this connection, it is of interest that the serum from AH136B tumor-bearing rats became much more potent for induction of cell aggregation according to the duration after intraperitoneal inoculation of the cells. The increase in potency was found to be due to an increased quantity of the unabsorbed factor in the serum, indicating the release by the cells of the unabsorbed factor into the body fluids. On the other hand, the quantity of the absorbed factor in the serum also remained unchanged independent of the duration after inoculation of tumor cells. Serum from healthy rats contained the absorbed factor (similarly less active), but not the unabsorbed factor, indicating that the absorbed factor was not tumor cell-specific in nature. As mentioned below, since the localization of the unabsorbed factor on the cell surfaces was confirmed by the immunofluorescence technique, this unabsorbed factor was termed the cell surface-associated adhesive factor, while the absorbed factor was termed the serum-associated adhesive factor.

2. Biochemical comparison

a) *Treatment with trypsin and periodate:* As is well known, protein portions have been shown to play a key role in the aggregating effect of sea sponge extract (8), the purified aggregation promoting factor of siliceous sponges (35) and of porcine thyroid cell extract (9). It seemed reasonable that the aggregating effects of the above cell surface- and serum-associated adhesive factor may be concerned with the protein portions in their molecules, and not with the carbohydrate portions, because these

factors were similarly sensitive to trypsin but resistant to periodate (10). The retina cell-adhesive substance was also sensitive to trypsin but resistant to periodate (11, 34). Accordingly, it was supposed that the aggregating effects of these adhesive factors may be initiated by interaction of the protein portions in their molecules with some components at the surface of the tumor cells.

b) Carbohydrate inhibition: Following the introduction of Landsteiner's hapten inhibition techniques, many hemagglutinins have been shown to react with specific carbohydrates on the erythrocyte surface (3, 18, 32). These studies have raised the possibility that carbohydrates may play an important part in the interaction between plant lectins and mammalian cell surfaces (1, 2). D-mannose and α -methyl-D-mannoside specifically inhibited tumor cell aggregation by the cell surface-associated factor; these sugars (100 mM) resulted in a complete inhibition of cell aggregation (10). On the other hand, the potency of the serum-associated factor was inhibited specifically by N-acetyl-D-glucosamine; this sugar (100 mM) resulted in a complete inhibition of cell aggregation. Thus, it seemed reasonable to suppose that adhesion of rat ascites hepatoma cells due to the cell surface-associated factor may be a consequence of the interaction of the protein structure in the molecule with certain carbohydrate molecules such as D-mannose at the cell surface, while that due to the serum-associated factor may operate by interaction of the protein portion in the molecule with certain carbohydrate molecules such as N-acetyl-D-glucosamine at the cell surface.

3. Morphological comparison

a) Effect of cell surface-associated factor: There remained the problem of which type of these adhesive factors separated was responsible for the development of junctional complexes. The cell contact observed at 24 hr incubation with the cell surface-associated factor was characterized by the development of well-defined junctional complexes, which were indistinguishable from those observed at 24 hr incubation with a mixed preparation of two adhesive factors (10); the adherent cells could not be dissociated by pipetting. In the presence of actinomycin D, the cell contact observed consisted of only simple apposition of plasma membranes; the aggregated cells were easily dissociated by pipetting.

b) Effect of serum-associated factor: In contrast, the cell contact observed at 24 hr incubation with the serum-associated factor with a similar activity consisted of only simple apposition. The intercellular spaces of the aggregated cells were larger, and the areas of cellular apposition were smaller; the aggregated cells were easily dissociated by pipetting. These experiments indicated a distinct functional difference between the cell surface- and serum-associated factors for the induction of junctional complexes. Thus, it is clear that the cell surface-associated factor is undoubtedly involved in the development of junctional complexes.

Characterization of Cell Surface-associated Adhesive Factor

1. Purification of the factor

The cell surface-associated factor described above gave two distinct precipitin lines when tested by agar immunodiffusion with rabbit antibody against the factor, while the adhesive factor, which was separated from tumor-bearing rat serum following the serum

procedures noted above, gave only one distinct precipitin line, which obviously corresponds to one of the two precipitin lines demonstrated (Photo 5A). Accordingly, the adhesive factor (from tumor cells) was applied to an immunoadsorbent column coupled with rabbit antibody against the adhesive factor (from tumor-bearing rat serum). The substance (corresponding to the cell surface-associated factor) was absorbed on the column and then eluted without loss of its activity in an acid condition (Table I) (24, 26). The adhesive factor, recovered from the column, produced only one distinct precipitin line, which is obviously common to the two adhesive factors (from tumor cells and tumor-bearing rat serum) when assayed by agar immunodiffusion with the above antibody (Photo 5B) (26). Polyacrylamide gel electrophoresis in the presence of SDS revealed that this factor shows a single band with a molecular weight of 70,000 (Photo 5C) (14). When estimated by gel filtration, its molecular weight was approximately 72,000 (26). This substance was a heat-stable and acidstable glycoprotein (quantitative analysis of the sugars in the molecule is in progress). Thus, approximately 220 μg of the purified factor could be obtained from the cell-free supernatant fluids (containing 40.0 mg) prepared from AH136B cells. Its minimum effective dose for induction of aggregation of AH109A cells ($1.5 \times 10^6/\text{ml}$) at 30 min incubation was approximately 10.0 μg (26). This factor aggregated tumor cells but not erythrocytes (untreated or trypsin glutaraldehyde-fixed) from rats, rabbits, or guinea pigs.

2. Binding of the factor to cancer cells

As mentioned above, the cell surface-associated adhesive factor (from tumor cells)

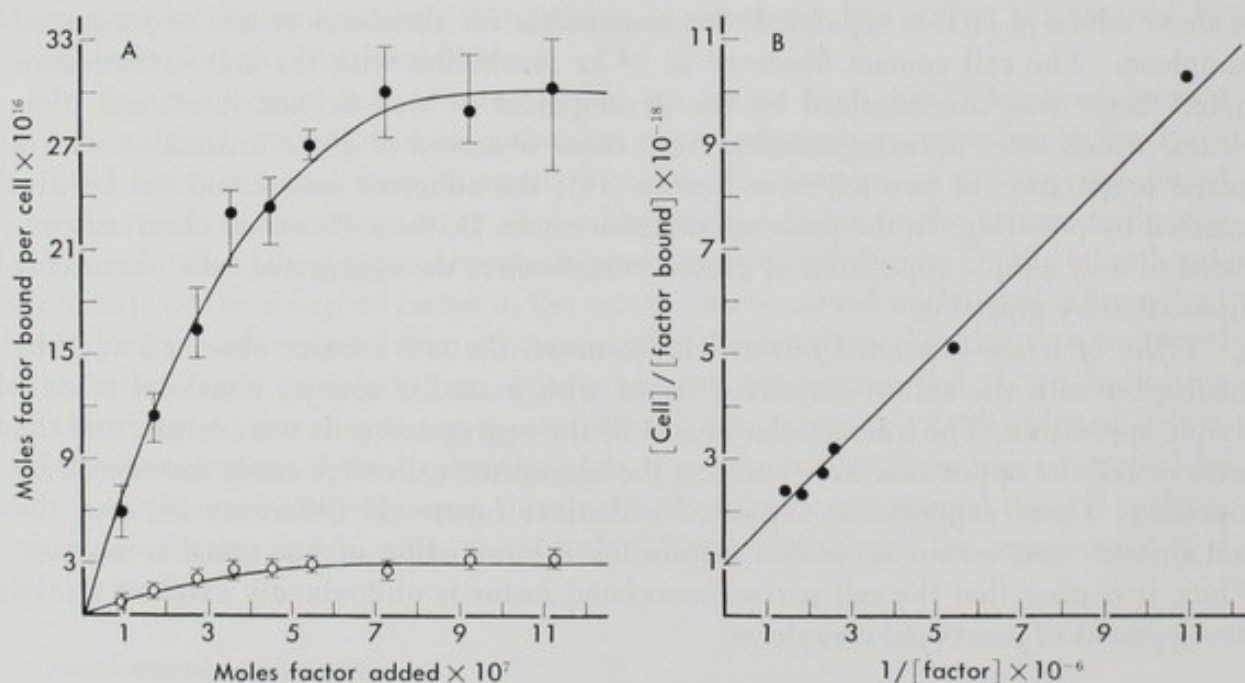


FIG. 1. A: Saturation curve of binding of cell surface-associated adhesive factor labeled with ^{125}I to AH109A cells. It reaches a plateau at a concentration of 50 $\mu\text{g}/\text{ml}$ of the factor. ● cell surface-associated factor; ○ the factor pretreated with D-mannose. B: Calculation of binding sites for cell surface-associated adhesive factor on AH109A cells. By plotting the binding data (presented in A) according to the Steck and Wallach (43) equations, the number of binding sites per cell is calculated to be 6×10^5 and the affinity constant (K_a) is 1.1×10^6 .

induced not only aggregation of tumor cells but also adhesiveness of the cells. In order to act on the tumor cells, this adhesive factor must bind to their surfaces, presumably through specific surface receptors. The purified cell surface-associated adhesive factor was labeled with ^{125}I . The labeled product was homogeneous and its biological activity remained unchanged after purification by affinity chromatography; its binding to AH109A cells noted above was specifically inhibited by D-mannose. The binding to the cells exhibited a simple saturation pattern, reaching its peak at a concentration of 50 $\mu\text{g}/\text{ml}$ (Fig. 1A). By plotting the binding data according to the Steck and Wallach (43) equations, the total numbers of binding sites per cell were calculated to be 6×10^5 and the affinity constant (K_a) was 1.1×10^6 (Fig. 1B) (14, 21). The binding of this adhesive factor to the cells was also demonstrated by the indirect immunofluorescent technique using rabbit antibody against the purified adhesive factor; this bound adhesive factor was found localized on the cell surface.

Synthesis of Cell Surface-associated Adhesive Factor

1. Synthesis of the factor by cancer cells and its localization

As mentioned above, the cell surface-associated adhesive factor functions as a trigger factor to develop junctional complexes in tumor cells, provided it was exogenously applied to the cells. In order to form cell islands characterized by junctional complexes without any addition of this component, tumor cells, *e.g.*, AH136B and AH7974 cells themselves, must synthesize this adhesive component. It seems possible that if these tumor cells could be maintained under physiological conditions but prevented from aggregating at a reasonably low cell density, the cells may continue to synthesize this component. The tumor cells, which were mechanically dissociated in Rabinowitz' balanced salt solution containing EDTA (1.2 mM), were suspended at a density of 2×10^4 cells/ml for cultivation. The synthesis (or regeneration) of this adhesive component was examined using ^{125}I -labeled rabbit antibody (IgG fraction) against the purified adhesive factor; ^{125}I -labeled rabbit IgG served as a control. The cultured cells were harvested after different cultivation times (0 to 24 hr).

The synthesis (as shown in the form of increased radioactivity specifically bound to the cells) began to rise rapidly; it increased 8-fold in 12 hr of cultivation, reaching its peak, *i.e.*, a 10-fold increase, in 24 hr of cultivation (14, 21) (Fig. 2). Since the adhesive component, which previously existed in the cells, was revealed during cell dissociation, it was scarcely detected in the inhibition of cultivation. This finding indicated that the release of this component from tumor cells occurs more easily than that of the cognin (12) from embryonic chick neural retina cells, because the adhesiveness of the tumor cells was less strong than that of the neural retina cells. The regeneration of the factor was strongly inhibited by the addition of actinomycin D or puromycin, indicating that the regeneration required protein synthesis (Fig. 2).

In contrast, this type of adhesive component was not detectable in AH109A and YS cells during 24 hr of cultivation (Fig. 2), although there remained some questions that this component might exist in an inaccessible state (hidden within the surface membrane layer or situated at the submembrane layer), or in a smaller quantity not demonstrable by this technique. However, biochemical evidence that this component could not be separated from those tumor cells by the same procedures as noted above (Table

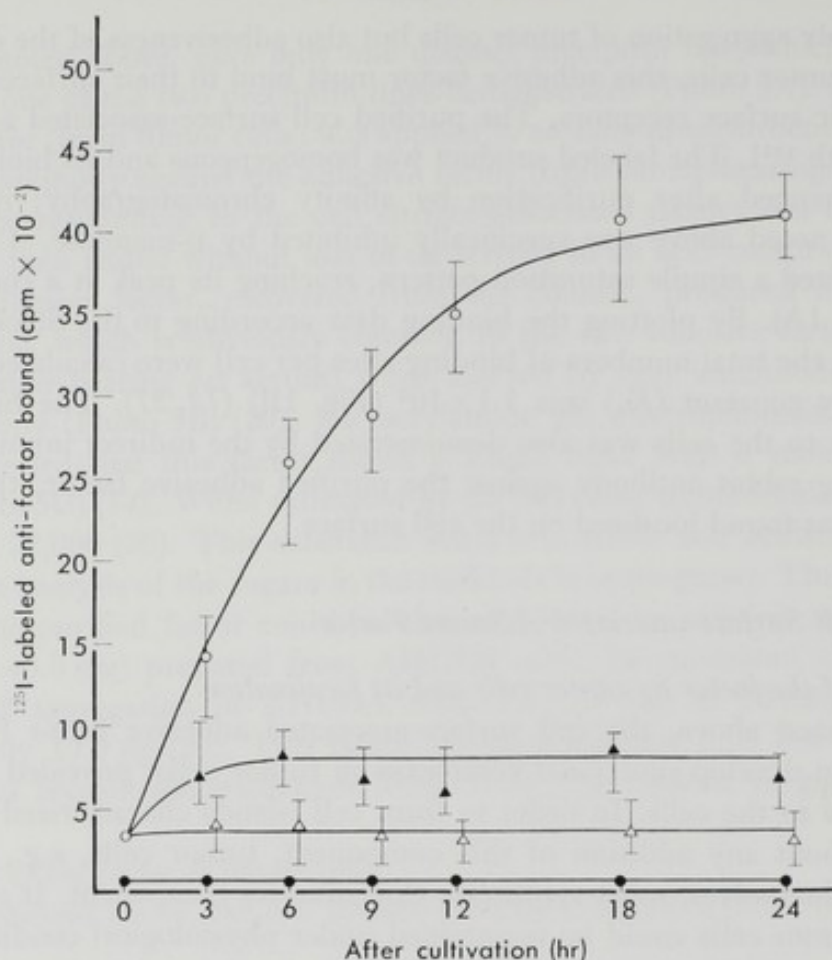


FIG. 2. Detection of synthesis of cell surface-associated adhesive factor by AH136B cells using ^{125}I -labeled antibody against the factor. The synthesis begins to rise rapidly; it increases to 8-fold in 12 hr cultivation, reaching its peak, *i.e.*, a 10-fold increase, in 24 hr cultivation. It is inhibited by actinomycin D or puromycin. ○ AH136B cells ($1 \times 10^6/50$ ml in minimum essential medium (MEM)); ▲ AH136B cells ($1 \times 10^6/50$ ml in MEM containing 12.5 mg actinomycin D); △ AH136B cells ($1 \times 10^6/50$ ml in MEM containing 125 mg puromycin); ● AH109A cells ($1 \times 10^6/50$ ml in MEM).

I) strongly suggested that this component may not be synthesized by the cells; only the serum-associated adhesive factor can be separated from the cells (22). As described above, although when the adhesive factor was exogenously applied AH109A and YS cells could form *in vitro* cell islands characterized by the development of junctional complexes, such adhering cells, like untreated AH109A and YS cells, proliferated as single cells when intraperitoneally inoculated (23).

Furthermore, localization of the regenerated adhesive component was examined by the indirect immunofluorescence test using the immune IgG described above and FITC-labeled goat anti-rabbit IgG; preimmune rabbit IgG served as a control. Since the immunofluorescence test showed a specific binding of the antibody to the surface of the live recovered cells, the surface localization of this component is reasonable; the intensity and distribution of the immunofluorescence increased in parallel to the duration of cultivation (14, 21). The cells at 2 hr culture exhibited faint patch-like fluorescence at the limited small area of the cell surface (Photo 6A); those at 6 hr culture showed bright fluorescence at the larger (but limited) area of the cell surface

(Photo 6B); those at 12 hr culture showed conspicuous fluorescence, which was diffusely distributed on the whole cell surface (Photo 6C); and those at 24 hr culture showed a similar but more conspicuous fluorescence (Photo 6D). Such an increase in immunofluorescence seems to correspond to the radioimmunologically detected increase in the synthesis of this component mentioned above. In contrast, when the cells were similarly tested within 1 hr after cultivation, they showed little or no immunofluorescence. Thus, the tumor cells could recover from the dissociative effect by at least 24 hr; such recovery did not occur in the presence of puromycin or actinomycin D. No immunofluorescence was revealed in tumor cells such as AH109A and YS cells. Hausman and Moscona (12) have shown the existence of the adhesive factor on the surface of embryonic chick neural retina cells by immunologic assays, *e.g.*, binding of antiserum to the surface of the recovered cells and complement-mediated cell lysis; retina cells were allowed to recover from trypsinization for 18 hr. Chang *et al.* (5) have also described immunologic detection of the adhesive factor on the surface of slime mold *Dictyostereum discoideum*, which may play a role in species-specific cell adhesions.

2. Induction of cancer cell adhesiveness by the synthesized factor

Tumor cells, which had completed the regeneration of the adhesive factor at 24 hr cultivation, adhered to each other, finally resulting in the development of junctional complexes, provided they were cultured at a reasonably high cell density (2×10^6 ml) possibly capable of inducing cell contact (14, 21). On the other hand, the cells, which had failed to regenerate this adhesive factor in the presence of actinomycin D or puromycin, did not adhere to each other. The process of cell adhesiveness observed was divided into three stages: (1) The cells aggregated in the form of a linear or branched chain within 3 hr of incubation (Photo 7A), resembling the picture observed at early stage of *in vitro* reaggregation of embryonic chick retina cells (41) or of Chinese hamster V79 cells (44), and such cell aggregation was specifically suppressed by the antibody (Fab fraction) against the adhesive factor; (2) the cell aggregates became spherical or grape cluster-like in shape due to fusion at 6 hr of incubation (Photo 7B) and since the contact of aggregated cells consisted of simple apposition of plasma membranes, the cells were easily dissociated by pipetting; and (3) the cell aggregates became oval in shape at 12 to 24 hr of incubation, closely resembling the external shape of AH136B cell islands (floating in the ascitic fluids) (Photo 7C, D) and since the contact of aggregated cells was characterized by the development of tripartite junctional complexes, the cells were not dissociated by pipetting. Tight junctions were found located only in the apical portion of the cell aggregates, while intermediate junctions and desmosomes were found in the inner portion; such development of junctional complexes was more frequent at 24 hr of incubation. No tight junctions were found in the inner portion of the cell aggregates. In contrast, AH109A and YS cells failed to adhere under the same conditions of incubation, because of their lack of potency in synthesizing the adhesive factor.

Further information on the adhesive factor has been obtained: 1) The substance, which is immunologically cross-reactive with the factor, can be extracted from embryonic rat liver suggesting that the adhesive factor may be one of carcinoembryonal proteins; 2) the adhesive factor exhibits a lectin-like potency, by which T lymphocytes

can be activated and release macrophage chemotactic lymphokine (16, 21, 28), suggesting that this factor might be concerned in immunologic reactions in tumor sites.

Acknowledgments

We are greatly indebted to Drs. Y. Koga, S. Tokuda, H. Kako, and S. Kurano for their invaluable cooperation. This work was supported in part by special grants for cancer research from the Japanese Ministry of Education, Science and Culture, and the Biological Institute of Shionogi Pharmaceutical Company, Osaka and the Society for Metabolism Research, Tokyo.

REFERENCES

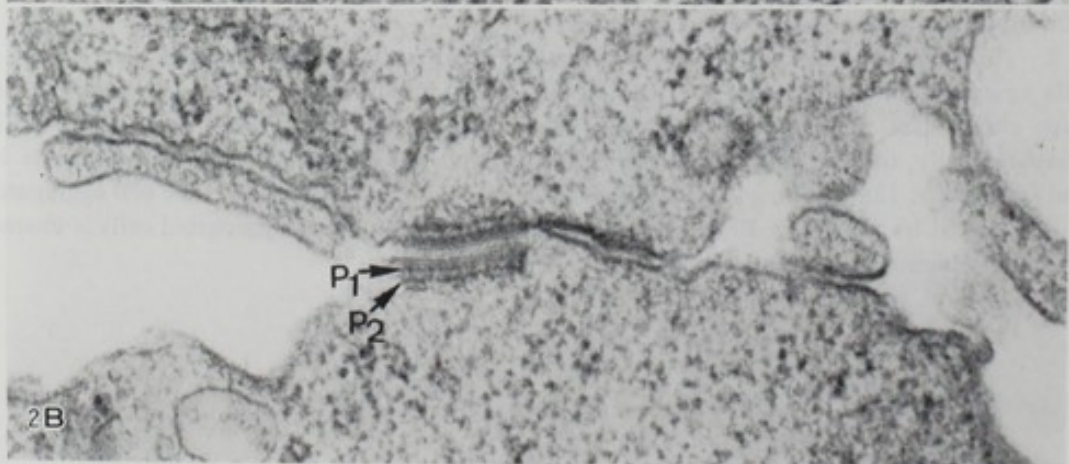
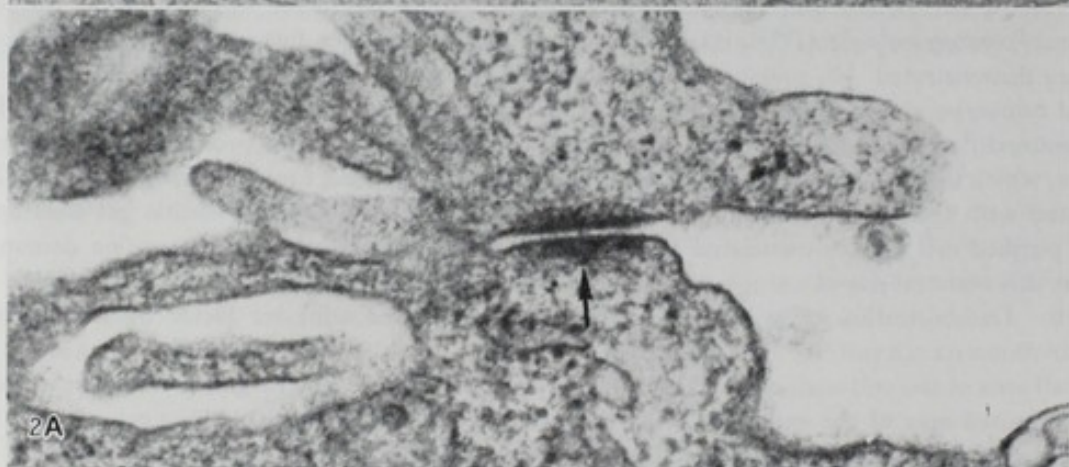
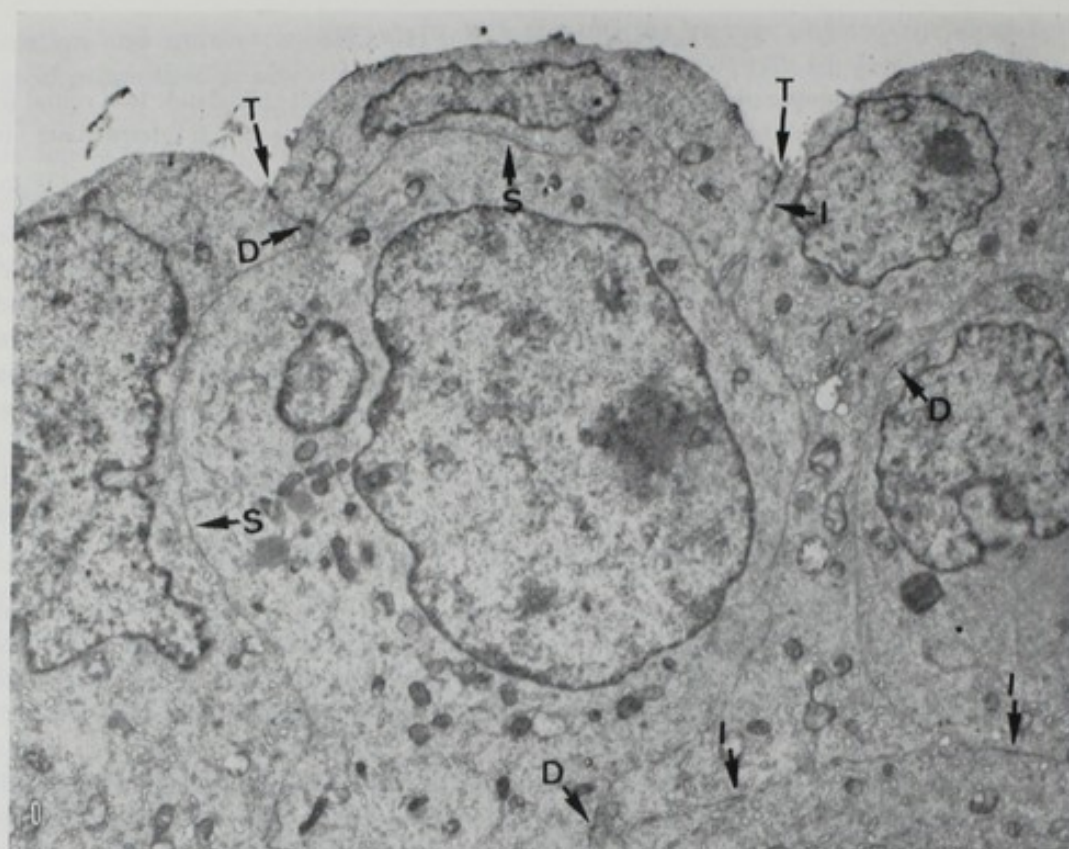
1. Aub, J. C., Sanford, B. H., and Cote, M. N. Reaction of normal and leukemic cell surface to a wheat germ agglutinin. *Proc. Natl. Acad. Sci. U.S.*, **54**, 400-402 (1965).
2. Burger, M. M. A difference in the architecture of the surface membrane of normal and virally transformed cells. *Proc. Natl. Acad. Sci. U.S.*, **62**, 994-1001 (1969).
3. Burger, M. M. and Goldberg, A. R. Identification of tumorspecific determinant on neoplastic cell surfaces. *Proc. Natl. Acad. Sci. U.S.*, **57**, 359-366 (1967).
4. Cauldwell, C. B., Henkart, P., and Humphreys, T. Physical properties of sponge aggregation factor. A unique proteoglycan complex. *Biochemistry*, **12**, 3051-3055 (1973).
5. Chang, C. M., Reitherman, R. W., Rosen, S. D., and Barondes, S. H. Cell surface location of discoidin, a developmentally regulated carbohydrate-binding protein from *Dictyostelium discoideum*. *Exp. Cell Res.*, **95**, 136-142 (1975).
6. Faquhar, M. G. and Palade, G. E. Junctional complexes in various epithelia. *J. Cell Biol.*, **17**, 375-412 (1963).
7. Garber, B. B. and Moscona, A. A. Reconstruction of brain tissue from cell suspensions. II. Specific enhancement of aggregation of embryonic cerebral cells by supernatant from homologous cell cultures. *Dev. Biol.*, **27**, 235-243 (1972).
8. Gasic, G. J. and Galanti, N. L. Proteins and disulfide groups in the aggregation of dissociated cells of sea sponges. *Science*, **151**, 203-205 (1966).
9. Giraud, A., Fayet, G., and Lissitzky, S. Thyrotropin-induced aggregation-promoting factors of adult cultured thyroid cells. *Exp. Cell Res.*, **87**, 359-364 (1974).
10. Hanaoka, Y., Kudo, K., Ishimaru, Y., and Hayashi, H. Biochemical and morphological comparison of two tumour-cell-aggregation factors from rat ascites hepatoma cells. *Br. J. Cancer*, **37**, 536-544 (1978).
11. Hausman, R. E. and Moscona, A. A. Purification and characterization of the retina-specific cell-aggregating factor. *Proc. Natl. Acad. Sci. U.S.*, **72**, 916-920 (1975).
12. Hausman, R. E. and Moscona, A. A. Immunologic detection of retina cognin of the surface of embryonic cells. *Exp. Cell Res.*, **119**, 191-204 (1979).
13. Hausman, R. E., Knapp, L. W., and Moscona, A. A. Preparation of tissue-specific cell-aggregating factors from embryonic neural tissue. *J. Exp. Zool.*, **198**, 417-422 (1976).
14. Hayashi, H. and Ishimaru, Y. Morphological and biological aspects of adhesiveness and dissociation of cancer cells. *Int. Rev. Cytol.*, in press.
15. Henkart, P., Humphreys, S., and Humphreys, T. Characterization of sponge aggregation factor. A unique proteoglycan complex. *Biochemistry*, **12**, 3045-3050 (1973).
16. Hifumi, M., Kuratsu, J., and Hayashi, H. Immunological function of cell surface-associated adhesive factor from rat ascites hepatoma cells: Production of macrophage chemotactic lymphokine. *Trans. Soc. Pathol. Japon.*, **69** (in Japanese), in press.
17. Humphreys, T. Chemical dissolution and *in vitro* reconstruction of sponge cell adhesions.

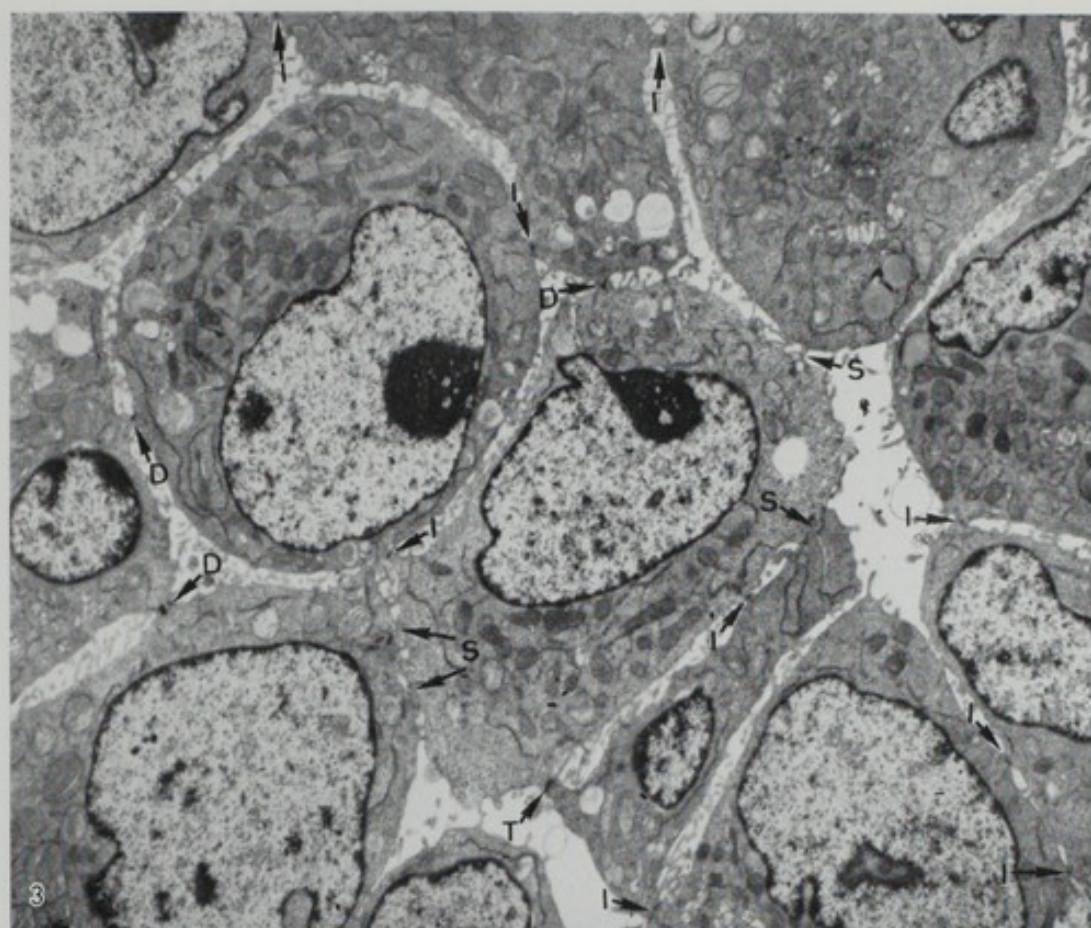
- I. Isolation and functional demonstration of the components involved. *Dev. Biol.*, **8**, 27-47 (1963).
18. Inbar, M. and Sachs, L. Structural difference in sites on the surface membrane of normal and transformed cells. *Nature*, **223**, 710-712 (1969).
 19. Ishihara, H., Ishimaru, Y., and Hayashi, H. Ultrastructural changes of intercellular junctions in rat ascites hepatoma cells with calcium depletion. *Br. J. Cancer*, **35**, 643-656 (1977).
 20. Ishimaru, Y., Ishihara, H., and Hayashi, H. An electron microscopic study of tumour cell adhesiveness induced by aggregation factor from rat ascites hepatoma cells. *Br. J. Cancer*, **31**, 207-217 (1975).
 21. Ishimaru, Y., Hifumi, M., Kurano, R., and Tokuda, S. Immunological function of cancer cell surface-associated adhesive glycoprotein: Evidence for lectin-like activity. *Infect. Inflam. Immun.* (in Japanese), in press.
 22. Ishimaru, Y., Kudo, K., Koga, Y., and Hayashi, H. A possible mechanism for island formation by rat ascites hepatoma cells with special reference to the function of aggregation factor at the cell surface. *J. Cancer Res. Clin. Oncol.*, **93**, 123-136 (1979).
 23. Ishimaru, Y., Kudo, K., Ishihara, H., and Hayashi, H. The induction of tumour cell adhesiveness and intercellular junctions by a glycoprotein of rat ascites hepatoma cell surface. *Br. J. Cancer*, **34**, 426-436 (1976).
 24. Kudo, K. and Hayashi, H. Cell aggregation factor from animal cells. In "Lectins," ed. T. Osawa and R. Mori, pp. 155-172 (1976) (in Japanese). Kodansha, Tokyo.
 25. Kudo, K., Hanaoka, Y., and Hayashi, H. Characterization of tumour cell aggregation promoting factor from rat ascites hepatoma cells: Separation of two factors with different antigenic property. *Br. J. Cancer*, **33**, 79-90 (1976a).
 26. Kudo, K., Hanaoka, Y., and Hayashi, H. Purification of a tumour cell aggregation-promoting factor associated with rat ascites hepatoma. *Br. J. Cancer*, **33**, 88-89 (1976b).
 27. Kudo, K., Tasaki, I., Hanaoka, Y., and Hayashi, H. A tumour cell aggregation promoting substance from rat ascites hepatoma cells. *Br. J. Cancer*, **30**, 549-559 (1974).
 28. Kuratsu, J., Yoshinaga, M., and Hayashi, H. Rat lymphocyte mitogenesis by aggregation factor from rat ascites hepatoma cell surface. *Br. J. Cancer*, **38**, 224-232 (1978).
 29. Kuroda, Y. Preparation of an aggregation-promoting supernatant from embryonic chick liver cells. *Exp. Cell Res.*, **49**, 626-637 (1968).
 30. Lilien, J. Specific enhancement of cell aggregation *in vitro*. *Dev. Biol.*, **17**, 657-678 (1968).
 31. Lilien, J. and Moscona, A. A. Cell aggregation: Its enhancement by a supernatant from cultures of homologous cells. *Science*, **157**, 70-72 (1967).
 32. Lis, H., Sela, B. A., Sachs, L., and Sharon, N. Specific inhibition by N-acetyl-D-galactosamine of the interaction between soybean agglutinin and animal cell surfaces. *Biochim. Biophys. Acta*, **211**, 582-585 (1970).
 33. Magoliash, E., Schenck, J. R., Hargie, M. P., Burokas, S., Richter, W. R., Barlow, H. H., and Moscona, A. A. Characterization of specific cell aggregating materials from sponge cells. *Biochem. Biophys. Res. Commun.*, **20**, 383-388 (1965).
 34. McClay, D. R. and Moscona, A. A. Purification of specific cell-aggregating factor from embryonic neural retina cells. *Exp. Cell Res.*, **87**, 438-443 (1974).
 35. Muller, W.E.G., Muller I., Kurelec, B., and Zahn, R. K. Species-specific aggregation factor in sponges. IV. Inactivation of the aggregation factor by mucoid cells from another species. *Exp. Cell Res.*, **98**, 31-40 (1976).
 36. Nishimura, K. The mechanisms of increased vascular permeability in tumor tissues;

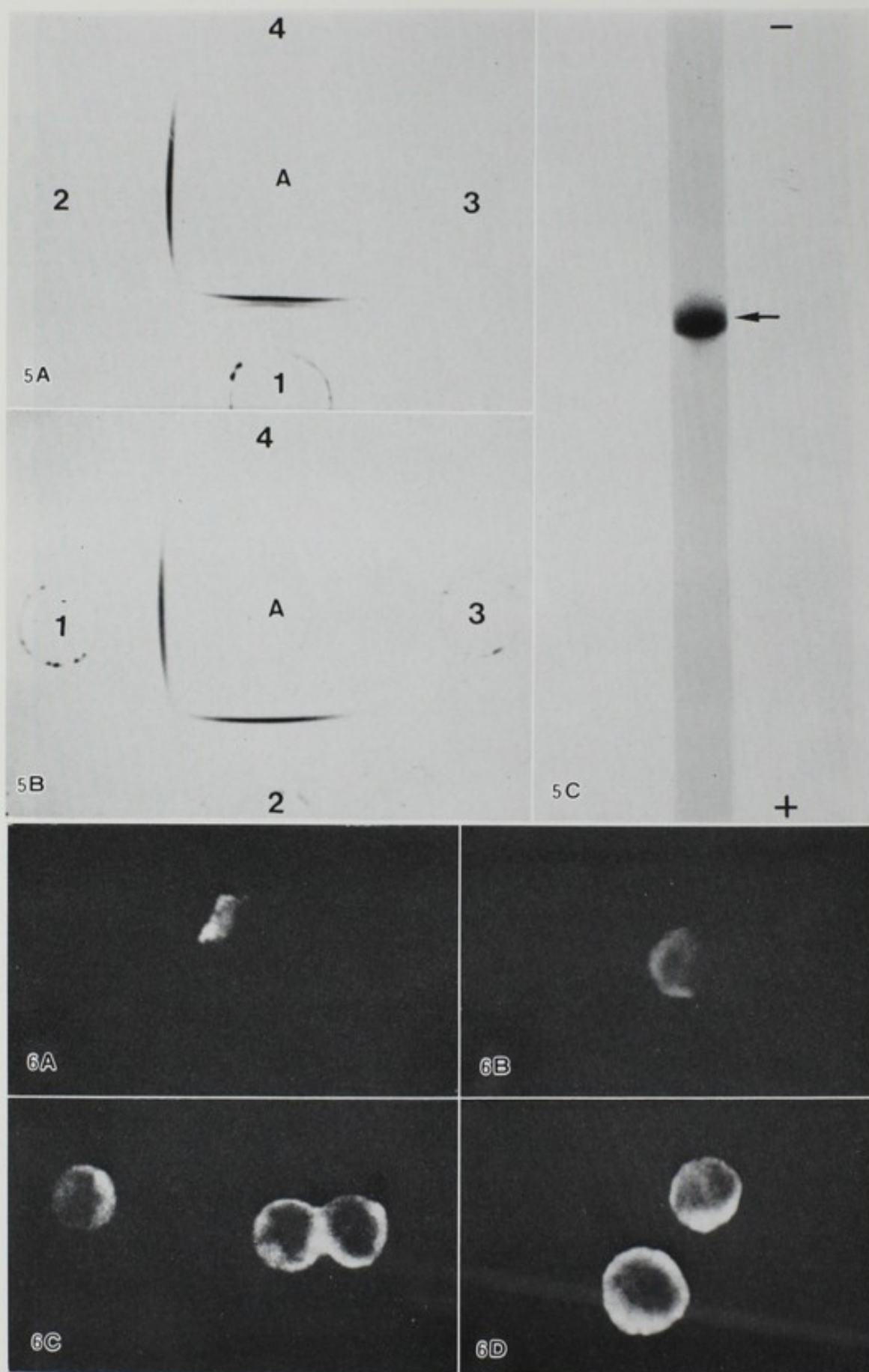
- Isolation and purification of permeability factors and their physico-chemical and biological properties. *J. Kumamoto Med. Soc.*, **44**, 298-318 (1970) (in Japanese).
37. Odashima, S. Comparative studies on the transplantability of liver cancers induced in rats fed with 3-methyl-4-dimethylaminoazobenzene for 3-6 month. *Gann*, **53**, 325-348 (1962).
 38. Odashima, S. Establishment of ascites hepatoma in the rat. *Natl. Cancer Inst. Monogr.*, **16**, 51-71 (1964).
 39. Overton, J. Experimental manipulation of desmosome formation. *J. Cell Biol.*, **56**, 636-646 (1973).
 40. Reich, E., Franklin, R. M., Shatkin, A. J., and Tatum, E. L. Effect of actinomycin D on cellular nucleic acid synthesis and virus production. *Science*, **134**, 556-557 (1961).
 41. Shimada, Y., Moscona, A. A., and Fischman, D. A. Scanning electron microscopy of cell aggregation: Cardiac and mixed retina-cardiac cell suspensions. *Dev. Biol.*, **36**, 428-446 (1974).
 42. Staehelin, L. A. Structure and function of intercellular junctions. *Int. Rev. Cytol.*, **39**, 191-283 (1974).
 43. Steck, T. L. and Wallach, D.F.H. The binding of kidney-bean phytohemagglutinin by Ehrlich ascites carcinoma. *Biochim. Biophys. Acta*, **97**, 510-522 (1965).
 44. Takeichi, M. Functional correlation between cell adhesive properties and some cell surface proteins. *J. Cell Biol.*, **75**, 464-474 (1977).
 45. Tasaki, I. and Hayashi, H. Aggregation factor from tumor cells of rat ascites hepatoma AH136B. *Proc. Jpn. Cancer Assoc.*, **28**, 154 (1969) (in Japanese).
 46. Tasaki, I. and Hayashi, H. Studies on effect of aggregation factor from rat ascites hepatoma AH136B cells. *Trans. Soc. Pathol. Japon.*, **60**, 124 (1971) (in Japanese).

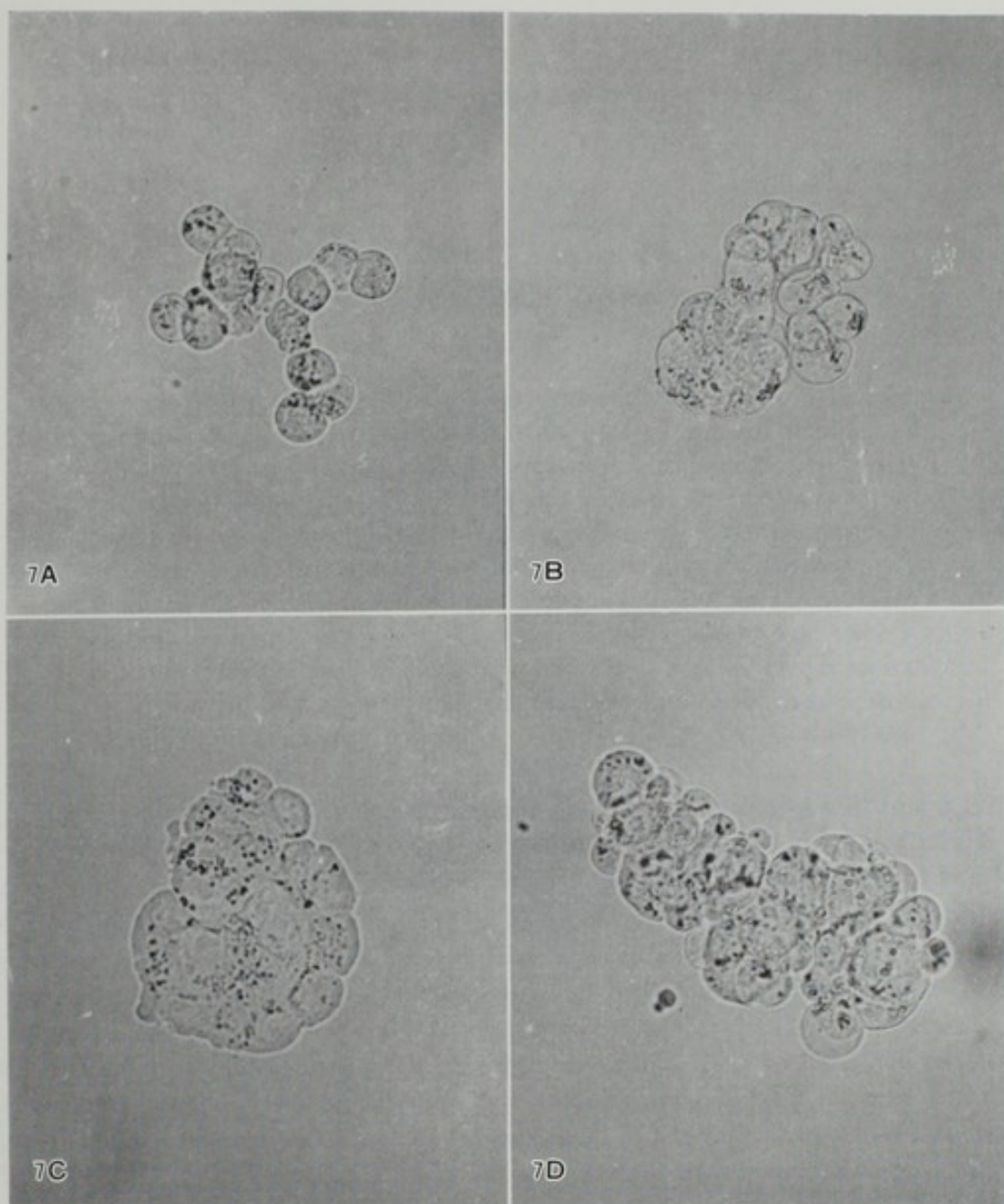
EXPLANATION OF PHOTOS

- PHOTO 1. Electron microscopic picture of rat ascites hepatoma AH136B cell island. It is round in shape and the individual cells adhere closely. T, tight junction; D, desmosome; I, intermediate junction; S, simple apposition. $\times 4,500$.
- PHOTO 2. A: Intermediate junction (indicated by arrow) observed in adherent AH109A cells after 12 hr incubation with the adhesive factor. Two outer leaflets are disposed in a parallel fashion and separated by a space of about 10 nm showing low electron density. In the cytoplasm subjacent to the inner leaflet, electron-dense materials are seen. $\times 60,000$. B: Desmosome observed in adherent AH109A cells after 12 hr incubation with the adhesive factor. Two outer leaflets are separated by a space of about 20 nm showing a central disc of electron-dense materials. Two electron-dense laminar plaques (P_1 and P_2) adjacent to the inner leaflet are found in the cytoplasm. Fibrils are seen in the cytoplasm, but they are not related to the plaques. $\times 68,000$.
- PHOTO 3. Adherent AH109A cells observed after 24 hr incubation with the adhesive factor. The adhesiveness of these cells becomes more close and characteristic. Cell surface regions showing close contact are increased. T, tight junction; D, desmosome; I, intermediate junction; S, simple apposition. $\times 4,500$.
- PHOTO 4. A: Desmosome observed in adherent AH109A cells after 24 hr incubation with the adhesive factor, which is characterized by one distinct laminar plaque (P). Many endoplasmic fibrils (indicated by arrows) are related to the plaque. $\times 68,000$. B: Tight junction observed in the same adherent cells, which is characterized by a narrow gap of less than 4 nm in distance and fusion of outer leaflets (F). $\times 80,000$.
- PHOTO 5. A: Agar immunodiffusion of cell surface-associated adhesive factor (after immunoadsorbent chromatography with rabbit anti-rat serum antibody). This factor (from tumor cells) (2) gives two precipitin lines when tested with rabbit antibody against the factor while the other factor (from tumor-bearing rat serum) (1) gives only one precipitin line, which fuses to one of the two precipitin lines demonstrated. No precipitin line is produced with the serum-associated factor (from normal and tumor-bearing rat serum) (3, 4). (1) 3 mg/ml; (2) 3 mg/ml; (3) 3 mg/ml; (4) 3 mg/ml. B: Agar immunodiffusion of purified cell surface-associated factor. This factor produces only one precipitin line, which is common to the two factors from tumor cells (1) and tumor-bearing rat serum (2) when tested with the above antibody. (1) 3 mg/ml; (2) 3 mg/ml. C: Polyacrylamide gel electrophoresis of purified cell surface-associated factor in the presence of sodium dodecyl sulfate demonstrating that this material shows a single band with a molecular weight of about 70,000.
- PHOTO 6. Demonstration of synthesized cell surface-associated adhesive factor by the indirect immunofluorescence test. A: AH136B cell at 2 hr culture exhibits patch-like fluorescence at the limited small area of the cell surface. B: AH136B cell at 6 hr culture shows bright fluorescence at the larger but limited area of the cell surface. C: AH136B cell at 12 hr culture exhibits conspicuous fluorescence, which is diffusely distributed on the whole cell surface. D: AH136B cells at 24 hr culture show similar but more conspicuous fluorescence.
- PHOTO 7. Adhesions of AH136B cells regenerating the cell surface-associated adhesive factor. A: The cells aggregate in the form of a branched chain at 3 hr culture. B: The cell aggregate becomes grape cluster-like in shape at 6 hr culture; it can be easily dissociated by pipetting. Electronmicroscopically, the cell contact consists of only simple apposition. C: The cell aggregate becomes oval in shape at 12 hr culture; it is difficult to dissociate by pipetting. D: The cell aggregate cannot be dissociated by pipetting. Electronmicroscopically, the contact of aggregated cells is characterized by the development of junctional complexes.











ISOLATION OF GROWTH INHIBITORY FACTOR FROM CELL SURFACE OF CULTURED CHICK EMBRYO FIBROBLASTS

Yoshihito YAOI and Kimiko MOTOHASHI

*Biology Division, National Cancer Center Research Institute**

Growth inhibitory activity was extracted from the cell surface of cultured chick embryo fibroblasts with urea-EDTA solution. The inhibitory activity was not destroyed by tryptic digestion. The inhibitor was metabolically labeled with ^3H -glucosamine, trypsinized and fractionated on a Sephacryl S-200 column. It was further fractionated into acidic glycopeptides and acid mucopolysaccharides, and the activity was found in the glycopeptide fraction. Improved methods for the extraction and purification of the growth inhibitory glycopeptide are described. The growth rate of cultured chick embryo fibroblasts was reduced remarkably by 100 $\mu\text{g/ml}$ of the purified factor. The possible role of the cell surface glycopeptide in density dependent inhibition of growth is discussed.

The proliferating activity of normal animal cells in monolayer cultures is regulated by cell density (11). The restriction of growth in dense cultures has attracted particular interest since malignant transformation of cells is often accompanied by the loss of density-dependent inhibition of growth. The regulation of cellular growth in culture is undoubtedly a complex phenomenon that may well involve cell-cell contact, staling of the culture medium, and accumulation of growth inhibitory substances produced by the cells. In this latter respect it is tempting to suppose that locally effective growth inhibitors might increase at the cell periphery in confluent cultures. This last assumption is based on the observations that very close apposition of cells, if not immediate contact, seems to be essential for the transmission of the inhibitory effects in confluent cultures (7, 13, 14). The role of cell surfaces in controlling cell division is also suggested by the ability of several proteolytic enzymes or serum factors to evoke a new round of DNA synthesis and cell division in density inhibited cells (2, 10). The primary site of action of the proteases or certain growth factors in serum is presumed to be at the cell surface. Cells in dense cultures would require a higher concentration of serum mitogens for their growth than in sparse cultures, possibly because of changes in cell surface architecture or accumulation of growth inhibitors on the cell membranes.

In a previous paper, we reported that a growth enhancing protein could be extracted from the cell surface of cultured chick embryo fibroblasts (CEF) with 1 M urea-5 mM EDTA solution. It has also been shown that some macromolecular growth inhibitors were contained in the crude cell surface components (8). The inhibitory activity, however, showed a high tendency to form a very large aggregate molecule so that it could hardly be separated from the other components (unpublished results).

* Tsukiji 5-1-1, Chuo-ku, Tokyo 104, Japan (矢迫義人, 本橋喜美子).

In the present study, attempts have been made to isolate a growth inhibitor from cell surface components by improving the extraction procedures, and this paper will report several unique properties of the inhibitory molecule.

Extraction of Cell Surface Material

Primary cultures of CEF were propagated in Eagle's minimum essential medium

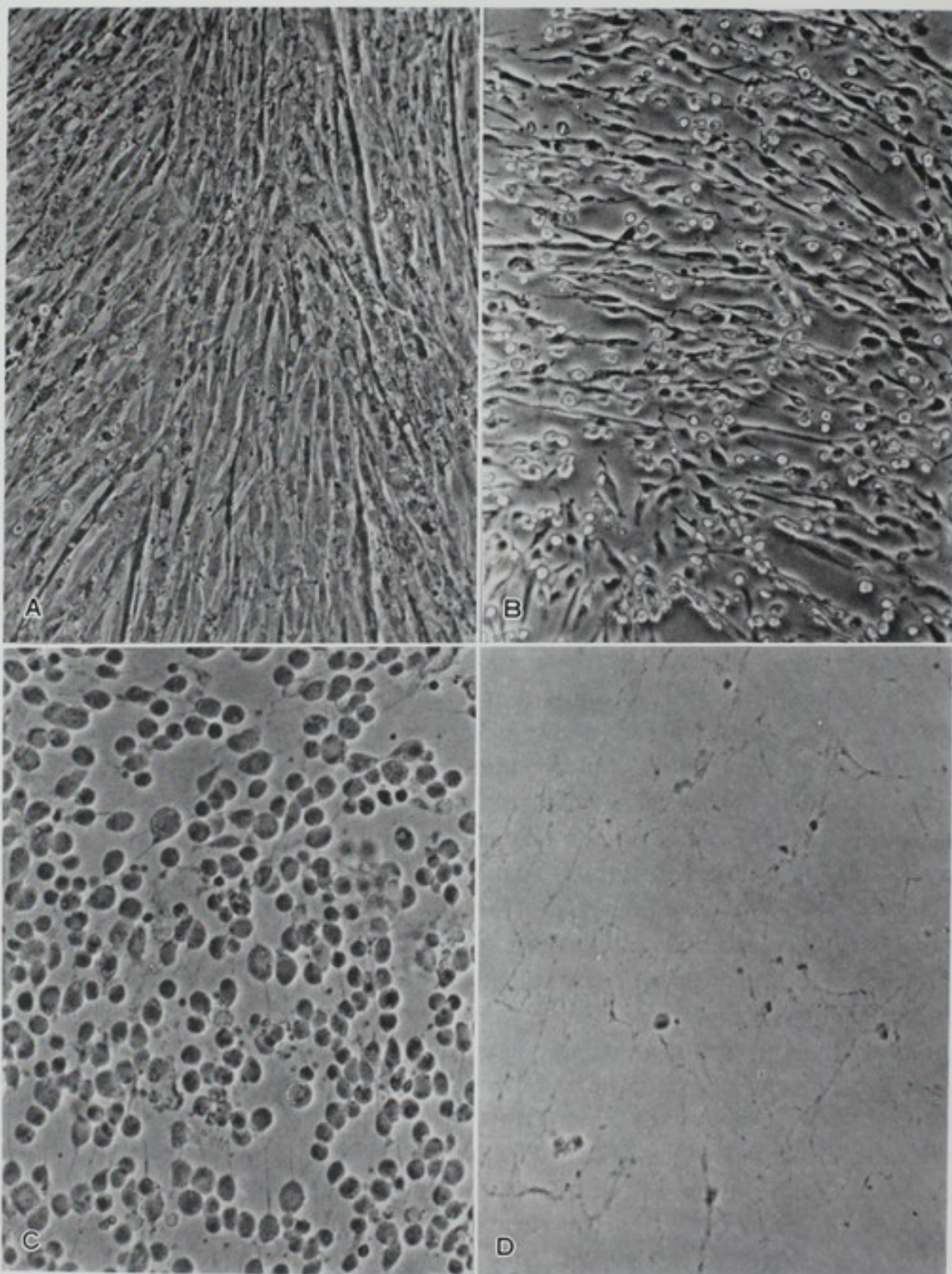


FIG. 1. Changes in cell shape during the extraction steps. A: Before treatment. B: After treatment with PBS-EDTA. C: During treatment with 1 M urea-5 mM EDTA. D: After detachment of cells. Phase-contrast microscopy.

(MEM) containing 7.5% fetal bovine serum in 174-cm² culture flasks. At a late log phase of the growth, the cells were washed twice with phosphate buffered saline (PBS) (—) and the cell surface material was extracted by the following three successive steps. At first, the cells were shaken gently in 15 ml of PBS(—) containing 5 mM EDTA at room temperature for 90 min. The cells became round, yet still remained on the flasks (Fig. 1). The supernatant solution (E1) was removed and the cells were further treated with 15 ml of PBS(—) containing 1 M urea and 5 mM EDTA at room temperature for 2 hr to obtain the second extract (E2). Although most cells were detached from the flasks by mild pipetting without any destruction of the cells (8), some fibrous structures were still observed on the bottom of the flasks after the detachment of cells (Fig. 1). They were finally dissolved with 6 M urea-10 mM EDTA (E3). All extracts were centrifuged to remove cells and debris, concentrated on collodion membranes and dialyzed against PBS(—). The protein contents of E1, E2, and E3 were 0.12, 1.66, and 0.20 mg from a flask, respectively.

Aliquots of these extracts were added to the cultures of CEF and the effects on the growth rate were examined. As shown in Table I, E1 and E2 enhanced the growth, probably owing to the growth-promoting factor as reported previously (8). On the other hand, E3 exerted an inhibitory effect on cellular growth, indicating that the last fraction was most enriched in the inhibitory substances. Although the yields of E3 were low, at first we have chosen fraction E3 as the starting material for the purification of the growth inhibitory activity.

Table I also shows that the inhibitory activity of E3 was not destroyed by digestion with trypsin (5 μ g/ml, 37°, 1 hr). On the other hand, all coomassie blue-positive bands, which were detected by SDS polyacrylamide gel electrophoresis of the undigested E3,

TABLE I. Effects of Cell Surface Substances on the Growth Rate of CEF

Dose of extract (μ g protein/ml)	Cell No. $\times 10^{-4}/\text{cm}^2$	% of control
Control	4.84 \pm 0.01	100
E1 3	4.96 \pm 0.23	102
6	5.06 \pm 0.03	105
12	5.95 \pm 0.62	123
E2 6	4.89 \pm 0.11	101
12	4.48 \pm 0.10	89
24	4.50 \pm 0.27	90
48	5.50 \pm 0.21	110
E3 5	4.23 \pm 0.36	87
10	4.28 \pm 0.05	88
20	3.68 \pm 0.03	74
40	3.16 \pm 0.14	65
E3 40, trypsinized	3.19 \pm 0.15	66
Trypsin control	4.82 \pm 0.04	99

CEF were seeded at 2×10^3 cells/cm² in plastic plates, and the cell numbers were determined after 5 days with the aid of a Coulter Counter. The protein content of each sample was determined by the method of Lowry *et al.* (9). Tryptic digestion of E3 was performed with 5 μ g/ml enzyme at 37° for 2 hr, and the dose was represented by the protein content before digestion. Mean values of duplicate experiments are presented.

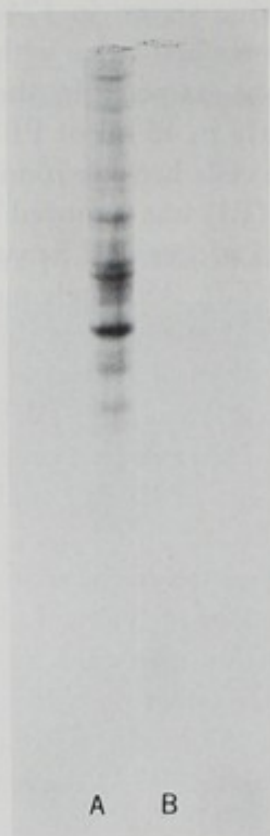


FIG. 2. SDS polyacrylamide electrophoresis of fraction E3 before (A) and after (B) tryptic digestion. The same amount of sample was loaded on each gel.

disappeared after tryptic digestion (Fig. 2). Further purification of the inhibitory factor was therefore carried out after tryptic digestion of E3.

Purification of Inhibitor

Primary cultures of CEF were labeled with ^3H -glucosamine throughout the cultivation period for 3 days, and the inhibitory fraction E3 was extracted as described above. The extract was digested with trypsin and then fractionated on a Sephacryl S-200 column (Pharmacia). As shown in Fig. 3, the inhibitory activity was eluted at the void volume position, coincident with the major peak of radioactivity and separated from the residual proteins. The inhibitory fraction showed no ultraviolet adsorption.

Since the inhibitory fraction seemed to contain mainly polysaccharides, it was examined by cellulose acetate electrophoresis in 0.15 M pyridine-formate buffer (pH 3.0, 1.5 mA/cm, 75 min). As shown in Fig. 4, several spots of acid mucopolysaccharides, including hyaluronic acid, chondroitin sulfate A, chondroitin sulfate B and/or heparan sulfate, were detected either by toluidine blue staining or by radioactivity. A major radioactive spot (designated as X in Fig. 4), however, did not agree with any known acid mucopolysaccharides; it was not stained with toluidine blue and migrated more slowly than hyaluronic acid.

Three volumes of ethanol were added and the fraction was kept at 2° overnight. The precipitate was collected by centrifugation, washed with 75% ethanol and dried. The supernatant was concentrated in a rotary evaporator and lyophilized. All mucopoly-

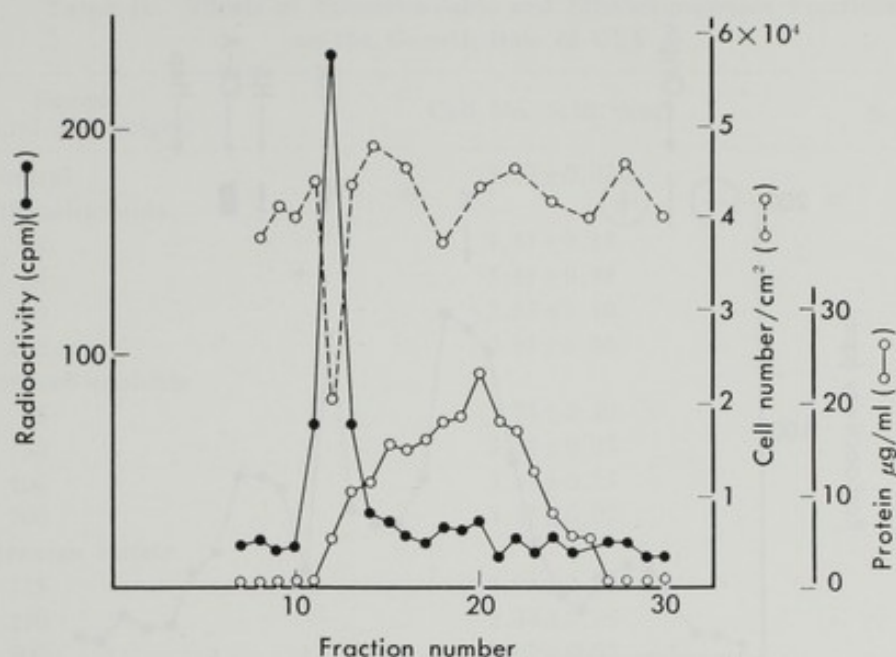


FIG. 3. Fractionation of the inhibitory factor on a Sephacryl S-200 column. Primary cultures of CEF were labeled with $0.025 \mu\text{Ci/ml}$ D-glucosamine-6- ^3H (20 Ci/mmol , Radiochemical Centre) for 3 days, and 6 M urea- 10 mM EDTA extract (E3) was prepared as described in the text. The extract from 30 culture flasks was digested with $5 \mu\text{g/ml}$ trypsin (Merck) at 37° for 1 hr, and fractionated on a Sephacryl S-200 column ($1.5 \times 40 \text{ cm}$) using PBS(—) as an elution buffer. An aliquot of 0.2 ml from each tube was subjected to assay for the growth-inhibitory activity as described in Table I. Radioactivity was determined in a liquid scintillation counter using Bray's solution (1).

saccharides, corresponding to about 50% of the total radioactivity in the fraction, were precipitated while component X remained completely soluble in 75% ethanol (Fig. 5A, B). Component X could thus be separated from other acid mucopolysaccharides. It did not migrate significantly upon electrophoresis in 0.1 M barium acetate buffer ($\text{pH } 7.1$, 1.5 mA/cm , 3 hr), probably because its acidic charge was neutralized by barium ions (Fig. 5C). Such electrophoretic behavior would be expected if the acidic charge of component X is due to sialic acid.

Table II shows the effects of 75% ethanol-soluble and -insoluble fractions on the growth rate of CEF. These results show that the soluble fraction, component X, was inhibitory to cellular growth at $200 \mu\text{g/ml}$, while the insoluble fraction, a mixture of known acid mucopolysaccharides, was not at similar concentrations.

Sulfated mucopolysaccharides have been sometimes suspected to be the probable growth inhibitors in the density-dependent inhibition of growth, since heparin (4), dextran sulfate (3, 4, 6) or sulfated agar (12) were shown to be potent inhibitors of cell proliferation. Cultured CEF, however, did not produce any heparin as revealed by electrophoresis. Among other mucopolysaccharides tested (chondroitin sulfate A, B, C, hyaluronic acid, and heparan sulfate), only heparan sulfate was somewhat inhibitory to cell growth, but its inhibitory activity was far less than component X (Table II). Other mucopolysaccharides somewhat enhanced growth at low concentrations but showed no growth-inhibitory activity at higher concentrations (results not shown).

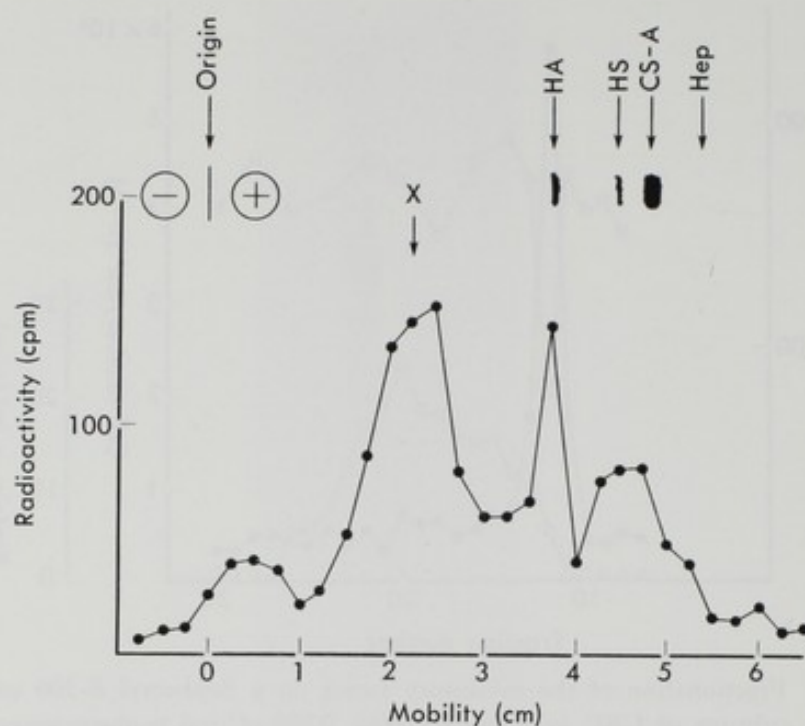


FIG. 4. Cellulose acetate electrophoresis of the inhibitory fraction in 0.15 M pyridine-formate buffer (pH 3.0, 1.5 mA/cm, 75 min) (5). After a cellulose acetate film was stained with 0.5% toluidine blue, it was cut into 0.25 cm pieces for determination of radioactivity in a liquid scintillation counter. Arrows indicate the positions of standard acid mucopolysaccharides, hyaluronic acid (HA), heparan sulfate (HS), chondroitin sulfate A (CS-A), and heparin (Hep).

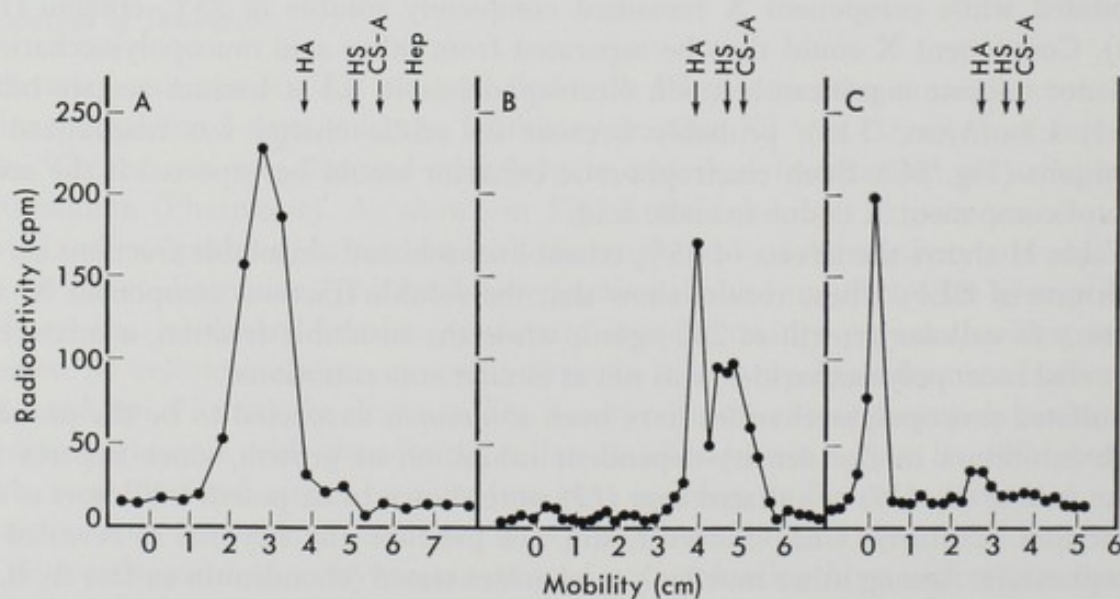


FIG. 5. Cellulose acetate electrophoresis of 75% ethanol-soluble (A, C) and-insoluble (B) fractions. Electrophoresis was performed in (A, B) pyridine-formate buffer as described in Fig. 2 or in (C) 0.1 M barium acetate (pH 7.1, 1.5 mA/cm, 3 hr) (15).

TABLE II. Effects of Ethanol-soluble and Ethanol-insoluble Fractions on the Growth Rate of CEF

Sample ($\mu\text{g/ml}$ dry weight)	Cell No. $\times 10^{-4}/\text{cm}^2$	% of control
Control	3.37 ± 0.07	100
Ethanol-soluble		
25	3.57 ± 0.15	106
50	3.17 ± 0.98	94
100	2.55 ± 0.10	76
200	0.91 ± 0.06	27
Ethanol-insoluble		
25	3.71 ± 0.20	110
50	3.64 ± 0.05	108
100	3.67 ± 0.25	109
200	3.47 ± 0.07	103
Heparan sulfate		
125	3.05 ± 0.06	91
250	2.48 ± 0.28	74
500	2.07 ± 0.02	61

Growth rate of CEF was determined as described in Table I. Effects of standard heparan sulfate (Seikagaku Kogyo, Tokyo) are also presented. Mean values of duplicate experiments are shown.

Component X, rather than the acid mucopolysaccharides, was therefore concluded to be the main growth inhibitor in this instance.

The following procedures were employed to obtain higher yields of the inhibitor. Confluent monolayer cultures of CEF, usually after cultivation for 4 days, were washed twice with PBS(−) and then treated with 0.05% trypsin-0.02% EDTA in PBS(−)

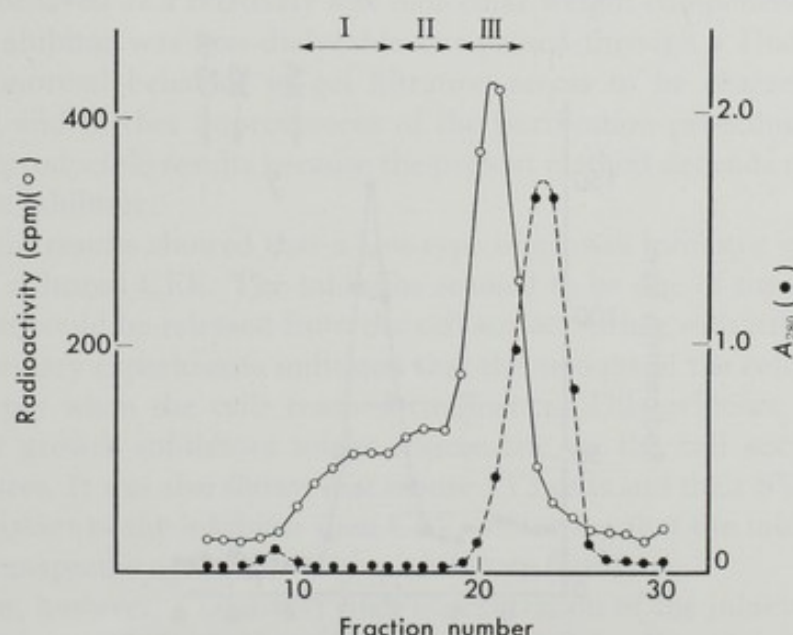


FIG. 6. Fractionation of inhibitor on a Sephacryl S-200 column. Trypsin-EDTA extract from 15 culture flasks (labeled with ^3H -glucosamine) was dissolved in 0.3 ml of 0.1 N acetic acid and loaded on a column of 1.5×40 cm. Elution was carried out with distilled water. Three fractions (I, II, and III) were collected separately and lyophilized.

TABLE III. Growth Inhibitory Effects of Sephacryl-fractionated Preparations

Dose ($\mu\text{g/ml}$ dry weight)	Cell No. $\times 10^{-4}/\text{cm}^2$	% of control
Control	10.56 ± 0.12	100
I 25	9.21 ± 0.10	87.2
50	4.87 ± 0.19	46.1
100	2.78 ± 0.18	26.4
II 50	8.01 ± 0.35	76.5
100	6.22 ± 0.08	58.9
III 50	10.24 ± 0.59	97.0
100	9.61 ± 0.22	91.1

Growth rate of CEF was determined as described in Table I.

at 37° for 15 min. After the dispersed cells were removed by centrifugation, the supernatant was further incubated with 1 mg/ml of the freshly added enzyme at 37° for 2 to 3 hr. The enzyme and residual proteins were removed by 5% trichloroacetic acid. The supernatant was neutralized and concentrated with a Diaflo UM-2 membrane. Acid mucopolysaccharides were removed by precipitation with three volumes of ethanol in the presence of 5% sodium acetate, and the supernatant was concentrated in a rotary evaporator. The solution was dialyzed against distilled water, lyophilized and dissolved in a small amount of 0.1 N acetic acid. It was loaded on a Sephacryl S-200 column and eluted with distilled water. The three fractions (I, II, and III in Fig. 6) were collected separately and lyophilized.

Table III shows the effects of these three fractions on the growth rate of CEF. Fraction I exhibited the highest inhibitory activity. The growth rate was significantly

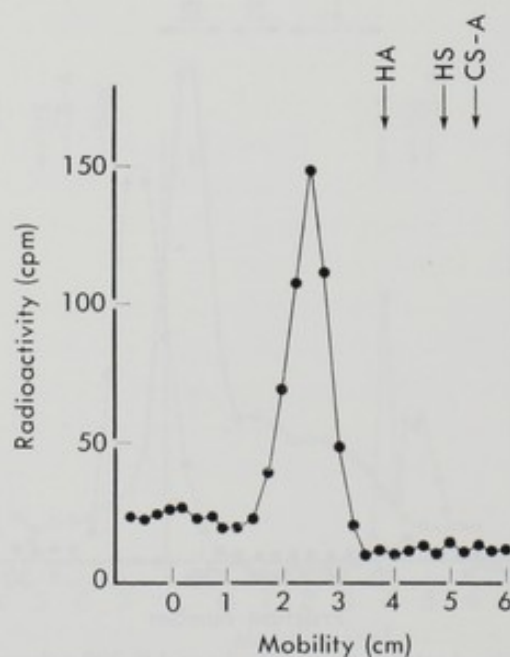


FIG. 7. Cellulose acetate electrophoresis of the purified inhibitor. The inhibitor (Fraction I in Fig. 4) was examined by electrophoresis in 0.15 M pyridine-formate buffer as described in Fig. 2.

reduced at 100 $\mu\text{g/ml}$. Neither cellular viability nor adhesiveness was affected under the experimental conditions. The inhibitor isolated here gave a sharp band on cellulose acetate electrophoresis (Fig. 7), as compared with the somewhat broad one of component X which had been obtained by the previous methods (Fig. 5). These results indicated that higher purification could be achieved by the later method. About 0.5 mg of the purified inhibitor was obtained from fifteen 174-cm² culture flasks. Lyophilized material was readily soluble in distilled water but insoluble in absolute ethanol or ether.

Inhibitory Properties

The isolated inhibitor was apparently an acidic glycopeptide generated by tryptic digestion of a certain cell surface glycoprotein, and it was readily distinguished from acid mucopolysaccharides by its solubility in 75% ethanol, electrophoretic mobility and staining with toluidine blue. The inhibitory activity might most likely be due to the sugar moiety of the glycopeptide. The protein moiety, however, might also play a part in the structural organization of the inhibitor molecule at the cell periphery, since the intact inhibitor was relatively insoluble as described in the extraction procedures, while the trypsin-isolated glycopeptide was highly soluble in water. Although the nature of the intact glycoprotein is still unknown, isolation of the intact inhibitor molecule, without any degradation of protein moiety, would be especially important to elucidate the physiological functions of the inhibitory factor.

Patterns of gel filtration of the inhibitor were influenced remarkably by the elution conditions, especially by the pH of the sample and elution buffers. The present results (Figs. 3 and 6) therefore do not allow a true estimate of the molecular weight of this compound. When the inhibitor was eluted from a Sephadex G-50 column with 0.01 N acetic acid, it behaved as a relatively low molecular weight component, about 6 to 8 K daltons. The inhibitor was non-dialyzable but passed through a Diaflo PM-10 membrane. The abnormal behavior in gel filtration seems to be characteristic of acidic carbohydrates, and further improvement of the purification procedures is required to obtain more reproducible results because the present method depends on such abnormal behavior of the inhibitor.

The present results showed that a new type of growth inhibitor was present at the cell surface of cultured CEF. The inhibitor seemed to be one of the pericellular components since it could be released from the cell surface either with urea-EDTA or with trypsin. Preliminary experiments indicated that the amount of the cell surface inhibitor increased sharply when the cells reached confluence. This evidence supports the assumption that growth inhibitors might accumulate on the cell surfaces in density-inhibited cultures. It was also shown that mouse 3T3 cells and their SV40 transformants were more resistant to the inhibitor than CEF, indicating that the inhibitory effect was not due to a nonspecific cytotoxicity of the inhibitory factor.

At present, however, a relatively high concentration of the inhibitor is required to obtain sufficient growth inhibition. The amount of the cell surface inhibitor in confluent cultures is assumed to be about 1.2 to 2.0 $\mu\text{g/ml}$, while about 100 $\mu\text{g/ml}$ of the purified inhibitor is required for the inhibition. In order to establish the physiological significance of the growth inhibitory glycopeptide, we have to eliminate more carefully

the possibility that the growth inhibition might be due to some contaminants present in low concentration. To this end, rigorous purification and chemical studies of the glycopeptide are in progress.

In spite of these reservations, the present results attract our particular interest since a great deal of recent evidence indicates drastic changes in the cell surface glycoproteins which are accompanied by cellular growth or malignant transformations. The inhibitory glycopeptide, therefore, seems to be one of the most probable growth regulators which might be related to the density-dependent inhibition of growth. Mitogenic activities of several proteolytic enzymes may be explained in part by the removal of the growth inhibitory glycopeptides from the cell surface of density-inhibited cultures.

On the other hand, Whittenberger and Graser (16) have reported that the DNA synthesis of mouse 3T3 cells was inhibited by addition of the plasma membrane fraction isolated from 3T3 cells, but not by that from SV40-transformed 3T3 cells. More recently Whittenberger *et al.* (17) have shown that the detergent-solubilized membrane fraction was also inhibitory to DNA synthesis. Their inhibitor(s) seems to be an intrinsic component of the cell membrane rather than the peripheral component of cells, and differs from our inhibitor in its chemical properties. The relationships between these two inhibitory principles are not yet clear.

REFERENCES

1. Bray, G. A. A simple efficient liquid scintillator for counting aqueous solution in a liquid scintillation counter. *Anal. Biochem.*, **1**, 279-285 (1960).
2. Burger, M. M. Proteolytic enzymes initiating cell division and escape from contact inhibition of growth. *Nature*, **227**, 170-171 (1970).
3. Clarke, G. D., Shearer, M., and Ryan, P. J. Association of polyanion resistance with tumorigenicity and other properties in BHK/21 cells. *Nature*, **252**, 501-503 (1974).
4. Clarke, G. D. and Stoker, M.G.P. Conditions affecting the response of cultured cells to the serum. In "Growth Control in Cell Cultures," ed. G.E.W. Woltenholme and J. Knight, pp. 17-32 (1971). Churchill Livingstone, Edinburgh and London.
5. Fransson, L.-A. and Rodén, L. Structure of dermatan sulfate. I. Degradation by testicular hyaluronidase. *J. Biol. Chem.*, **242**, 4161-4169 (1967).
6. Goto, M., Kataoka, Y., Kimura, T., Goto, K., and Sato, H. Decrease of saturation density of cells of hamstar cell lines after treatment with dextran sulfate. *Exp. Cell Res.*, **82**, 367-374 (1973).
7. Gurney, T. Local stimulation of growth in primary cultures of chick embryo fibroblasts. *Proc. Natl. Acad. Sci. U.S.A.*, **62**, 906-911 (1969).
8. Igarashi, Y. and Yaoi, Y. Growth-enhancing protein obtained from cell surface of cultured fibroblasts. *Nature*, **254**, 248-250 (1975).
9. Lowry, O. H., Rosebrough, N. J., Farr, A. L., and Randall, R. J. Protein measurement with the folin phenol reagent. *J. Biol. Chem.*, **193**, 265-275 (1951).
10. Sefton, B. N. and Rubin, H. Release from density dependent growth inhibition by proteolytic enzymes. *Nature*, **227**, 843-845 (1970).
11. Stoker, M.G.P. and Rubin, H. Density dependent inhibition of cell growth in culture. *Nature*, **215**, 171-172 (1967).
12. Temin, H. M. Studies on carcinogenesis by avian sarcoma viruses. III. The differential effect of serum and polyanions on multiplication of uninfected and converted cells. *J. Natl. Cancer Inst.*, **37**, 167-175 (1966).

13. Todaro, G., Matsuya, Y., Bloom, S., Robbins, A., and Green, H. Stimulation of RNA synthesis and cell division in resting cells by a factor present in serum. In "Growth Regulatory Substances for Animal Cells in Culture," ed. V. Defendi and M. Stoker, pp. 87-101 (1967). Wister Institute Press, Philadelphia.
14. Weiss, R. A. The influence of normal cells on the proliferation of tumor cells in culture. *Exp. Cell Res.*, **63**, 1-18 (1970).
15. Wessler, E. Analytical and preparative separation of acidic glycosaminoglycans by electrophoresis in barium acetate. *Anal. Biochem.*, **26**, 439-444 (1968).
16. Whittenberger, B. and Glaser, L. Inhibition of DNA synthesis in cultures of 3T3 cells by isolated surface membranes. *Proc. Natl. Acad. Sci. U.S.*, **74**, 2251-2255 (1978).
17. Whittenberger, B., Raben, D., Lieberman, M. A., and Glaser, L. Inhibition of growth of 3T3 cells by extract of surface membranes. *Proc. Natl. Acad. Sci. U.S.*, **75**, 5457-5461 (1978).

CHANGE IN SURFACE MUCOPOLYSACCHARIDES DURING THE DIFFERENTIATION AND TRANSFORMATION OF BLOOD CELLS

Chikako SATO,^{*1} Kiyohide KOJIMA,^{*2} Takahiko MIYAZAWA,^{*1}
Kimiko NISHIZAWA,^{*1} Minoru OKAYAMA,^{*3} and Kayoko OGURI^{*3}

*Laboratory of Experimental Radiology, Aichi Cancer Center Institute,^{*1}*

*Department of Oncological Pathology, Nara Medical University,^{*2}*

*and Blood Disease Center, Nagoya National Hospital^{*3}*

In two experimental systems, changes in the organization and biosynthesis of cell surface acidic sugars were detected by means of cell electrophoresis and chemical analysis of labeled glycosaminoglycans. During a very early stage of erythroid differentiation of Friend leukemic cells by dimethyl sulfoxide (DMSO), the cell electrophoretic mobility decreased in highly-inducible clones but not in noninducible clones. When the cells were treated with DMSO for longer than 20 hr, the mobility reduction became irreversible and hemoglobin synthesis was induced. The mobility decrease was attributed to the shedding of macromolecules from the cell surface, major molecules of which were identified as heparan sulfate. Matured erythrocytes neither contained nor synthesized heparan sulfate.

In the system of phytohemagglutinin (PHA)-induced blast formation of human T-lymphocytes, an early translocation of hyaluronic acid to the cell periphery within 15 min of PHA addition and later activated biosynthesis of chondroitin sulfate C were detected. Several agents which block blast formation also blocked the translocation of hyaluronic acid at the same concentrations. The presence of chondroitin sulfate in the cell periphery was also detected electrophoretically in T-cell type leukemia cells (MOLT-4B).

The presence of these glycosaminoglycans at the surface of immature or leukemic cells and the loss of them with blood cell differentiation suggest their role in maintaining cell proliferation.

Glycosaminoglycans of extracellular matrix have been long investigated. Its study as a cell surface component, however, has a history of less than ten years. Changes in the composition and the biosynthesis of glycosaminoglycans during the differentiation and the transformation of chondrocytes (15, 26) have been well investigated. Recently the association of hyaluronate with the surface of several types of cultured cells and modulation of the levels and distribution of this polysaccharide under different physiological conditions have been reported. We indicated the dislocation of hyaluronate in

^{*1} Kanokoden 81-1159, Tashiro-cho, Chikusa-ku, Nagoya 464, Japan (佐藤周子, 宮沢宇彦, 西沢きみ子).

^{*2} Shijo-cho, Kashihara 634, Japan (小島清秀).

^{*3} San-nomaru 4, Naka-ku, Nagoya 460, Japan (岡山 実, 小栗佳代子).

the cell surface after X-irradiation and its recovery by added ATP (20). In general transformed fibroblasts produce significantly more hyaluronic acid than their parent counterparts (8). The involvement of hyaluronic acid in cell-to-cell adhesion (28) and in attachment to substratum (2) suggested its role in cellular migration and developmental morphogenesis. Enhanced biosynthesis of hyaluronic acid at the early S phase was proposed as signal for the initiation of DNA synthesis (25). Heparan sulfate seems to be also a general cellular constituent rather than a differentiated cell product (11). Cell-cycle-dependent desquamation of heparan sulfate from the cell surface was indicated (12). Little is known, however, on the glycosaminoglycans of hemopoietic cells.

We employed two experimental systems to study the role of glycosaminoglycans in the differentiation of blood cells. That is, erythroid differentiation of Friend leukemia cells by dimethyl sulfoxide (DMSO) *in vitro* (4), and the blastformation of human T-lymphocytes by phytohemagglutinin (PHA). These two systems have some advantages for analysis as follows: 1) Differentiation and dedifferentiation can be reversibly controlled by the duration and concentration of inducing agents; 2) the existence of easily detectable markers of differentiation such as hemoglobin or cell size or stop of proliferation; and 3) the existence of several cloned cells which have different inducibility. Our strategy was first to survey the presence and organization of glycosaminoglycans on the cell surface by means of cell electrophoresis combined with specific enzymes and various ionic strengths, and next to confirm the results by the chemical analysis of labeled glycosaminoglycans from the point of molecular species and the rate of their biosynthesis.

Decrease in Electrophoretic Mobility (EPM)

Figure 1 shows the change in the EPM with the time of incubation with 1.5% DMSO. In C-10-6 and TSFAT-3 cells (7), it decreased evidently within 15 min of

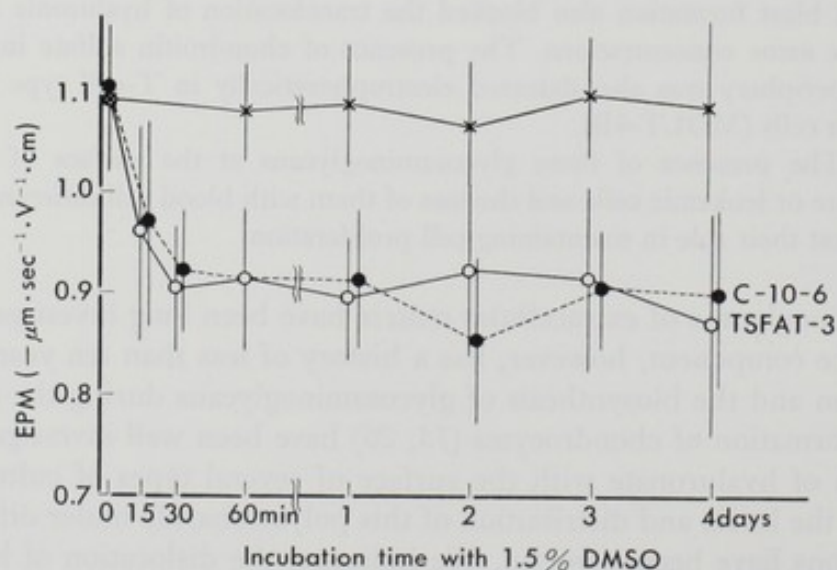


FIG. 1. Change in the electrophoretic mobility ($-\mu\text{m}\cdot\text{sec}^{-1}\cdot\text{V}^{-1}\cdot\text{cm}$) with time of incubation with 1.5% DMSO in noninducible cell line C-9-9 (x), highly inducible cell line C-10-6 (●) and cell line TSFAT-3 (○). Vertical line is S.D. for 30 measurements.

treatment and reached a minimum in 30 min. The reduced EPM continued for 4 days of incubation with DMSO. In C-9-9 cells, however, the EPM remained unchanged for 4 days. The difference between the EPM of control and DMSO-treated cells was significant ($p < 0.05$) in C-10-6 and TSFAT-3 cells but not in C-9-9 cells. The fractions of benzidine-positive cells which had synthesized hemoglobin on Day 5 were: C-10-6 cells, 62%; TSFAT-3 cells, 57%; and C-9-9 cells 1.9%. These results indicate that EPM reduction took place only in differentiation inducible clones (18).

To determine which acidic sugars are responsible for the EPM in each cell line, EPM measurement was carried out after the removal of sugars by their specific enzymes. Digestion with neuraminidase to remove sialic acid resulted in about a 60% reduction in the EPM in every three cell lines, irrespective of DMSO treatment. Digestion with chondroitinase-ABC caused no change in all three kinds of cells, with or without DMSO treatment. These results suggest that sialic acid is the major cell surface component responsible for the EPM, and chondroitin sulfate A, B, and C are not in the three cell lines. This situation was not affected by DMSO. On the other hand, digestion with hyaluronidase, heparitinase or heparanase caused a significant EPM reduction in untreated C-10-6 cells and TSFAT-3 cells. These three enzymes, however, had no effects on the EPM of the two inducible cells treated with DMSO for 2 days. The results in C-10-6 cells are shown in Fig. 2. In noninducible C-9-9 cells, hyaluronidase had no effects on the untreated cells but caused EPM reduction in

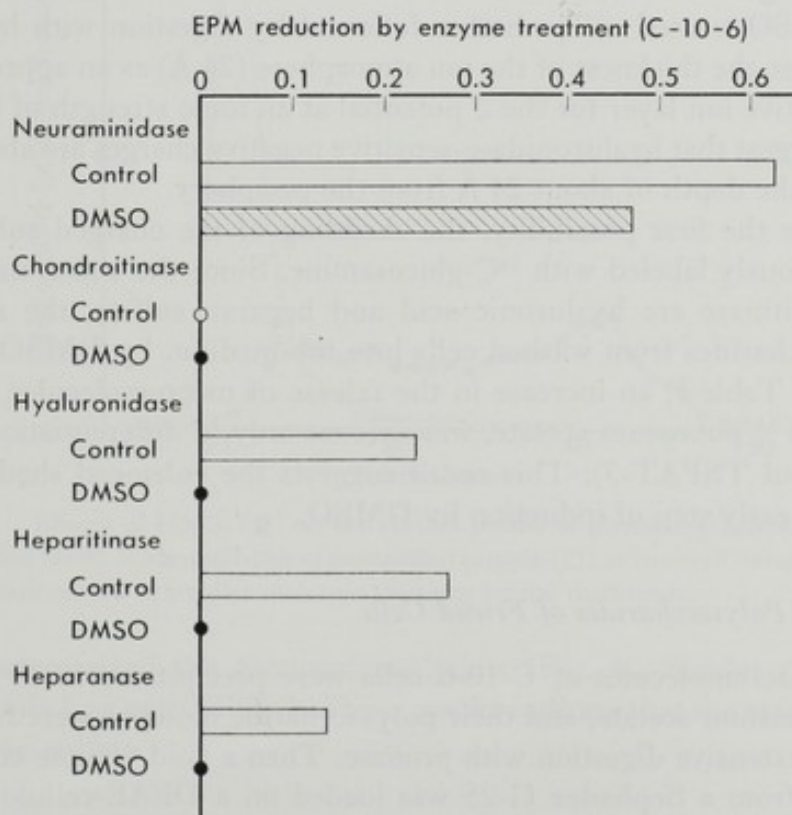


FIG. 2. Decrease in the electrophoretic mobility ($-\mu\text{m}\cdot\text{sec}^{-1}\cdot\text{V}^{-1}\cdot\text{cm}$) by digestion with specific enzymes in control and DMSO-treated C-10-6 cells. The length of the column represents the relative amount of each acidic sugar at the peripheral zone of 0-7.5 Å.

TABLE I. Release of ^{14}C -labeled Macromolecules of the Cell to Phosphate-buffered Saline (PBS) during Incubation with or without DMSO for 30 Min at 4°

Cell line	PBS (cpm)	1.5% DMSO in PBS (cpm)	% increase
C-9-9	12,248	13,096	6.5
C-10-6	10,958	13,772	20.4
TSFAT-3	6,368	8,124	21.6

Cells were preincubated with ^{14}C -glucosamine for 16 hr at 37° and washed before treatment with DMSO.

DMSO-treated cells. Heparitinase and heparanase caused a similar decrease in the EPM in C-9-9 cells, irrespective of DMSO treatment.

From these results, two explanations are possible for the EPM reduction by DMSO in differentiation-inducible clones. One is the loss of hyaluronidase-, heparitinase-, and heparanase-sensitive negatively charged substance from the cell surface by the treatment with DMSO, and the other is the dislocation of these negative charges from the periphery into a deeper layer so as not to contribute to the EPM. To examine the latter possibility, mobility was measured using a buffer solution of lower ionic strength, down to 0.0167, which allows the negative charges of the deeper layer to contribute to the EPM. The EPM of cells treated with DMSO for 30 min was significantly lower ($p < 0.05$) than that of nontreated cells by a similar magnitude at every ionic strength. Hyaluronidase-digested cells without DMSO treatment showed an EPM similar to that of the DMSO-treated cells whether followed by digestion with hyaluronidase or not. When we use the thickness of the ion atmosphere (24 \AA) as an approximate estimation of the effective ion layer for the ζ potential at an ionic strength of 0.0167 (20, 21), these results suggest that hyaluronidase-sensitive negative charges are absent in DMSO-treated cells to the depth of about 24 \AA from the periphery.

To examine the first possibility, the shedding of the charged substance, C-10-6 cells were previously labeled with ^{14}C -glucosamine. Since the substrates of hyaluronidase and heparitinase are hyaluronic acid and heparan sulfate, the release of these labeled polysaccharides from washed cells into the medium by DMSO was examined. As indicated in Table I, an increase in the release of macromolecules, precipitated in 70% ethanol + 1% potassium acetate, was evident only in differentiation-inducible cell lines (C-10-6 and TSFAT-3). This result suggests the enhanced shedding of macromolecules is an early step of induction by DMSO.

Identification of Polysaccharides of Friend Cells

Labeled macromolecules of C-10-6 cells were precipitated in 70% ethanol containing 1% potassium acetate, and their polysaccharide moieties were freed by alkaline treatment and extensive digestion with pronase. Then a void volume containing glycosaminoglycans from a Sephadex G-25 was loaded on a DEAE-cellulose column, and eluted with 20 mM to 1 M NaCl in 20 mM Tris-HCl pH 7.29. As shown in Fig. 3, radioactivity due to glycosaminoglycans was detected in the eluate between 0.25 to 0.5 M NaCl. These fractions were combined and treated with nitrous acid or heparitinase. Gel filtration of the digested sample on a Sephadex G-50 revealed that both

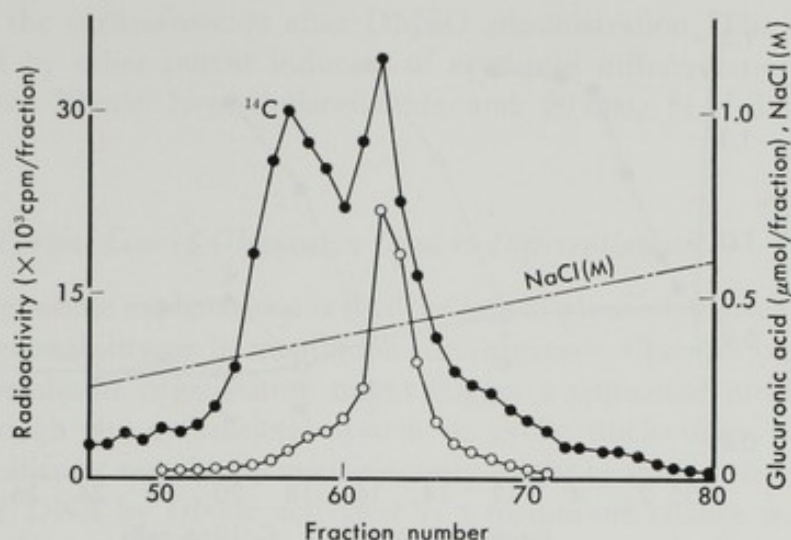


FIG. 3. Elution profile of macromolecular fraction with increasing concentration of NaCl in 20 mM Tris-HCl, pH 7.29, from DEAE cellulose column. ● radioactivity of glycosaminoglycans; ○ amount of glucuronic acid. The scale for the concentration of NaCl (M) is the same as the one for glucuronic acid.

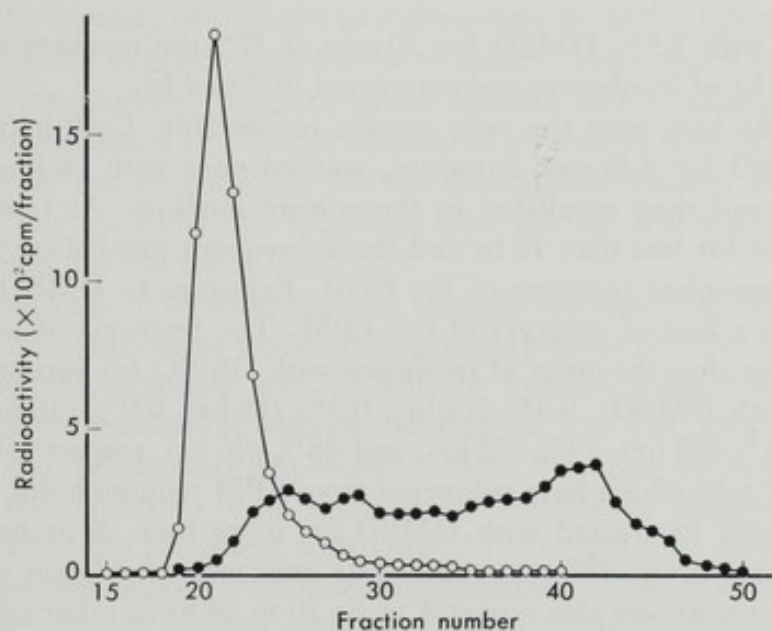


FIG. 4. Effects of HNO_2 (●) on the elution profile of glycosaminoglycans from Sephadex G-50. Radioactivities of nontreated sample (○) at the void volume fractions were moved to smaller molecule fractions by the treatments.

treatments depolymerized the glycosaminoglycans (Fig. 4). Similar results were obtained after the labeling with $^{35}\text{SO}_4^{-2}$. These results indicate that the major glycosaminoglycan is heparan sulfate.

Recovery of EPM and Stop of Differentiation

The DMSO-treated C-10-6 cells were washed once with Dulbecco's phosphate-buffered saline, and then incubated in a fresh culture medium (F12+10% calf serum).

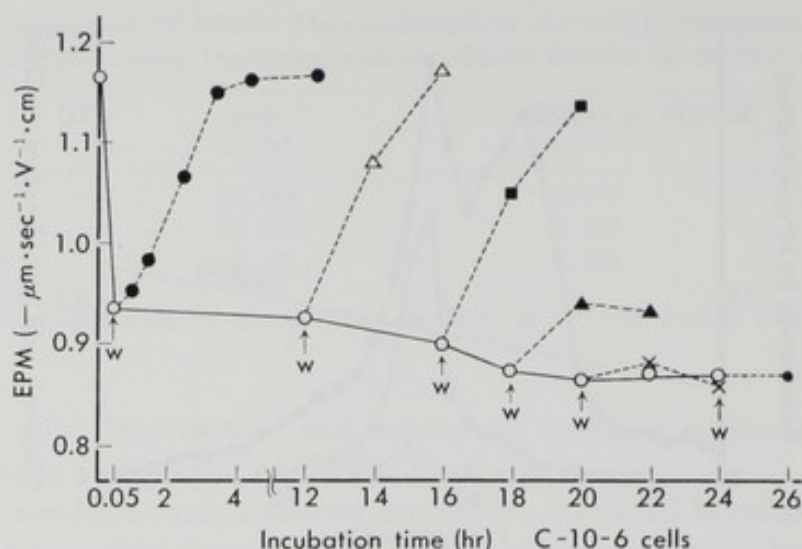


FIG. 5. Change in the electrophoretic mobility of C-10-6 cells with time of treatment with 1.5% DMSO (○) and its recovery after washing out DMSO at 30 min (●), 12 hr (△), 16 hr (■), 18 hr (▲), 20 hr (×), and 24 hr (•), respectively.

After treatment with 1.5% DMSO for 30 min at 37°, the recovery of the EPM was evident within 1 hr of incubation and completed in 3 to 4 hr.

To determine how long the cells remain recoverable, C-10-6 cells were treated with 1.5% DMSO for different durations, washed once with Dulbecco's phosphate-buffered saline, and then incubated in the culture medium. As indicated in Fig. 5, DMSO treatment for less than 16 hr and the subsequent incubation without the drug resulted in the complete recovery of the EPM. Exposure to DMSO for longer than 20 hr resulted in a loss of recovery of the EPM. The fractions of benzidine-positive cells tested 5 days after the onset of treatment with DMSO for various durations were 0.3% (30 min with DMSO), 0.3% (12 hr), 0.3% (16 hr), 0.9% (18 hr), 1.9% (20 hr), 4.7% (24 hr), 26% (48 hr), 39% (72 hr), and 48% (96 hr), respectively. These results suggested that 1) cells which have recovered from EPM reduction did not differentiate, and 2) cells should be treated with DMSO for more than 20 hr before irreversible commitment to erythroid differentiation. The existence of a latent period before irreversible commitment was also reported to be 20 to 24 hr in other cell lines (5). After this latent period of exposure to DMSO, subsequent expression of erythroid functions follows without DMSO. This latent period or commitment process precedes or accompanies the increase in cytoplasmic globin mRNA (17). What the commitment process is and the primary site of DMSO action are unknown. There is a hypothesis that the initial effects of DMSO are on the membrane (6). Accumulation of erythrocyte membrane antigen (24) and spectrin (1) occurs 1 to 2 days after DMSO treatment. Increased agglutinability by lectins (3), reduced membrane permeability, and increased membrane microviscosity are relatively early events. A good correlation was found between increased membrane microviscosity and the spectrin or hemoglobin level in individual cells (1). Local anesthetics prevent induction of erythroid differentiation of Friend cells by DMSO and also prevent the change in microviscosity of the lipid membrane. The loss of macromolecules from the cell surface that we found in this experi-

ment is one of the earliest events after DMSO administration. The EPM reduction was also caused by other potent inducers of erythroid differentiation such as 1 mM sodium butyrate, 30 mM N-methylacetamide and 20 mM, N,N-dimethylacetamide (21).

How Could the Partial Loss of Glycocalyx Lead to Differentiation?

One of the possible explanations is that the loss of glycocalyx gives rise to a change in membrane permeability or in membrane conformation. Changes in local ionic concentration or membrane organization might trigger a sequential process for cell differentiation through the cytoskeletal system or cyclic nucleotides. Enhancement of lectin agglutinability or membrane microviscosity might be one of the sequential processes. Breakage of DNA by DNase activated by a membrane change was postulated as an early step in the control of differentiation through gene activation (23).

The second possible explanation is that the partial loss of glycocalyx might result in the exposure of membrane receptors to the inducers for erythroid differentiation in the serum. This hypothesis agrees with the following findings: (a) prior treatment of Friend cells with DMSO renders them slightly sensitive to erythropoietin (16); (b) serum enhances the capacity of the cells to differentiate by DMSO (9); (c) the effect of DMSO varies markedly depending on the lot of serum. The concept of two sequential programs, first a commitment program by an inducer and a subsequent expression program, has been postulated (5). Partial removal of glycocalyx may facilitate the action of inducers but may not be sufficient for the final differentiation. If the glycocalyx was repaired and the cell EPM was recovered after DMSO was washed out, the erythroid differentiation did not take place.

As another explanation of differentiation through the loss of glycocalyx, the effect of DMSO on the biosynthesis of glycosaminoglycans should be considered. The EPM reduction after 30 min treatment with DMSO or hyaluronidase was completely recovered by subsequent incubation without the drug for 3 to 4 hr, presumably by rapid biosynthesis. In our preliminary experiment, rapid turnover of heparan sulfate of Friend cells and the inhibition of its synthesis by DMSO are suggested. The loss of recovery of the EPM after treatment with DMSO for longer than 20 hr seems to suggest the loss of normal biosynthesis and reorganization of the glycocalyx. Since the matured erythrocyte is not covered with glycosaminoglycans and its EPM is not reduced by hyaluronidase (19) or heparitinase, the loss of glycosaminoglycans of Friend cells by DMSO through its early shedding and subsequent inhibition of biosynthesis can be regarded as a process of erythroid differentiation in itself.

Composition of Acidic Sugars on Lymphocytes

A T-cell-rich fraction and a B-cell-rich fraction were isolated from healthy human peripheral blood based on their different adhesiveness to plastic dish walls and nylon fibers. Figure 6 is the schematic presentation of the relative amount of each acidic sugar in the surface of T-cells or B-cells before or after PHA treatment for 24 hr. The EPM reduction by each enzymatic digestion measured at ionic strength 0.167 is shown as a column on the line of 7.5 Å, and the further EPM reduction detected at lower ionic

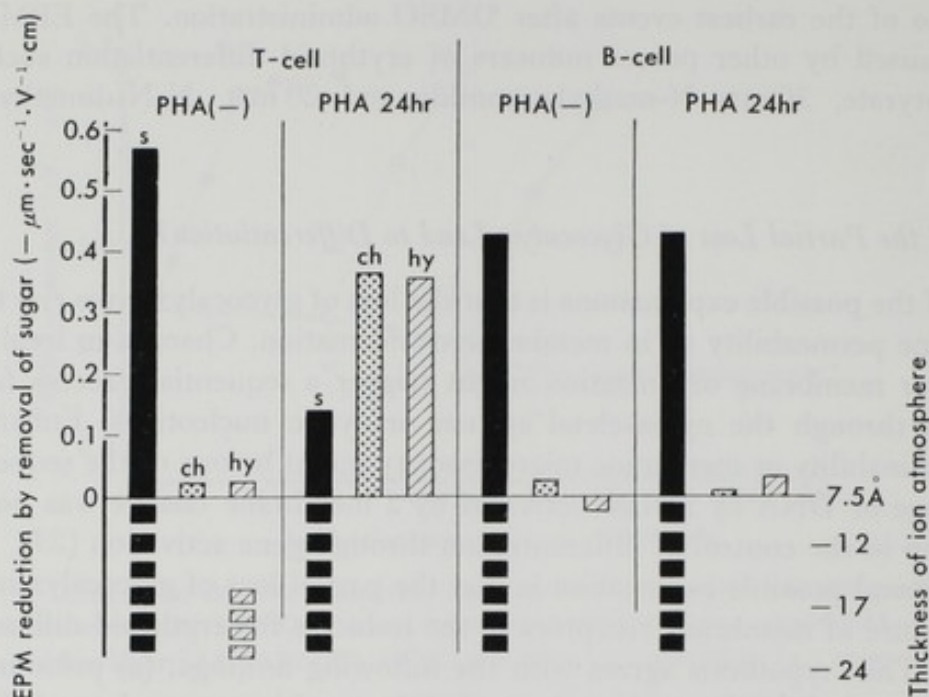


FIG. 6. Histogram of the composition of acidic sugars in the surface of lymphocytes with or without stimulation. EPM reduction at ionic strength 0.167 by each enzymatic digestion is shown as a column above the line of 7.5 Å thickness of the ion atmosphere. Further EPM reductions detected at lower ionic strengths are illustrated as blocks at the bottom part, one block referring to an EPM reduction by 0.1. (The length of a column above the 7.5 Å line)+(the number of blocks \times 0.1) shows EPM reduction detected at a low ionic strength, which represents the relative amount of the acidic sugar within the corresponding thickness of the ion atmosphere. Closed columns represent EPM reduction by treatment with 20 units/ml neuraminidase; dotted columns refer to EPM reduction by 1 unit/ml chondroitinase-ABC; and shaded columns show that by 10 units/ml hyaluronidase.

strengths is illustrated as blocks at the bottom part, one block referring to an EPM reduction by 0.1. (The length of a column above the 7.5 Å line)+(the number of blocks \times 0.1) shows the EPM reduction detected at a low ionic strength, which represents the relative amount of the acidic sugar within the corresponding thickness of the ion atmosphere. In B-cells, only neuraminidase caused EPM reduction. Chondroitinase-ABC and hyaluronidase had no effects on the EPM at any ionic strength tested. The pattern of the composition of the acidic sugars of B-cells remained unchanged after incubation with PHA for 24 hr. In contrast, the presence of PHA for 24 hr induced substantial change in T-cells. EPM reduction by chondroitinase-ABC and hyaluronidase was detected at ionic strength 0.167, which suggests the appearance of these glycosaminoglycans in the peripheral layer of 0–7.5 Å. In nonstimulated T-cells, hyaluronic acid was detected electrophoretically around 17 Å. Treatment with neuraminidase gave rise to increasing EPM reduction with decreasing ionic strength. This result suggests the uniform distribution of sialic acid through every layer depth. During 24 hr of incubation with 1% PHA, 96% of the T-cells enlarged with the synthesis of macromolecules, while B-cells remained unchanged in size.

Time Course Change after PHA Administration

Figure 7 exhibits the time course change in EPM reduction by each enzyme at an ionic strength of 0.167. Hyaluronic acid was detected at the peripheral layer by as early as 30 min and remained unchanged thereafter. On the other hand, chondroitin sulfate appeared on the periphery after 4 hr of PHA administration, and the extent of its contribution to the EPM increased thereafter. In parallel with the change in chondroitin sulfate, the extent of EPM reduction by neuraminidase decreased with time. Since the presence of chondroitin sulfate was not detected at any tested ionic strength in non-stimulated T-cells and was detected with increasing magnitude after 4 hr, an enhanced synthesis of chondroitin sulfate and its overspread on neuraminic acid of glycoprotein was assumed.

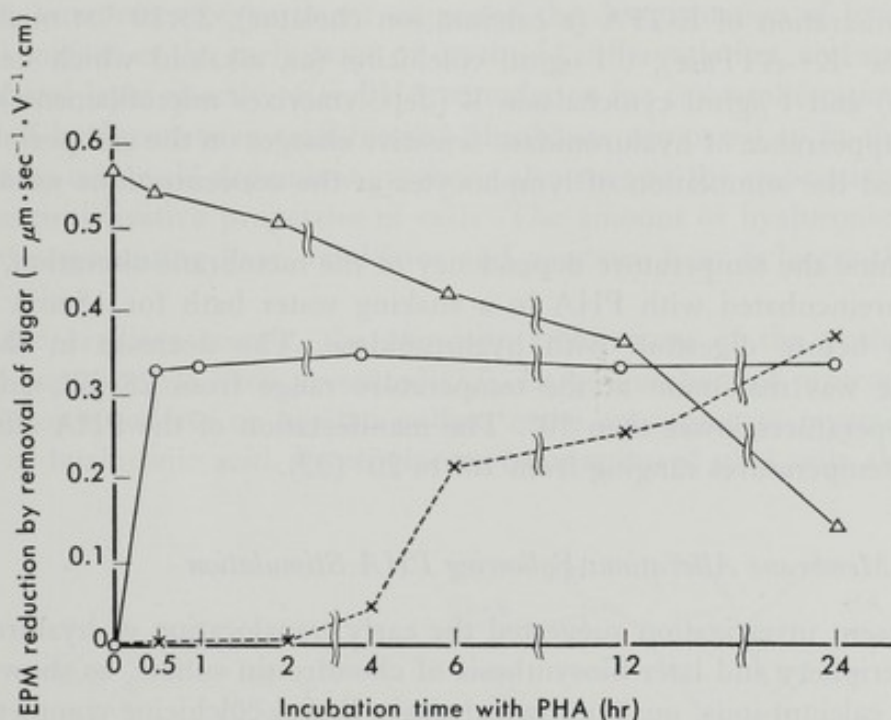


FIG. 7. Decrease in electrophoretic mobility by digestion with 20 units/ml neuraminidase (Δ), 10 turbidity reducing units (TRU)/ml hyaluronidase (\bullet) or 1 unit/ml chondroitinase-ABC (\times) in T-lymphocytes.

Enhanced Synthesis of Chondroitin Sulfate after PHA Stimulation

After the incorporation of ^{14}C -glucosamine for 24 hr with or without 1% PHA, labeled glycosaminoglycans of lymphocytes were purified on a Sephadex G-50 column following extensive digestion with pronase. Paper chromatography of the glycosaminoglycans subsequent to the digestion with chondroitinase ABC revealed a 4.3-fold increase in the synthesis of chondroitin sulfate C. About 30% of it remained on the cells, and the other 70% was released into the medium. The biosynthesis of chondroitin sulfate A or B also increased four-fold after the stimulation; most of these two, however, were released to the medium (22).

Effects of Chondroitinase on MOLT Cells

On the hypothesis that proliferating lymphoblastoid cells have a cell coat of chondroitin sulfate, T-cell-type human leukemia cells (MOLT-4B) were examined. Digestion with chondroitinase-ABC resulted in a marked reduction in the EPM ($-0.594 \pm 0.041 \mu\text{m} \cdot \text{sec}^{-1} \cdot \text{V}^{-1} \cdot \text{cm}$) compared with the control (-0.800 ± 0.064) (22).

Effects of Inhibitors and Temperature on the Membrane Change

To investigate whether the appearance of hyaluronic acid on the surface is relevant to mitogenic stimulation, some inhibitors of blastogenesis were utilized. T-cells were incubated in the presence of both inhibitors and 1% PHA-M in the culture medium for 30 min at 37°, and then digested with hyaluronidase before measurement of the EPM. Administration of EGTA (a calcium ion chelator), 2×10^{-7} M ouabain (an inhibitor of Na^+/K^+ -ATPase), 0.1 $\mu\text{g}/\text{ml}$ colchicine (an alkaloid which depolymerizes microtubules) and 1 $\mu\text{g}/\text{ml}$ cytochalasin B (depolymerizes microfilaments) completely blocked the appearance of hyaluronidase-sensitive charges on the cell periphery. These agents blocked the stimulation of lymphocytes at the concentrations used in this experiment.

To examine the temperature dependency of the membrane alteration, T-lymphocytes were preincubated with PHA in a shaking water bath for 15 min at different temperatures before digestion with hyaluronidase. The decrease in the EPM by hyaluronidase was maximum at the temperature range from 25–37°, and was very slight at temperatures lower than 10°. The manifestation of the PHA effect changed markedly at temperatures ranging from 10° to 20° (22).

Summary of Membrane Alterations Following PHA Stimulation

The present investigation suggested the early translocation of hyaluronic acid to the T-cell periphery and later biosynthesis of chondroitin sulfate, as shown in Fig. 8. Chelators of calcium ions, ouabain, cytochalasin B and colchicine completely blocked both changes in hyaluronic acid and blast formation. These results suggest that the early topological change in hyaluronic acid might be caused through the microtubules-

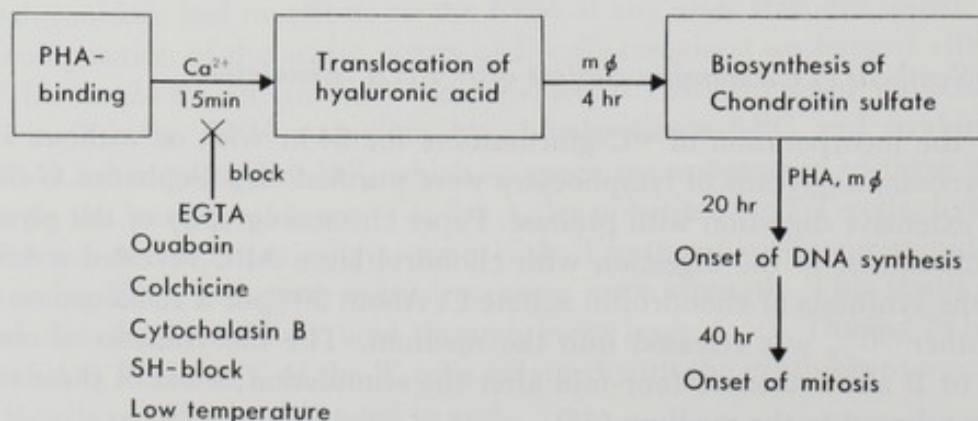


FIG. 8. PHA effects on glycosaminoglycans of T-lymphocytes.

microfilament system subsequent to Ca^{2+} - and Na^{+} -influx. Transitional fluidization of membrane lipids also occurs 15–30 min after the addition of PHA (27). A marked change in the temperature dependency of the PHA effect on hyaluronic acid at around 15° also supports the idea of the reorganization of membrane components. A similar temperature dependency was obtained in the topological change in sialoprotein of erythrocyte membrane after X-irradiation (19). As for the activation of the biosynthesis of chondroitin sulfate, the requirement of a macrophage has been suggested in our preliminary experiment. Further analysis of macrophage-lymphocyte interaction is now under investigation.

Is Hyaluronic Acid a Scaffold for Proteoglycans?

If we believe in the purity and specificity of hyaluronidase from *Streptomyces hyalurolyticus*, our present experiment suggested the desquamation of hyaluronic acid from the cell surface at the early stage of erythroid differentiation, and its appearance on the peripheral layer shortly after PHA stimulation for cell proliferation. Enhanced biosynthesis of hyaluronate in transformed fibroblasts compared to in their counterparts (8), and its cell-cycle-dependent synthesis also suggest the association of hyaluronate with the proliferative properties of cells. The amount of hyaluronic acid in the early stage of regenerating liver, fetal liver and newborn liver is larger than in adult liver (10).

As for the cartilage matrix, the exquisite architecture of the proteoglycan-hyaluronic acid complex has been presented (13). Large numbers of proteoglycans containing chondroitin sulfate or keratan sulfate make an aggregate reversibly along a single chain of hyaluronic acid. Proteoglycans from cultured glial cells also aggregate

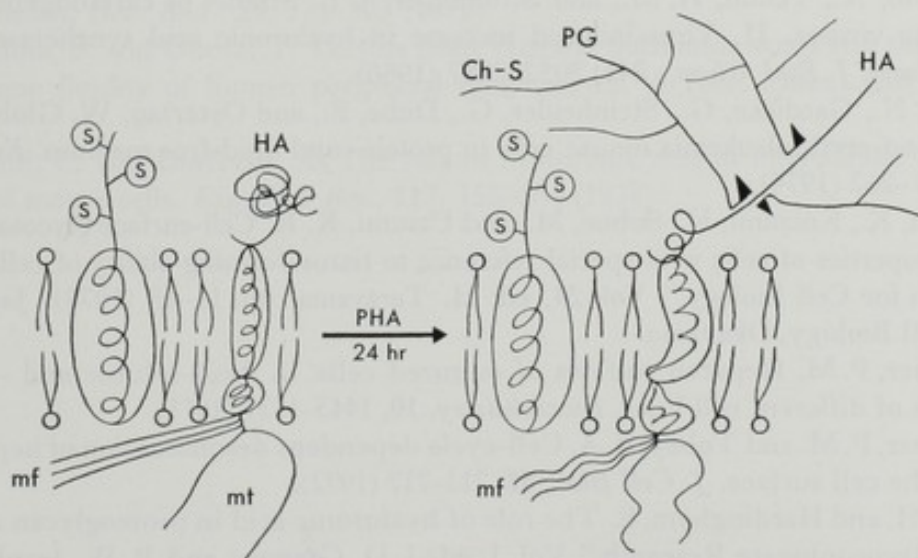


FIG. 9. Model of membrane alterations induced by PHA in T-lymphocytes to explain our results. Early conformational change in hyaluronic acid provides the binding sites for chondroitin sulfate proteoglycans to be actively synthesized later. Ultimately the proteoglycan-hyaluronate complex spread over sialoproteins. HA, hyaluronic acid; Ch-S, chondroitin sulfate; PG, proteoglycan; S, sialic acid; mf, microfilament; mt, microtubules.

with hyaluronic acid *in vitro* (14). We propose here the organization change of the T-lymphocyte surface by PHA as shown in Fig. 9. The early conformational change in hyaluronic acid provides the binding sites for chondroitin sulfate proteoglycans, which are actively synthesized later. The function of these thick aggregates on the cell surface that masks receptors for hormones and other regulating agents, modulation of antigenic expression, cell-to-cell interaction and cell-to-matrix interaction is now a project of extensive research.

REFERENCES

1. Arndt-Jovin, D., Ostertag, W., Eisen, H., Kfimek, F., and Jovin, T. M. Studies of cellular differentiation by automated cell separation. Two model systems: Friend virus-transformed cells and *Hydra attenuata*. *J. Histochem. Cytochem.*, **24**, 332-347 (1976).
2. Atherly, A. G., Barnhart, B. J., and Kraemer, P. M. Growth and biochemical characteristics of a detachment variant of CHO cells. *J. Cell Physiol.*, **90**, 375-386 (1977).
3. Eisen, H., Nasi, S., Georgotoulou, C., Arndt-Jovin, D., and Ostertag, W. Surface changes in differentiating Friend erythroleukemic cells in culture. *Cell* **10**, 689-695 (1977).
4. Friend, C., Scher, W., Holland, J. G., and Sato, T. Hemoglobin synthesis in murine virus-induced leukemic cells *in vitro*: stimulation of erythroid differentiation by dimethylsulfoxide. *Proc. Natl. Acad. Sci. U.S.A.*, **68**, 378-382 (1971).
5. Gusella, J., Geller, R., Clarke, B., Weeks, V., and Housman, D. Commitment to erythroid differentiation by Friend erythroleukemia cells: a stochastic analysis. *Cell*, **9**, 221-229 (1976).
6. Harrison, P. R. The biology of the Friend cell. In "Biochemistry of Cell Differentiation," Vol. 15, ed. J. Paul, pp. 227-267 (1977). University Park Press, Baltimore.
7. Ikawa, Y., Aida, M., and Inoue, Y. Isolation and characterization of high and low differentiation-inducible Friend leukemia lines. *Gann*, **67**, 767-770 (1976).
8. Ishimoto, N., Temin, H. M., and Strominger, J. L. Studies of carcinogenesis by avian sarcoma viruses. II. Virus-induced increase in hyaluronic acid synthetase in chicken fibroblasts. *J. Biol. Chem.*, **241**, 2052-2057 (1966).
9. Kluge, N., Gaedicke, G., Steinheider, G., Dube, S., and Ostertag, W. Globin synthesis in Friend-erythroleukemia mouse cells in protein- and lipid-free medium. *Exp. Cell Res.*, **88**, 257-262 (1974).
10. Kojima, K., Koizumi, K., Sobue, M., and Utsumi, K. R. Cell-surface glycosaminoglycans and properties of cells with special reference to tissue-forming ability of cells. In "Symposium for Cell Biology," Vol. 24, ed. H. Terayama, pp. 11-18 (1973). Japan Society for Cell Biology, Okayama.
11. Kraemer, P. M. Heparan sulfates of cultured cells. II. Acid-soluble and -precipitable species of different cell lines. *Biochemistry*, **10**, 1445-1451 (1971).
12. Kraemer, P. M. and Tobey, R. A. Cell-cycle dependent desquamation of heparan sulfate from the cell surface. *J. Cell Biol.*, **55**, 713-717 (1972).
13. Muir, H. and Hardingham, E. The role of hyaluronic acid in proteoglycan aggregation. In "Glycoconjugate Research," Vol. 1, ed. J. D. Gregory and R. W. Jeanloz, pp. 375-391 (1979). Academic Press, New York.
14. Norling, B., Glimelius, B., Westermarck, B., and Wasteson, Å. A chondroitin sulphate proteoglycan from human cultured glial cell aggregates with hyaluronic acid. *Biochem. Biophys. Res. Commun.*, **84**, 914-921 (1978).
15. Okayama, M., Yoshimura, M., Muto, M., Chi, J., Roth, S., and Kaji, A. Transformation of chicken chondrocytes by Rous sarcoma virus. *Cancer Res.*, **37**, 712-717 (1977).

16. Preisler, H. and Giladi, M. Erythropoietin responsiveness of differentiating Friend leukemia cells. *Nature*, **251**, 645-646 (1974).
17. Ross, J., Ikawa, Y., and Leder, P. Globin messenger-RNA induction during erythroid differentiation of cultured leukemia cells. *Proc. Natl. Acad. Sci. U.S.*, **69**, 3620-3623 (1972).
18. Sato, C. and Kojima, K. Phytohemagglutinin-induced change in the distribution of acidic sugars in surface membrane of lymphoid cells and blocking of the radiation effect. *Exp. Cell Res.*, **98**, 90-94 (1976).
19. Sato, C., Kojima, K., and Nishizawa, K. Target of X-irradiation and dislocation of sialic acid in decrease of cell surface charge of erythrocytes. *Radiat. Res.*, **69**, 367-374 (1977).
20. Sato, C., Kojima, K., and Nishizawa, K. Translocation of hyaluronic acid in cell surface of cultured mammalian cells after X-irradiation and its recovery by added adenosine triphosphate. *Biochim. Biophys. Acta*, **470**, 446-452 (1977).
21. Sato, C., Kojima, K., Nishizawa, K., and Ikawa, Y. Early decrease in hyaluronidase-sensitive cell surface charge during the differentiation of Friend erythroleukemic cells by dimethyl sulfoxide. *Cancer Res.*, **39**, 1113-1117 (1979).
22. Sato, C., Miyazawa, T., Nishizawa, K., Kojima, K., and Okayama, M. Changes in the organization and biosynthesis of cell surface acidic sugars during the phytohemagglutinin-induced blast formation of human T-lymphocytes. *Exp. Cell Res.*, **124**, 285-292 (1979).
23. Scher, W. and Friend, C. Breakage of DNA and alterations in folded genomes by inducers of differentiation in Friend erythroleukemic cells. *Cancer Res.*, **38**, 841-849 (1978).
24. Sugano, H., Furusawa, M., Kawaguchi, T., and Ikawa, Y. Enhancement of erythrocytic maturation of Friend virus-induced leukemia cells *in vitro*. *Bibl. Haematol.*, **39**, 943-959 (1973).
25. Tomida, M., Koyama, H., and Ono, T. Induction of hyaluronic acid synthetase activity in rat fibroblasts by medium change of confluent cultures. *J. Cell Physiol.*, **86**, 121-130 (1975).
26. Tool, B. P. Hyaluronate turnover during chondrogenesis in the developing chick limb and skeleton. *Dev. Biol.*, **29**, 321-329 (1972).
27. Toyoshima, S. and Osawa, T. Lectins from Wistaria floribunda seeds and their effect on membrane fluidity of human peripheral lymphocytes. *J. Biol. Chem.*, **250**, 1655-1660 (1975).
28. Underhill, C. and Dorfman, A. The role of hyaluronic acid in intercellular adhesion of cultured mouse cells. *Exp. Cell Res.*, **117**, 155-164 (1978).

STROMA AS A RATE LIMITING FACTOR FOR GROWTH OF TUMORS IN VIVO

David P. Kufe

Department of Pathology, Dana-Farber Cancer Institute, Boston, Massachusetts 02115

CELL KINETICS OF NORMAL AND NEOPLASTIC TISSUES

1. The stroma of the tumor is a complex of normal connective tissue cells and extracellular matrix. The stroma is a rate limiting factor for the growth of a tumor in vivo.

2. The stroma of the tumor is a complex of normal connective tissue cells and extracellular matrix. The stroma is a rate limiting factor for the growth of a tumor in vivo.

3. The stroma of the tumor is a complex of normal connective tissue cells and extracellular matrix. The stroma is a rate limiting factor for the growth of a tumor in vivo.

4. The stroma of the tumor is a complex of normal connective tissue cells and extracellular matrix. The stroma is a rate limiting factor for the growth of a tumor in vivo.

5. The stroma of the tumor is a complex of normal connective tissue cells and extracellular matrix. The stroma is a rate limiting factor for the growth of a tumor in vivo.

During the past few years, the stroma of the tumor has been recognized as a rate limiting factor for the growth of a tumor in vivo. The stroma is a complex of normal connective tissue cells and extracellular matrix. The stroma is a rate limiting factor for the growth of a tumor in vivo.

The stroma of the tumor is a complex of normal connective tissue cells and extracellular matrix. The stroma is a rate limiting factor for the growth of a tumor in vivo.

In conclusion, the stroma of the tumor is a complex of normal connective tissue cells and extracellular matrix. The stroma is a rate limiting factor for the growth of a tumor in vivo.

CELL KINETICS OF NORMAL
AND NEOPLASTIC TISSUES

STROMA AS A RATE LIMITING FACTOR FOR GROWTH OF TUMORS *IN VIVO*

Setsuya FUJITA

*Department of Pathology, Kyoto Prefectural University of Medicine**

In vivo cancer cell proliferation and tumor growth were analyzed by means of tritiated thymidine autoradiography, and tumor volume- or cell number-measurements.

1. On an average, doubling times of human tumors were found ten times as long as the generation times of cancer cells that constitute the tumors. The discrepancy is explained by the presence of a large amount of cell loss.

2. Mechanism of the cell loss was investigated and it was found that much slower growth of the stroma limits the rate of growth of the entire tumor mass thereby producing the loss of cancer cells.

3. In hormone dependent mammary tumors of rats induced by dimethylbenzanthracene (DMBA), it was found that, here too, the stroma, being a primary target of the hormone, acts as a controlling factor of tumor growth.

4. The growth-controlling factors were further analyzed in experimental ascites tumor (Yoshida sarcoma) in chemical and physical terms and it was found that glucose supply *via* stroma from the blood plays the most important role of rate limitation in the tumor growth.

Based on these observations, the role of stroma as a rate limiting factor of tumor growth is discussed.

Among the various features that characterize malignant tumors, "excessive growth" is considered the most fundamental. Beyond doubt, growth is realized by the proliferation of tumor cells. However, the proliferation of cancer cells and growth of the tumor are by no means the same phenomena. In most cases of human cancers, the doubling times that characterize tumor growth and the generation times of the cells constituting the tumor differ by a factor of 10 or so. The proliferation of cancer cells contributes only partly to the growth of the tumor, due to a large amount of cell loss.

The cause of the cell loss is investigated in the present paper and it was concluded that growth of the stroma of which cells proliferate ten times slower than the parenchymal cancer cells limits the rate of the growth of the entire tumor mass. The stroma that supports the cancer cells functions at the same time as a rate limiting factor of cancer growth.

If, in most tumors, the stroma acts as a rate limiting factor in growth control, does it also function as such in hormone-dependent tumors? We studied dimethylbenzanthracene (DMBA)-induced experimental mammary carcinomas of rats that show estrogen-dependent growth. Ovariectomy and testosterone therapy on these tumor-

* Kajii-cho-465, Kawaramachi, Kamikyo-ku, Kyoto 602, Japan (藤田哲也).

bearing rats resulted in tumor regression that first became manifest on the second or the third day following the therapy. However, already at 24 hr, microscopic examination revealed marked changes in the stroma while the proliferation and morphology of the cancer cells were still unchanged. It was concluded that, even in hormone-dependent growth of mammary carcinoma, the stroma plays a leading role in the growth control of the cancer.

What are the chemical factors that underlie this regulation mechanism? We analyzed the growth of rat ascites tumors (Yoshida sarcoma) after a single-cell transplantation into the peritoneal cavity of young rats. Examination of the physical and chemical changes in the ascitic fluid following the implantation revealed that a shortage of glucose supply occurring at 8.5 days triggered marked cell loss in the growing tumor. It is concluded that glucose supply from the blood plays the most important role in the rate-limiting process in malignant tumors growing *in vivo*, and that the meaning of the slow growth of the stroma and genesis of blood vessels in the growth control of tumors may be understood in this context.

Difference between Cancer Growth and Cancer Cell Proliferation

All the investigations so far made concerning the growth of human tumors have reached the unanimous conclusion that there is a marked discrepancy between the volume doubling time (D) of a tumor and the generation time (T) of parenchymal cancer cells composing the tumor (8, 10, 13, 17). In most human tumors, the ratio of T to D amounts to 1 to 10 or more as seen in Table I. This discrepancy has been explained by the presence of a large amount of cell loss in the proliferating cancer cell population in human tumors (4, 9, 10, 13). Figure 1 illustrates how cell loss slows down tumor growth. Then the question is raised: What is the cause of the marked cell loss in human cancers growing *in vivo*? If we can understand this mechanism thoroughly, we may control growth of the tumors just by enhancing this mechanism that occurs naturally in the human body. In this context, it is important to realize that, for clinical progression of malignant diseases, tumor growth has an essential meaning; even if cancer cells pro-

TABLE I. Volume Doubling Times (D) and Generation Times (T) in Human Cancers (9, 10)

Type of tumor	No. of cases	D (days)	Type of cell	No. of cases	T (days)
			Adenocarcinomas (lymph node metastasis)	4	6.6-12.8
			Squamous cell carcinomas (lymph node metastasis)	2	6.3-7.1
Bronchial carcinomas	89	17-480			
Metastatic lung cancers	202	7-465			
Gastric carcinomas					
Metastasis	4	16-60		6	3-12.3
Advanced stage	4	105-305 ^a		5	4-15
Early	15	555-2,405 ^a		5	4-15
Colonic carcinomas	21	138-1,155 ^a		2	4.2-7.9
Mean values		(7)-30-100-(more than 1,000 years)			3-10

^a D 's of cancers growing in gastrointestinal tract are much longer than others.

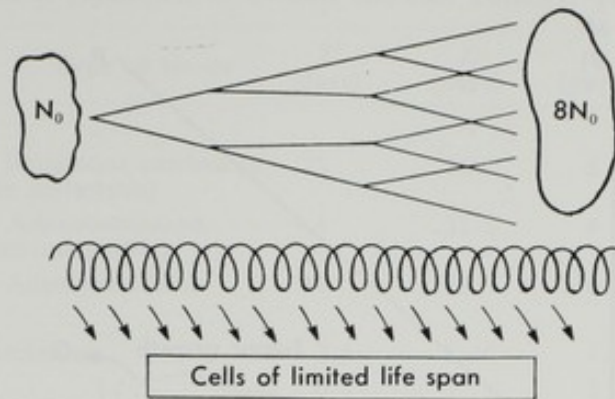


FIG. 1. Cell loss in tumor growth. While the tumor grows, many cells are lost as *CLLS* (cells of limited life span). As a result, cell cycles are repeated ten times or more until a tumor doubles its cell number or volume. *CLLS* comprise dying cells and non-proliferative cells that ultimately die (5).

liferate very vigorously, the disease of cancer is not aggravated, if half or more of its daughter cells are continuously lost (4). In adult normal tissues the same thing happens; generative cells in the gastrointestinal mucosa, hematopoietic tissue or epidermis proliferate very actively with generation times of 1 to 4 days (10, 17), but half of the cells are continuously lost so that the tissue size remains constant throughout the life.

Possible Mechanism Causing the Discrepancy between Proliferation of Tumor Cells and Tumor Growth

Seeking a possible answer to this question, I studied autoradiographic materials of more than 100 cases of human tumors labeled with tritiated thymidine and found that the labeling indices of stromal cells are always markedly lower than those of parenchymal cancer cells (5, 11). There were no exceptions to this rule. The difference in the labeling index is especially marked in autoradiographs taken after several days of cumulative labeling with tritiated thymidine. The ratio of the labeling indices in stromal and cancer cells appeared somewhat near 1 to 10. These findings gave us an idea that this difference in the labeling indices may explain the difference in the ratios of proliferation of tumor cells (T), and tumor growth (D). It is possible that cell proliferation (more correctly growth) of the stroma parallels the growth of the entire tumor mass.

A tumor is believed to grow excessively in an uncontrolled fashion. But this does not mean that the tumor grows independently of any factors in its environment. Tumor cells require, as any cells do, chemical as well as physical support from the stroma. If we boil down the problem, the term "stroma" will ultimately mean "tissue fluid that interfaces between tumor cells and the host." However, in solid tumors, the capillary and connective tissue around it that assure the circulation of the tissue fluid would be important. A capillary and connective tissue around it constitute the elementary unit of the stroma.

If the elementary unit is present only in a given amount, the maximum number of tumor cells that can be supported is necessarily limited. In tumors growing *in vivo*, cancer cells are supposed to parasitize around the elementary units of the stroma already supporting the maximum number. It is thus necessary for the stromal units to double

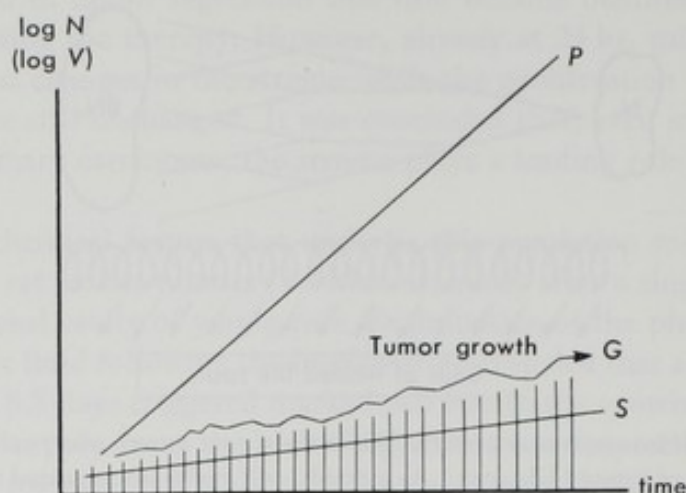


FIG. 2. Stroma as a rate limiting factor for tumor growth. Tumor cells proliferate rapidly. Line P indicates potential growth of the tumor that would be realized if none of the daughter cells were lost in the tumor. However, the stroma grows very slowly (S) so that the actual tumor growth (G) is forced to follow this slope. The difference between P and G represents cell loss. The abscissa represents time, and the ordinate, the logarithm of volume or cell number of tumor.

their number before the cancer cells can do so. The schema shown in Fig. 2 illustrates this relationship.

If cancer cells proliferate without cell loss, the tumor should grow purely exponentially as shown by the straight line P in Fig. 2. However, the proliferation (or more exactly, growth) of the stroma is so slow, as shown by the hatched line S , the tumor cells supported by the stroma can only grow along with this line. Thus the actual growth will become a curve something like that marked with G . The discrepancy between lines P and G represents the cell loss.

Obviously, the stroma functions to support and nourish the cancer cells, on the one hand, but also brakes the growth of the cancer, on the other. It has been disputed by pathologists for a long time whether the stroma is "*den Weg bahnend*" or "*das Wachstum blemsend*" for the cancer (12). It is interesting to find out in the present investigation that the stroma performs these two-faced functions at the same time, as will be shown below.

Figuratively speaking, the situation is just like an over-crowded society of animals; since the capacity for survival is limited, a population explosion cannot occur despite the high birth rate of the members. In order to accept an enlarging population, supplies of food and space should increase proportionally.

In order to test the idea that the stroma may play a role as a rate limiting factor in tumor growth, we have to investigate cancer growth and cell proliferation in the same tumor. It was a difficult task to find suitable cases for this purpose in human tumors. However, we were able to collect 3 human cases in which the volume doubling time (by direct size measurements) and generation time (by tritiated thymidine autoradiography) were determined in the same tumor (5). In addition to human tumors, rat mammary tumors produced by DMBA injection and transplanted Yoshida sarcoma grown in rat subcutis were studied (5, 11). The results are shown in Table II. In the 3 cases of human tumors, most cancer cells incorporated tritiated thymidine during the

TABLE II. Kinetic Parameters of Cancers and Cell Turnover Time in Stroma (5)

Name	Location	Type of tumor	T (days)	D (days)	t_a (days) ^a	LIs (%) ^b	T_{100} (days) ^c
Human							
M. K.	Maxilla	Squamous carcinoma (lymph node metastasis)	11	14.2	6	42	14.2
Y. N.	Rectum	Adenocarcinoma (subcutaneous metastasis)	4	31.5	4	13	30.7
Y. Y.	Breast	Adenocarcinoma	11	175	8	3	266
Rat							
DMBA	mammary carcinoma		2.1	5-10	1.5	13	11.5
Yosida	Sarcoma (subcutaneous transplantation)		0.7	3	3	98-100	3

^a Duration of cumulative labeling with tritiated thymidine in days.

^b Labeling index in the stroma after t_a days of cumulative labeling.

^c Extrapolated value, suggesting average turnover time (or doubling time) of stromal cells.

cumulative labeling while stromal cells showed much lower labeling indices as shown in Table II. The latter labeling indices were counted only in areas where the diffuse distribution of labeled cancer cells assured availability of tritiated thymidine during the cumulative labeling. Therefore, the labeled cells in the stroma, though low in labeling indices, represent all the cells that synthesized DNA during the period of the cumulative labeling.

In these materials, first, I attempted to count the cells constituting vascular walls and the fibroblasts surrounding them separately. But identification was frequently impossible so that I counted both elements together. In flash labeling autoradiographs of these human tumors, the labeling indices of stromal cells were extremely low (5), so that I interpreted the labeling indices after cumulative labeling, LIs (cf. Table II), as indicating the total fraction of the cells which have flowed into the DNA-synthetic phase during the duration t_a of the cumulative labeling. Extrapolating these LIs -values to 100%, I calculated the turnover time, T_{100} , of the stromal cells (Table II). It is evident that these data (T_{100}) show little correlation with the generation time (T) of the respective tumor cells, but that they are closely correlated with the volume doubling time (D) of the tumors.

These correlations can also be confirmed with experimental DMBA mammary tumors (Photos 1, 2) and subcutaneously transplanted Yoshida sarcoma (Table II). In the latter, the measured turnover time of the stromal cells (T_{100}) gave exactly the same figure as the volume doubling time (D) of the tumor.

Hormone and Stromal Control of Tumor Growth

In some human mammary carcinomas, estrogen plays an essential growth-promoting role and in such cases ovariectomy with or without accompanying testosterone therapy has been proved highly effective to control the growth of the tumors. It has been believed that estrogen receptors in the cancer cells receive and transmit the information carried by estrogen to the machinery of cancer cells of the mammary gland to maintain cell proliferation (15). However, as I discussed previously (7), cancer cells usually lose the normal susceptibility in subtle control of cell proliferation and differentiation from

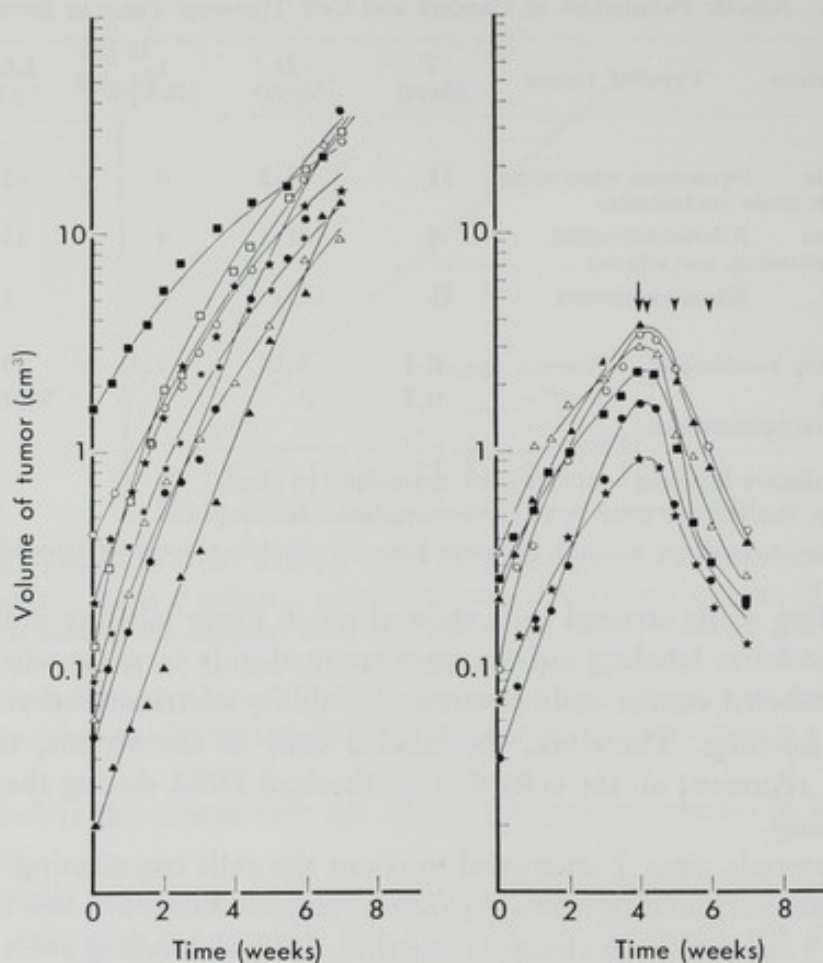


FIG. 3 (left). Growth curves of DMBA-mammary carcinomas of rats (14). Rapidly growing tumors before ovarectomy. Abscissa, weeks after measurements of tumor size started; ordinate, volume of the tumors in cubic centimeters on logarithmic scale.

FIG. 4 (right). Effect of ovarectomy and testosterone on growth curves of DMBA-mammary carcinoma of rats (14). Arrow indicates time of ovarectomy, and arrowhead, administration of 5 mg testosterone.

the environment when they are transformed into a malignant state, and keep proliferating rather blindly. Therefore, it should be questioned again whether the growth control of mammary cancer by hormone therapy is realized directly in the cancer cells or indirectly through the growth controlling function of the stroma.

To answer the question, we (5, 14) prepared hormone dependent mammary carcinomas of rats by intravenous injection of DMBA. The DMBA-mammary carcinomas are usually multiple and highly susceptible to ovarectomy and/or testosterone therapy (*cf.* Figs. 3 and 4). Multiple tumors are especially suitable for kinetic studies of the growth (by serial measurements of tumor sizes) and of the proliferation of parenchymal and stromal cells (by tritiated thymidine autoradiography). We used tumors less than 2 cm in diameter produced in 55 Sprague-Dawley rats. The results are shown in Figs. 3, 4, and 5. The mean volume doubling times of rapidly growing tumors were estimated at 5 to 10 days (Fig. 3) and the generation time of rapidly proliferating cancer cells at 51 hr with the DNA-synthetic time 9 hr, by the cumulative labeling method (Fig. 5, *cf.* Photos 1 and 2). Already 24 hr after the combined hormone treatment (ovarectomy

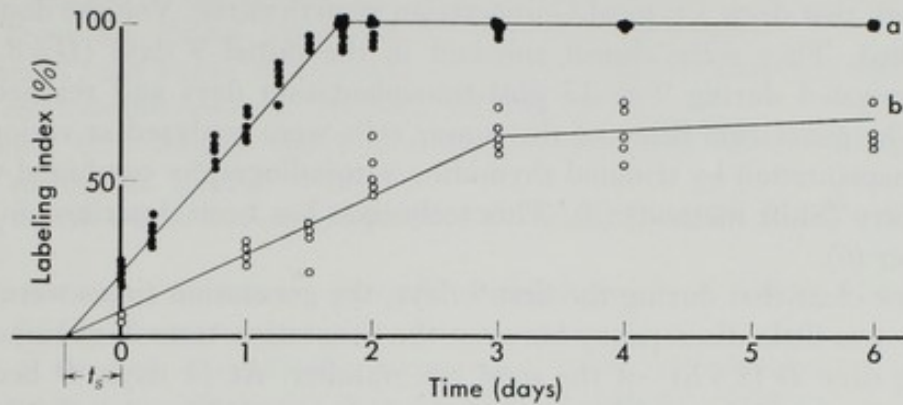


FIG. 5. Increase in labeling indices during cumulative labeling with tritiated thymidine (cancer cells of DMBA-mammary carcinoma). (●) indicates labeling indices counted in rapidly proliferating population in medullary area of the tumor, and (○) represents those in more differentiated cells forming tubulo-cystic structures. Abscissa, days of cumulative labeling; ordinate, labeling indices in percent.

and testosterone administration) (Photo 3), diffuse necrosis was observed in the corresponding capillaries which contain many nucleated blood elements, and labeling indices in the stromal cells showed drastic reduction, whereas the parenchymal cancer cells demonstrated little change in morphology and in the pattern of uptake of tritiated thymidine. Only several days after the commencement of the therapy, cancer cells showed signs of reduction of proliferative activity and partial necrosis (*cf.* Figs. 3 and 4). From repeated experiments, it was confirmed that the initial response is always in the stroma (14).

Although it has been well established that estrogen stimulates the proliferation of epithelial cells in the female reproductive system (3, 16), its effect on cancer cells or the presence of receptors in cancer cells have not been confirmed directly. Reports so far made have been concerned only with cancer tissues. It is possible that also in hormone-dependent tumors control of cancer growth is realized indirectly by the stroma.

Since the stroma is a host tissue, it should be within the range of normal control of cell proliferation and differentiation while the cancer cells are abnormal cells that are outside the range. These findings suggest that, in strategy for the control of cancer growth and cancer progression, much effort in the future should be focused on the stroma rather than on cancer cells alone.

Chemical Nature of the Rate Limiting Factor of the Stroma on Tumor Growth

Now I want to ask the third question: What is the rate limiting factor of the stroma that controls the growth of the tumor *in vivo*? In order to answer this question, we used a transplantable rat tumor (Yoshida sarcoma) growing in the ascites. Since the ascitic cavity can be regarded as a magnified space of tissue-fluid circulation in connective tissue, study of the environmental factors which influence tumor growth in the ascites may reveal the true nature of the rate limiting factor acting in the stroma.

We first studied (1) growth kinetics by counting the number of tumor cells growing in the ascites at various intervals after transplantation of a single tumor cell. After the single cell transplantation, the increase in cell number followed a remarkably repro-

ducible pattern that drew a typical Gompertzian growth curve. Volume doubling times were calculated. They were almost constant in the initial 9 days ($D=8.5$ hr), then gradually elongated during 9 to 13 post-transplantation days and reached a plateau thereafter. The generation times of the tumor cells were analyzed at various intervals after the transplantation by tritiated thymidine autoradiography combined with DNA-cytofluorometry (Shift method) (2). This technique has been described in detail in a separate paper (6).

It became clear that during the first 9 days, the generation times were 8.1 to 13.2 hr and there was little discrepancy between the generation time T of tumor cells and the doubling time D (8.5 hr) of the total cell number. At 11 days, D became 28 hr, while T remained at 8.1 to 13.2 hr. At 13 days, D was 115 hr and T 8.3 to 22.2 hr. Gradually, the discrepancy between T and D became manifest after 9 days post-transplantation (2).

These results revealed that the generation time of rapidly proliferating tumor cells remained relatively unchanged throughout the course of the growth of the tumor, although the fraction of more slowly proliferating cells increases with time. This rigid character of the generation time in cancer cells seems to be a characteristic feature of malignant tumor cells (7).

Meanwhile, the growth of the ascitic tumor slowed down from 9 days post-implantation onwards. This is beyond doubt due to the increase in cell loss after 9 days. Ashihara and I studied the changes in physical and chemical properties of the ascitic fluid during the whole experimental period, with special reference to those changes around 9 days.

The physical and chemical properties we studied were: volume of ascites, exchange rates of tritiated water between circulating blood and ascites, P_{O_2} , P_{CO_2} , pH, total cholesterol, total protein, and glucose concentration. The most significant change around 9 days was in glucose concentration, which decreased abruptly from 170–140 mg/dl to 7–5 mg/dl at 8.5 days just before the deceleration of growth began. Partial oxygen pressure, P_{O_2} , decreased from 40–35 mmHg to 7–4 mmHg thereafter, during days 9 and 10.

The primary change in the properties of the tissue fluid in the peritoneal cavity that influences the growth of the tumor seems to be that of glucose concentration. The decrease in the partial pressure of oxygen became manifest only after the deprivation of glucose and was probably enhanced by the Crabtree effect. From these experiments, it was concluded that cell loss in the tumor is primarily determined by glucose supply from the blood, and contrary to our expectation, a shortage of oxygen and changes in other factors followed that of glucose.

It is concluded that glucose supply from the blood plays the most important role in the rate-limiting process in cancers growing *in vivo*, and that the meaning of the slow growth of the stroma and genesis of blood vessels in the growth control of malignant tumors may be understood in this context.

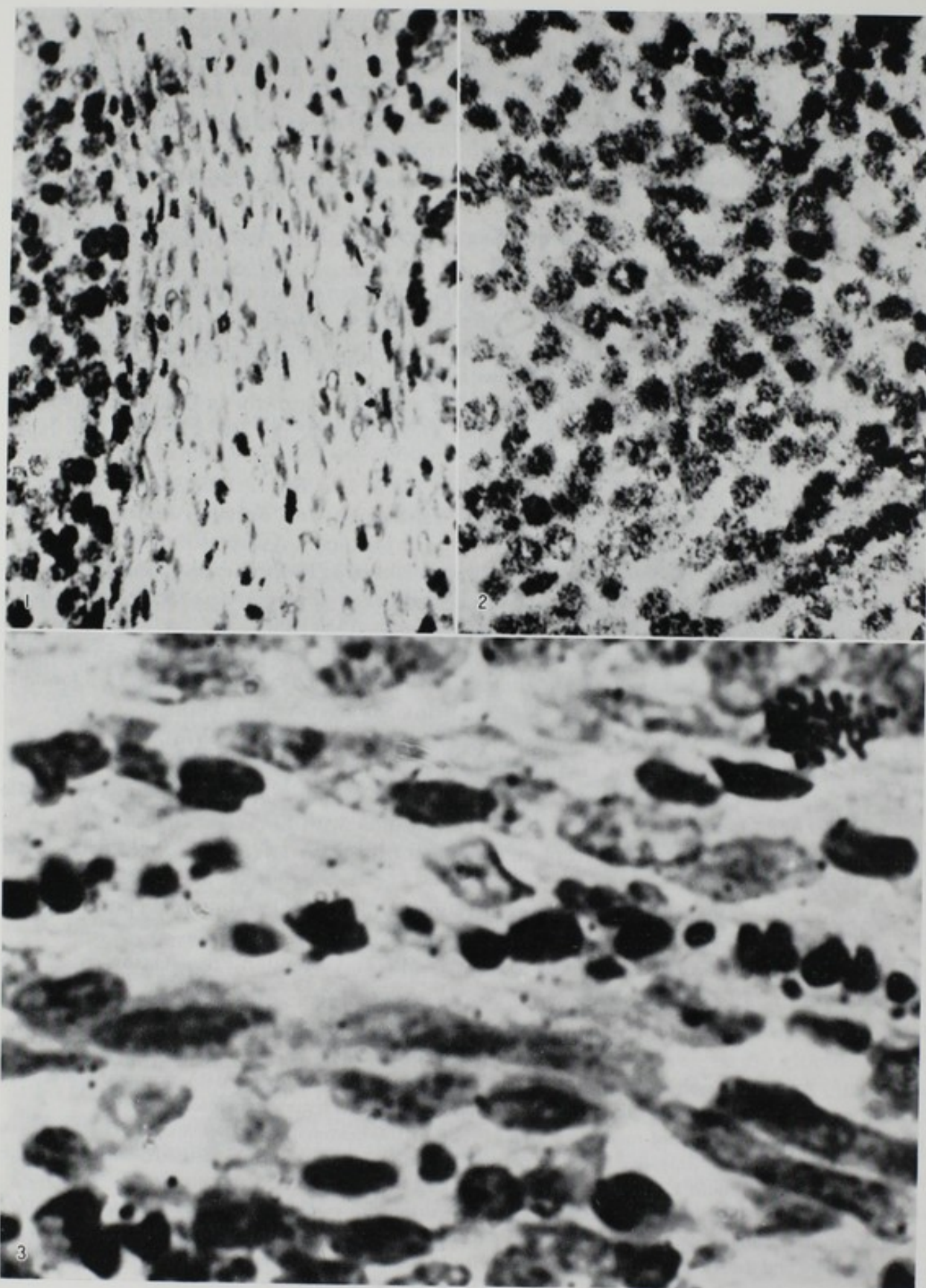
REFERENCES

1. Ashihara, T. and Fujita, S. Proliferation and differentiation of cancer cells *in vivo*. XLVI.

- Kinetic analysis of cell proliferation in incipient growth of Yoshida sarcoma in ascitic form. *Trans. Soc. Pathol. Japon.*, **63**, 193-194 (1974) (in Japanese).
2. Ashihara, T. and Fujita, S. Cell cycle analysis of Yoshida ascites sarcoma grown after a single cell transplantation. *J. Cell Biol.*, **70**, 236a (1976).
 3. Epifanova, O. I. Mitotic cycles of estrogen-treated mice: A radioautographic study. *Exp. Cell Res.*, **42**, 562-577 (1966).
 4. Fujita, S. Growth of human cancers *in vivo*. *Nihon Rinsho*, **29**, 111-116 (1971) (in Japanese).
 5. Fujita, S. Stroma as a factor controlling cancer growth. *J. Cancer Clin.*, **18**, 596-599 (1972) (in Japanese).
 6. Fujita, S. Analysis of cytokinetics by means of Feulgen cytofluorometry combined with ^3H -thymidine autoradiography. *Exp. Cell Res.*, **88**, 395-401 (1974).
 7. Fujita, S. Population kinetics of human cancer cells *in vivo*. *J. Cancer Clin.*, **21**, 654-659 (1975) (in Japanese with English abstract).
 8. Fujita, S. Kinetics of cancer cell proliferation and cancer growth. In "Modern Biological Sciences," Vol. 15, ed. T. Sugimura and Y. Yamamura, pp. 248-261 (1976) (in Japanese). Iwanami-Shoten, Tokyo.
 9. Fujita, S. Biology of early gastric carcinoma. *Path. Res. Pract.*, **163**, 297-309 (1978).
 10. Fujita, S. and Ashihara, T. Growth and Proliferation. In "Tumor Pathology," ed. H. Sugano and H. Kobayashi, pp. 39-60 (1970) (in Japanese). Asakura-Shoten, Tokyo.
 11. Fujita, S., Maekawa, J., Matsumoto, H., and Ashihara, T. Proliferation and differentiation of human cancer cells *in vivo*. XXXI. Stromal proliferation as a factor determining velocity of cancer growth. *Proc. Jpn. Cancer Assoc.*, 148 (1971).
 12. Hamperl, H. Die Morphologie der Tumoren. In "Handbuch der Allgemeinen Pathologie," Vol. VI, pt. 3, ed. A.v. Albertin, A. Butenandt, H. Dannenberg, G. Domagk, W. Fister, and H. Hamperl, pp. 18-106 (1956). Springer-Verlag, Berlin.
 13. Lamerton, L. F. Tumour cell kinetics. *Br. Med. Bull.*, **29**, 23-28 (1973).
 14. Maekawa, J. Regression of DMBA-induced mammary carcinoma and hormone-dependent changes of its blood vessels studied by ^3H -thymidine autoradiography. *J. Kyoto Pref. Univ. Med.*, **88**, 1199-1218 (1979) (in Japanese with English abstract).
 15. McGuire, W. L. Estrogen receptors in human breast cancer. *J. Clin. Invest.*, **52**, 73-77 (1973).
 16. Perrota, C.A.U. Initiation of cell proliferation in the vaginal and uterine epithelia of the mouse. *Am. J. Anat.*, **111**, 195-204 (1962).
 17. Steel, G. G. "Growth Kinetics of Tumours" (1977). Clarendon Press, Oxford.

EXPLANATION OF PHOTOS

- PHOTO 1. Autoradiograph of stroma after 1.5 days of cumulative labeling (DMBA-mammary carcinoma of rat). Thirteen percent of the stromal cells has incorporated tritiated thymidine. $\times 400$.
- PHOTO 2. Autoradiograph of medullary area of the DMBA-mammary carcinoma after 1.5 days of cumulative labeling. Ninety-five to -eight percent of cancer cells has incorporated tritiated thymidine. Compare with Photo 1 and Fig. 5. $\times 400$.
- PHOTO 3. Autoradiograph of the stroma of DMBA-mammary carcinoma 24 hr after ovariectomy (14). A capillary runs transversely in the middle of the photograph. Necrotic changes corresponding the capillary and drastic reduction of labeling index in the stroma are already manifest. However, at this stage, no change is observed in parenchymal cancer cells. $\times 1,000$.



COMPUTER ANALYSIS OF DECYCLING PROCESSES

Manabu TAKAHASHI and Michiyoshi MASUDA

*Department of Pathology, Yamaguchi University School of Medicine**

An automatic method for the analysis of decycling processes was developed to calculate decycling rate, cell loss rate, cell loss factor, birth rate or cell production rate (growth rate in no-loss condition), virtual growth rate (growth rate in non-decycling condition) and other parameters of the cell loss process using data on the fraction of labeled mitoses (FLM), labeling index (LI), and actual growth rate (E). The basis for this analysis is the compartment model that was introduced by D. G. Kendall (10) for the multiple phase birth process. The calculation proceeds in conjunction with the automatic FLM curve analysis, the program for which was modified from that reported previously (23). Since the cell loss rate equals the difference between the actual growth rate and the birth rate, the central problem was how to calculate the latter. A sample calculation using experimental data was presented to show that the results change appreciably depending upon the assumption as to the location of the decycling point within the cell cycle.

Cell loss analysis has been an important subject of investigation for more than a decade and has added much to the knowledge of tumor growth. Of the methods now available, the one that was introduced by Steel and Bensted (20) and further refined by Steel (19) for the measurement of the cell loss factor is the most powerful tool. It involves a technique of cell labeling with tritiated thymidine, but unlike the stathmokinetic method (8, 16), it uses no mitotic inhibitor which may interfere with the progression of cells through interphase or may fail to block mitoses completely. In this respect, his method seems to be advantageous over the others. However, in order that his method be applicable, the cell population must satisfy the requirements that: (1) There is no variability in phase transit time; (2) a cell leaves the cycle only at the post-mitotic boundary; and (3) the specific cell loss rates in proliferative and quiescent cell compartments (P and Q compartments) are identical.

Despite an increasing number of cell loss experiments there exist only a few theoretical works (4, 6, 15, 17, 19). The present report is to propose an automatic method of calculating the cell loss rate and other related parameters. The model is based on the multiple-phase birth-and-death process (22) which was developed from the model introduced by D. G. Kendall (10). The experimental data to be used are the same as in Steel's method but the way in which the data are processed is different. Because a cell loss rate equals the difference between birth rate and growth rate, our attention will be focused upon how to estimate the rate of cell flow across the mitotic boundary from the fraction of labeled mitoses (FLM) curve and the observed growth

* Kogushi 1144, Ube 755, Japan (高橋 学, 益田道義).

rate. It demands modification of the current program for automatic FLM curve analysis (23) so as to be compatible with a decycling population. A newly-developed program and its application to the actual data will be described.

Principle of Analysis

In a cell population growing by binary fission, one cell is added to the population at each cell division and under the condition that no cell is lost, the growth rate should equal the cell production rate or birth rate, defined as the rate at which cells cross the division boundary. If cells are lost, the actual growth rate E is less than the birth rate κ_P and the difference may be equated to a cell loss rate κ_L :

$$\kappa_L = (a-1)\kappa_P - E \quad (1)$$

where $a=2$, for example, corresponds to binary fission (Fig. 1). It holds universally, independent of the relative cell loss rates in the P and Q compartments or variable phase transit time. In a cell population with stabilized age distribution the specific growth rates of the P and Q compartments are equal so that the increased P cell loss rate results in a decrease in the growth rate E of the whole population. However, loss of Q cells does not affect E and increases κ_L . It does not contradict Eq. (1) because κ_P is increased and the increased Q cell loss rate raises the growth fraction (see Eq. (8)).

In the stathmokinetic method κ_P is estimated from the rate of accumulation of arrested mitoses. It would be an ideal method if an agent is available which effects a complete block of cells at mitosis with no interference with the cell progression through other phases. In the labeling method of Steel (19), the cell loss factor, *i.e.*, the ratio of

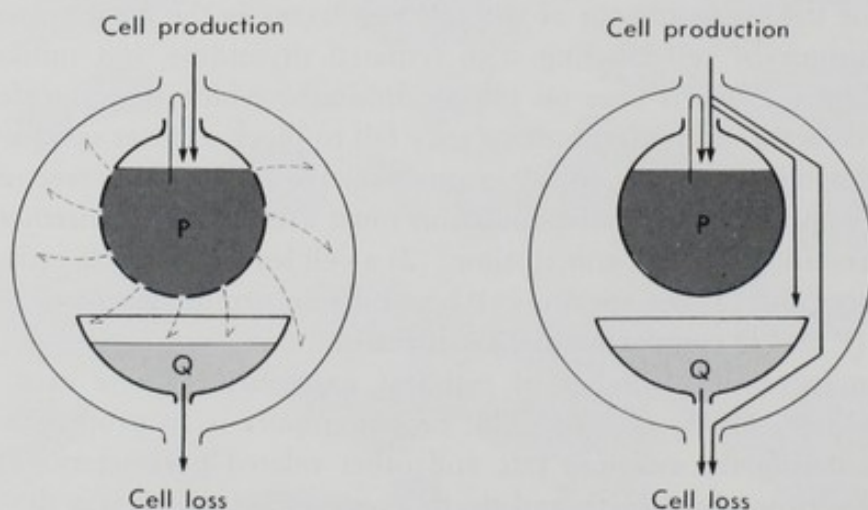


FIG. 1. A block diagram showing the relation among influx, efflux, and growth. Siphoned water is doubled in volume before it returns to P. The one volume replaces water that was withdrawn and another may be interpreted as influx into the system (outer circle) from outside. The influx which equals the rate of withdrawal can be read from a flow meter in the siphon. The efflux is given by the difference between the influx and the rate of increase of the total volume. The left side of the figures represents random decycling (Model A) and the other, post-mitotic decycling (Model B).

κ_L to κ_P , is calculated by the well-known equation which involves the potential doubling time T_d^{pot} (doubling time of a no-loss population)

$$\phi = 1 - \frac{T_d^{\text{pot}}}{T_d} \quad (2)$$

It is valid if and only if

$$\kappa_P = \frac{\ln 2}{T_d^{\text{pot}}} \quad (\text{see Discussion}) \quad (3)$$

because

$$E = \frac{\ln 2}{T_d^{\text{pot}}} \quad (4)$$

T_d^{pot} is estimated according to

$$\frac{\ln 2}{T_d^{\text{pot}}} = \frac{\ln \alpha}{T_C} \quad (5)$$

where T_C is the cell cycle time and α is the number of P cells to be born per division which is related to the growth fraction GF:

$$\alpha - 1 = \text{GF} \quad (6)$$

However, a nonvariable transit time is a necessary condition for Eq. (5) and two additional assumptions (see p. 67) for Eq. (6). A calculation of the growth fraction in a post-mitotically decycling population poses another problem.

Therefore, a calculation of the birth rate is a central problem in cell loss analysis and it will be achieved by formulating the rate of cell flow across the end of the cell-cycle in terms of the parameters to be obtained from the FLM analysis.

Birth Rate of Decycling Population

According to the compartment model (22), a cell progression through the cycle constitutes a Poisson process in which the cell moves from one compartment to the next with a transition probability density $\lambda_i (i=1, 2, \dots, K)$. Therefore, the rate of P cell flow across the division boundary is

$$\kappa = \lambda_K \cdot f_K \quad (7)$$

where f_K is the relative number of cells in the last compartment (Fig. 2) and λ_K and f_K are measured by FLM analysis.

The available programs (1, 3, 5, 21, 23) assume a non-decycling population and these programs do not apply exactly to a decycling population. Although the best-fitting FLM curve may be identical, the parameters associated with it are different. As discussed in the Appendix, the shape of the FLM curve depends more or less on the decycling unless it occurs at random throughout the cycle. It leads to the consequence that a probability density of decycling δ must be known in advance to analyze the FLM curve correctly. On the other hand, in order to determine δ , correct estimates of the mean phase transit time $\bar{T}(j)$ and the number of compartments $k(j)$ are needed. Therefore, δ , $\bar{T}(j)$, and $CV(j)$ must be optimized simultaneously and progressively so as to make them consistent both with the given FLM curve and the growth rate. This

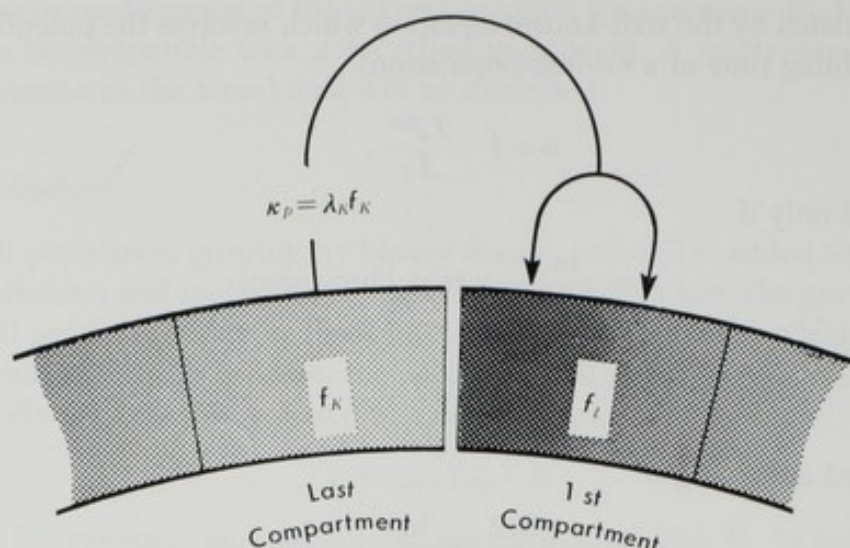


FIG. 2. The rate of crossing a division boundary. It equals the rate at which cells are added to the population (see Fig. 1).

can be achieved by adjusting δ properly by the growth rate equation, Eq. (13), at each step of the optimization of other parameters (see next Section).

If κ is obtained by Eq. (7), a specific birth rate in the whole population κ_P is given by

$$\kappa_P = \kappa \cdot GF \quad (8)$$

or

$$\kappa_P = \lambda_K \cdot f_K \cdot GF \quad (9)$$

where GF is the growth fraction to be calculated from labeling indices within P compartment LI_P and of the whole population LI_{P+Q} :

$$GF = \frac{LI_{P+Q}}{LI_P} \quad (10)$$

In the following, Model A and Model B will be considered. Model A assumes random decycling occurring at a uniform rate δ (decycling probability density) throughout the entire cycle and Model B assumes that decycling occurs only at one of the phase boundaries.

FLM Analysis for Decycling Population

Model A: In a random-decycling population, the distribution of cells around the cell cycle is independent of the decycling probability density δ . Therefore, the FLM curve as well as the relative cell number in each compartment f_i are the same as in the non-decycling counterpart and $\lambda(j)$ can be calculated from

$$\bar{T}_0(j) = \frac{k(j)}{\lambda(j)} \quad (11)$$

where $\bar{T}_0(j)$ and $k(j)$ are the mean transit time and the number of compartments obtained from FLM curve analysis using the Takahashi-Hogg-Mendelsohn (THM)

program (23) without any modification. However, $\bar{T}(j)$ true for a random-decycling population must be corrected according to Eq. (12) after δ is calculated. This argument is intuitively correct but it can be confirmed by using a procedure that optimizes $\bar{T}(j)$ and δ simultaneously. Although the THM program operates on $\bar{T}_0(j)$, it can be converted to

$$\bar{T}(j) = \frac{k(j)}{\lambda(j) + \delta} \quad (12)$$

using solution δ of

$$\prod_{j=1}^4 \left(1 + \frac{1}{\lambda(j)} (E + \delta) \right)^{k(j)} = a \quad (\text{growth rate equation}). \quad (13)$$

In any other respect the procedure is the same as described previously (23) and f_i is given by recurrence formulae:

$$f_i = \begin{cases} f_{i-1} \cdot \frac{\lambda(j)}{\lambda(j) + \delta + E} & [\sum_{l=1}^{j-1} k(l) < i \leq \sum_{l=1}^j k(l)] \end{cases} \quad (14)$$

$$f_i = \begin{cases} f_{i-1} \cdot \frac{\lambda(j)}{\lambda(j+1) + \delta + E} & [i = 1 + \sum_{l=1}^j k(l)] \end{cases} \quad (15)$$

where Eq. (15) is for the first compartment of each phase.

As discussed in the Appendix, the shape of the FLM curve is determined by a set of *characteristic roots* (i.e., $E + \delta$, real or imaginary) of the growth rate equation, Eq. (13). Therefore, $\lambda(j)$'s $k(j)$'s and a set of $E + \delta$ are the parameters that can be determined from FLM analysis. The largest one of the characteristic roots represents the virtual growth rate E_0 to be attained in the assumed absence of decycling

$$E_0 = E + \delta \quad (16)$$

and it is the parameter that can be measured and is required to calculate f_i (Eqs. (14) and (15)). It implies that as long as a random-decycling population is concerned, the matter of δ may be forgotten in calculating κ_p .

Model B: If the decycling occurs at the end of the j -th phase, the influx into the next phase is diminished by a factor r called the "reproductive coefficient" (22) that satisfies the growth rate equation:

$$\prod_{j=1}^4 \left(1 + \frac{E}{\lambda(j)} \right)^{k(j)} = ar \quad (\text{see Eq. (A10)}). \quad (17)$$

Therefore, the next compartment obeys

$$\frac{d}{dt} n_{i+1}(t) = r \cdot \lambda(j) n_i(t) - \lambda(j+1) n_{i+1}(t) \quad [i = \sum_{l=1}^j k(l)] \quad (18)$$

whereas the equations for other compartments are unchanged from those for the non-decycling population. Since no decycling occurs within each phase,

$$\bar{T}(j) = \frac{k(j)}{\lambda(j)}. \quad (19)$$

Recurrence formulae for f_i are the same as Eqs. (14) and (15) except that

$$\delta = 0 \quad (20)$$

and

$$f_{i+1} = r \cdot f_i \frac{\lambda(j)}{\lambda(j+1) + E} \quad [i = \sum_{l=1}^j k(l)] \quad (21)$$

which is for the first compartment of the $(j+1)$ -th phase. This causes the difference in the calculation of LI_P and GF.

Miscellaneous Parameters of Decycling Processes

During the calculation of the cell loss factor ϕ several other parameters were obtained such as the birth rate κ_P (Eq. (9)), cell loss rate κ_L (Eq. (1)) and growth fraction GF (Eq. (10)). The reproductive coefficient defined as a probability for a newly born cell to complete the cycle can be obtained from Eq. (17) for Model B. The corresponding value for Model A is given by

$$r = \prod_{j=1}^4 \left(\frac{\lambda(j)}{\lambda(j) + \delta} \right)^{k(j)} \quad (22)$$

where δ can be estimated from Eq. (16) (see also Eq. (12)). By analogy, a decycling coefficient may be defined as the probability that a newly born cell fails to divide, *i.e.*,

$$d = 1 - r. \quad (23)$$

It seems to be of some value to introduce a decycling rate κ_D and a decycling factor ϕ_D which are comparable to the cell loss rate and cell loss factor, respectively

$$\kappa_D = \delta \cdot GF \quad (24)$$

and

$$\phi_D = \frac{\kappa_D}{\kappa_P}. \quad (25)$$

These parameters can be calculated for a Model B population as well because r is known for Model B from Eq. (17) and the equivalent δ can be obtained by solving Eq. (22). The virtual growth rate E_0 is the largest real root of

$$\prod_{j=1}^4 \left(1 + \frac{E}{\lambda(j)} \right)^{k(j)} = a \quad (26)$$

and can be approximated by

$$E_0 = \frac{2^{CV^2c} - 1}{CV^2c} \cdot \frac{1}{T_c} \quad (\text{see Eq. (A12)}). \quad (27)$$

Sample Calculation

The entire procedure of calculations was programmed in FORTRAN for a FACOM 230-75 (Kyushu University Computer Center) and was applied to the culture line derived from diethylstilbestrol-induced renal carcinoma of Syrian hamsters.

TABLE I. Cell Cycle Parameters vs. Decycling Modes

Mode of decycling	G1	S	G2	M	C	S. D.
Post-mitotic	11.70 [9]	12.43 [3]	4.98 [3]	0.86 [3]	29.97 (0.289)	0.07313
Pre-synthetic	11.72 [9]	12.43 [3]	4.98 [3]	0.86 [3]	29.98 (0.289)	0.07312
Post-synthetic	11.55 [9]	12.40 [3]	4.80 [3]	1.12 [3]	29.87 (0.288)	0.07339
Pre-mitotic	11.55 [9]	12.40 [3]	4.80 [3]	1.12 [3]	29.87 (0.288)	0.07339
Random	11.91 [7]	12.35 [3]	4.91 [3]	0.96 [3]	30.13 (0.296)	0.07328

The figures are mean phase lengths in an hour and the number of compartments [] or coefficient of variation of cell cycle time (). S. D. is the standard deviation of the FLM data from regression (in FLM units).

TABLE II. Parameters Relevant to Cell Loss Process

Mode of decycling	λ_K	f_K	GF	LI_P	κ_P	κ_L	ϕ	E_0	r	δ
Post-mitotic	350.55	0.78	63.80	38.03	1.73	0.26	15.13	2.38	76.44	0.91
Pre-synthetic	350.59	0.68	72.54	34.44	1.73	0.26	15.14	2.38	76.62	0.91
Post-synthetic	266.98	0.82	61.13	40.68	1.32	-0.15	-11.17	2.39	76.20	0.92
Pre-mitotic	266.95	0.79	63.19	39.39	1.32	-0.15	-11.18	2.39	76.20	0.92
Random	312.57	0.74	66.48	37.46	1.54	0.07	4.66	2.32	77.25	0.85

$$E = 1.47 \text{ (\%/hr)} \quad LI_{P+Q} = 24.9 \text{ (\%)}$$

Dimension: λ_K (% of K -th compartment cells/hr), f_K (% of P cells), GF (%), LI_P (% of P cells), κ_P (%/hr), κ_L (%/hr), ϕ (%/division), E_0 (%/hr), r (%/cycle), and δ (%/P cells/hr).

The input data (14) were: (1) Actual specific growth rate ($E=0.0147 \text{ hr}^{-1}$) or population doubling time ($T_d=47.2 \text{ hr}$); (2) pulse labeling index ($LI_{P+Q}=0.249$), and (3) the fraction of labeled mitoses and the initial M/L ratio ($M/L=0.06$).

The estimate of mean phase lengths (except \bar{T}_M) varied only slightly depending upon the presumed mode of decycling, and \bar{T}_M was 30% greater when a decycling point was located behind the end of the S phase than elsewhere (Table I). The effect on the estimate of the cell loss rate or cell loss factor was more pronounced (Table II).

The assumption of post-mitotic or pre-synthetic decycling has led to more than three times as large a ϕ as the estimate based on a random decycling model. Furthermore, by assuming post-synthetic decycling, ϕ became negative indicating that such an assumption is unacceptable in this example, but a random decycling model cannot be rejected. Therefore, unless further experimental evidence about the decycling mode is given, a tentative conclusion would be that ϕ is in between 15.1% and 4.7%, which corresponds to G1 decycling and random decycling, respectively. According to Steel's method (19) ϕ was estimated as 8%. It is 47% less than the corresponding value (15.1%) calculated by the present method, and the difference may be attributed partly at least to his assumption of an equal cell loss rate in the P and Q compartments which may not be valid in an actual population. However, it was within the range of uncertainty.

Should no decycling occur in mitosis, the same birth rate should be obtained by the application of the above-described principle to the pre-mitotic boundary and this was confirmed by actual calculation.

The calculation of the decycling probability density was less sensitive to the pre-

sumed mode of decycling and it was estimated that 0.9% of P cells leave from the cycle per hr (the decycling rate: 0.6% of population/hr and decycling factor: 34–44% per division).

Comment

A phenomenon called decycling shares conceptual overlapping with the cell loss that refers to a substantial loss of volume or of cell number because some proliferative cells disappear immediately after dropping off the cycle by lysis. However, decycling is not identical to the cell loss because the latter includes the loss of quiescent cells (Q cells) and because some cells coming out of the cell cycle are not lost and remain in the Q compartment.

Decycling is the only factor that counteracts growth that is driven by the cell cycling. A loss of noncycling cells, on the other hand, has no effect at all on the specific growth rate E although it increases the growth fraction GF. This will be realized if one pays attention to an equality of the specific growth rates of the P and Q compartments in a stabilized exponential growth. In contrast, the loss of noncycling cells increases the specific birth rate κ_P by increasing the growth fraction (see Eq. (9)) and leads to an increase in the cell loss rate κ_L (see Eq. (1)). Noting that the loss of Q cells has no effect on the specific growth rate and the population doubling time, it will be clear, by analogy, that a potential doubling time T_d^{pot} (doubling time in the assumed absence of cell loss) does not reflect the Q cell loss rate which has to be taken into account in the calculation of the cell loss factor ϕ . Therefore, ϕ cannot be determined from T_d^{pot} and T_d except under a special condition.

From the discrepancy between the cell cycle time T_c and the population doubling time T_d one can calculate the decycling rate, but these measurements are not enough to calculate κ_L or ϕ . In the present analysis the labeling index LI_{P+Q} is used in addition to the growth rate and the cell cycle parameters. Although the birth rate κ_P (cell production rate) plays a central role in this method, it may as well be regarded as a numerical technique of adjusting κ_L (within a constraint from a given FLM curve) in such a way that both of the calculated LI_{P+Q} and E of the model are equalized to the corresponding experimental data.

One of the characteristics of the present method is that no restrictive assumption is made as to the relative cell loss rates in the P and Q compartments. At first glance, it may appear justifiable to include all the cell loss into Q cell loss assuming that a loss of a P cell is actually a loss of a Q cell at zero age, but it is not truly so. However, if P cell loss is defined as such, the P cell loss rate should be infinitesimal as compared to the Q cell loss rate which is represented by the whole area under the distribution curve of Q cell survival time. It also raises a semantic problem when considering a situation in which a P cell is lost accidentally by metastasis or exfoliation while the cell is still going on in the cell cycle. Therefore, the possibility must be admitted that a cell may be lost directly from the P compartment. In such a case, P cell loss should be regarded as an age-independent random process. Based on the experimental data, Lala (12) argued in favor of a preferential loss from the noncycling compartment and Mendelsohn and Dethlefsen (15) demonstrated that the P cell loss rate was practically zero in two out of three tumor strains examined. Consequently, it seems appropriate to assume that

the actual cell population is represented by a mixture of Model A and Model B processes until further evidence is provided to choose one over the other. Another point of interest in connection with the calculation of the cell loss rate is the mode of decycling, which affects age distribution and hence the relative cell number in the S phase. The sample calculation also demonstrated that this was actually the case. Of the five decycling modes that were examined, decycling at the post-synthetic or pre-mitotic phase boundary was found to be unacceptable in this particular example because a negative value is obtained for the cell loss factor ϕ . On the other hand, post-mitotic or pre-synthetic decycling was considered to be possible and this is in accordance with a widely held view that cells enter G_0 post-mitotically or during passage through G_1 (2, 7, 11, 13). Steel's method (19) was also based on the assumption of post-mitotic decycling. Nevertheless, other possibilities such as random decycling from the entire cycle are by no means excluded. The present investigation undertaken to relax the necessary condition of equal cell loss rate in the P and Q compartments has ended up with a need for an assumption on the mode of decycling which is not known exactly. However, because the actual mode of decycling may coincide with either one of the assumptions or with a combination thereof, the program that was developed in this study permits calculation of the probable range in which the true solutions would fall.

In the application of this method the tumor volume must be corrected for the necrotic fraction. It is only with this precaution that the loss from the viable compartment (including conversion to necrotic mass) is measurable. If no such correction is made, the non-viable fraction is operationally included into the Q compartment and the calculated cell loss rate represents the total resorption rate in the whole tumor mass. This point seems to be important in the study of solid tumors.

Acknowledgments

We express our sincere thanks to Dr. Joe W. Gray and Dr. Mortimer L. Mendelsohn of Lawrence Livermore Laboratory for their valuable discussions and suggestions. Without their help, this paper would not have been completed. We are also grateful to Mrs. N. Fukuda for her skillful assistance in the programming. This work was supported in part by a Grant-in-aid for Cancer Research (No. 901005) from the Ministry of Education, Science and Culture of Japan.

MATHEMATICAL APPENDIX

According to the compartment model of the cell cycle (22), cell population kinetics can be described by the matrix equation (state equation)

$$\frac{d}{dt} \mathbf{n}(t) = \phi \mathbf{n}(t) \quad (\text{A1})$$

where ϕ is the growth rate matrix. Depending upon whether decycling occurs at random or at a phase boundary,

$$\phi = \begin{pmatrix} -(\lambda_1 + \bar{\delta}) & \cdot & \cdot & \cdot & \cdot & a\lambda_K \\ \lambda_1 & -(\lambda_2 + \bar{\delta}) & & & & \\ & \cdot & \cdot & & & \\ & & \cdot & \cdot & & \\ & & & \cdot & \cdot & \\ & & & & \cdot & \\ & & & & & \lambda_{K-1} & -(\lambda_K + \bar{\delta}) \end{pmatrix} \quad (\text{A2})$$

or

$$\phi = \begin{pmatrix} -\lambda_1 & \cdot & \cdot & a\lambda_K \\ \lambda_1 & -\lambda_2 & & \\ & \cdot & \cdot & \\ & & r\lambda_i & -\lambda_{i+1} \\ & & & \cdot \\ & & & & \lambda_{K-1} & -\lambda_K \end{pmatrix} \quad [i = k(j)] \quad (\text{A3})$$

In a population with stabilized age distribution (whether stationary or growing exponentially), the initial condition $\mathbf{n}(0)$ as well as the later development $\mathbf{n}(t)$ are all specified by ϕ . As described in the preceding paper (22), the matrix equation Eq. (A1) can be solved using the Laplace transform in the form of

$$\mathbf{n}_i(t) = \sum_{j=1}^K C_{ij} \exp(e_j t) \quad (\text{see Eq. (A6) for } C_{ij}) \quad (\text{A4})$$

where

$$e = (e_1, e_2, \dots, e_K)$$

is the eigenvalue spectrum of ϕ and the element e_j (eigenvalue of ϕ) is the characteristic root of

$$|\phi - xU| = 0 \quad (\text{A5})$$

which also serves as the growth rate equation (see Eqs. (A9) and (A10)) and the coefficient C_{ij} is given by

$$C_{ij} = g_i(e_j)/g'(e_j) \quad (\text{A6})$$

where $g'(x)$ is the derivative of the left side of Eq. (A5) and $g_i(x)$ is a determinant made by replacing the i -th column of $\phi - xU$ with $\mathbf{n}(0)$. Therefore, the kinetic behavior in the steady state including the fraction of the labeled mitoses curve is uniquely determined by ϕ .

Automatic FLM analysis is a computerized technique of optimizing the elements of ϕ (assuming $\bar{\delta}=0$ and $r=1$) by way of fitting the associated FLM curve to the data whereby the mean and the coefficient of the variation in phase transit time are calculated according to

$$\bar{T}(j) = \frac{k(j)}{\lambda(j)} \quad (\text{A7})$$

and

$$CV(j) = k(j)^{-1/2}. \quad (\text{A8})$$

In the THM program (23), additional information on the ratio of mitoses to labeled cells (M/L ratio) is utilized in order to measure λ in the M phase. However, because

the information about a net increase of labeled cells is abolished in the FLM data by taking the ratio to total mitoses, the specific growth rate E is required to determine δ or r . The newly developed program makes use of E to control δ or r in such a way that it satisfies the growth rate equation which is either

$$\prod_{j=1}^4 \left(1 + \frac{1}{\lambda(j)} (x + \delta) \right)^{k(j)} = a \quad [\text{Model A}] \quad (\text{A9})$$

or

$$\prod_{j=1}^4 \left(1 + \frac{1}{\lambda(j)} x \right)^{k(j)} = ar \quad [\text{Model B}]. \quad (\text{A10})$$

Virtual growth rate in the assumed absence of decycling E_0 is the real root of Eq. (A9) or Eq. (A10) with $\delta=0$ or $r=1$. When considering a cell population having the same λ for all the compartments, the equation can be solved in the form of

$$E_0 = \lambda(a^{1/K} - 1) \quad (\text{A11})$$

or

$$E_0 = \frac{a^{CV^2c} - 1}{CV^2c} \cdot \frac{1}{T_0}. \quad (\text{A12})$$

REFERENCES

1. Ashihara, T. Computer optimization of the fraction of labeled mitoses analysis using the fast Fourier transform. *Cell Tissue Kinet.*, **6**, 447-452 (1973).
2. Augenlicht, L. H. and Baserga, R. Changes in the G0 state of WI-38 fibroblasts at different times after confluence. *Exp. Cell Res.*, **89**, 255-262 (1974).
3. Barrett, J. C. Optimized parameters for the mitotic cycle. *Cell Tissue Kinet.*, **3**, 349-353 (1970).
4. Bjerknes, R. Exponential growth. *Eur. J. Cancer*, **10**, 165-168 (1974).
5. Brockwell, P. J., Trucco, E., and Fry, R.J.M. The determination of cell cycle parameters from measurements of the fraction of labeled mitoses. *Bull. Math. Biol.*, **34**, 1-12 (1972).
6. Chuang, S. N. and Lloyd, H. H. Mathematical analysis of cancer chemotherapy. *Bull. Math. Biol.*, **37**, 147-160 (1975).
7. Epifanova, O. I. and Tersikh, V. V. On the resting periods in the cell life cycle. *Cell Tissue Kinet.*, **2**, 75-193 (1969).
8. Iversen, O. H. Kinetics of cellular proliferation and cell loss in human carcinomas. *Eur. J. Cancer*, **3**, 389-394 (1967).
9. Jagers, P. and Norrby, K. Estimation of the mean and variance of cycle time in cinemicrographically recorded cell populations during balanced exponential growth. *Cell Tissue Kinet.*, **7**, 201-211 (1974).
10. Kendall, D. G. On the role of variable generation time in the development of a stochastic birth process. *Biometrika*, **34**, 316-330 (1948).
11. Lajtha, L. G. Cytokinetics and regulation of progenitor cells. *J. Cell Physiol.*, **67** (Suppl. 1), 113-148 (1966).
12. Lala, P. K. Evaluation of the mode of cell death in Ehrlich ascites tumor. *Cancer*, **29**, 261-266 (1972).
13. Lala, P. K. and Patt, H. M. A characterization of the boundary between the cycling and resting states in ascites tumor cells. *Cell Tissue Kinet.*, **1**, 137-146 (1968).
14. Masuda, M. The effects of diethylstilbestrol (DES) on the cell cycle of DES-induced

- renal carcinoma of Syrian hamster *in vitro*. *Bull. Yamaguchi Med. Sch.*, **22**, 227-238 (1975).
15. Mendelsohn, M. L. and Dethlefsen, L. A. Cell kinetics of breast cancer: The turnover of nonproliferating cells. *Recent Results Cancer Res.*, **42**, 73-86 (1973).
 16. Refsum, S. B. and Berdal, P. Cell loss in malignant tumours in man. *Eur. J. Cancer*, **3**, 235-236 (1967).
 17. Shackney, S. E. A cytokinetic model for heterogeneous mammalian cell populations. I. Cell growth and cell death. *J. Theor. Biol.*, **38**, 305-333 (1973).
 18. Steel, G. G. Cell loss factor in the growth rate of human tumours. *Eur. J. Cancer*, **3**, 381-387 (1967).
 19. Steel, G. G. Cell loss from experimental tumours. *Cell Tissue Kinet.*, **1**, 193-207 (1968).
 20. Steel, G. G. and Bensted, J.P.M. *In vitro* studies of cell proliferation in tumours. *Eur. J. Cancer*, **1**, 275-279 (1966).
 21. Steel, G. G. and Hanes, S. The technique of labeled mitoses: Analysis by automatic curve-fitting. *Cell Tissue Kinet.*, **4**, 93-105 (1971).
 22. Takahashi, M. Theoretical basis for cell cycle analysis. II. Further studies on labeled mitosis wave method. *J. Theor. Biol.*, **18**, 195-209 (1968).
 23. Takahashi, M., Hogg, J. D., and Mendelsohn, M. L. The automatic analysis of FLM curves. *Cell Tissue Kinet.*, **4**, 505-518 (1971).
 24. Takahashi, M. Kinetic analysis of decycling cell population by the application of a compartment model of the cell cycle. In "Mathematical Models in Cell Kinetics," ed. A-J. Valleron, pp. 29-30 (1975). European Press Medikon, Ghent Belgium.

PRIMORDIAL GERM CELL PROLIFERATION AND ITS
RELATION TO TERATOCARCINOGENESIS IN MICE

Takehiko NOGUCHI

*Genetic Stock Center, National Institute of Genetics**

The proliferative behavior of primordial germ cells (PGC) during the fetal age covering the critical period for teratocarcinogenesis was studied for several sublines of 129 mice which differ in the incidence of congenital testicular teratomas. 1) In sublines with low tumor incidences, the mitotic activity of PGC started to decrease precipitously from in the fetal age at about late in the 13th day of gestation. This pattern of decline in mitotic activity exactly, but with a short lag period, paralleled that of susceptibility of fetal testes to experimental teratocarcinogenesis by the transplantation method of Stevens. This suggests that the risk group PGC in teratocarcinogenesis may be those retaining this proliferative capacity. 2) In a subline with the highest incidence of the tumor (33%), several unusual phenomena in PGC proliferation were found in some of the testes: (i) a decrease in dividing cell number per testis at the 13th day of gestation; (ii) an extension of the PGC proliferative period; (iii) a marked reduction in PGC number. 3) Based on the pattern of PGC proliferation, testes of the subline with the highest tumor incidence fell into three subgroups: (i) normal testes (Group 1), (ii) testes with longer proliferative period (Group 2), (iii) testes having the longest proliferative period and sparse PGC (Group 3). 4) Teratoma incidences estimated for Groups 1, 2, and 3 testes were 7%, 50%, and near 90%, respectively. It is suggested that the longer proliferative period of PGC is correlated with the higher incidence of testicular teratomas in strain 129 mice. 5) Fetuses having Group 2 and those having Group 3 testes had high incidences of bilateral teratomas.

Testicular teratomas in inbred strain 129 mice are derived from primordial germ cells (PGC) (10, 11, 15, 16). The earliest recognizable teratomatous foci appear as clusters of multipotential embryonic cells within the seminiferous tubule of the fetus (7, 15, 16). Teratomas are formed as the result of the growth and differentiation of these embryonic cells (6, 7, 15, 16). The incidence of the tumor is, therefore, primarily dependent on the frequency of the conversion of PGC into multipotential embryonic cells. This conversion has been believed to be an epigenetic change rather than to be a mutational one. Little is known about the specific mechanism underlying this mis-differentiation of PGC.

Many genetic and nongenetic factors are known to influence the incidence of teratomas (8, 9, 11-14). The incidence of spontaneous teratomas varies among sublines of strain 129 and in strains derived from them. Evidence hitherto accumulated (7, 8,

* Yata 1111, Mishima 411, Japan (野口武彦).

9, 14) suggests that the critical period for the conversion resides in a rather narrow period of fetal development. On the other hand, it is known that after migration into the genital ridge PGC continue to divide for a short period of time and then enter a mitotically quiescent stage (4). We noticed that the critical period for teratocarcinogenesis roughly coincides with the period when a decline in mitotic activity of PGC occurs. We therefore performed a quantitative analytical study on the proliferative behavior of PGC in fetal testes in relation to the incidence of congenital testicular teratomas. We compared the proliferative pattern of PGC among three sublines of 129 mice with high, intermediate and low incidences of teratomas using serial histological sections of a large number of fetal testes. This paper will review the results, especially the unusual proliferative behavior of PGC found in some testes of a strain of mice with a high incidence of spontaneous testicular teratomas (3).

Critical Period of Teratocarcinogenesis and PGC Differentiation

1. Critical period of teratocarcinogenesis in strain 129 mice

The first recognizable teratomatous foci appear at the 15th day of gestation in 129/Sv mice, and the 16th day in 129/Sv-ter mice (7, 13). On the other hand PGC in 12-day male genital ridges retain full susceptibility to experimental teratocarcinogenesis by the transplantation method of Stevens (8, 9). The conversion of PGC into multipotent embryonic cells may, therefore, be initiated during the period between the 13th and the 14th day in 129/Sv mice, and during the period between the 13th and the 15th day in 129/Sv-ter mice.

2. Proliferative activity of PGC as an indicator of PGC maturation

Peters (4) reported that after being enveloped in the seminiferous cord PGC continue to divide for a short period of time and then stop dividing temporarily when the supporting cells (Sertoli cells) are arranged around the periphery of the cord, leaving the PGC in the center. This observation implies that a drastic change in the mitotic activity of PGC occurs during the period from the 13th to the 15th day of gestation. Franchi and Mandel (2) described that in fetal rat testes accumulation of mitochondria at one pole of the cell occurs at 16.5 days post coitum. They pointed out the possibility that the mitochondrial polarization may be in some way related to cessation of PGC mitotic activity. The mitotic activity of PGC was, therefore, considered to be an indicator of PGC maturation.

Comparative Studies on Proliferative Activity of PGC in Developing Fetal Testes among 129 Mice Sublines

The incidence of teratomas varies among sublines of strain 129. It is high (33%) in subline 129/Sv-ter Hi-line (hereafter referred to as Hi-line) (13), intermediate (10%) in subline 129/Sv-ter Lo-line (hereafter referred to as Lo-line), and low (0.07%) in subline 129/Sv-+/A^y (hereafter referred to as A^y). Proliferative patterns of PGC in these sublines were compared.

The proliferative activity of PGC was studied using two kinds of indices: the total number of dividing PGC/testis and the mitotic index (dividing cells/dividing+non-

dividing cells). For identification of PGC, the criteria described by Clermont and Perey (1) were adopted. For quantitative staging of fetuses, the maximum head length (hereafter referred to as head length) which was defined as the interval length (mm) between the tip of the nose to the margin of the back of the head, was used because: (1) it could be easily and precisely measured; and (2) it could be easily correlated to gestational days since head length was in direct proportion to the gestational day. Early twelve day fetuses had a head length of about 4 mm. With every one-day increase in fetal age, head length increased by 1 mm.

1. Total number of dividing PGC/testis

Although this index was not in direct proportion to PGC mitotic activity, it was a more sensitive marker, and was more easily determined than the mitotic index. The pattern of change in dividing cell number/testis was first compared among the three sublines of 129 mice. Figure 1 is a summary of the results.

In subline A^y, the indices made a curve with a sharp peak at a head length between 5 and 6 mm. Most of the PGC became mitotically quiescent at about 7 mm head length (the 15th day). In Lo-line, the pattern of change in the index was similar to that of A^y, except that the average value at the peak area was smaller ($P < 0.001$) than that of A^y.

In Hi-line, the peak value became lower ($P < 0.001$) than that of Lo-line. As far as these sublines are concerned, the intensity of this tendency is correlated with a

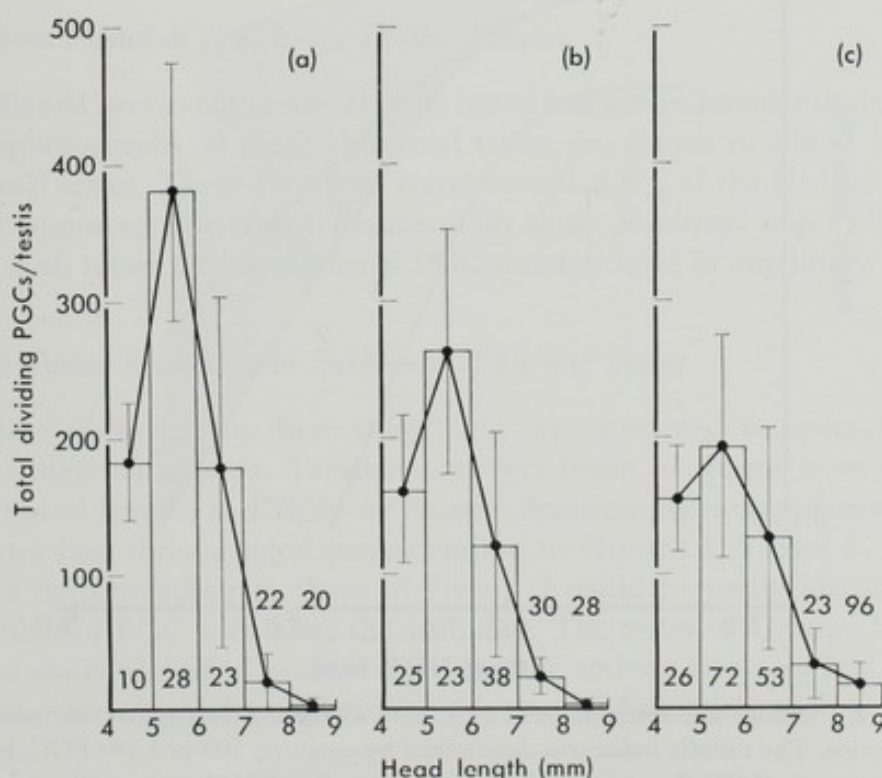


FIG. 1. Change in total number of dividing PGC/testis with increasing fetal age in sublines of 129 mice. The total number of dividing cells was estimated by counting dividing PGC every two sections. (a) 129/Sv-+/A^y. (b) 129/Sv-ter Lo-line. (c) 129/Sv-ter Hi-line. Figures in or above the columns represent the number of testes analyzed.

higher incidence of teratomas. This is the earliest recognizable unusual phenomenon found in strain 129 mice during the critical period of teratocarcinogenesis. The indices of Hi-line testes were distributed in a broader area than those of A^y and Lo-line. Another unusual point in the pattern was that at the tailing area the average index values of Hi-line were larger ($P < 0.1$, between 7 and 8 mm; $P < 0.001$, between 8 and 9 mm) than those of A^y and Lo-line. Testes of A^y and Lo-line rarely contained more than 20 dividing cells at a head length area from 8 to 9 mm. But many Hi-line testes had more than 20 dividing cells even in this late developmental stage, when the testes were old enough to have teratomatous foci. One of the interesting findings here was that the testes having more than 20 dividing cells had teratomas several times more often than testes having less than 20 dividing cells. Another finding of interest was that some of the Hi-line testes had seminiferous tubules with sparse PGC (Fig. 3). Most of these testes had an abnormally small number of dividing PGC at the peak area (5 to 6 mm).

2. Mitotic index

The pattern of change in the mitotic index in developing Hi-line testes was compared to those of A^y and Lo-line. The pattern of decline of mitotic indices of strains A^y and Lo-line were approximately the same. The area in which most of the values of A^y and Lo-line testes fell is schematically shown in Fig. 3 as zone I. Between 5 and

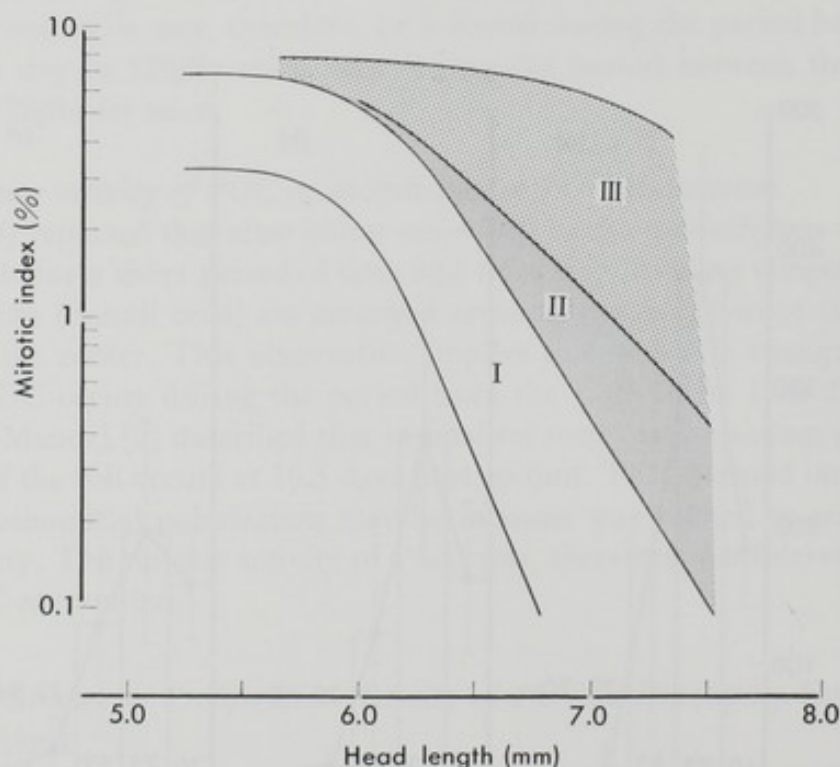


FIG. 2. Change in mitotic index of PGC with increasing fetal age in sublines of 129 mice. The mitotic index was determined by counting 800 to 3,500 PGC, but when testes contained sparse PGC, the index was determined with smaller numbers of PGC. Zone I, almost all of the indices of testes of A^y and Lo-line fell here. Zone II and Zone III, some indices of Hi-line testes fell here, see the text for details. Forty seven testes of A^y, 40 testes of Lo-line, and 166 testes of Hi-line were analyzed.

6 mm head length the indices were maintained as high as 3 to 6%, then decreased precipitously. At 7 mm head length most of the indices became less than 0.5%.

When male genital ridges from 12 1/2-day 129 fetuses were transplanted into adult scrotal testes, 80% of them developed into testes with teratomas (8, 9). When 13 1/2-day and 14 1/2-day genital ridges were similarly transplanted, only 15% and 8% of them had teratomas (9). Accordingly the pattern of change in the mitotic index closely paralleled the pattern of decline in the susceptibility of genital ridges to the experimental teratocarcinogenesis.

The pattern of change in the mitotic index in Hi-line testes again differed from those of A^y and Lo-line. Many index values of Hi-line testes fell in zone I. But some others scattered over zone I during a head length area larger than 6 mm. This suggests that PGC in some Hi-line testes have a longer proliferative period. The testes showing unusual mitotic indices fell in two groups. One group of testes had a normal PGC number level. The other group of testes had a remarkably reduced PGC number. Most of the former group of testes fell in zone II, and the latter group of testes fell in zone III in Fig. 2. Accordingly Hi-line testes finally fell in three subgroups. The first, Group 1 testes, had a normal number of PGC and a normal proliferative pattern. The second, Group 2 testes, had a normal number of PGC, but had a longer proliferative period as suggested by the pattern of the mitotic index. The third, Group 3 testes, were those having an unusually reduced number of PGC, and having a remarkably extended proliferative period.

Abnormal Testes Found in 129/Sv-ter Hi-line Fetuses

As mentioned previously, some Hi-line testes had seminiferous tubules with sparse PGC. Microphotographs of these abnormal testes are shown in Fig. 3 together with those of normal testes. These abnormal testes occupied 8% of the Hi-line testes. These testes always appeared bilaterally. Fetuses with these abnormal testes often coexisted with fetuses with testes having a normal PGC number level in one litter.

Estimation of Tumor Incidences in Subgroups of Hi-line Testes

As Hi-line testes fell in three subgroups, we attempted to estimate the tumor incidences in these subgroups. Teratomatous foci begin to appear from the 16th day (about 8 mm head length) in 129/Sv-ter fetuses. Accordingly it was necessary to divide 16th day testes into three groups corresponding to Groups 1, 2, and 3. As shown in Fig. 3, testes corresponding to those of Group 3 could be easily identified by their reduced number of PGC even after the 16th day. The testes of Groups 1 and 2 were, however, less easily identified because PGC mitotic activity was very low at this stage. A method was then devised to subgroup 16th day Hi-line testes with a normal PGC number level.

As shown in Figs. 1 and 2, the proliferative activity of PGC decreased in a continuous fashion. It is therefore reasonable to consider that the testes of Group 2 were the antecedents of most of the 16th-day testes having a normal number of PGC, but having an unusually high dividing cell number level. Accordingly the 16th day Hi-line

TABLE I. Incidences of Teratomas in Three Subgroups of Fetal Testes from 129/Sv-*ter* Hi-line

Group of testes	Quantity of PGC	Proliferative period of PGC	% testes with teratomas
1 ^a	Normal	Normal	7
2 ^b	Normal	Moderately extended	50
3 ^c	Reduced	Markedly extended	92

^a Testes having 20 or less than 20 dividing PGC, from 29 fetuses with head length 8.2 to 8.6 mm.

^b Testes having more than 20 dividing PGC, from 15 fetuses with head length 8.2 to 8.6 mm.

^c Testes having an extremely reduced number of PGC, from 6 fetuses with head length 8.3 to 11.5 mm.

testes having a normal number of PGC were divided into two groups corresponding to Groups 1 and 2 based on the level of dividing cell number. Table I summarizes the character of the three subgroups of testes and their tumor incidences. The incidences varied greatly among the subgroups.

Group 3 testes always appeared bilaterally. Accordingly fetuses with Group 3 testes had a high tendency to have bilateral teratomas (5/6). Group 2 testes did not necessarily appear bilaterally. Fetuses having at least one Group 2 testis also showed a high incidence of bilateral teratomas (6/15). On the contrary fetuses having Group 1 testes rarely had bilateral teratomas (0/29).

Comment

This is the first experiment that determined quantitatively the pattern of developmental change in the proliferative activity of PGC in the testes of fetal mice. The mitotic index was 3 to 6% until late in the 13th day, and decreased precipitously. This pattern of change in PGC proliferation exactly paralleled the declining pattern of the susceptibility of fetal testes to experimental teratocarcinogenesis. PGC lose their susceptibility to teratocarcinogenesis as they lose their capacity to proliferate.

By comparing the proliferative pattern of PGC in the subline with the highest incidence of teratomas to those of sublines with low incidences of the tumors, three unusual phenomena in the proliferative behavior of PGC were revealed in the subline with the highest incidence. Among these, a decrease in the total number of PGC observed at the 13th day and extension of the proliferative period observed between the 13th day and 15th day were correlative to a high incidence of teratomas. It is possible that the extension of the proliferative period of PGC may enhance, in some way, the risk of conversion of PGC into teratomas.

This experiment showed that the fetuses of strain 129/Sv-*ter* Hi-line are heterogeneous in respect to the character of the testes. The author recently found that some ovaries from Hi-line fetuses had a remarkably reduced number of PGC (unpublished data). Such abnormal ovaries occurred bilaterally as in the case of the testes. The cause of this heterogeneity has not yet been clarified. But the author now has a hypothesis explaining this heterogeneity. The mice strain, 129/Sv-*ter* Hi-line might have a hidden recessive mutation (tentatively called *ter*) which causes the abnormality in the fetal gonad. If male mice have bilateral teratomas, most of them become sterile (13). It is possible that the females with the abnormal ovaries may have some disadvantage in

reproduction. Accordingly this hypothesis implies that it would be very hard to get a subline of mice homozygous for *ter* mutation because of the high risk of sterility. This also means that a Hi-line mice colony might be composed of animals with genotypes of $+/+$, $ter/+$, and ter/ter . This might be the reason why the Hi-line testes were heterogeneous in respect to the proliferative behavior of PGC.

Acknowledgments

The author is very grateful to Dr. Leroy C. Stevens for his cooperation in this work and encouragement. A part of this work was done in the Jackson Laboratory, Bar Harbor, Maine. This work was supported in part by Grants-in-Aid for Scientific Research from the Ministry of Education, Science and Culture, and in part by grant CA02662 from the National Cancer Institute.

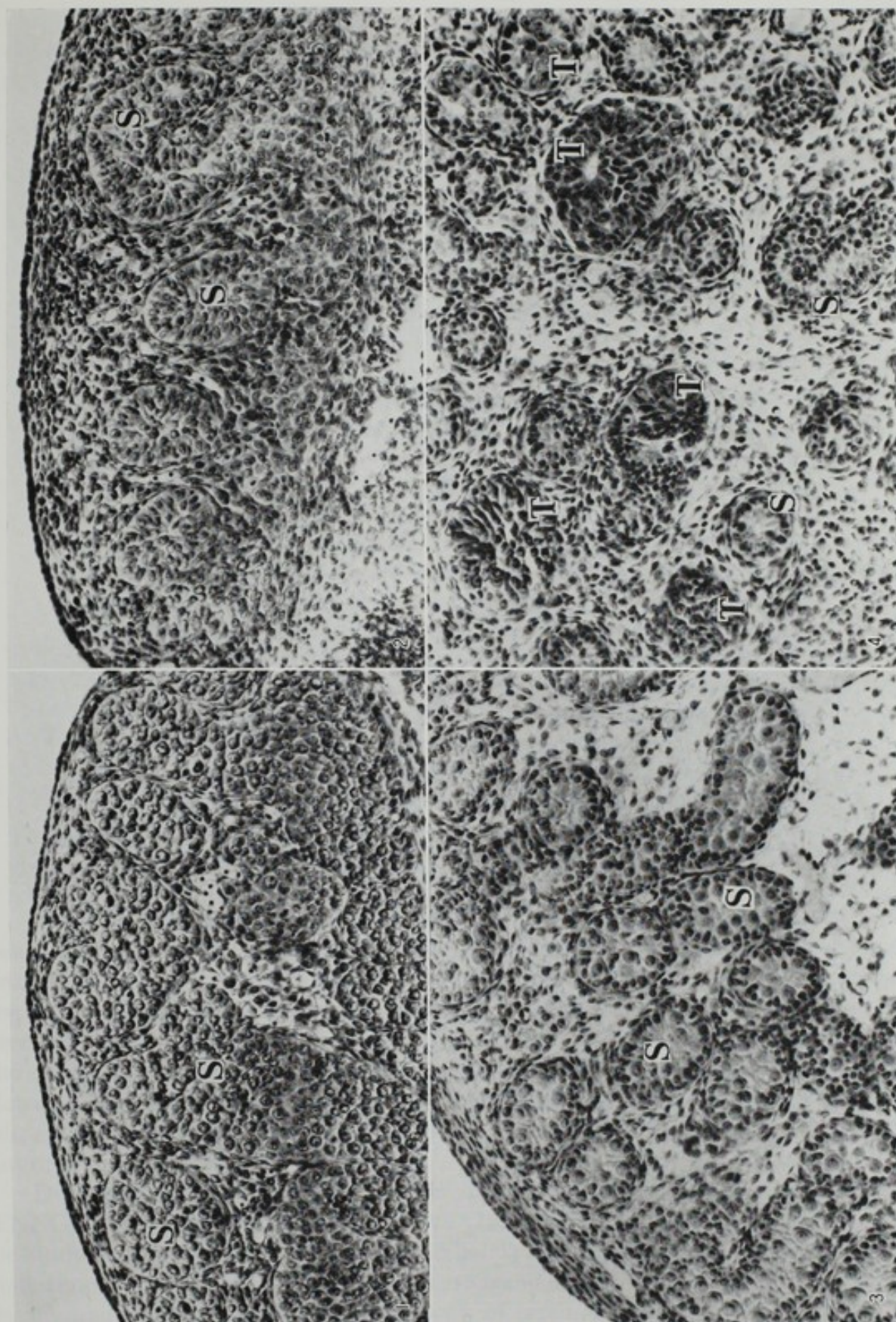
REFERENCES

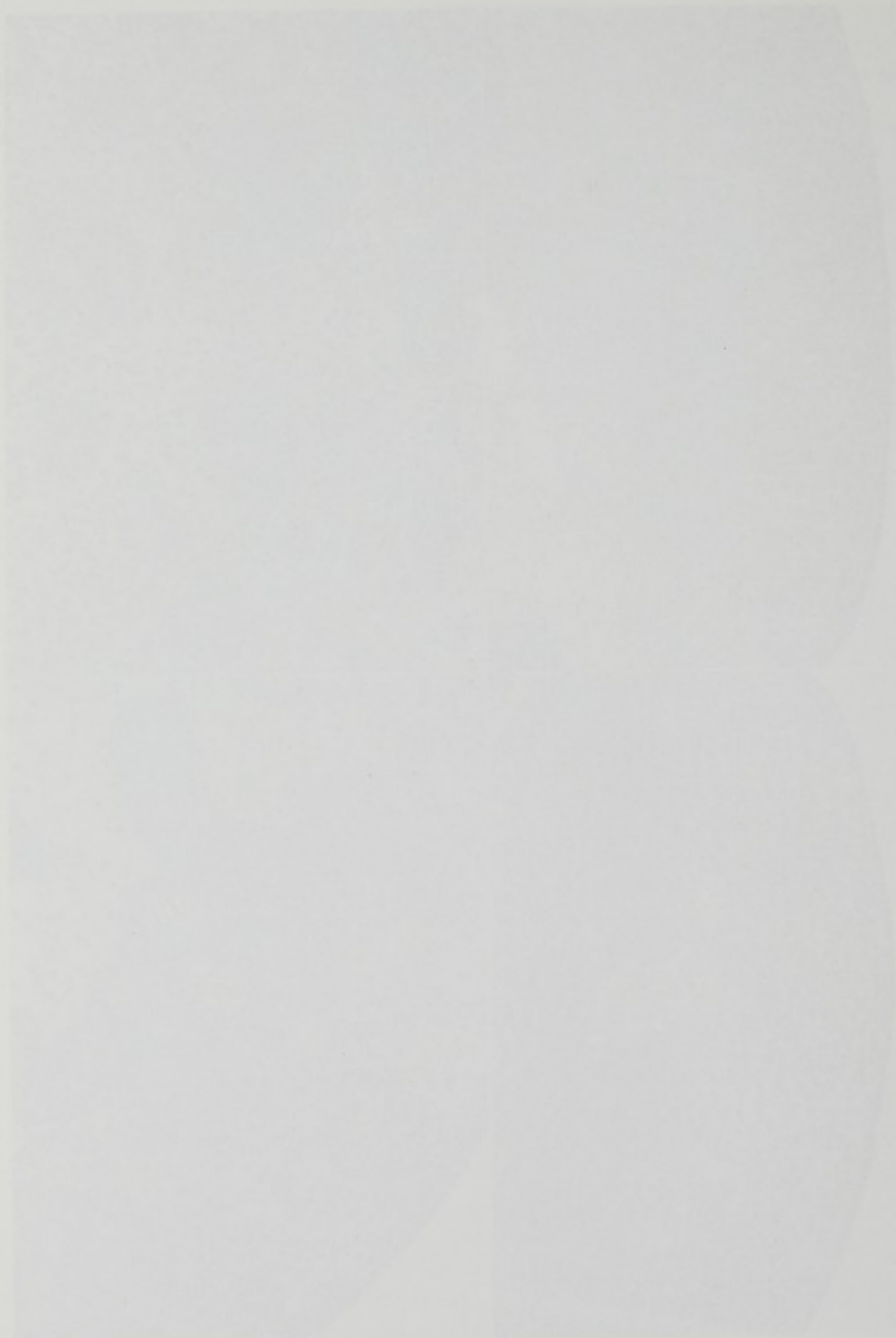
1. Clermont, Y. and Perey, B. Quantitative study of the cell population of the seminiferous tubules in immature rats. *Am. J. Anat.*, **100**, 241-267 (1957).
2. Franchi, L. L. and Mandl, A. M. The ultrastructure of germ cells in foetal and neonatal male rats. *J. Embryol. Exp. Morphol.*, **12**, 289-308 (1964).
3. Noguchi, T. and Stevens, L. C. Primordial germ proliferation in fetal testes of a strain of mice with high incidence of congenital testicular teratomas (in preparation for submission to *J. Natl. Cancer Inst.*).
4. Peters, H. Intrauterine gonadal development. *Fertil. Steril.*, **27**, 493-500 (1976).
5. Stevens, L. C. and Little, C. C. Spontaneous testicular teratomas in an inbred strain of mice. *Proc. Natl. Acad. Sci. U.S.*, **40**, 1080-1087 (1954).
6. Stevens, L. C. Embryology of testicular teratomas in strain 129 mice. *J. Natl. Cancer Inst.*, **23**, 1249-1295 (1959).
7. Stevens, L. C. Testicular teratomas in fetal mice. *J. Natl. Cancer Inst.*, **28**, 247-267 (1962).
8. Stevens, L. C. Experimental production of testicular teratomas in mice. *Proc. Natl. Acad. Sci. U.S.*, **52**, 654-661 (1964).
9. Stevens, L. C. Development of resistance to teratocarcinogenesis by primordial germ cells in mice. *J. Natl. Cancer Inst.*, **37**, 859-867 (1966).
10. Stevens, L. C. Origin of testicular teratomas from primordial germ cells in mice. *J. Natl. Cancer Inst.*, **38**, 549-552 (1967).
11. Stevens, L. C. The biology of teratomas. *Adv. Morphol.*, **6**, 1-31 (1967).
12. Stevens, L. C. Environmental influence on experimental teratocarcinogenesis in testes of mice. *J. Exp. Zool.*, **174**, 407-413 (1970).
13. Stevens, L. C. A new inbred subline of mice (129/*ter*Sv) with a high incidence of spontaneous congenital testicular teratomas. *J. Natl. Cancer Inst.*, **50**, 235-242 (1973).
14. Stevens, L. C. Developmental biology of teratomas in mice. In "ICNUCLA Symposia on Developmental Biology," Vol. 2, pp. 186-204 (1975). Academic Press, New York.
15. Stevens, L. C. Teratocarcinogenesis and spontaneous parthenogenesis in mice. In "Developmental Biology of Reproduction," (1975). Academic Press, New York.
16. Stevens, L. C. Comparative development of normal and parthenogenetic mouse embryos, early testicular and ovarian teratomas, and embryoid bodies. In "Teratomas and Differentiation," pp. 17-32 (1975). Academic Press, New York.

EXPLANATION OF PHOTOS

PHOTOS 1 and 2. Normal and abnormal testes (of Hi-line testes) from littermates having a head length of 5.6 mm and 5.8 mm, respectively.

PHOTOS 3 and 4. Normal and abnormal testes (of Hi-line testes) from littermates having a head length of 10.5 mm and 10.9 mm, respectively. T, teratomatous focus; S, seminiferous tubule. Note the reduced population density of PGC in the tubules in Photos 2 and 4.





CELL KINETICS OF DUODENAL CANCER INDUCED BY N-ETHYL-N'-NITRO-N-NITROSOGUANIDINE IN C3H/He MICE

Masao ITO,^{*1} Seiji YAMADA,^{*1} Mutsushi MATSUYAMA,^{*2}
and Takeo NAGAYO^{*1}

*Laboratories of Pathology^{*1} and Ultrastructure Research,^{*2}
Aichi Cancer Center Research Institute*

Cell kinetics of duodenal cancer in mice induced by N-ethyl-N'-nitro-N-nitrosoguanidine (ENNG) were studied. Well differentiated tubular adenocarcinomas of multiple origin and with homogenous cellular atypia were found in 100% of the duodenal mucosa of C3H/He female mice, induced by oral administration of high doses of ENNG. According to the growth grades, the cancerous lesions were classified into three stages. The mitotic indices were significantly lower in the cancer cells in each stage than those in normal and cancer-bearing but non-tumorous crypt cells. Labeling indices 1 hr after an intraperitoneal injection of tritiated thymidine were also slightly lower in cancer cells in each stage than the indices in normal and non-tumorous crypt cells. The cell cycles of the cancer cells were prolonged for about 4 hr as compared with those of their normal counterparts. The prolongation mainly occurred in the G1 phase. No significant difference in the cell cycles however, was observed between each stage of the cancerous growths. The mode of the invasive growth of duodenal cancer was discussed from the dual viewpoints of histology and cell kinetics.

The idea that cancer cells proliferate more rapidly than normal cells has been assumed for a long time among most investigators, based on the rapid growth of tumor tissues with frequent mitotic figures. Recently however, kinetic studies with autoradiography have revealed that the mitotic indices of leukemic cells or of ascitic tumor cells were rather lower than those of normal proliferative cells and that the cell cycle was also more prolonged in the tumor cells than in their normal counterparts (3, 4, 7, 8). However, the cell kinetics of solid cancers have not been elucidated as those of leukemic cells and of ascitic tumor cells have been, because of technical difficulties and the mosaic nature of solid cancers.

Duodenal cancer in mice induced by N-ethyl-N'-nitro-N-nitrosoguanidine (ENNG), as reported by Matsuyama *et al.* (12, 17), has the following advantages in the study of cell kinetics of solid cancer cells: 1) the method to induce the cancer is quite simple and effective; 2) the cancers are composed of morphologically and functionally uniform cells (13, 14); 3) the process of carcinogenesis from the initial to the

^{*1, *2} Kanokoden 81-1159, Tashiro-cho, Chikusa-ku, Nagoya 464, Japan (伊藤正夫, 山田靖治, 松山睦司, 長与健夫).

advanced stage is observable in a short period; 4) as a typical permanent cell-reproductive system, the cell kinetics of the small intestine of normal mice have been intensively studied by many investigators (6, 10, 16, 18) and there are enough reliable data on the kinetics.

For these reasons, we tried to study the cell kinetics of duodenal cancer induced by ENNG as a representative of solid carcinomas.

Cell Kinetics of Duodenal Cancer Induced by ENNG

Sixty female C3H/He mice of 8 weeks old (Hoshino Laboratory Animals Co., Saitama) were given water containing 500 mg/l of N-ethyl-N'-nitro-N-nitrosoguanidine (ENNG, Jyoko Chemicals Co., Nagoya) for 9 weeks and then water without the carcinogen for 3 weeks. Twenty-six control mice were given tap water for 12 weeks. All the mice were fed with a laboratory diet (CE-2, CLEA Japan Inc., Tokyo). At the end of the 12th week, all the mice in both the experimental and control groups were intraperitoneally injected with 1 μ Ci/g body weight of tritiated thymidine (specific activity 20 Ci/mmol, New England Nuclear, Boston). Two or three mice in the experimental group were killed consecutively under ether anaesthesia from 0.5 hr to 26 hr after the injection and the same treatments were carried out on control group mice. When sacrificed, each animal was infused with 3 ml of 10% formalin into the stomach cavity and duodenum by a gastric tube and the mucosae were fixed for 5 min. Then the duodenum 5 cm from the pyloric ring was removed, opened, extended on a filter paper and fixed again with 10% formalin for more than 1 week. After fixation, the whole duodenum was cut into four slices and embedded in paraffin with routine procedures. Sections 5 μ m thick were cut semi-serially; three sections were picked up and the next five were discarded, and thus about 270 sections per mouse (90 sets of three serially cut sections) were obtained. Therefore the sections were separated from each other by a distance of over 25 μ m. The number of detectable cancerous tubules was increased by this method. One section of each serially cut set was stained with hematoxylin and eosin (HE) for the detection of tumor lesions.

For autoradiographic studies, about 2,000 sections were selected from experimental groups. They were covered with nuclear track film emulsion (NTB-2, Eastman Kodak Co., U.S.A.) by the dipping method and were exposed for a week at 4° in dark boxes, desiccating with silica gel. After the exposure, they were developed with D-19 (Eastman Kodak) for 5 min at 18°, fixed in an acidic fixative for 15 min and thereafter washed in running water. All specimens were stained with HE.

For calculations of mitotic index, labeling index and cell cycle, the epithelial cells in the proliferative zone of normal duodenal crypts in the control group, those of the non-tumorous crypts in the cancer-bearing mice of the experimental group and the induced cancer cells were examined as the targets of the calculations. Mitotic indices were measured by counting the cells in mitosis per 5,000 cells of the duodenal crypts in both control and experimental mice. In cases with cancer, the mitotic indices were measured by counting the mitotic cells per the whole number of cells composing the carcinoma on all the semi-serially sectioned and H-E stained specimens. The labeling indices of normal and non-tumorous cells were measured by counting the labeled cells per 5,000 cells of the duodenal crypts in both control and experimental mice, which

were injected with tritiated thymidine 1 hour before sacrifice. The labeling indices of tubular adenocarcinoma were measured by counting the labeled cancer cells per the total number of cancer cells. Calculations in the normal and non-tumorous crypts were repeated in over ten areas of each specimen.

The cell cycles were calculated by the labeled mitoses method, which is regarded as the most reliable at the present time (18). Labeled mitoses curves were obtained by plotting chronologically the percentage of the labeled cells in 200 mitotic cells of the duodenal crypts of both the control and experimental groups. The curves in the tumor cells were obtained by plotting the percentage of the labeled mitoses in the adenocarcinoma cells observable in each specimen.

As the results, the incidence of carcinoma in the experimental mice was 100% at the end of the experiment. All the tumors were observed in the duodenum, located within 5 cm of the pyloric ring and they were usually multiple in number.



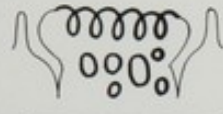
The tumors showed a histologic pattern of well-differentiated tubular adenocarcinoma and their cellular atypicality was almost uniform throughout every stage of growth.

According to the sizes of the tumor lesions, they were classified into three types as follows; Type A: the tumor growth was limited to a single gland and located in a crypt or in a villus; Type B: the tumorous tubules were branched out but remained in a crypt or in a villus; Type C: tumor tubules had already invaded into several crypts and villi. Type A and B correspond to intra-villus lesions and Type C to micro-crater lesions according to Matsuyama's classification (12, 14).

In this experiment, the tumors had not yet invaded the submucosa and no metastases were observed. The histologic features of the tumors of each type are shown in Photos 1 to 4. Average number of tumor lesions in each duodenum was 44 Type A, 33 Type B, and 13 Type C (Table I).

The mean cell number per tumor in microscopic specimens was 121 in Type A, 217 in Type B, and 496 in Type C. The total cell number of tumors detected in each mouse was 4,435 in Type A, 9,805 in Type B and 6,697 in Type C. These numbers were calculated from 60 mice in the experimental group. Mitotic tumor cells per mouse were 212 in Type A, 331 in Type B, and 335 in Type C. More than 5,000 tumor cells were calculated for the mitotic and labeling indices and more than 200 mitotic cells could be counted in tumor lesions of each type, so it was considered that the standard

TABLE I. Number of Tumor Cells per Tumor, Number of Tumors, Total Tumor Cells, and Mitotic Cells in the Tumors of Each Type

Type of carcinoma	A	B	C
			
Calculated No. of Tumors ^a	44	33	13
Cells per tumor	121	217	496
Total tumor cells ^a	4,435	9,805	6,697
Mitotic tumor cells ^a	212	331	355

^a Per mouse.

TABLE II. Mitotic Indices and Labeling Indices in the Normal and Non-tumorous Crypt Cells and in Tumor Cells of Each Type

	Mitotic index (%)	Labeling index (%)
Normal crypt	6.0 ± 0.15	34.3 ± 0.61
Non-tumorous crypt	6.1 ± 0.13	35.2 ± 0.98
Tumor cells		
Type A	4.8 ± 0.15	31.6 ± 0.59
Type B	4.8 ± 0.08	31.5 ± 0.41
Type C	4.6 ± 0.11	29.3 ± 1.37

error of the calculation of cell cycles by the labeled mitoses method was in the range of ± 0.5 hr.

The mitotic index of normal crypt cells in control mice was 6.0% and that of the non-tumorous crypt cells in experimental mice was 6.1%. No difference in the mitotic index between them was observed. The mitotic indices of tumor cells were 4.8% in Type A, 4.8% in Type B, and 4.6% in Type C (Table II). It is evident that the mitotic indices of the carcinoma cells were lower than those of the normal and non-tumorous crypt cells and the differences in the mitotic indices between each type of tumor were not significant. Autoradiograms of the tumors of each type are shown in Photos 5-7.

The labeling indices were 34.3% in normal crypt cells and 35.2% in non-tumorous crypt cells, while those of cancer cells were 31.6% in Type A, 31.5% in Type B, and 29.3% in Type C. Significant differences in the labeling index were not observed between normal, non-tumorous, and cancer cells even though the index was slightly lower in the latter.

Labeled mitoses curves in the normal and in non-tumorous crypt cells are shown in Fig. 1. The patterns of the curves were quite similar in both groups. On the other hand, the curves in the three types of tumor cells were different from that of the non-tumorous crypt cells (Fig. 2). The values of the cell cycles were shown in Table III.

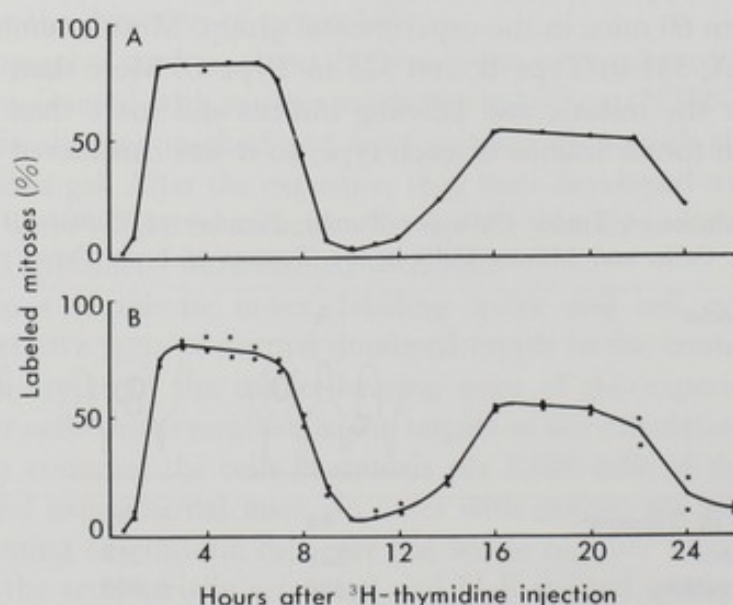


FIG. 1. Labeled mitoses curves in normal and non-tumorous crypt cells.

A: Normal crypt. B: Non-tumorous crypt.

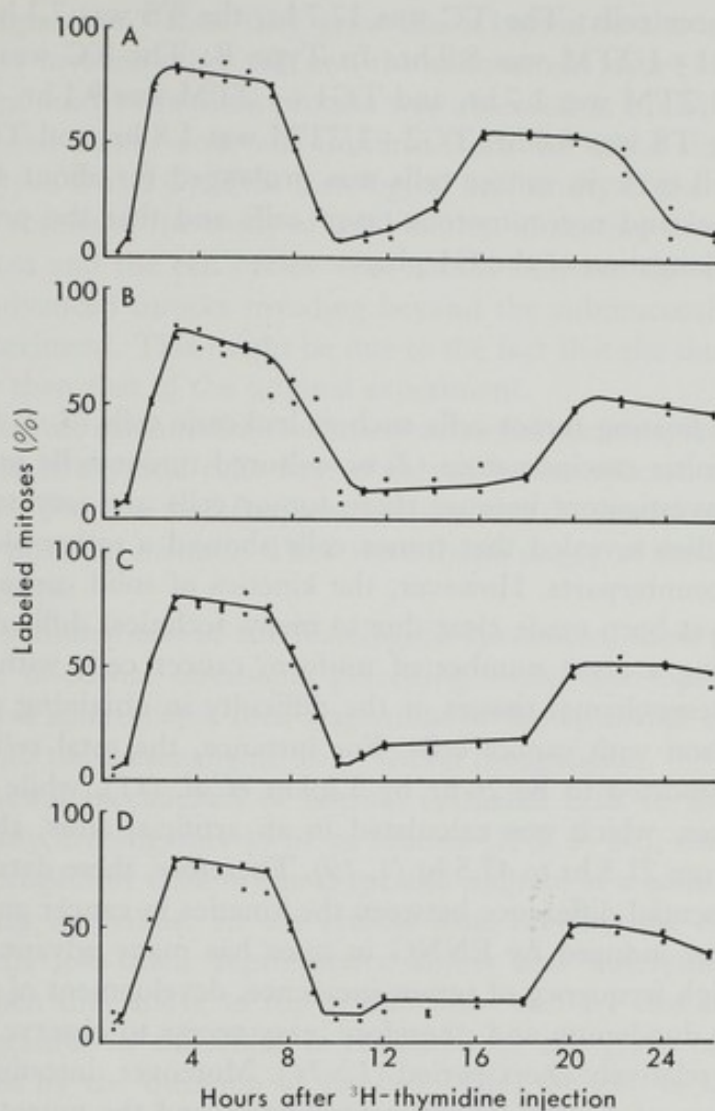


FIG. 2. Labeled mitoses curves in tumor cells of each type. A: Non tumorous crypt. B: Carcinoma A. C: Carcinoma B. D: Carcinoma C.

TABLE III. The Values of Cell Cycles of Normal Crypt and Non-tumorous Crypt Cells and of Tumor Cells in Each Type

	TC	TS	TG2+1/2TM	TG1+1/2TM
Normal crypt	13.7	6.6	1.4	5.7
Non-tumorous crypt	13.6	6.8	1.5	5.3
Tumor cells				
Type A	17.7	7.1	1.7	8.9
Type B	17.7	6.9	1.7	9.1
Type C	17.5	6.6	1.8	9.1

The period of the total cell cycle (TC) in the normal crypt cells was 13.6 hr, the period of active synthesis of DNA (TS) was 6.9 hr, the period of post DNA synthesis (TG2)+1/2 mitotic period (1/2TM) was 1.4 hr, and the period of pre DNA synthesis (TG1)+1/2TM was 5.7 hr. The TC of non-tumorous crypt cells was 13.7 hr, the TS was 6.8 hr, TG2+1/2TM was 1.5 hr, and TG1+1/2TM was 5.3 hr. The values in both the normal and non-tumorous crypt cells were nearly equal.

In Type A cancer cells: The TC was 17.7 hr, the TS was 7.1 hr, $TG2+1/2TM$ was 1.7 hr, and $TG1+1/2TM$ was 8.9 hr. In Type B: The TC was 17.7 hr, the TS was 6.9 hr, $TG2+1/2TM$ was 1.7 hr, and $TG1+1/2TM$ was 9.1 hr. In Type C: The TC was 17.5 hr, the TS was 6.6 hr, $TG2+1/2TM$ was 1.8 hr, and $TG1+1/2TM$ was 9.1 hr. Thus the cell cycle in cancer cells was prolonged for about 4 hr as compared with those of normal and non-tumorous crypt cells and that the prolongations were mainly due to a prolongation of the G1 phase.

Comment

The kinetics of floating tumor cells such as leukemic cells (3, 7, 8), ascitic cells in patients with peritonitis carcinomatosa (2) or cultured tumor cells *in vitro*, have been studied by many investigators because these tumor cells are easy to handle and are uniform. These studies revealed that tumor cells showed a rather slower growth rate than their normal counterparts. However, the kinetics of solid cancer cells developed in a host have not yet been made clear due to many technical difficulties, such as the difficulty in obtaining a great number of uniform cancer cells without their normal counterparts and mesenchymal tissues or the difficulty in obtaining a suitable control system for comparison with cancer cells. For instance, the total cell cycle of human rectal cancer was reported to be 26 hr by Lipkin *et al.* (11), while the cell cycle of normal rectal mucosa, which was calculated in an artificial anus, showed broad and ambiguous values from 21.5 hr to 47.5 hr (1, 19). Therefore, these data are not adequate to determine the essential difference between the kinetics in cancer and normal cells.

Duodenal cancer induced by ENNG in mice has many advantages in the study of cell kinetics; a high frequency of tumor incidence, development of tumors in certain limited areas of the duodenum and, therefore, easy access to observe various stages of tumor growth in a relatively short period (12-14). Moreover, intestinal epithelial cells in mice have a system of permanent cell reproduction and the mucosa of the intestine can clearly be differentiated into proliferative and functional zones.

The cell cycle of the intestinal mucosa in normal mice in this experiment was calculated to be 13.6 hr and this value closely resembled that in C57BL mice reported by Matsuzawa (15). The value for non-tumorous crypt cells in ENNG drinking mice was 13.9 hr. These results seem to be sufficiently reliable to serve for the control in the kinetics of duodenal cancer cells. Prolongation of the total cell cycles with the decline in the mitotic indices was observed in all tumor stages and these results conformed the data obtained in leukemic or ascitic tumor cells.

Therefore, it is concluded that the proliferation of solid tumor cells is not more rapid than that of normal proliferative cells but rather slower. It is also supposed that this duodenal cancer will proliferate constantly from the initial stage to the more advanced stages, because no differences in the growth rate were observed between each stage of tumor growth.

Matsuyama *et al.* reported that the duodenal carcinoma induced by ENNG was composed of almost uniform tumor cells both morphologically and histochemically, resembling the proliferative cells in the normal duodenal crypt. He concluded from histological observation of tumor tissues in serial sections that the carcinoma cells developed in the duodenal crypt and invaded the surrounding mesenchyme of the villus

as a "lateral invagination," then they grew like a balloon in the mesenchymal tissues and afterward they invaded other villi and the submucosal layer (14).

In the present study, the same process was observed in tumor growth. The atypicality of the induced cancer cells was uniform from the initial stage (Type A) to the advanced one (Types B and C). This histological uniformity of the tumor cells was also supported by the results of the study of cell kinetics, indicating that the mitotic indices, the labeling indices and the cell cycles were almost uniform throughout each stage of tumor growth. Advanced tumors invading beyond the submucosal layer were not observed in this experiment. This might be due to the fact that the duration of the experiment was shorter than that of the original experiment.

In the histological examinations of many subserial sections, small foci which were composed of 20 to 30 atypical cells were observed in the affected mucosa as shown in Photos 8A and 8B. The foci had frequent mitoses and the nuclei of these atypical cells were arranged in piled up manner. They were found singly at the base of the villi, but were rare in the crypt.

From serial examinations of the histological specimens, these foci seemed to be a proto-type of the duodenal carcinoma preceding tumor development. Following the appearance of these microscopic foci, stagnation of the epithelial cells does occur and then they grow into the mesenchyme as a "lateral invagination."

The cell renewal mechanism of normal epithelial cells in the small intestine is considered by many investigators to be as follows (5, 6, 9, 16); the cells are produced by mitosis from progenitor cells in the crypt and migrate at a constant speed along the epithels composing the villus. In the critical zone between the crypt and the villus, the immature cells lose their reproductive ability and differentiate into absorptive epithelial cells, then they move to top of the villus and are cast off the surface. The speed of cell migration in the villus is regulated by the grade of cell reproduction, which is controlled by the duration of the cell cycle, the rate of the proliferative cell compartment in crypt cells and the speed of cell loss from the top of the villus.

On the other hand, the cancer cells developed by doses of ENNG from progenitor cells in the crypt migrate to the critical zone, but they do not have the ability to differentiate and maintain only reproductive ability.

For an explanation of the mode of the invasive growth of cancer cells, many factors has been mentioned, *e.g.*, active movement of cancer cells and mesenchymal cells, loss of contact inhibition of tumor cells, looseness of the binding of cancer cells and discharge of a proteolytic enzyme from cancer cells.

From the viewpoints of histology and cell kinetics, the invasion mechanism of duodenal cancer induced by ENNG is supposed to be as follows: If cancer cells having a slower growth rate than normal proliferating cells develop in the stream of normal cell migration from the crypt to the top of the villus, stagnation of the epithelial cells may occur and owing to the maintenance of their proliferating nature, they are pushed aside into the mesenchymal tissue by the force of the normal cell stream.

It is hoped that these hypotheses may be confirmed by future studies.

REFERENCES

1. Bleiberg, H. and Galand, P. *In vitro* autoradiographic determination of cell kinetic

- parameters in adenocarcinomas and adjacent healthy mucosa of the human colon and rectum. *Cancer Res.*, **36**, 325-328 (1976).
2. Clarkson, B., Ota, K., Ohkita, T., and O'Connor, A. Kinetics of proliferation of cancer cells in neoplastic effusions in man. *Cancer*, **18**, 1189-1213 (1965).
 3. Clarkson, B., Ohkita, T., Ota, K., and Fried, J. Studies of cellular proliferation in human leukemia. I. Estimation of growth rates of leukemic and normal hematopoietic cells in two adults with acute leukemia given single injections of tritiated thymidine. *J. Clin. Invest.*, **46**, 506-529 (1967).
 4. Cronkite, E. P. and Flidner, T. M. Granulocytopoiesis. *N. Engl. J. Med.*, **270**, 1347-1352, 1403-1408 (1964).
 5. Friedman, N. B. Cellular dynamics in the intestinal mucosa; The effect of irradiation on epithelial maturation and migration. *J. Exp. Med.*, **81**, 553-557 (1945).
 6. Fujita, S. Analysis of cell proliferation and differentiation by microautoradiography. In "Shin-Saibo-Gaku," 2nd ed., ed. S. Seno and Y. Takagi, pp. 605-674 (1965) (in Japanese). Asakura-Shoten, Tokyo.
 7. Gavosto, F., Pileri, A., Gabutti, V., and Masera, P. Cell population kinetics in human acute leukemia. *Eur. J. Cancer*, **3**, 301-307 (1969).
 8. Greenberg, M. L., Chanana, A. D., Cronkite, E. P., Giacomelli, G., Rai, K. R., Schiffer, L. M., Stryckmans, P. A., and Vincent, P. C. The generation time of human leukemic myeloblasts. *Lab. Invest.*, **26**, 245-252 (1972).
 9. Leblond, C. P. and Stevens, C. E. The constant renewal of the intestinal epithelium in the albino rat. *Anat. Rec.*, **100**, 357-378 (1948).
 10. Leshner, S., Fry, R. J. M., and Kohn, H. I. Age and the generation time of the mouse duodenal epithelial cell. *Exp. Cell Res.*, **24**, 334-343 (1961).
 11. Lipkin, M., Bell, B., and Sherlock, P. Cell proliferation kinetics in the gastrointestinal tract of man. I. Cell renewal in colon and rectum. *J. Clin. Invest.*, **42**, 767-776 (1963).
 12. Matsuyama, M., Nakamura, T., and Nagayo, T. Early morphological changes in carcinogenesis by N-ethyl-N'-nitro-N-nitrosoguanidine in mouse duodenum. *Abst. Int. Cancer Congr.*, **11**, 673-674 (1974).
 13. Matsuyama, M., Ito, M., Yamada, S., Nakamura, T., and Nagayo, T. Histochemical patterns in early lesions and infiltrating adenocarcinomas induced in mouse duodenum by N-ethyl-N'-nitro-N-nitrosoguanidine. *J. Natl. Cancer Inst.*, **56**, 791-795 (1976).
 14. Matsuyama, M., Nakamura, T., Suzuki, H., Ito, M., Yamada, S., and Nagayo, T. Early lesions in carcinogenesis by N-ethyl-N'-nitro-N-nitrosoguanidine in mouse duodenum. In "Pathophysiology of Carcinogenesis in Digestive Organs," ed. E. Faber *et al.*, pp. 269-283 (1977). Japan Scientific Societies Press, Tokyo/University Park Press, Baltimore.
 15. Matsuzawa, T. and Wilson, R. The intestinal mucosa of germfree mice after whole-body X-irradiation with 3 kiloroentgens. *Radiat. Res.*, **25**, 15-24 (1965).
 16. Messier, B. and Leblond, C. P. Cell proliferation and migration as revealed by radioautography after injection of thymidine-³H into male rats and mice. *Am. J. Anat.*, **106**, 247-285 (1960).
 17. Nakamura, T., Matsuyama, M., and Kishimoto, H. Tumors of the esophagus and duodenum induced in mice by oral administration of N-ethyl-N'-nitro-N-nitrosoguanidine. *J. Natl. Cancer Inst.*, **52**, 519-522 (1974).
 18. Quastler, H. and Sherman, F. G. Cell population kinetics in the intestinal epithelium of the mouse. *Exp. Cell Res.*, **17**, 420-438 (1959).
 19. Terz, J. J., Curutchet, H. P., and Lawrence, W. J. Analysis of the cell kinetics in five human solid tumors. *Cancer*, **28**, 1100-1110 (1971).

EXPLANATION OF PHOTOS

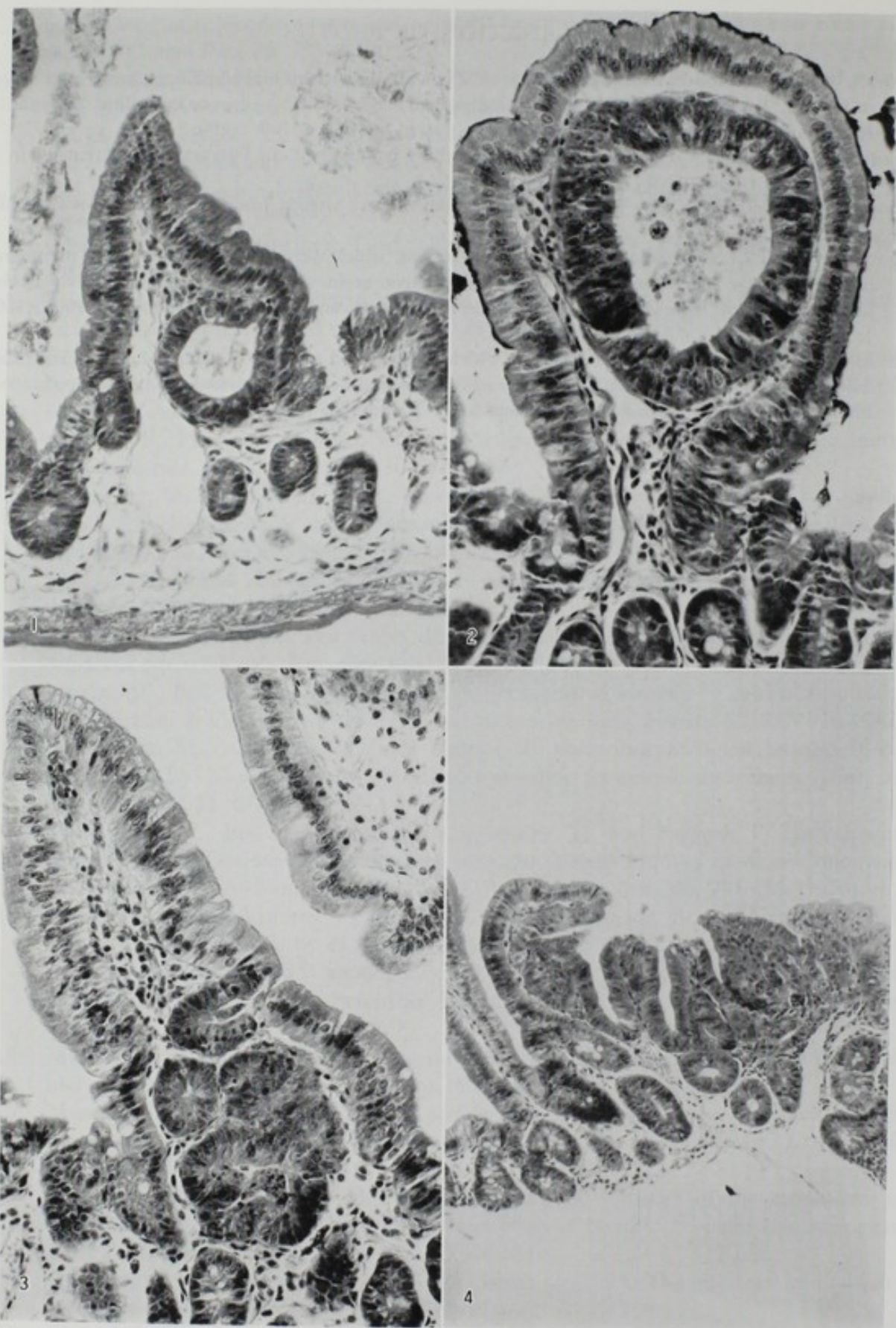
PHOTOS 1 and 2. Duodenal adenocarcinomas of Type A, induced by oral administration of high doses of ENNG. Tumor growth is limited to a single gland and located in a crypt or in a villus. The tubule in Photo 1 is in an earlier stage of growth than that in Photo 2. $\times 100$, $\times 200$.

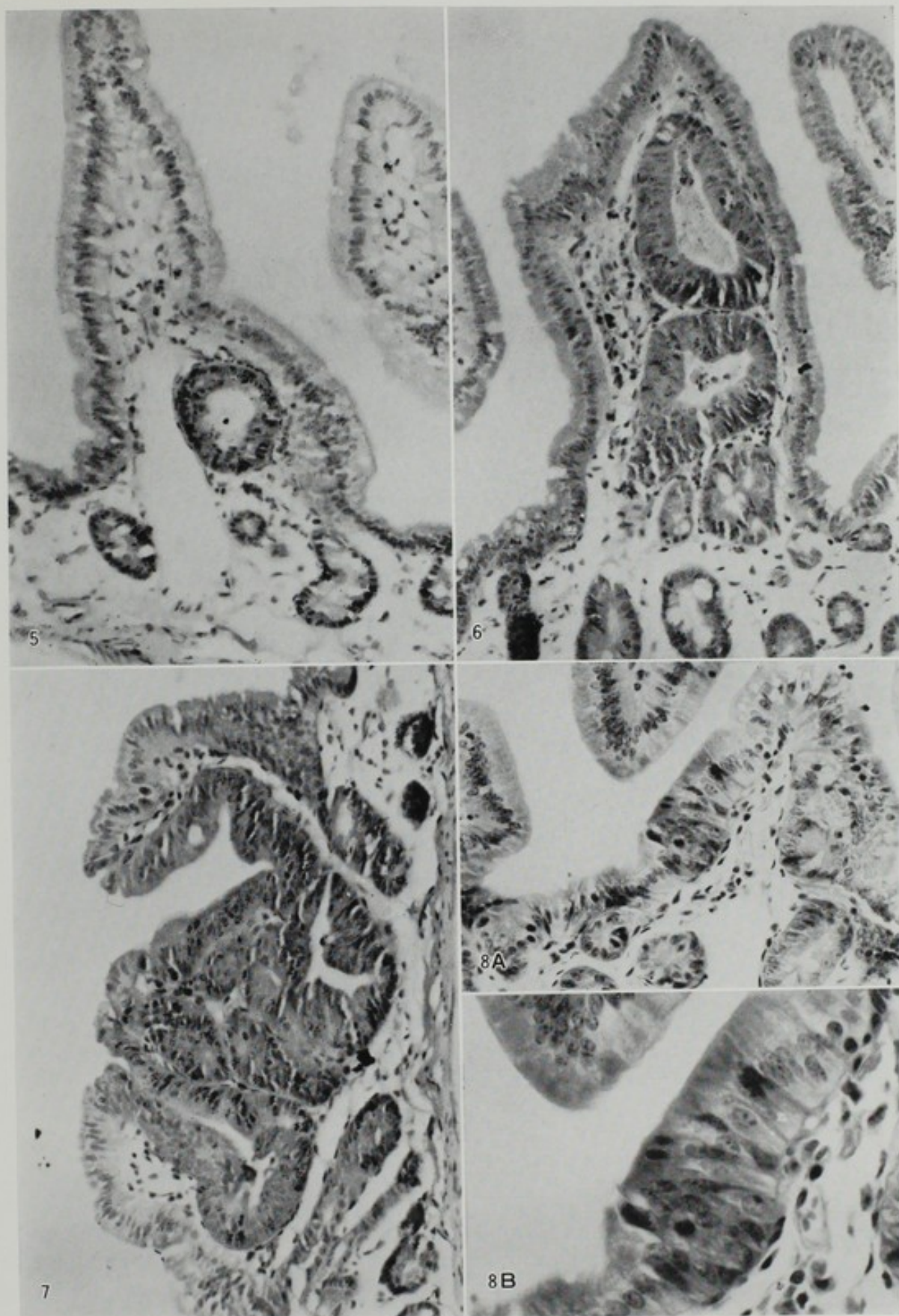
PHOTO 3. Carcinoma of Type B; the cancerous tubule is branched out into several but remains in a crypt or in a villus. $\times 200$.

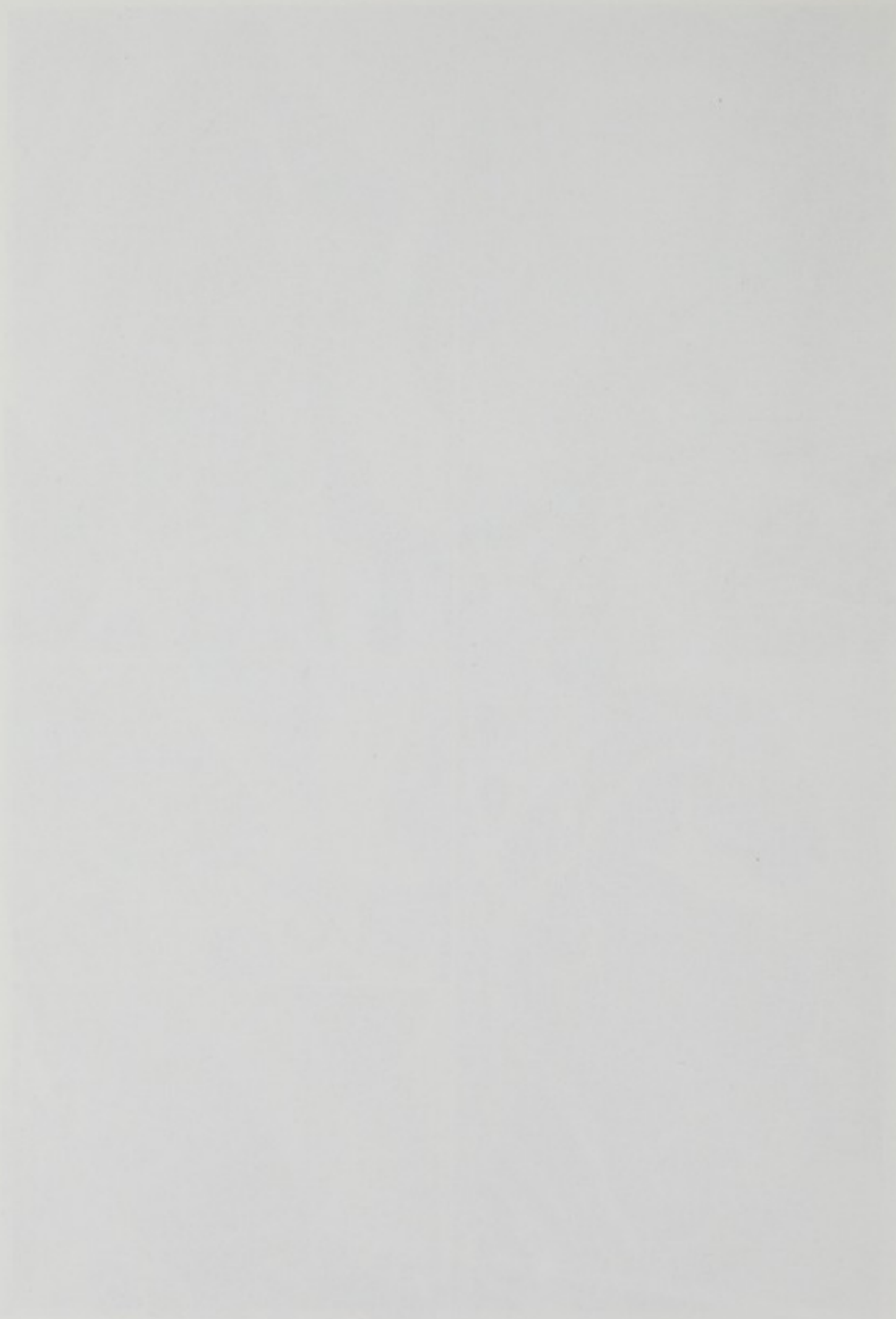
PHOTO 4. Carcinoma of Type C; the cancerous tubules have already invaded several crypts and villi. $\times 40$.

PHOTOS 5, 6, and 7. Autoradiogram of cancerous lesions, which were injected with tritiated thymidine intraperitoneally 1 hr before the mice were killed. Silver grains are frequently observed on the nuclei of tumor cells of Type A (Photo 5), of Type B (Photo 6), and of Type C (Photo 7). $\times 100$, $\times 100$, $\times 100$.

PHOTO 8. Initial lesion of duodenal cancer, which is composed of 20 to 30 atypical cells. This small lesion has frequent mitoses and the nuclei of these atypical cells were arranged in piled up manner. Photo 8B is a higher magnification of Photo 8A. $\times 200$, $\times 400$.







HISTOCHEMICAL INVESTIGATION OF PRECANCEROUS CHANGES INDUCED BY 3-ME OLE IN RAT LIVER

Shih-Hsiung Yang, Tzong-Shyan Shieh, Shih-Hsiung Yang, Shih-Hsiung Yang,
Shih-Hsiung Yang, Shih-Hsiung Yang, Shih-Hsiung Yang, Shih-Hsiung Yang

ANALYSIS OF MORPHOLOGY AND FUNCTION OF PRECANCEROUS CHANGES

Changes in morphology and function of liver cells induced by 3-methylcholanthrene (3-MC) were studied in rat liver. The results showed that 3-MC induced a series of changes in the morphology and function of liver cells, including the appearance of large, pale, foamy cells, the enlargement of the nucleus, and the appearance of large, pale, foamy cells.

The changes in morphology and function of liver cells induced by 3-MC were studied in rat liver. The results showed that 3-MC induced a series of changes in the morphology and function of liver cells, including the appearance of large, pale, foamy cells, the enlargement of the nucleus, and the appearance of large, pale, foamy cells.

A series of experiments have been conducted to study the changes in morphology and function of liver cells induced by 3-MC. The results showed that 3-MC induced a series of changes in the morphology and function of liver cells, including the appearance of large, pale, foamy cells, the enlargement of the nucleus, and the appearance of large, pale, foamy cells.

One of the problems in studying the changes in morphology and function of liver cells induced by 3-MC is the lack of a suitable method for the study of the changes in morphology and function of liver cells. In this study, a series of experiments have been conducted to study the changes in morphology and function of liver cells induced by 3-MC. The results showed that 3-MC induced a series of changes in the morphology and function of liver cells, including the appearance of large, pale, foamy cells, the enlargement of the nucleus, and the appearance of large, pale, foamy cells.

Received 10/10/77, revised 11/10/77, accepted 12/10/77. This work was supported by the National Science Foundation, Grant No. 12345678.

ANALYSIS OF MORPHOLOGY AND
FUNCTION OF PRECANCEROUS
CHANGES

HISTOCHEMICAL INVESTIGATION OF PRECANCEROUS LESIONS INDUCED BY 3'-ME-DAB IN RAT LIVER

Michio MORI, Tohru KAKU, Kimimaro DEMPO, Masaaki SATOH,
Aiko KANEKO, and Tamenori ONOÉ

*Department of Pathology, Sapporo Medical College**

A histochemical investigation was carried out in serial sections of the liver from rats fed a diet containing 0.06% 3'-methyl-4-(dimethyl-amino)azobenzene (3'-Me-DAB) for 10 or 12 weeks, in an attempt to identify hyperplastic areas and hyperplastic nodules as clearly as possible.

Gamma glutamyl transpeptidase (GGT) was shown to be a sufficient marker for the demonstration of hyperplastic areas, while non-specific esterase (ES) histochemistry was useful in dividing hyperplastic nodules into two further subgroups (nodule I and nodule II).

Quantitative analysis on the fluctuation of these lesions after withdrawal of the carcinogen was attempted. The result indicated that most hyperplastic areas underwent remodelling and only 0.15% of them contributed to the development of liver cancer. Less than half of nodule I became remodelled and 2% of them developed into cancer. On the other hand, it was shown that 7% of nodule II progressed into liver cancer.

A series of sequential changes in hepatocytes appears in the liver during the course of chemical hepatocarcinogenesis. These changes include the occurrence of hyperplastic areas, hyperplastic nodules, and liver cancer. Although hyperplastic areas and hyperplastic nodules are generally considered to be precursor lesions for liver cancer in many instances (5), the interrelation between these lesions and cancer has not yet been fully documented due to the paucity of quantitative information.

One of the problems in performing quantitative studies of these lesions in the process of hepatocarcinogenesis is the difficulty in the identification of such lesions. It is especially true in the early stage of hepatocarcinogenesis, because hyperplastic areas are hardly recognizable in conventional histological specimens. These areas can be identified from the surrounding liver tissue by their low or deficient activities of some enzymes, such as glucose-6-phosphatase (G-6-Pase), ATPase, and β -glucuronidase (5). However, enzyme deficiency seems not to be a sufficient marker for tracing the fate of hyperplastic areas, because the activities of these enzymes vary among individual hyperplastic areas, and even in the normal liver, parenchymal cells show a considerable heterogeneity in enzyme activity within a liver lobule (15). On the contrary, γ -glutamyl transpeptidase (GGT) is shown to have a valuable role as a marker for focal hyper-

* Minami-1-jo, Nishi-17-chome, Chuo-ku, Sapporo 060, Japan (森 道夫, 賀来 享, 伝法公麿, 佐藤昌明, 金子愛子, 小野江為則).

plastic lesions (6). It was demonstrated that the numbers of hyperplastic areas detected by positive GGT reaction were significantly greater than those indicated by enzyme deficiency (7).

Therefore in the present study, parallel histochemical analyses of GGT (22), G-6-Pase (23), and nonspecific esterase (ES) (2) activities were carried out in serial sections of the liver from rats fed a diet containing 0.06% 3'-methyl-4-(dimethyl-amino)azobenzene (3'-Me-DAB), in an attempt to identify these lesions as clearly as possible. Subsequently we examined the sequential changes in these lesions in the course of hepatocarcinogenesis to elucidate the significance of such lesions in the development of liver cancer.

Histochemical Identification of Hyperplastic Areas

The histological, biochemical, immunohistochemical, and ultrastructural changes in the liver during the course of hepatocarcinogenesis in rats fed a diet containing 0.06% 3'-Me-DAB were described previously (3, 4, 8-13, 16-21, 24).

At around week 6 of azo-dye feeding, several hyperplastic areas appeared in the liver of some rats. These areas consisted of hepatocytes with rather abundant cytoplasm, but were hardly distinguishable from the surrounding liver tissue in conventional histological specimens (Photo 2A). When serial sections were reacted for G-6-Pase and GGT, hyperplastic areas were demonstrated as the areas that were low or deficient in G-6-Pase (Photo 1) and positive for GGT (Photo 2B). The GGT activity was demonstrated strongly on the entire surface of hepatocytes in the hyperplastic areas, making a sharp contrast to the complete absence of GGT staining in the surrounding liver tissue (Photo 4). GGT activity was also shown to be positive in the areas of bile duct proliferation, but these lesions were easily discernible from hyperplastic areas by referring to the hematoxylin- and eosin stained sections.

Method of Quantitative Evaluation of Precancerous Lesions

The whole areas of liver specimens were measured directly with a semi-automatic quantitative image analyzer (Kontron MOP system, West Germany) by tracing the outline of histochemically-stained liver sections with stylos. The number of hyperplastic areas, hyperplastic nodules, and liver cancer was counted under a light microscope. The number of these lesions per cm² in the liver specimens was calculated.

Fate of Hyperplastic Areas after Withdrawal of Carcinogen

By utilizing GGT histochemistry, many hyperplastic areas were demonstrated in the liver of rats given azo-dye for 10 weeks (Photo 3). The average number of these areas in each cm² of the liver specimen was 78 (Fig. 1). When the animals were returned to a normal diet after 10 weeks of azo-dye feeding, the number of hyperplastic areas decreased significantly with the lapse of time. Eight weeks after withdrawal of the carcinogen, the average number of hyperplastic areas diminished to approximately one third of that seen before removal of the carcinogen (Table I), suggesting that 65% of hyperplastic areas undergo remodelling and become indistinguishable from the sur-

TABLE I. Changes in the Number of Hyperplastic Areas and Nodules after Withdrawal of Carcinogen

	Area	Nodule
3'-Me-DAB10W	78.85	1.15
3'-Me-DAB10W+BD4W	35.82	1.24
3'-Me-DAB10W+BD8W	26.68	1.76

Number of GGT positive areas per cm².

TABLE II. Changes in the Number of Nodules and Cancer after Withdrawal of Carcinogen

	Nodule I	Nodule II	Cancer
3'-Me-DAB12W	1.639	0.345	0.086
3'-Me-DAB12W+BD4W	1.735	0.450	0.128
3'-Me-DAB12W+BD8W	0.876	0.510	0.183

Number of nodules per cm².

rounding tissue during 8 weeks of normal diet feeding. Ogawa *et al.* (17) reported that more than 90% of hyperplastic areas underwent a process of maturation and remodelling, in rats which received a single dose of diethylnitrosamine (200 mg per kg body weight). Such a discrepancy may reflect the difference in the effect of the carcinogens used.

On the other hand, it was shown that 33% of hyperplastic areas persisted for at least 8 weeks even in the absence of any carcinogen. Judging from the number of liver cancer which appeared in the liver in a late phase of carcinogenesis, it was shown that 0.15% of hyperplastic areas contributed to the development of liver cancer. It was also indicated that approximately 1% of hyperplastic areas progressed to hyperplastic nodules.

Histochemical Characterization of Hyperplastic Nodules

Several hyperplastic nodules appeared in the liver at around week 12 of azo-dye feeding. These nodules were generally demarcated from the surrounding liver tissue, so that they were easily identified even in conventional histological sections. However, as pointed out by Kitagawa, the hyperplastic nodules could be individually heterogeneous (14). When serial sections were reacted for G-6-Pase and ES, it was found that hyperplastic nodules were divided into two further subgroups: 1) Nodules exhibiting a positive reaction for ES (Photo 7) but deficient in G-6-Pase (Photo 6); 2) those deficient in both ES (Photo 8) and G-6-Pase. Such a difference was clearly shown when the intensity of the reaction product for ES was quantitatively measured through a densitometer (Photos 9 and 10).

These two kinds of nodules were named "nodule I" and "nodule II" respectively (21). The latter was found less frequently in the liver than the former (Table II).

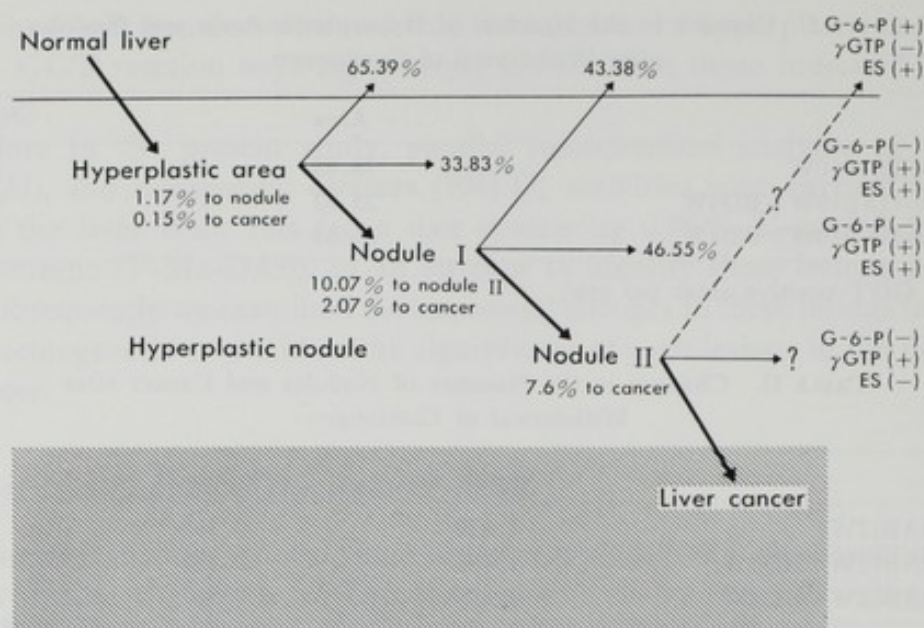


FIG. 1. Relation of hyperplastic areas, nodules and liver cancer.

Histological and Ultrastructural Characteristics of Nodules I and II

Nodule I consisted of rather large cells with eosinophilic abundant cytoplasm (Photo 11), which often contained glycogen accumulation on fasting, and some lipid droplets. The liver cell plates were thick and tortuous. Electron microscopically the cells composing nodule I were identical with hepatocytes of adult rat liver in revealing abundant cytoplasm with well-developed cytoplasmic organelles. A proliferation of the smooth endoplasmic reticulum (ER in Photo 13) occupied large portions of the cytoplasm. Large glycogen-containing autophagic vacuoles and glycogen areas (1) were seen in the cytoplasm, suggesting disturbed carbohydrate metabolism in these cells. The large nucleus was round in configuration with one to two dominant nucleoli. The nucleoplasm was electron lucent because of the condensation of chromatin toward the nuclear envelope (Photo 14). Dilatation of the bile canaliculi lumen with a loss of microvilli was often encountered (Photo 15), in accordance with the observation of hepatocytes in hyperplastic nodules induced by diethylnitrosamine (DEN) followed by 2-acetylaminofluorene (2AAF), and in regenerating liver after partial hepatectomy (17).

On the other hand, nodule II consisted of basophilic small hepatocytes with scanty cytoplasm (Photo 12). Ultrastructurally the cells in nodule II showed certain similarities to liver cancer (17). That is, they contained abundant polysomes in the cytoplasm, but only a few cytoplasmic organelles. The nucleus was irregular in outline and often contained intranuclear inclusions (Photo 16).

Fate of Hyperplastic Nodules after Withdrawal of Carcinogen

When ES histochemistry was applied to the liver specimens from rats fed a diet containing azo-dye for 12 weeks, the average number of nodule II was shown to be about one-fifth that of nodule I (Table II). From the fluctuation in the number of

nodules after withdrawal of the carcinogen, it was shown that 43% of nodule I underwent remodelling during 8 weeks of normal diet feeding, while 46% of them persisted in the absence of the carcinogen. It was also noted that 10% of nodule I progressed to nodule II, and 2% of them developed into liver cancer.

On the other hand, 7.6% of nodule II progressed to liver cancer even after withdrawal of the carcinogen (Table II).

Conclusion

By utilizing several histochemical techniques in serial sections of the liver from rats fed a diet supplemented with 3'-Me-DAB at a concentration of 0.06%, identification of precancerous lesions became possible, and consequently follow-up studies of these lesions in the course of hepatocarcinogenesis could be accomplished.

It was indicated that in the early stage of carcinogenesis most of the lesions were reversible and they became remodelled when the carcinogen was withdrawn from the diet. In the late phase of carcinogenesis, the rate of irreversible lesions increased concomitant with the prolonged exposure to the carcinogen. It was shown that the hyperplastic nodules, especially those designated as nodule II, contributed to the development of liver cancer in a very high frequency.

Acknowledgment

This study was supported by a Grant-in-Aid for Cancer Research (301062) from the Ministry of Education, Science and Culture, Japan.

REFERENCES

1. Bannasch, P. The cytoplasm of hepatocytes during carcinogenesis; electron and light microscopic investigations of the nitrosomorpholine-intoxicated rat liver. *Recent Results Cancer Res.*, **19**, 1-100 (1968).
2. Burstone, M. S. The cytochemical localization of esterase. *J. Natl. Cancer Inst.*, **18**, 167-172 (1957).
3. Dempo, K., Chisaka, N., Yoshida, Y., Kaneko, A., and Onoé, T. Immunofluorescent study on α -fetoprotein-producing cells in the early stage of 3'-methyl-4-dimethylaminoazobenzene carcinogenesis. *Cancer Res.*, **35**, 1282-1287 (1975).
4. Enomoto, K., Dempo, K., Mori, M., and Onoé, T. Histopathological and ultrastructural study on extramedullary hematopoietic foci in early stage of 3'-methyl-4-dimethylaminoazobenzene hepatocarcinogenesis. *Gann*, **69**, 249-254 (1978).
5. Farber, E. Hyperplastic areas, hyperplastic nodules, and hyperbasophilic areas as putative precursor lesions. *Cancer Res.*, **36**, 2532-2533 (1976).
6. Fiala, S. and Fiala, A. E. Activation by chemical carcinogens of γ -glutamyl transpeptidase in rat and mouse liver. *J. Natl. Cancer Inst.*, **51**, 151-158 (1973).
7. Hirota, N. and Williams, G. M. The sensitivity and heterogeneity of histochemical markers for altered foci involved in liver carcinogenesis. *Am. J. Pathol.*, **95**, 327-328 (1979).
8. Inaoka, Y. Significance of the so-called oval cell proliferation during azo-dye hepatocarcinogenesis. *Gann*, **58**, 355-366 (1967).
9. Iwasaki, T., Dempo, K., Kaneko, A., and Onoé, T. Fluctuation of various cell populations and their characteristics during azo-dye carcinogenesis. *Gann*, **63**, 21-30 (1972).

10. Kaneko, A., Dempo, K., Iwasaki, T., and Onoé, T. Changes in the activities of glucose-6-phosphatase, aldolase, and alkaline phosphatase during azo-dye carcinogenesis. *Gann*, **63**, 31-39 (1972).
11. Kaneko, A., Dempo, K., Yoshida, Y., Chisaka, N., and Onoé, T. Deviation in esterase isozyme pattern during early stage of hepatocarcinogenesis by 3'-methyl-4-dimethylaminoazobenzene. *Cancer Res.*, **34**, 1816-1821 (1974).
12. Kaneko, A., Yoshida, Y., Yokoyama, S., Dempo, K., and Onoé, T. Some properties and electrophoretic patterns of rat liver esterases in relation to hepatocarcinogenesis by 3'-methyl-4-(dimethylamino)azobenzene. *Gann*, **67**, 331-337 (1976).
13. Kaneko, A., Chisaka, N., Enomoto, K., Kaku, T., Dempo, K., Mori, M., and Onoé, T. A microsomal butyryl esterase appearing in rat liver during development, regeneration, and carcinogenesis, and after phenobarbital treatment. *J. Natl. Cancer Inst.*, **62**, 1489-1495 (1979).
14. Kitagawa, T. Sequential phenotypic changes in hyperplastic areas during hepatocarcinogenesis in the rat. *Cancer Res.*, **36**, 2534-2539 (1976).
15. Novikoff, A. B. Cell heterogeneity within the hepatic lobule of the rat (Staining reactions). *J. Histochem. Cytochem.*, **7**, 240-244 (1956).
16. Ogawa, K., Minase, T., and Onoé, T. Demonstration of glucose-6-phosphatase activity in the oval cells of rat liver and the significance of the oval cells in azo-dye carcinogenesis. *Cancer Res.*, **34**, 3379-3386 (1974).
17. Ogawa, K., Medline, A., and Farber, E. Sequential analysis of hepatic carcinogenesis. A comparative study of the ultrastructure of preneoplastic, malignant, prenatal, postnatal, and regenerating liver. *Lab. Invest.*, **41**, 22-35 (1979).
18. Onoé, T., Dempo, K., Kaneko, A., and Watabe, H. Significance of α -fetoprotein appearance in the early stage of azo-dye carcinogenesis. *GANN Monogr. Cancer Res.*, **14**, 233-247 (1973).
19. Onoé, T., Mori, M., Kaneko, A., Dempo, K., and Ogawa, K. Significance of the appearance of α -fetoprotein in the early stage of azo-dye hepatocarcinogenesis. *Tumor Res.*, **8**, 75-78 (1973).
20. Onoé, T., Kaneko, A., Dempo, K., Ogawa, K., and Minase, T. α -fetoprotein and early histological changes of hepatic tissue in DAB-hepatocarcinogenesis. *Ann. N. Y. Acad. Sci.*, **259**, 168-180 (1975).
21. Onoé, T., Kaneko, A., Dempo, K., Chisaka, N., Yokoyama, S., and Ogawa, K. Histochemical and biochemical studies on carcino-fetal protein during 3'-methyl-4-dimethylaminoazobenzene hepatocarcinogenesis. In "Onco-Developmental Gene Expression," ed. W. H. Fishmann and S. Sell, pp. 227-236 (1976). Academic Press, New York.
22. Rutenburg, A. L., Kim, H., Fischbein, J. W., Hanker, J. S., Wasserkrug, H. L., and Seligman, A. M. Histochemical and ultrastructural demonstration of γ -glutamyl transpeptidase activity. *J. Histochem. Cytochem.*, **17**, 517-526 (1969).
23. Wachstein, M. and Meisel, E. On the histochemical demonstration of glucose-6-phosphatase. *J. Histochem. Cytochem.*, **4**, 592 (1956).
24. Yoshida, Y., Kaneko, A., Chisaka, N., and Onoé, T. Appearance of intestinal type of tumor cells in hepatoma tissue induced by 3'-methyl-4-dimethylaminoazobenzene. *Cancer Res.*, **38**, 2753-2758 (1978).

EXPLANATION OF PHOTOS

Photos 1-4 show liver specimens of rats fed azo-dye for 10 weeks.

PHOTO 1. G-6-Pase reaction in a fresh frozen section. The hyperplastic area is shown as an enzyme deficient area. $\times 160$.

PHOTO 2 A: HE stained section of acetone-fixed-paraffin-embedded material, corresponding to the area shown in Photo 2B. $\times 50$.

B: Hyperplastic areas demonstrated by GGT histochemistry. $\times 50$.

PHOTO 3. Low power view of GGT-stained sections of the liver. N, hyperplastic nodules. $\times 4$.

Photos 5-8 show liver specimens of rats fed azo-dye for 12 weeks.

PHOTO 5. GGT reaction in the hyperplastic nodule. $\times 130$.

PHOTO 6. G-6-Pase reaction in the hyperplastic nodule. $\times 140$.

PHOTO 7. ES reaction in nodule I. ES activity is higher than the surrounding liver tissue. $\times 80$.

PHOTO 8. ES reaction in nodule II. ES activity is lower than the surrounding liver tissue. $\times 50$.

PHOTO 9. Densitometry of ES reaction products in nodule I.

PHOTO 10. Densitometry of ES reaction products in nodule II.

PHOTO 11. Histological appearance of nodule I. HE stain, $\times 130$.

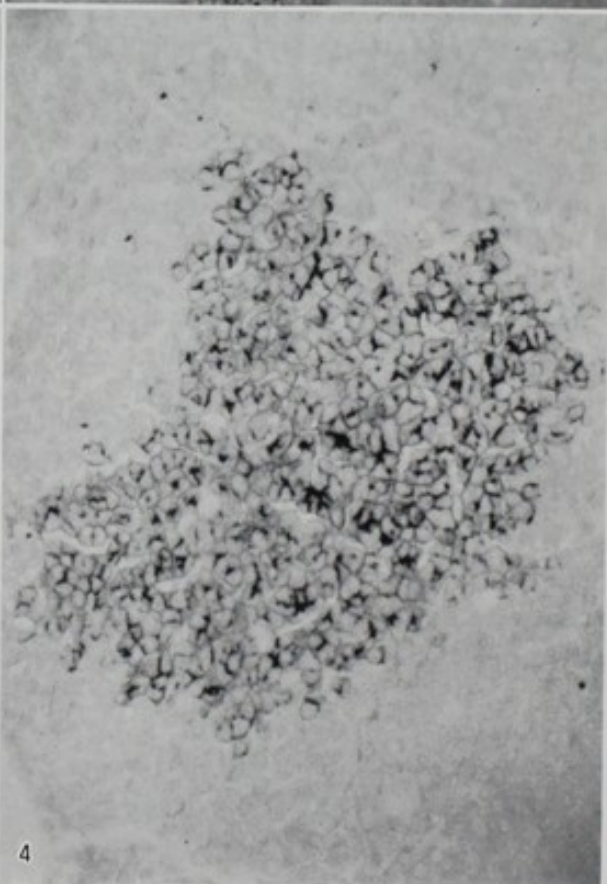
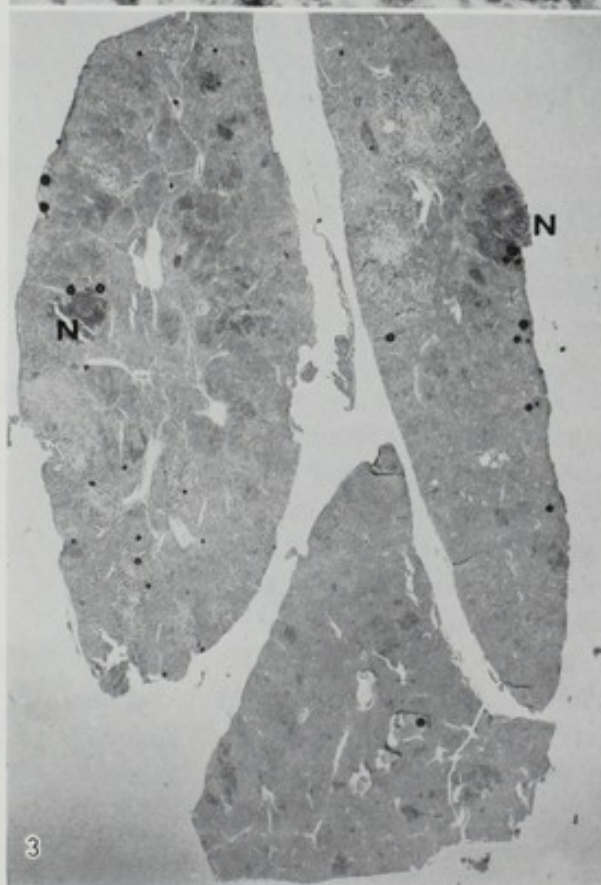
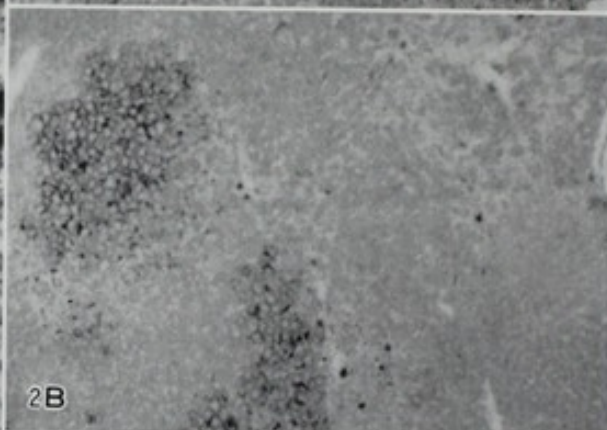
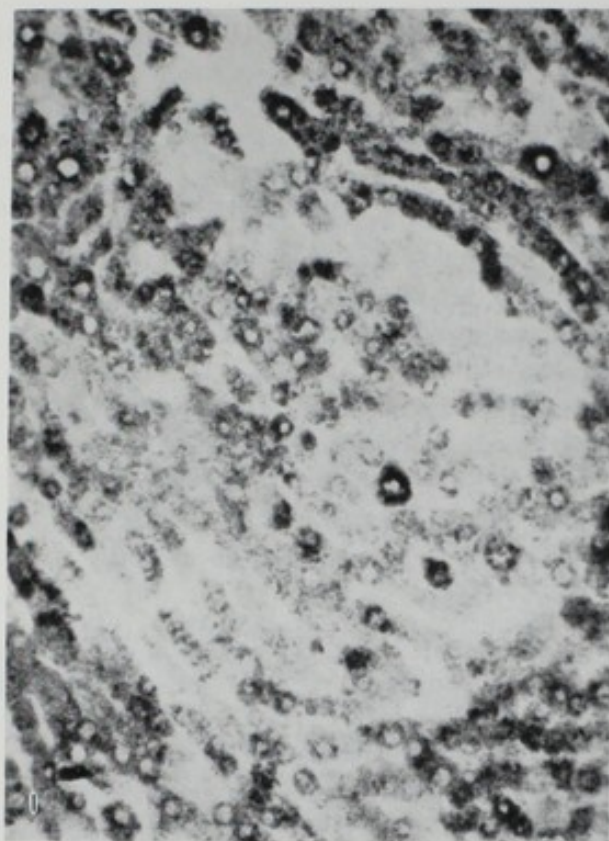
PHOTO 12. Histological appearance of nodule II. HE stain, $\times 40$.

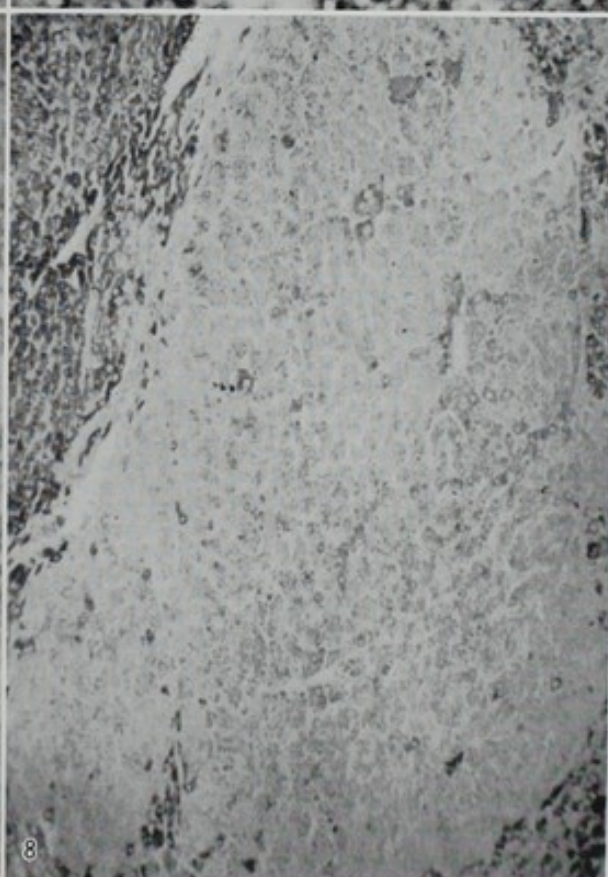
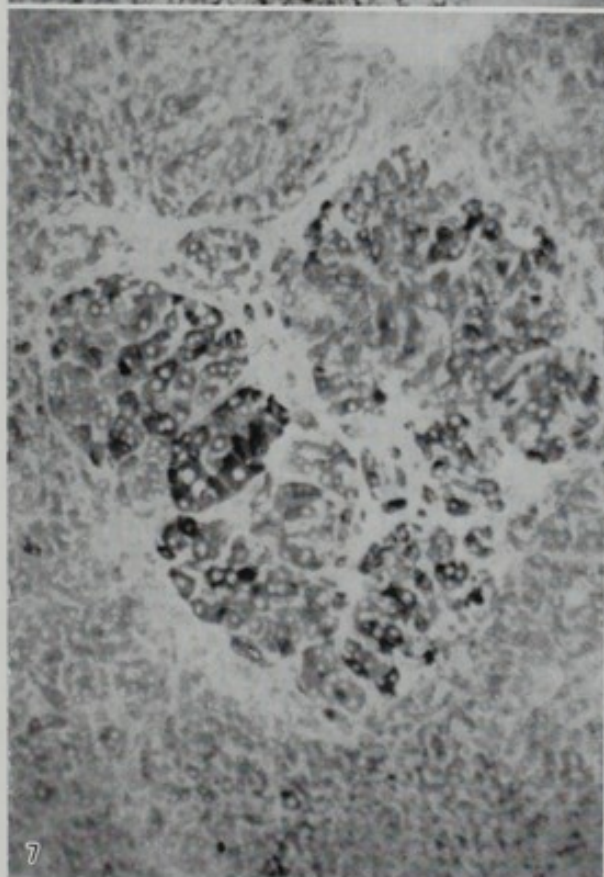
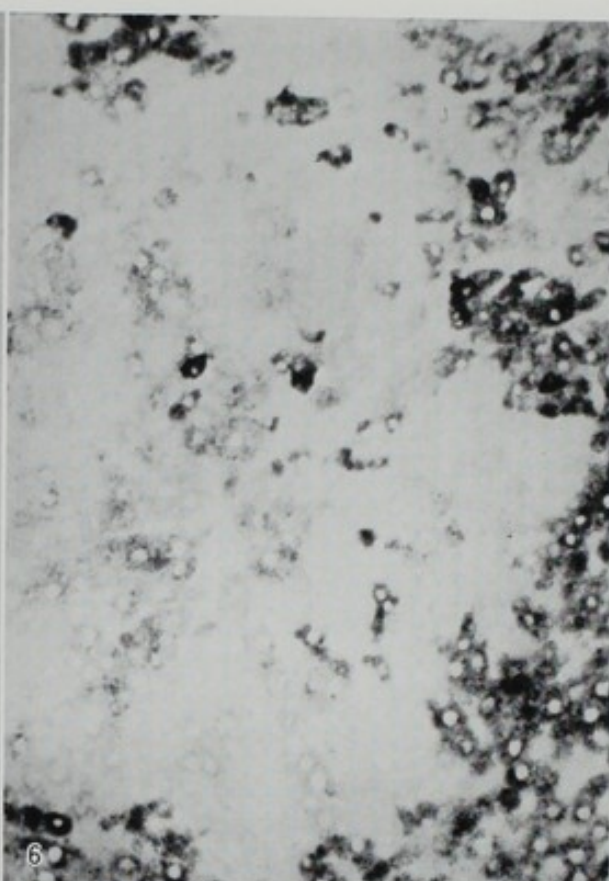
PHOTO 13. Low power electron micrograph of a portion of nodule I. ER, aggregation of smooth surfaced endoplasmic reticulum; GL, glycogen area; arrows, autophagic vacuoles containing glycogen particles.

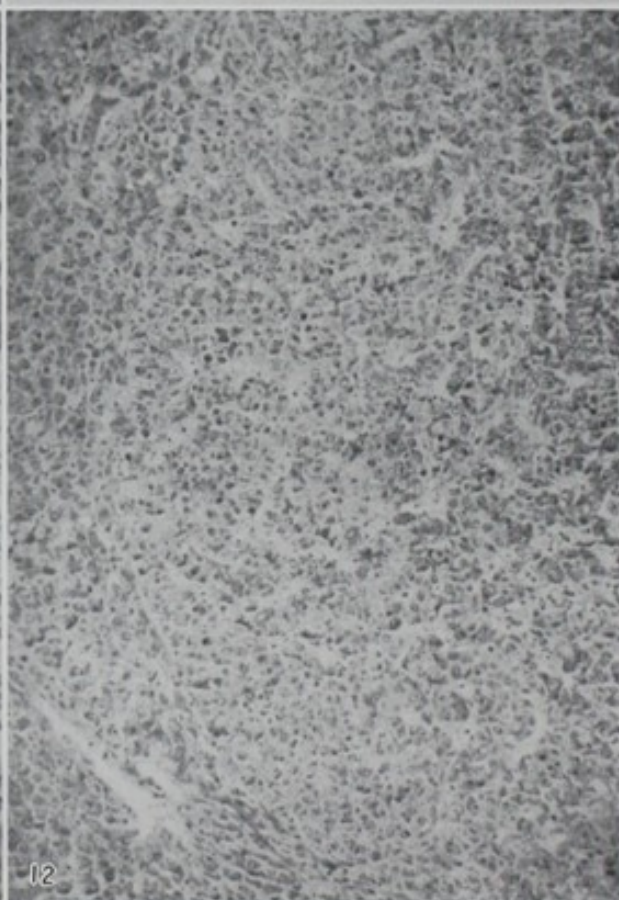
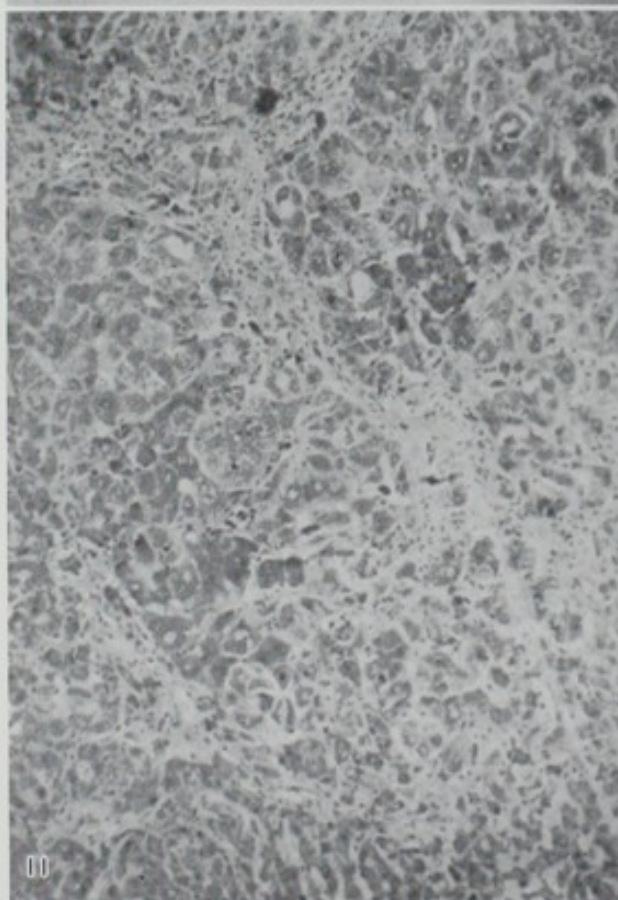
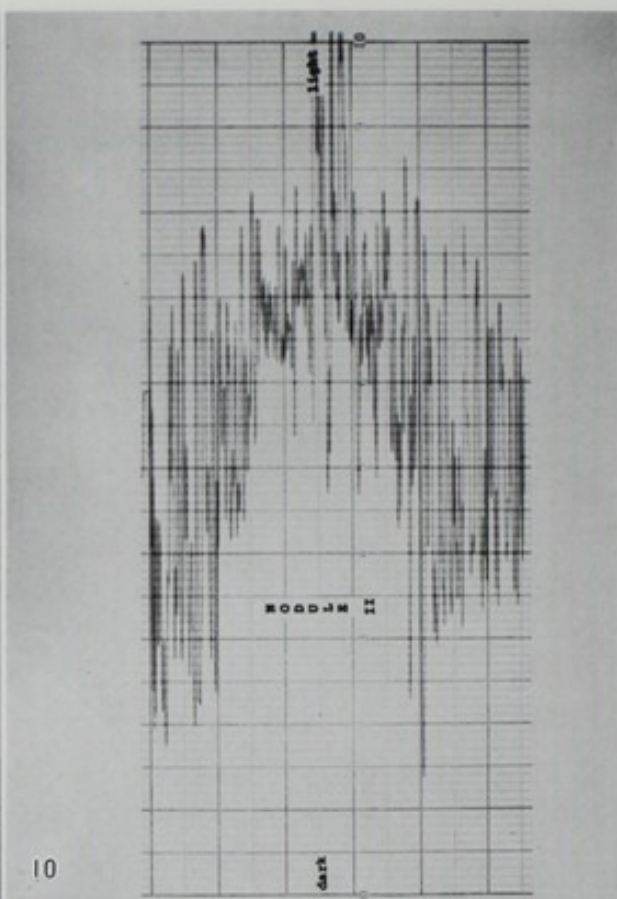
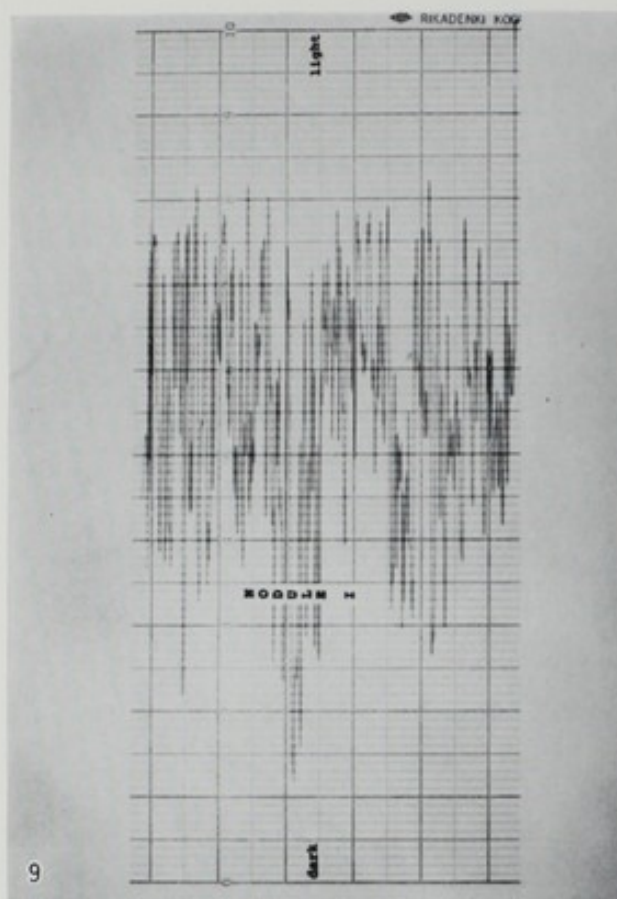
PHOTO 14. Nucleus with smooth outline is a general feature of the cells in nodule I. NL, nucleolus.

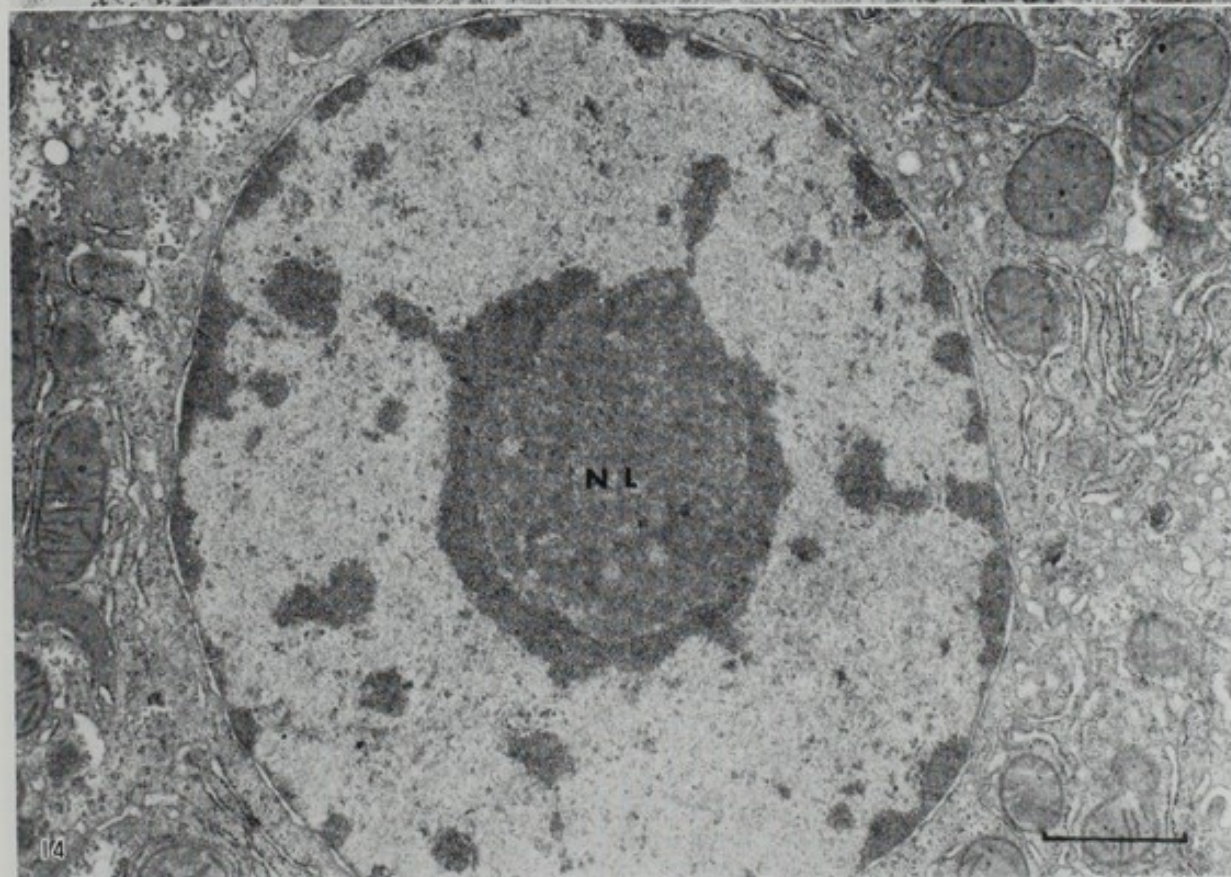
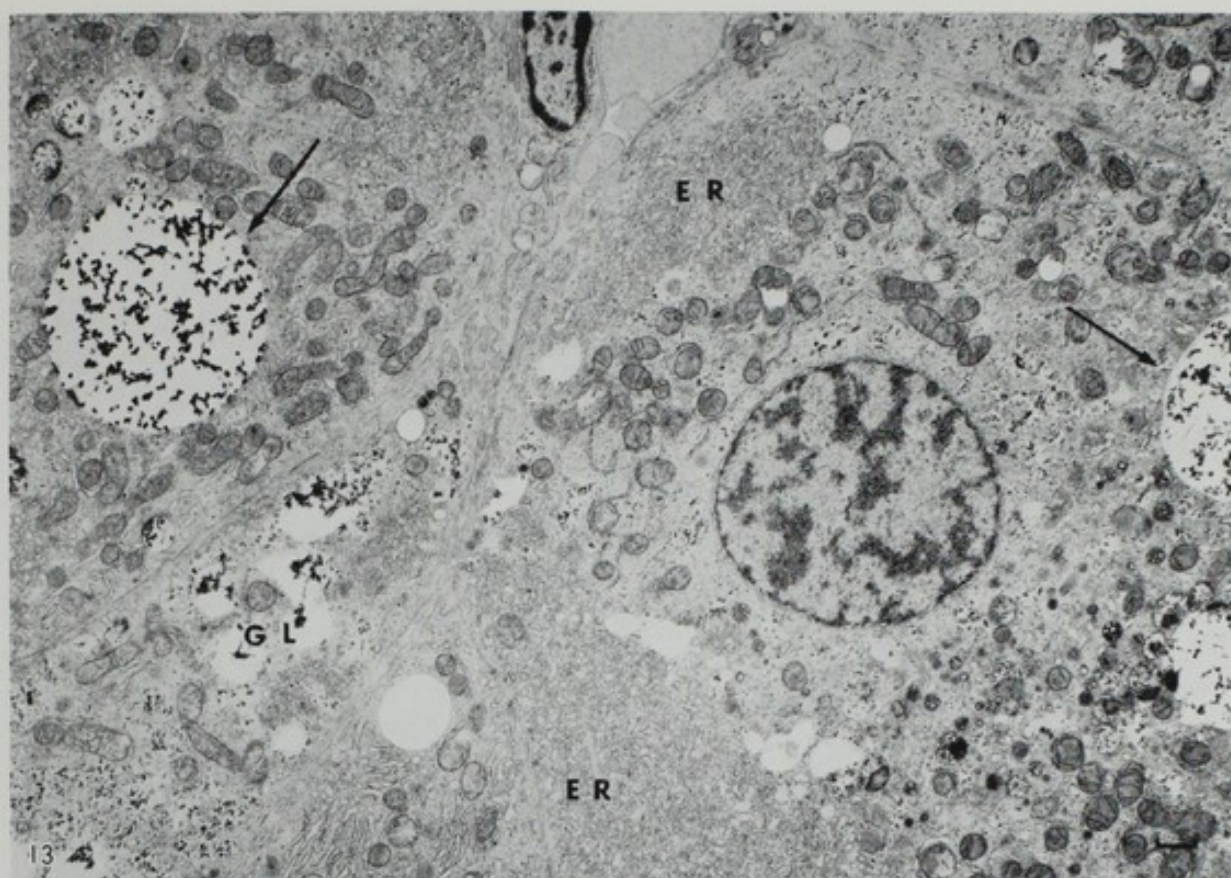
PHOTO 15. Dilated bile canaliculus (BC) with a few microvilli is seen between the cells in nodule I.

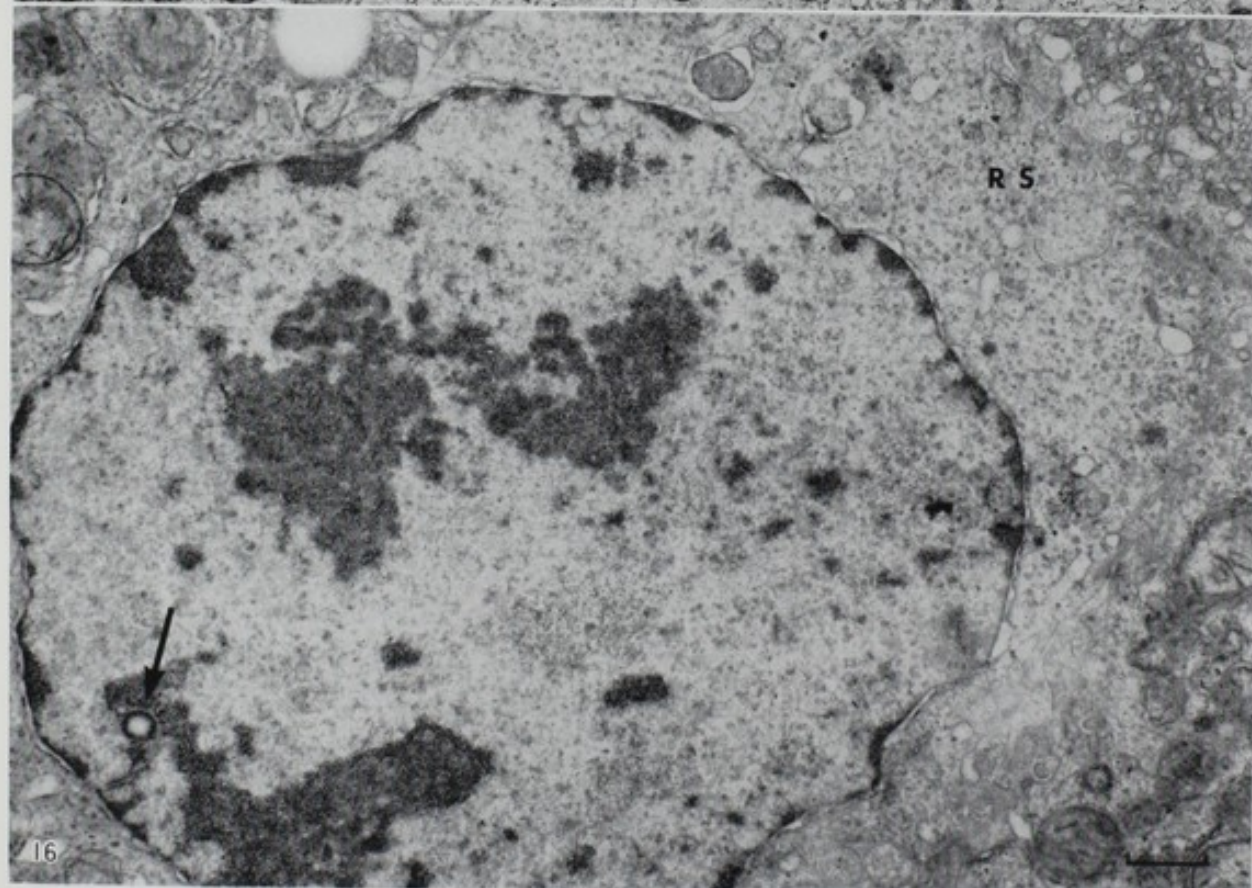
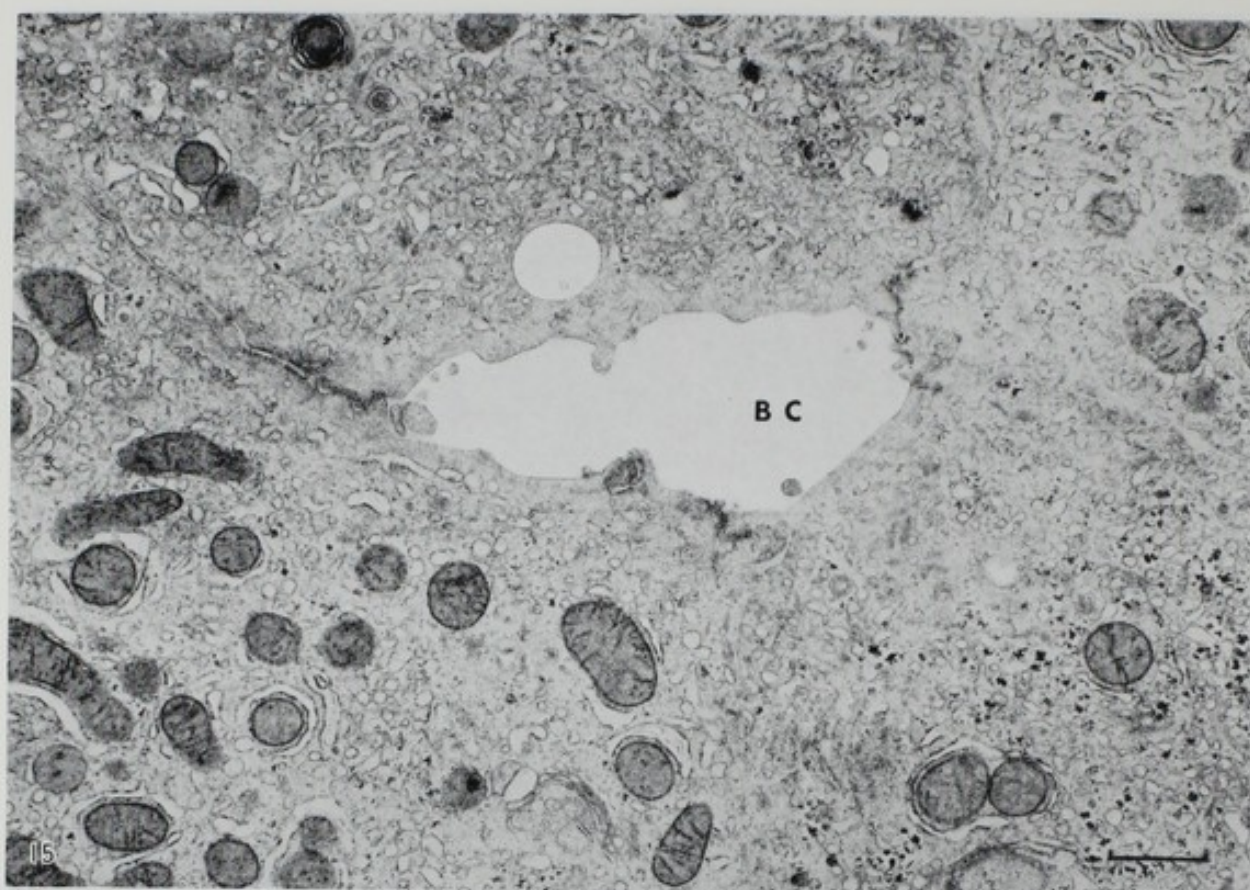
PHOTO 16. A portion of the cell seen in nodule II. RS, polysomes in the cytoplasm. Nucleus is irregular and contains an intranuclear inclusion (arrow).











CHARACTERISTICS OF CULTURED FIBROBLASTS OF SKIN FROM PATIENTS WITH ADENOMATOSIS COLI AND PEUTZ-JEGHERS' SYNDROME

Michiko MIYAKI,^{*1} Noriko AKAMATSU,^{*1} Utako HIRONO,^{*1}
Kazutoshi SUZUKI,^{*1} Makoto ROKUTANDA,^{*1} Tetsuo ONO,^{*1}
Masao S. SASAKI,^{*2} Akira TONOMURA,^{*2}
and Joji UTSUNOMIYA^{*3}

*Department of Biochemistry, Tokyo Metropolitan Institute of Medical Science^{*1}
and Department of Cytogenetics, Medical Research Institute^{*2} and
Department of Surgery and Polyposis Center,^{*3}
Tokyo Medical and Dental University*

1) Skin fibroblasts from individuals with manifest adenomatosis coli (AC) were two to three times more sensitive than normal cells to the cytotoxicity of 4-nitroquinoline-1-oxide (4NQO) and mitomycin C. The 4NQO-sensitive cells were found to have increased 4NQO-reductase activity. But the sensitivity of AC cells to UV light and N-methyl-N'-nitro-N-nitrosoguanidine was normal. Peutz-Jeghers' (PJ) cells did not exhibit increased sensitivity to these carcinogens. 2) The manifest AC and manifest PJ fibroblasts were up to five times more susceptible to morphological transformation by murine sarcoma virus (murine leukemia virus) of rat 78A1 cells, 78A1-MSV (MLV), than those from normal individuals. The fibroblasts from nonmanifest family members of AC patients included two types of cell strains: One was as highly susceptible to MSV (MLV) as the manifest AC, and the other had a sensitivity similar to normal cells. The cultures of AC cells, which were highly susceptible to MSV (MLV), released more infectious MSV and MLV than normal cells after infection with MSV (MLV). None of the fibroblasts were transformed by infection with xenotropic MLV alone. Similar amounts of ³H-uridine-labeled virus were incorporated into AC and normal cells, suggesting that some process other than adsorption or penetration of virus may increase the susceptibility of AC and PJ cells to transformation. 3) The growth rates of AC and PJ cells were the same as those of normal cells in the presence of 1% and 15% serum. The saturation densities and plating efficiencies of AC and PJ cells were 10% to 20% higher than those of normal cells. The morphology of some colonies of AC and PJ cells differed from normal cells. These characteristics of cultured skin fibroblasts seem to reflect a genetic predisposition to cancer in AC and PJ patients and thus may be useful for detection of latent cases.

^{*1} Honkomagome 3-18-22, Bunkyo-ku, Tokyo 113, Japan (宮木美知子, 赤松紀子, 広野詩子, 鈴木一年, 六反田亮, 小野哲生).

^{*2, *3} Yushima 1-5-45, Bunkyo-ku, Tokyo 113, Japan (佐々木正夫, 外村 晶, 宇都宮譲二).

Colon cancer is increasing by degrees in Japan. Inherited factors as well as environmental factors are known to play a role in the development of this cancer. Adenomatosis coli (AC) (12, 20, 31) and Peutz-Jeghers' syndrome (PJ) (6, 32), characterized by multiple adenomas and a high incidence of cancer in the colon and other organs, have been shown to be autosomal dominant traits. Surveys of these high risk groups in Japan were started in 1961, and 850 AC patients from 300 families have been registered by Tokyo Medical and Dental University (33), and 3,400 possible carriers now require examination. However, the genetic factors of these precancerous diseases are still not clear.

Consistent with the idea that a genetic predisposition to cancer is imposed by environmental factors, increased sensitivity of skin fibroblasts of affected individuals to X-ray and UV light irradiation and to various chemical carcinogens has been demonstrated in cases of recessively inherited disorders (24). High susceptibilities to morphological transformation by the DNA and RNA tumor viruses SV40 and murine sarcoma virus (MSV) have also been demonstrated in cells from individuals with neoplasia and genetic abnormalities (8, 14, 30).

To look at possible expressions of the genetic factor in the skin of AC and PJ patients, we have cultured fibroblasts from the skin biopsies of individuals with manifest AC (20 subjects) and with manifest PJ (5 subjects), and from family members of AC patients (9 subjects) in Japan. We have observed the unusual properties of these cells with regard to susceptibility to chemical carcinogens and to murine sarcoma virus, and their growth characteristics as described below.

Sensitivity of AC and PJ Cells to Chemical Carcinogens

Cells from recessively-inherited disorders have been reported to be defective in the repair of damage by certain kinds of chemical mutagens and carcinogens (24). These cells exhibit increased sensitivities to the cytotoxicity of the carcinogens, *e.g.* xeroderma pigmentosum cells are sensitive both to UV light (2) and 4-nitroquinoline-1-oxide (4NQO) (28), ataxia telangiectasia cells to X-rays (29), and Fanconi's anemia cells to mitomycin C (22, 23). In our present study, measuring the colony-forming ability of cells after treatment with carcinogens, revealed that above 50% of the AC cell strains had increased susceptibility to 4NQO as shown in Fig. 1A. AC cells that were sensitive to 4NQO were also sensitive to mitomycin C (Fig. 1B). The repair mechanism for DNA damage by 4NQO has been known to be similar to that for UV repair (9), and 4NQO sensitive cells usually are also sensitive to UV light (28). But the sensitivity of AC cells to UV light was normal, suggesting that they are not deficient in UV-type repair. Incorporation of ^{14}C -4NQO into AC cells did not differ from that into normal cells (Table I), and the rate of release of ^{14}C -4NQO from AC cells by post-incubation was the same as that from normal cells. However, the size of the DNA fragments produced by 4NQO-treatment of AC cells was smaller than normal when measured by alkaline sucrose density gradient centrifugation immediately after treatment (Fig. 2). The result indicated that the number of single-strand scissions in DNA caused by 4NQO or the number of 4NQO molecules bound to DNA was more in AC cells than in normal cells.

Since 4NQO is well known to be converted to 4-hydroxyaminoquinoline 1-oxide,

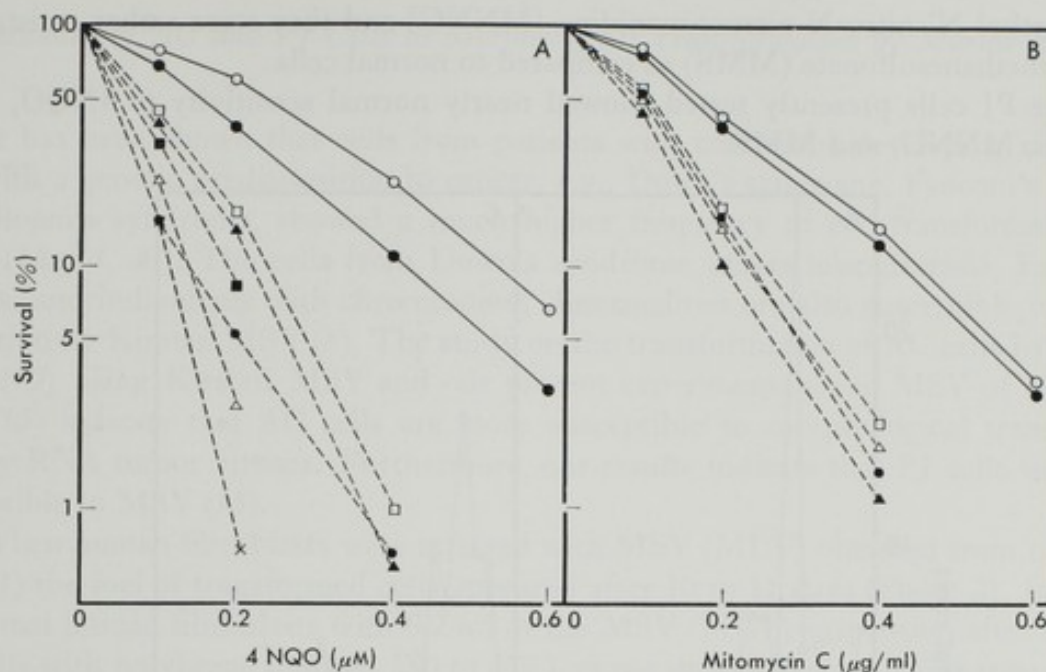


FIG. 1. Effect of 4NQO and mitomycin C on cell survival of normal and AC fibroblasts. The cells were seeded at 400 cells per 100 mm dish, and 20 hr later were treated with 4NQO or mitomycin C for 1 hr at 37° in minimum essential medium (MEM) without serum. Then they were washed and cultivated in MEM containing 15% serum. The colonies were counted after cultivation for 20 days. A: 4NQO; B: Mitomycin C. ○, ● normal cells; □, ■, △, ▲, •, × AC cells.

TABLE I. Incorporation of ^{14}C -4NQO into Normal and AC Cells

Cells	^{14}C -4NQO, cpm/ 10^6 cells	
	2 μM	4 μM
Normal (N2)	553	1,712
Normal (C4)	680	2,093
AC (PL78)	764	2,281
AC (PL40)	684	2,287

The cells were seeded at $1 \times 10^6/100$ mm dish. After 20 hr ^{14}C -4NQO in MEM was added and the cells were incubated at 37° for 1 hr. Then they were washed, detached with pronase E and EDTA, collected on a glass fiber filter and washed with NaCl solution. The radioactivity incorporated into the cells was measured after solubilizing the cells with Soluene 350.

which has the ability to bind to DNA (27), the 4NQO-reductase activity (4, 26) of cell lysates was measured. A higher activity of reductase was observed in the lysate of the higher 4NQO-sensitive cells, as shown in Table II. It has been reported that individuals with a genetically high activity of arylhydrocarbon hydroxylase, an activating enzyme of carcinogenic arylhydrocarbons, have a greater risk of developing lung cancer due to smoking than do those with low hydroxylase activity (7). The mechanism of sensitivity of AC cells to mitomycin C is not yet clear, but the 4NQO sensitivity was parallel with the sensitivity to mitomycin C, which has been known to be activated by cellular reducing enzymes. The increased sensitivity of other AC cells to mitomycin C has also been observed by Sasaki (21). The AC cells did not exhibit increased sensitivity

to N-methyl-N'-nitro-N-nitrosoguanidine (MNNG) and they were rather resistant to methyl methanesulfonate (MMS) as compared to normal cells.

The PJ cells presently tested showed nearly normal sensitivity to 4NQO, mitomycin C, MNNG, and MMS.

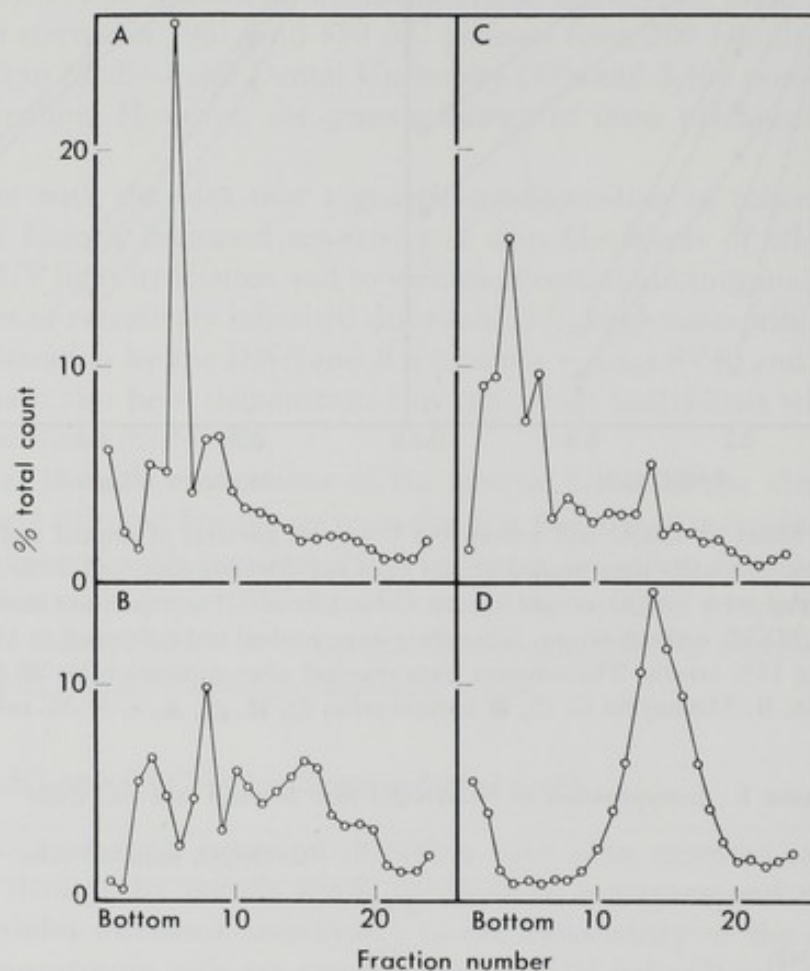


FIG. 2. Alkaline sucrose density gradient centrifugation of DNA from normal and AC cells treated with 4NQO. The ^3H -thymidine-labeled cells were treated in a suspension with $1\ \mu\text{M}$ 4NQO at 37° for 10 min. After washing with MEM, the cells were lysed at 20° for 30 min on top of alkali-SDS which was layered over 5–20% alkaline sucrose gradient, and then centrifuged at 25,000 rpm for 1 hr. A: Normal cells, control. B: Normal cells, 4NQO-treated. C: AC cells, control. D: AC cells, 4NQO-treated.

TABLE II. 4NQO-reductase Activity of Normal and AC Cells

Cells	Oxidized NADH (nmol/min/mg protein)	Inhibition of colony formation at $0.2\ \mu\text{M}$ 4NQO (%)
Normal (N2)	22	45
Normal (C4)	25	63
AC (PL78)	48	85
AC (PL40)	77	97

The cells were disrupted by sonication with 0.25 M sucrose (pH 7.4) and centrifuged at $60,000 \times g$ for 1 hr. The supernatant was assayed for 4NQO-reductase activity in a reaction mixture containing 0.06 M phosphate (pH 6.4), 0.2 mM 4NQO, and 0.15 mM NADH. The enzyme activity was calculated from the decrease in absorbance at 340 nm.

Susceptibility of AC and PJ Cells to Morphological Transformation by Murine Sarcoma Virus

It has been shown that cells from patients with conditions developing neoplasia and with a genetic predisposition to cancer, *e.g.*, Down's syndrome, Fanconi's anemia and Bloom's syndrome, showed a much higher frequency of cell transformation by SV40 (13, 14, 30). The cells from Down's syndrome, ataxia telangiectasia, Fanconi's anemia, and individuals with chromosomal abnormalities are also susceptible to transformation by Kirsten MSV (8). The study on the transformation of AC cells by Pfeffer *et al.* (19) using Kirsten MSV and our present experiments using MSV of rat 78A1 cells (15) indicate that AC cells are more susceptible to morphological transformation by RNA tumor viruses. Furthermore, our results indicate that PJ cells were also susceptible to MSV (15).

When human fibroblasts were infected with MSV (MLV) obtained from rat 78A1 cells (1) the foci of transformed cells appeared after 10 to 11 days (Photo 2). Infection of normal human fibroblasts with 0.2 ml of the MSV (MLV) suspension after treating the cells with polybrene induced 150 to 470 foci per dish, whereas similar treatment of cells from manifest AC induced 600 to 2,000 foci as shown in Fig. 3. The cells from family members of AC patients included two groups. One group showed a sensitivity as low as normal cells and the other exhibited an increased sensitivity to the MSV (MLV) similar to manifest AC, and the latter seemed to be latent cases of AC. The cells from individuals with PJ syndrome also showed a high sensitivity to transformation by MSV (MLV), and the fibroblasts from two subjects having Gardner's syndrome showed a transformation frequency of 700. These AC and PJ cells were also sensitive to transformation by three kinds of pseudotypes of Moloney MSV containing amphotropic MLV, xenotropic MLV, and dualtropic MLV (15), although they were not transformed by infection with standard Moloney MSV (MLV).

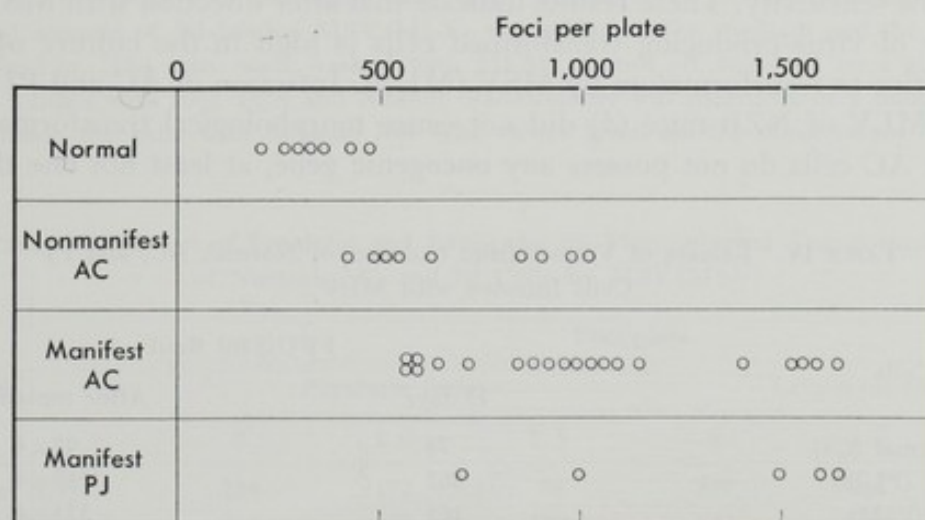


FIG. 3. Susceptibility of skin fibroblasts to transformation by MSV(MLV). The cells were seeded at 2×10^5 cells per 60 mm dish. After 20 hr, the cells were treated with polybrene and infected with 0.2 ml of 1-, 5-, 25-, and 125-fold diluted MSV(MLV) suspension obtained from rat 78A1 cells. After incubation for 12 days, the number of foci was counted and extrapolated to the value at 1-fold dilution.

TABLE III. Release of Viruses from Culture of Normal, AC, and PJ Cells Infected with MSV (MLV)

Cells	Foci per plate on day 11	FFU/5 ml fluid		
		MSV 16 days	MLV 16 days	After replating ^a
Normal (C4)	290	156	910	1,980×4
AC (PL78)	1,340	468	4,950	7,455×4
PJ (PJ22)	790	168	1,160	2,800×4

The cells were infected with 0.2 ml of 78A1-MSV (MLV). After cultivation for 16 days with a change of medium every third day, 24-hr culture fluids were added to 2×10^5 mink cells or S+L- mink cells and incubated for 7 days. FFU's (focus-forming units) of MSV and MLV in the fluids are indicated by the number of foci which are assayed on the mink cells and the S+L- mink cells, respectively. Each value given is the mean value from duplicate experiments.

^a FFU of MLV in fluids on day 14 after replating of cells at 1/4 the cell density.

Addition of the culture fluids from cells infected with MSV (MLV) to uninfected cells also caused transformation, and the difference between the number of foci in AC cells and normal cells was greater than that observed in the original infection experiments with MSV (MLV). This suggested that infected AC cell cultures released more infectious MSV (MLV) particles. Therefore, the titers of MSV and MLV in the culture fluid of the first infection experiment were assayed using normal and S+L- mink cells (17). The titers of infectious MSV and MLV in the fluids were consistent with the sensitivity of the cells to transformation by MSV (MLV) (Table III). Replating the infected cultures increased the titer of the viruses, indicating that the production of viruses is affected by the conditions of cell growth, but that the amount of viruses released from the highly-sensitive cells after replating was still larger than that from the cells with low sensitivity (Table III). The reverse transcriptase activity of the fluid from this culture of highly sensitive cells was also higher than that of infected cells with low sensitivity. These results indicate that after infection with MSV (MLV), the number of virus-producing transformed cells is high in the culture of AC cells highly sensitive to transformation by MSV (MLV). Infection of AC and PJ cells with xenotropic MLV of NZB mice (5) did not cause morphological transformation, suggesting that AC cells do not possess any oncogenic gene, at least not one that is res-

TABLE IV. Release of Viruses from Cultures of Normal, AC, and PJ Cells Infected with MLV

Cells	FFU/5 ml fluid	
	15 days	After replating ^a
Normal (C4)	75	92×4
AC (PL78)	385	749×4
PJ (PJ22)	165	333×4

The cells were infected with 0.2 ml of xenotropic MLV from NZB-mouse cells. After cultivation for 15 days, with a change of medium every third day, 24-hr culture fluids were added to 2×10^5 S+L- mink cells and incubated for 7 days. Each value is the mean number of foci from duplicate experiments.

^a FFU of MLV in fluids on day 7 after replating at 1/4 the cell density.

cuable by murine type C viruses. But when the cells were infected with xenotropic MLV, much infectious MLV was released into the culture fluid by AC cells which were highly sensitive to transformation by MSV (MLV) (Table IV).

When the fibroblasts were incubated with ^3H -uridine-labeled MSV (MLV) after treatment with polybrene, about 7% of the added radioactivity was adsorbed to the cells during a 1-hr period of incubation. Similar amounts of labeled MSV (MLV) were adsorbed to AC and normal cells (Table V), indicating that the increased sensitivity of AC cells to transformation by MSV (MLV) is not due to more efficient adsorption of virus to the AC cells but to other processes, such as uncoating or integration and expression of the virus genome. It has been suggested that protease activity is associated with the production and maintenance of transformation (34), and the protease inhibitor pepstatin has been demonstrated to reduce the formation of foci in mouse cells caused by MSV (35). The presence of pepstatin or leupeptin at the time of virus infection of AC cells and throughout cultivation reduced their transformation frequency to the level of normal cells but also reduced that of the normal cells, as indicated in Table VI. On the other hand, tetradecanoylphorbol acetate (TPA) added to the culture medium after infection with MSV (MLV) increased the number of foci in cultures of both AC and normal cells (Table VII). Reduction of the transformation frequency by protease inhibitors and its enhancement by TPA suggest that the level of a specific protease affects morphological transformation. It is interesting that AC cells have a

TABLE V. Adsorption of ^3H -labeled MSV (MLV) to Normal and AC Cells

Cells	^3H , cpm adsorbed/ 10^6 cells	
	^3H -MSV (MLV) suspension added	
	0.05 ml	0.15 ml
Normal (C4)	3,920	11,465
AC (PL78)	3,928	10,392

The cells were treated with polybrene 20 hr after seeding at 5×10^5 cells per 60 mm dish. Then the indicated amount of ^3H -labeled MSV (MLV) was added to the medium and the cultures were incubated for 1 hr. The cells were washed with MEM, scraped off, collected on a glass fiber filter and washed 5 times with 10% TCA and ethanol. Radioactivity was measured in a toluene scintillator after solubilizing the cells with Soluene 350. The values given are the mean values from duplicate experiments.

TABLE VI. Effect of Pepstatin and Leupeptin on Morphological Transformation of Normal, AC, and PJ Cells by MSV (MLV)

Cells	Foci/plate					
	Pepstatin (mM)			Leupeptin (mM)		
	0	1.0	1.5	0	1.0	1.5
Normal (C4)	284	172	68	269	216	146
AC (PL78)	864	272	180	ND	ND	ND
PJ (PJ22)	ND	ND	ND	975	780	510

Pepstatin and leupeptin were added to the cell cultures at the time of infection and were present throughout the culture period until counting of foci. The values given are the mean values from duplicate experiments.

TABLE VII. Effect of TPA on Morphological Transformation of Normal and AC Cells by MSV (MLV)

Cells	Foci/plate	
	-TPA	+TPA
Normal (C4)	300	620
AC (PL78)	1,479	2,957
AC (PL77)	1,093	1,736

TPA at 1 ng/ml was added to the cell cultures 3 days after infection with MSV (MLV), and the medium was changed every 3 days. Foci were counted 12 days after infection. The values given are the mean values from triplicate experiments.

higher level of plasminogen activator than normal cells, as reported by Kopelovich (10). The spontaneously increased level of protease activity in AC cells may affect the sensitivity to transformation by MSV (MLV).

Growth Characteristics of AC and PJ Cells

Although Pfeffer *et al.* have reported a difference in growth rates between AC and normal cells in a medium containing 1% serum (18), our experiments as well as that of Hamaguchi (3) showed that the population-doubling time of AC and PJ cells did not differ from that of normal cells in the presence of both 15% and 1% fetal calf serum (Fig. 4). However, the saturation densities of AC and PJ cells were 10% to 20% higher than those of normal cells. The plating efficiencies of AC and PJ cells were higher than normal cells (Table VIII), and some of their colonies, composed of spindle shaped small

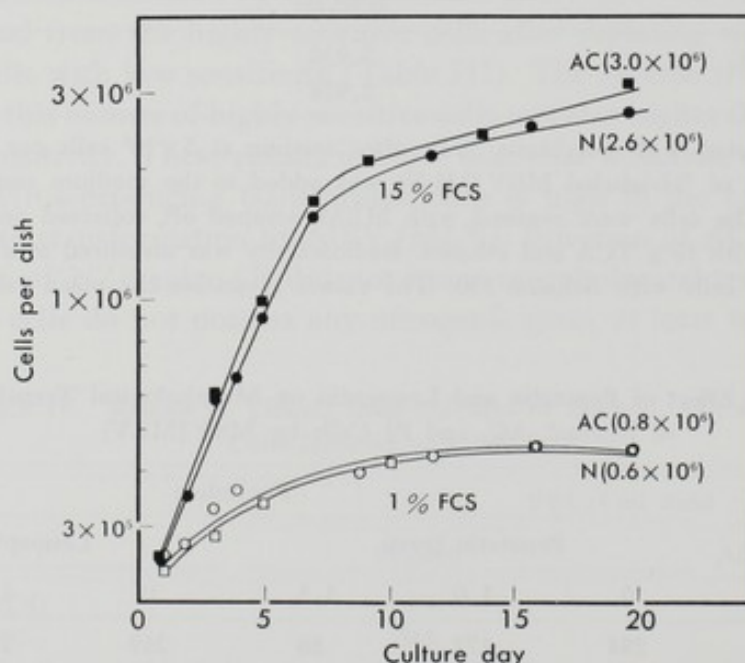


FIG. 4. Growth curves of normal and AC cells. The cells were inoculated at 2×10^5 cells per 60 mm dish and cultivated for the days indicated with a change of medium every third day. The number of cells was counted after treatment with pronase E and EDTA. The values in parentheses indicate the saturation densities. ●, ○ normal cells (C4); ■, □ AC cells (PL78).

TABLE VIII. Plating Efficiency of Normal, AC, and PJ Cells

Cells	Number of cell strain	Plating efficiency in liquid medium (%)
Normal (volunteers)	7	18.8±1.6
Normal (nonmanifest AC)	8	20.6±3.2
AC (manifest AC)	22	24.4±1.1
PJ (manifest PJ)	6	25.7±2.1

The cells were inoculated at 400 cells per 100 mm dish, cultured for 14 days and the number of colonies containing more than 100 cells/colony was counted. The values given are the mean±S.E. from 2 to 10 experiments for each cell strain.

fibroblasts, were more tightly formed with more uniform peripheries (Photo 4); colonies of normal cells, in contrast, had large fibroblasts and diffused peripheries (Photo 3). This morphological difference in colonies was also observed by Sasaki (21). The colony-forming abilities of AC cells in soft agar were also higher than those of normal cells.

These characteristics of AC cells seem to reflect a predisposition to formation of many polyps. But the mechanism of expression of the growth abnormalities is not understood yet. The AC cells have increased plasminogen activator activity (10) and defective actin organization (11). Our preliminary experiment indicated that protease activity in culture fluids from AC cells was higher than normal although the intracellular protease activity of AC cells did not differ from normal. It may be noted that some of the AC cells exhibited a high frequency of spontaneous reciprocal translocation of chromosomes (21) and that increased tetraploidy was observed in cultured Gardner's syndrome cells (25). We recently observed the enhanced inducible chromosomal aberration and transformation of AC cells after treatment with a chemical carcinogen (16). Further studies of chromosomal aberration should be carried out.

Acknowledgments

We are grateful to Dr. H. Yoshikura, Institute of Medical Science, University of Tokyo, for providing S+L- mink cells and four pseudo types of Moloney MSV (MLV) and to Dr. R. Hirai, of this institute, for xenotropic MLV. This work was supported in part by grants for cancer research from the Ministry of Education, Science and Culture, and the Ministry of Health and Welfare of Japan.

REFERENCES

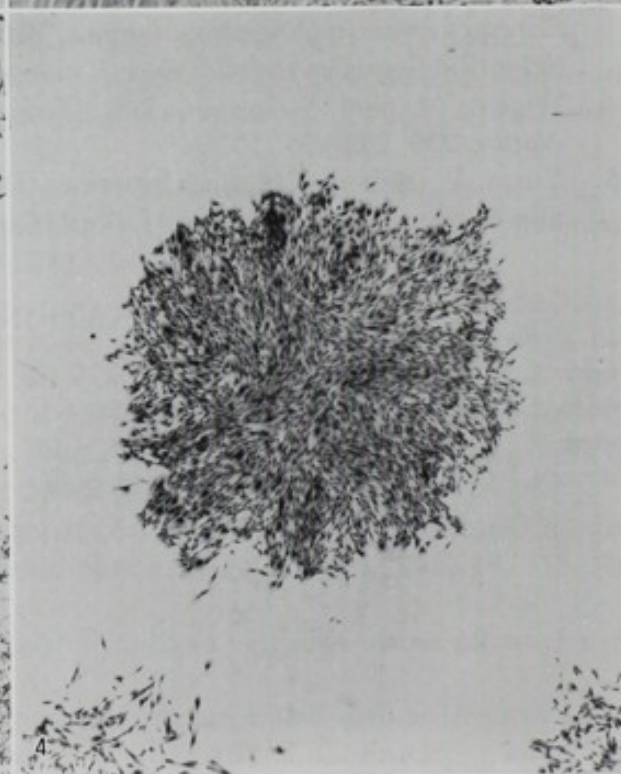
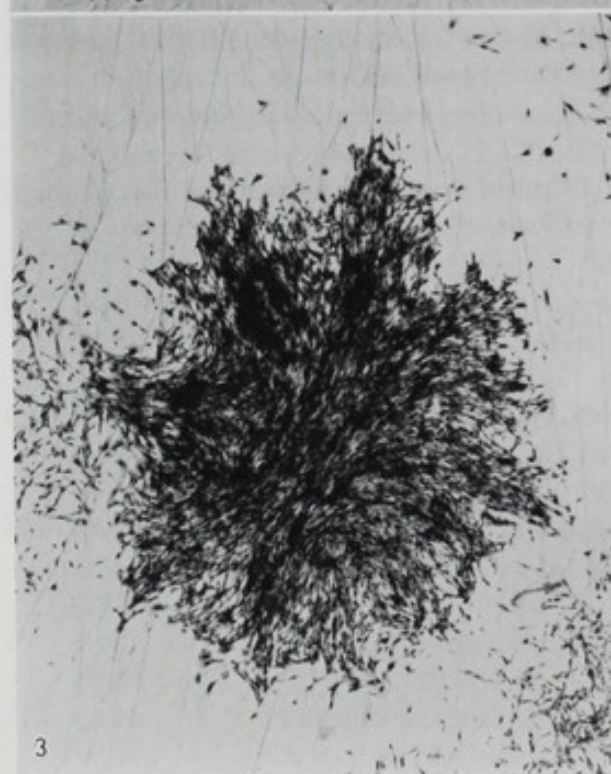
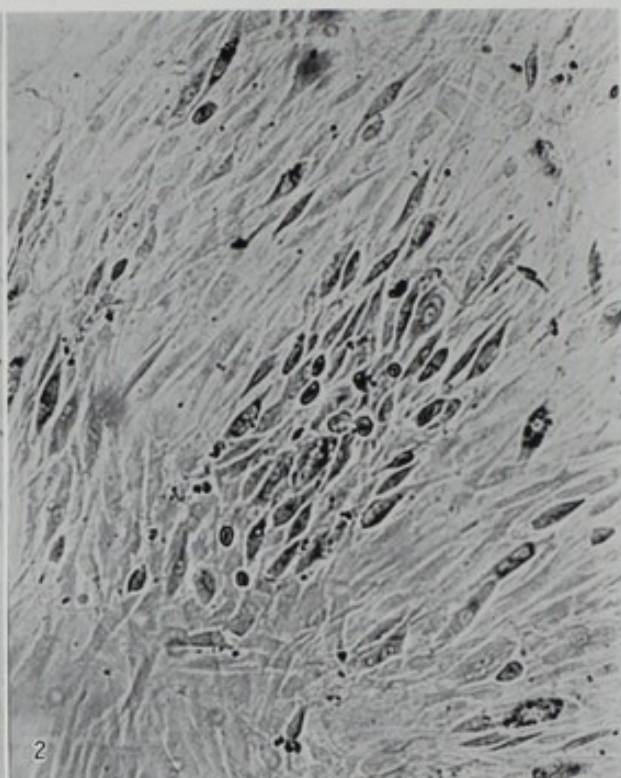
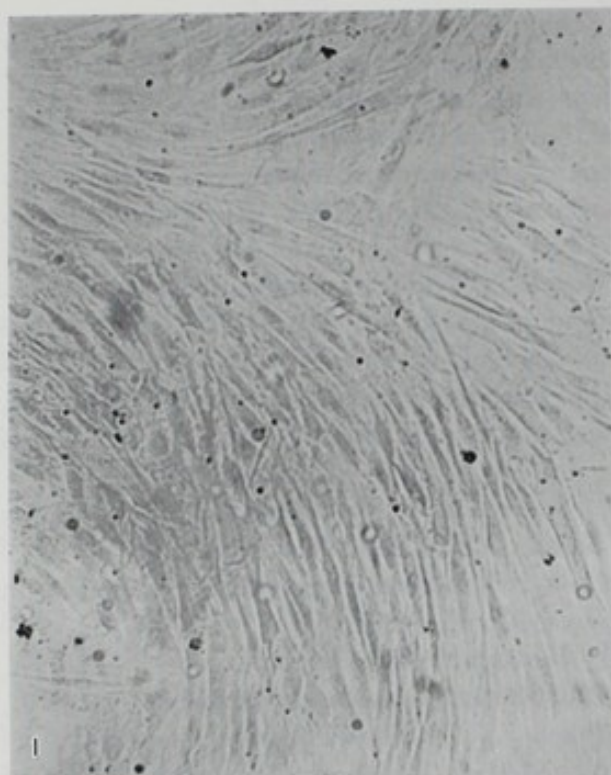
1. Bernard, C., Boiron, M., and Lansneret, J. Transformation et infection chronique de cellules embryonnaires de rat par le virus du sarcome de Moloney. *C. R. Acad. Sci. Paris*, **264**, 2170-2173 (1967).
2. Cleaver, J. E. Defective repair replication of DNA in xeroderma pigmentosum. *Nature*, **218**, 652-656 (1968).
3. Hamaguchi, H. Personal communication.
4. Hashimoto, Y., Terasawa, M., and Toriyama, M. Metabolism of 4-nitro-quinoline-1-oxide. *Seikagaku*, **36**, 556 (1964) (in Japanese).
5. Hirai, R., Yuasa, Y., and Yamamoto, T. Heat-labile character of murine sarcoma-xenotropic leukemia virus complex in duck. *Cell Virol.*, **96**, 615-621 (1979).
6. Jeghers, H., McKusik, V. A., Kermit, H., and Katz, K. Generalized intestinal polyposis

- and melanin spots of the oral mucosa, lips and digits. *N. Engl. J. Med.*, **241**, 1031-1036 (1949).
7. Kellermann, G., Shaw, C. R., and Luyten-Kellermann, M. Aryl hydrocarbon hydroxylase inducibility and bronchogenic carcinoma. *N. Engl. J. Med.*, **289**, 934-937 (1973).
 8. Klement, V., Freedman, M. H., McAllister R. M., Nelson-Rees, W. A., and Heubner, R. J. Differences in susceptibility of human cells to mouse sarcoma virus. *J. Natl. Cancer Inst.*, **47**, 65-73 (1971).
 9. Kondo, S., Ichikawa, H., Iwo, K., and Kato, T. Base-change mutagenesis and prophage induction in strains of *E. coli* with different DNA repair capacities. *Genetics*, **66**, 187-217 (1970).
 10. Kopelovich, L. Phenotypic markers in human skin fibroblasts as possible diagnostic indices of hereditary adenomatosis of the colon and rectum. *Cancer*, **40**, 2534-2541 (1977).
 11. Kopelovich, L., Conlon, S., and Pollack, R. Defective organization of actin in cultured skin fibroblasts from patients with inherited adenocarcinoma. *Proc. Natl. Acad. Sci. U.S.*, **74**, 3019-3022 (1977).
 12. Lockhart-Mumme, J. P. and Dukes C. E. Familial adenomatosis of colon and rectum, its relation to cancer. *Lancet*, **i**, 586-589 (1939).
 13. Lubiniecki, A. S., Blattner, W. A., and Fraumeni, J. F. Jr., Elevated expression of T-antigen in simian papovavirus 40-infected skin fibroblasts from individuals with cytogenetic defects. *Cancer Res.*, **37**, 1580-1583 (1977).
 14. Miller, R. W. and Todaro, G. J. Viral transformation of cells from persons at high risk of cancer. *Lancet*, **i**, 81-82 (1969).
 15. Miyaki, M., Akamatsu, N., Rokutanda, M., Ono, T., Yoshikura, H., Sasaki, M. S., Tonomura, A., and Utsunomiya, J. Increased sensitivity of fibroblasts of skin from patients with adenomatosis coli and Peutz-Jeghers' syndrome to transformation by murine sarcoma virus. *Gann*, **71**, 797-803 (1980).
 16. Miyaki, M., Akamatsu, N., Hirono, U., Ono, T., Tonomura, A., and Utsunomiya, J. Transformation of fibroblasts from a patient with adenomatosis coli by treatment with a chemical carcinogen. *Gann*, **71**, 741-742 (1980).
 17. Peeble, P. T. An *in-vitro* focus-induction assay for xenotropic murine leukemia virus, feline leukemia virus C and the feline primate virus RD-114/CCC/M-7. *Virology*, **67**, 288-291 (1975).
 18. Pfeffer, L., Lipkin, M., Stutman, O., and Kopelovich, L. Growth abnormalities of cultured human skin fibroblasts derived from individuals with hereditary adenomatosis of the colon and rectum. *J. Cell Physiol.*, **89**, 29-38 (1976).
 19. Pfeffer, L. M. and Kopelovich, L. Differential genetic susceptibility of cultured human skin fibroblasts to transformation by Kirsten murine sarcoma virus. *Cell*, **10**, 313-320 (1977).
 20. Reed, T. E. and Neel, J. V. A genetic study of multiple polyposis of the colon. *Am. J. Hum. Genet.*, **7**, 236-263 (1955).
 21. Sasaki, M. S. Fanconi's anemia: A condition possibly associated with a defective DNA repair. In "DNA Repair Mechanisms," ed. P. C. Hanawalt, E. C. Friedberg, and C. F. Fox, pp. 657-684 (1978). Academic Press, New York.
 22. Sasaki, M. S. and Tonomura, A. A high susceptibility of Fanconi's anemia to chromosome breakage by DNA cross-linking agents. *Cancer Res.*, **33**, 1829-1836 (1973).
 23. Sasaki, M. S. Is Fanconi's anemia defective in a process essential to the repair of DNA cross links. *Nature*, **257**, 501-503 (1975).
 24. Setlow, R. B. Repair deficient human disorders and cancer. *Nature*, **271**, 713-717 (1978).
 25. Shannon, D. Increased tetraploidy: cell-specific for the Gardner gene in the cultured cells. *Cancer*, **38**, 1983-1988 (1976).

26. Sugimura, T., Okabe, K., and Nagao, M. The metabolism of 4-nitroquinoline-1-oxide, a carcinogen. III. An enzyme catalyzing the conversion of 4-nitroquinoline-1-oxide to 4-hydroxyaminoquinoline-1-oxide in rat liver and hepatomas. *Cancer Res.*, **26**, 1717-1721 (1966).
27. Tada, M. and Tada, M. Enzymatic activation of the carcinogen 4-hydroxyaminoquinoline-1-oxide and its interaction with cellular macromolecules. *Biochem. Biophys. Res. Commun.*, **46**, 1025-1032 (1972).
28. Takebe, H., Furuyama, J., Miki, Y., and Kondo, S. High sensitivity of xeroderma pigmentosum cells to the carcinogen 4-nitroquinoline-1-oxide. *Mutat. Res.*, **15**, 98-100 (1972).
29. Taylor, A.M.R., Harnden, D. G., Arlett, C. F., Harecourt, S. A., Lehman, A. R., Stevens, S., and Bridges, B. A. Ataxia telangiectasia: a human mutation with abnormal radiation sensitivity. *Nature*, **258**, 427-429 (1975).
30. Todaro, G. J., Green, H., and Swift, M. R. Susceptibility of human diploid fibroblasts strains to transformation by SV-40 virus. *Science*, **153**, 1252-1254 (1966).
31. Utsunomiya, J. and Nakamura, T. The occult osteomatous change in the mandible in patients with familial polyposis coli. *Br. J. Surg.*, **2**, 45-51 (1975).
32. Utsunomiya, J., Gocho, H., Miyanaga, T., Hamaguchi, A., Kashimura, A., Aoki, N., and Komatsu, I. Peutz-Jeghers' syndrome and its natural cause. *Johns Hopkins Med. J.*, **136**, 71-82 (1975).
33. Utsunomiya, J. Present status adenomatosis coli in Japan. In "Pathophysiology of Carcinogenesis in Digestive Organs," ed. E. Farber *et al.*, pp. 305-321 (1977). Japan Scientific Societies Press, Tokyo/University Park Press, Baltimore.
34. Wigler, M. and Weinstein, I. B. Tumor promoter induced plasminogen activator. *Nature*, **259**, 232-233 (1976).
35. Yuasa, Y., Shimojo, H., and Umezawa, H. Effect of protease inhibitors on focus formation by murine sarcoma virus. *J. Natl. Cancer Inst.*, **54**, 1255-1256 (1975).

EXPLANATION OF PHOTOS

- PHOTO 1. Uninfected AC fibroblasts. PL78, $\times 150$.
PHOTO 2. AC fibroblasts infected with MSV(MLV). PL78, $\times 150$.
PHOTO 3. Colony of normal fibroblasts. C4, $\times 10$.
PHOTO 4. Colony of AC fibroblasts. PL40, $\times 10$.



ADENOMATOUS HYPERPLASIA IN LIVER CIRRHOSIS: AN APPROACH FROM A MICROANGIOGRAPHICAL POINT OF VIEW

Kenichi SASAKI

*Department of Pathology, School of Medicine, Kitasato University**

For the evaluation of adenomatous hyperplasia of the liver, which is a peculiar lesion easily mistaken for hepatocellular carcinoma (HCC), 83 cirrhotic livers with or without HCC were examined by means of gelatine injection methods. Nine cases with 11 lesions of adenomatous hyperplasia were found in this study (10.8%). Microangiographically, adenomatous hyperplasia was disclosed to be characterized by hypovascularity, a stretched but not enclosed vascular network enclosing the nodule and draining vessels with ordinary tapering. Corresponding to the microangiography, the presence of terminal portal triads was basically noted in the nodule. Results of the nuclear DNA estimation on adenomatous hyperplasia by microspectrophotometry also revealed different values from those of HCC. As to its possible precancerous state, adenomatous hyperplasia seems to be far distant from HCC.

Although recent advances based on a number of newly established laboratory and diagnostic procedures have disclosed some characteristics of hepatic tumors, a lot of issues still remain to be settled.

Adenomatous hyperplasia of the liver has been called by various names, *e.g.*, multiple nodular hyperplasia, nodular hepatitis, nodular hyperplasia, regenerative nodules, and so on (7), and designated by the formation of sizeable nodules following liver injury, submassive hepatic necrosis or cirrhosis of the liver (8, 25). The size of nodules in liver cirrhosis are usually 2 to 5 mm in diameter. However adenomatous hyperplasia may occasionally develop to one or more centimeters in the greatest dimension, even up to 8 cm.

The lesions of adenomatous hyperplasia in cirrhosis of the liver may occasionally show quite similar morphological appearances to that of hepatocellular carcinoma (HCC) macroscopically. Namely, they have distinct demarcation by fibrous stroma, and a tan, gray-whitish or greenish tint on the cut-surface, *etc.* Even by microscopical examination, not infrequently they may show similar features to those of HCC. Meanwhile, it is well known that HCC may reveal a broad spectrum of cellular atypism, from minimal-deviated to anaplastic carcinomas. Controversies are still present on the diagnostics of some lesions of adenomatous hyperplasia in cirrhotic liver in autopsy materials and surgical specimens.

The purpose of this article is to elucidate the differential characteristics of this

* Kitasato 1-15-1, Sagamihara 228, Japan (佐々木憲一).

borderline lesion, adenomatous hyperplasia from hepatocellular carcinoma, especially from a microangiographical point of view.

Cases Surveyed in Our Department

Eighty-three livers of cirrhosis, including 50 cases with HCC, were submitted for this study. These cases of cirrhosis were classified into types as shown in Table I.

Forty-nine livers of 83 cirrhosis were subjected to gelatine injection study. The hepatic artery and/or the portal vein of the removed livers were cannulated in the hepato-duodenal ligament. 50% Mika Conc (X-ray contrast meal) in 5% gelatine solution colored 5% gelatine (by 5% Carmin or 5% Berlin Blue, Merck Co.) were injected into the vessel with a syringe with manual pressure. The gelatine-injected livers were stored in ice-cold 10% formol for gelling.

Stereographic angiography was performed using a soft X-ray apparatus (Softex CBM type, Softex Co., Ltd. and Sofron SRO-M50s type, Sohken Co., Ltd.) on the whole livers and serial large liver slices of 1–2 cm in thickness, as well as on thinner slices of 3–5 mm in thickness. Stereomicroscopic observations were also carried out on

TABLE I. Cases Examined

		Adenomatous hyperplasia	
Cirrhosis without HCC	33	1	
Male		26	0
Female		7	1
Cirrhosis with HCC	50	8	
Male		39	2
Female		11	6
Total	83	9	
Male		65	2
Female		18	7

TABLE II. Cases Examined with Adenomatous Hyperplasia

Case No.	Age	Sex	HBAg	HBAb	AFP (ng)	Cirrhosis (type)	HCC	Adenomatous hyperplasia	Size (cm)
1.	65	M	/	/	/	B	+ rt	rt, superior	1.4×1.0
2.	64	F	+	/	8.4×10 ⁴	B	+ lt	mid, inferior	2.5×2.3
3.	76	F	—	/	100	B	+ mid	mid, superior	1.5×1.2
4.	75	F	+	/	51	B	+ lt	rt	1.1×1.0
5.	64	F	—	/	—	B	+ mid	rt	2.0×1.5
6.	63	F	—	/	—	B	+ rt & lt	mid	1.5×1.2
7.	68	M	—	±	—	B	(+ rt) post-operation	rt, superior & rt, lateral	1.5×1.3 1.0×0.8
8.	73	F	—	—	2,220	B	+ rt	rt, superior	1.1×1.0
9.	58	F	—	/	12	B	—	rt mid	1.3×1.2 1.0×1.0

Type of liver cirrhosis was classified according to Nagayo and Miyake's classification, and type B is almost identical to post-hepatic type cirrhosis. lt, anatomical left lobe; mid, surgical middle lobe; rt, surgical right lobe; AFP, α -fetoprotein. +, positive; —, negative; /, not examined.

the cleared tissue slices with methylsalicylate for further microangiographical analysis.

Histological examination was done on all the cases examined for the evaluation of the lesions and for exclusion of hepatocellular carcinoma. In 83 cases of liver cirrhosis, large nodules of adenomatous hyperplasia, more than 1 cm in dimension, were consequently disclosed in 9 cases (10.8%) (Table II).

For estimation of dyskaryosis (nuclear pleomorphism and hyperchromatism) in adenomatous hyperplasia and related lesions, tissue sections of 15 microns in thickness were stained by Feulgen's reaction, and nuclear DNA was measured by an Olympus microspectrophotometer (BHQ) with a wavelength of 545 nm.

Incidence of Adenomatous Hyperplasia

Adenomatous hyperplasia, greater than 1 cm in dimension, was disclosed in 9 cases of 83 examined, the incidence being 10.8% (Table I). Some laboratory data and pathological findings on the livers in these 9 cases are shown in Table II. Eleven lesions were encountered in the 9 cases: 7 lesions in the right lobe and 4 in the middle lobe of the liver. All but one were found in the cirrhotic liver with HCC foci. Sex predominance was higher in females than males (2: 7).

Gross and Microangiographical Findings of Adenomatous Hyperplasia

Macroscopically, the lesions of adenomatous hyperplasia were similar to those of HCC in cirrhotic liver. However, the vasculatures of each respective lesion were distinctly different.

Several case presentations would make it easier to recognize the differential characteristics of adenomatous hyperplasia and hepatocellular carcinoma.

Case 4.

A 75-year-old female was admitted to the Kitasato University Hospital, having arrived in shock shortly after a sudden onset of severe epigastric pain. She had a previous history of acute hepatitis. After 6 hr she was dead due to uncontrolled severe anemia and respiratory insufficiency.

Autopsy examination revealed massive intraperitoneal hemorrhage of an estimated amount of 3,100 ml. Grossly, the liver was atrophic and showed a diffusely granular appearance, weighing 1,090 g. In the left lobe, there was a large tumor mass, measuring $7.5 \times 8.0 \times 4.0$ cm in the greatest dimensions, a ruptured focus for the intraperitoneal bleeding. X-ray contrast meal was injected into the common hepatic artery for microangiography.

A sectioned slice showed a well-circumscribed tumor mass, gray whitish in color with some hemorrhagic and necrotic foci, which was confirmed to be hepatocellular carcinoma histologically. Apart from the tumor mass in the left lobe, another tan, fairly well-circumscribed nodule, measuring 1.1×1.0 cm in dimensions, was found in the right lobe.

Soft X-ray examination revealed that the tumor of the left lobe indicated a typical hypervascularity, which is characteristically identical to HCC. On the contrary, the nodule of the right lobe was hypovascular and the only finding noted was displacement

of the adjacent arterial branches (Photo 1). The latter was identified as adenomatous hyperplasia later.

Case 7.

A 68-year-old male was admitted to our University Hospital in shock with a blood pressure of 70/30 mmHg in September, 1977. An abdominal echogram disclosed a solid mass in the liver, and selective angiography revealed a hypervascular mass in the right lobe of the liver. On October 27th, 1977, partial lobectomy of the right hepatic lobe was performed, and the tumor mass was determined histologically, to be well-differentiated hepatocellular carcinoma, that had arisen in liver cirrhosis. Unfortunately, the patient was readmitted to the hospital because of resistant ascites and hepatic encephalopathy 7 months after the operation, and died from complicated bronchopneumonia.

An autopsy revealed that the liver was atrophic and diffusely fine granular, weighing 750 g, and it had two nodular lesions in it. One of the lesions was greenish in color and located in the upper portion of the right lobe, measuring 1.5×1.3 cm in size (Photo 2). The other one was gray-whitish and located in the lateral area of the right lobe, 1.0×0.8 cm in size.

Microangiographically, these nodular lesions were hypovascular in comparison with the surrounding cirrhotic liver. However, some draining branches of the hepatic artery with tapering were observed in the lesions (Photo 3). Venous lake figures were absent. These lesions were determined to be adenomatous hyperplasia.

Case 8.

A 73-year-old female had a history of diabetes mellitus since 10 years before the first admission. She was then admitted on December 22nd, 1975, with complaints of pretibial edema and abdominal distension. Abdominal laparoscopy disclosed cirrhosis of the liver. At that time, hepatitis B antigen was negative in serum and the estimation of alpha fetoprotein was below 10 ng/ml in serum.

However, when she was readmitted on April 11th, 1978, serum alpha fetoprotein was elevated to 4,030 ng/ml. Coeliac arteriography disclosed a hypervascular mass in the right lobe of the liver, and she was diagnosed as HCC arising in cirrhotic liver. Although anti-cancerous chemotherapy was introduced, she died due to rupture of the hepatic tumor.

At autopsy a tumor mass of 6.0×6.0 cm in the greatest dimensions, located in the right lobe was recognized. Gelatine injection with 50% X-ray contrast meal was performed.

A sectioned surface of the tumor showed a large green tumor mass compatible with the hypervascular lesion by coeliac angiography, and beside this large mass a greenish nodule, measuring 1.1×1.0 cm in size, was found. Both lesions gave a similar macroscopical appearance. Microangiography by soft X-ray disclosed that both lesions had quite different vascularities, namely, the former was hypervascular and the latter hypovascular (Photo 4). A close-up view of the latter nodule denoted that the thicker arterial branches were pushed out and displaced by the nodule, but several arterial branches were still draining into the nodule with proportional taperings, corresponding to the vessels in portal triads (Photo 5).

TABLE III. Macroscopical and Angiographical Findings of Adenomatous Hyperplasia and HCC

Adenomatous hyperplasia	HCC
Macroscopical	Macroscopical
Fairly well-circumscribed	Well-circumscribed
Tan, gray-white, green or yellow	Gray-white, green or yellow
Angiographical	Angiographical
Hypovascular	Hypervascular
Draining arteries with few ramifications	Draining arteries with irregular ramifications
Venous lake: absent	Venous lake: present
Stretching of surrounding arteries	Basket-like figure

Case 9.

A 58-year-old female visited the Kitasato University Hospital in January, 1978, with complaints of easy fatiguability and abdominal distension. Clinical examinations revealed cirrhosis of the liver, ascites, esophageal varices, and hypersplenism. On March 1st, 1978, she had an episode of bleeding from the esophageal varices, and embolization by "Alon Alpha" in the vena gastrica sinistra was performed. After a transient lull, however, she died due to another massive hematoemesis from the esophageal varices.

Autopsy examination was carried out. Grossly, the liver was markedly atrophic, weighing 680 g, showing diffuse micronodular from 3 to 7 mm in size. Several cysts were also noted. Gelatine injection with X-ray contrast meal was performed.

By serial sectioning a gray-whitish nodule, 1.0 cm in dimension, was found in the convex area of the right hepatic lobe (Photo 6). Soft X-ray microangiography of the sliced liver disclosed that the nodule was hypovascular and it was surrounded by a relatively dense vascular network (Photo 7). This vascular network looked like that of the basket-like figure encountered in HCC, but the surrounding network of this nodule was mainly composed of an accumulation of stretched arterial branches and was different from the basket-like figure of HCC.

Additionally, stereomicroscopic investigation on the cleared tissue slices of the above-mentioned lesions of adenomatous hyperplasia revealed further evidence for the different vascular pattern from that of HCC as shown in Photo 8.

In summary, the macroscopic and microangiographic findings of adenomatous hyperplasia of the liver are indicated in Table III, with comparisons of those of HCC.

Microscopical Findings in Adenomatous Hyperplasia

The nodules of adenomatous hyperplasia were fairly well demarcated by fibrous stroma which contained a number of hepatic arterial and portal branches, as well as proliferated bile ductuli (Photo 9). This finding indicates that the stroma surrounding the nodules may be formed by an accumulation of ordinary stroma of the cirrhotic liver, due to pressure of regenerating nodules. In the marginal area of adenomatous hyperplasia the stroma was irregular. A marked increase in portal branches, which may be frequently observed in HCC arisen in cirrhosis, could not be noted in the surrounding stroma. A number of terminal portal triads were identified in the peripheral area

TABLE IV. Histological Findings of Adenomatous Hyperplasia and HCC

	Adenomatous hyperplasia	HCC
Portal triads	Present	Absent
Hepatic veins in nodule	Present	Absent
Neovascularization	Minimal	Prominent
Kupffer cells	Abundant	Sparse
Arrangement of hepatocytes	Plate- or cord-like	Trabecular
Iron	Positive in parenchymal cells	Almost negative in tumor cells

as well as in the center of the nodules (Photo 9). Some portal triads were distorted in arrangement and a decrease in portal branches and/or bile ducts was also observed. However, lympho-plasmacytic infiltration was recognized in these areas, as seen in unaltered portal triads. Some central veins were also present in the nodule. These findings would suggest that the presence of portal triads, even if altered, and occasionally of central veins, is an essential architectural component of adenomatous hyperplasia. Newly-formed blood vessels characterized by thin-walled vessels with large lumens were scarcely seen.

Hepatic cells, consisting of the nodules, were fairly swollen, but eosinophilic granularity in the cytoplasm was well preserved. Nuclear pleomorphism in adenomatous hyperplasia was milder than in the dyskaryotic area of the surrounding cirrhosis. Pseudo-glandular patterns, frequently containing bile plugs, were observed in some cases. The cells were arranged in plate- or cord-like patterns, which were easily recognized by reticulin stain. Iron granules could be demonstrated in the hepatocytes of adenomatous hyperplasia, the same as in the surrounding cirrhotic areas, especially in cases with intensive siderosis. Lihoral cells including Kupffer's cells were rich in nodules.

Microscopical differences between adenomatous hyperplasia and hepatocellular carcinoma are summarized in Table IV.

Histogram of Nuclear DNA in Adenomatous Hyperplasia, as Compared with That of Liver Cirrhosis and HCC

For the estimation of nuclear pleomorphism in hepatic lesions, the nuclear DNA value was measured with an Olympus Microspectrophotometer, BHQ. One hundred nuclei in each case were estimated in sections stained by Feulgen reaction. Technical discrepancies among cases through the staining process were revised on the mean value of lymphocytes in each slides.

The histograms of normal liver distributed in the range of 2.0 to 4.0 (Fig. 1a) and the mean value was 2.60 ± 0.74 . In liver cirrhosis, nuclear pleomorphism was variable from nodule to nodule and from case to case. Figure 1c is a histogram of cirrhosis with minor nuclear pleomorphism. Figures 1e and 1f are examples of cirrhosis with dyskaryosis.

Histograms of adenomatous hyperplasia were similar to that of cirrhosis of minor pleomorphism (Fig. 1d). The mean value of nuclear DNA in adenomatous hyperplasia was 2.84 ± 1.02 , almost equal to that of supposed stable cirrhosis (2.81 ± 1.05).

Meanwhile, the histograms of nuclear DNA in tumor cells of hepatocellular car-

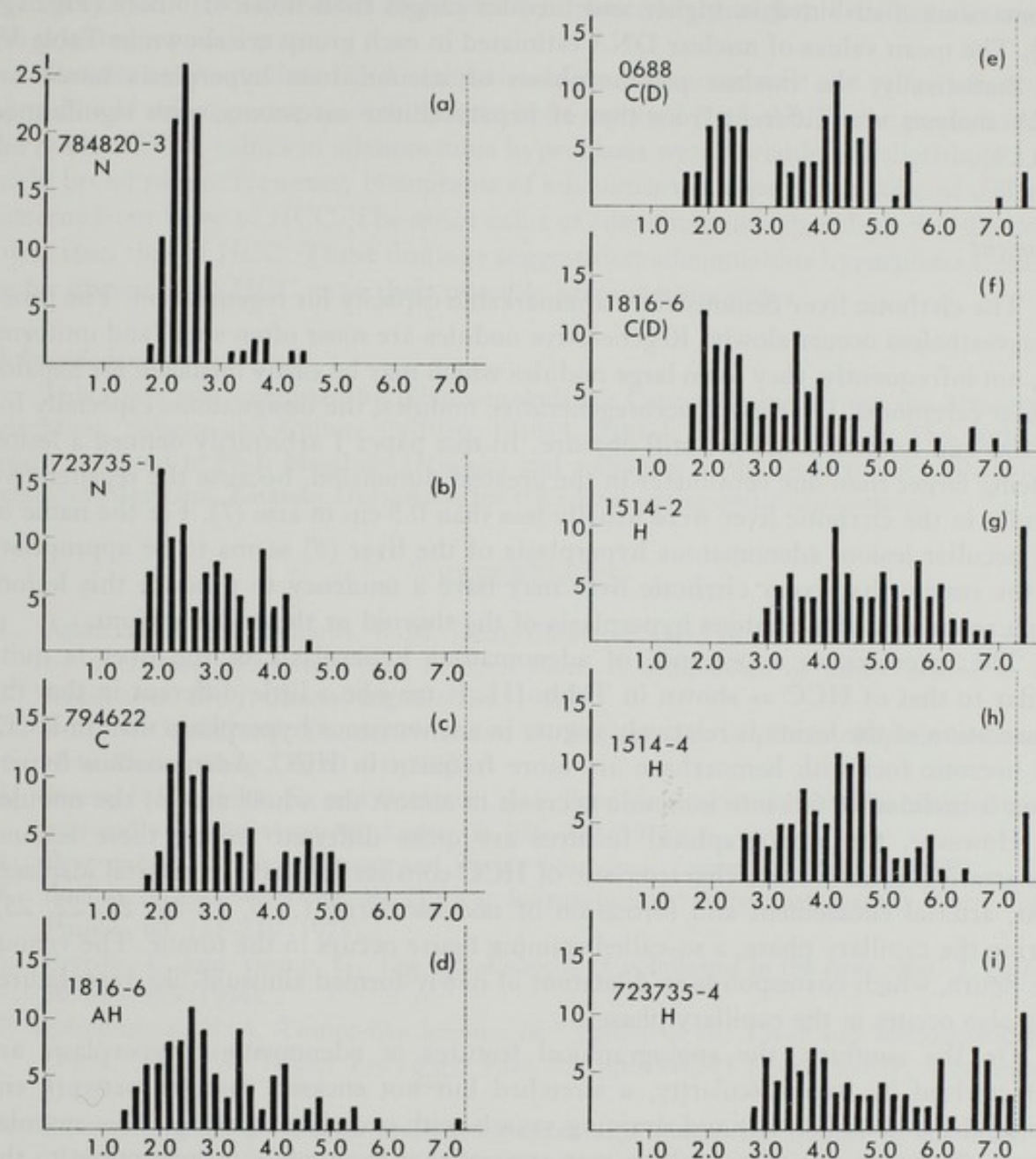


FIG. 1. Histogram of the nuclear DNA. a: Normal liver. b and c: Cirrhosis with minor pleomorphism. d: Adenomatous hyperplasia. e and f: Cirrhosis with dyskaryosis. g, h, and i: HCC.

TABLE V. Mean Value of Nuclear DNA by Microspectrophotometry

Group	Number of cases examined	Nuclear DNA Mean \pm S.D.
Normal	5	2.60 ± 0.74
Cirrhosis minor pleomorphism	10	2.81 ± 1.05
Cirrhosis with dyskaryosis	6	4.31 ± 1.65
Adenomatous hyperplasia	4	2.84 ± 1.20
Hepatocellular carcinoma	11	4.98 ± 1.61

cinoma were distributed in higher and broader ranges than those of others (Fig. 1g, h, i). The mean values of nuclear DNA estimated in each group are shown in Table V.

Statistically, the nuclear pleomorphism of adenomatous hyperplasia based on DNA analysis was different from that of hepatocellular carcinoma, with significance at 0.1%.

Comment

The cirrhotic liver demonstrates a remarkable capacity for regeneration. The process nevertheless occurs slowly. Regenerative nodules are most often small and uniform, but, not infrequently, they form large nodules which may be easily mistaken for hepatocellular carcinoma. On these macroregenerative nodules, the designations especially for the size and nomenclature are still obscure. In this paper I arbitrarily defined a lesion as being larger than one centimeter in the greatest dimension, because the regenerative nodules in the cirrhotic liver were usually less than 0.5 cm in size (7). For the name of this peculiar lesion, adenomatous hyperplasia of the liver (8) seems to be appropriate for the reason that every cirrhotic liver may have a tendency to produce this lesion, which resembles adenomatous hyperplasia of the thyroid or the endometrium.

The macroscopic appearance of adenomatous hyperplasia of the liver is quite similar to that of HCC as shown in Table III. It may be a little different in that the demarcation of the lesion is relatively vaguer in adenomatous hyperplasia than in HCC, and necrotic foci with hemorrhage are more frequent in HCC. Adenomatous hyperplasia is inclined to fall into ischemic necrosis in almost the whole area of the nodule.

However, the angiographical features are quite different among these lesions. The arteriographic feature characteristic of HCC consists basically of arterial displacement, arterial encasement and formation of neovascularity (2, 6, 15-19, 21, 22, 25). During the capillary phase, a so-called staining figure occurs in the tumor. The venous lake figure, which corresponds to dilatation of newly-formed sinusoid-like vasculatures (24), also occurs in the capillary phase.

On the contrary, the angiographical features of adenomatous hyperplasia are characterized by hypovascularity, a stretched but not encased vascular network enclosing the nodule (20, 26) and draining vessels with ordinary tapering. This vascular feature of adenomatous hyperplasia may suggest that the nodule is susceptible to the hypovolemic effect of systemic circulation and is inclined to fall into ischemic necrosis. Slight neovascularization is also of the utmost importance for differentiation.

Focal nodular hyperplasia (FNH) is designated as the non-encapsulated focal area of the hyperplastic nodule which develops in non-cirrhotic liver, and it usually occurs solitarily and locates subcapsularly (10, 12, 13). Its female predominance has been described. The macroscopical and histological features of FNH seem to resemble that of adenomatous hyperplasia except for the absence of cirrhosis. However, the reported arteriograph of FNH is different from that of adenomatous hyperplasia. Hypervascularity and neovascularity of varying degrees, although they develop in the peripheral area of the lesion, are common in FNH (9, 10).

Since Baum *et al.* (3) reported seven cases of benign hepatic tumors occurring in women taking oral contraceptives, the etiological possibilities of steroids have been pointed out. Controversies still remain (3, 4, 11, 14). It is interesting that the female

predominance of adenomatous hyperplasia is noticed, although all the females are in the post-menopausal state.

Results on the nuclear DNA estimation of several tumor cells and related disorders by means of microspectrophotometry have been reported (1, 5, 23). In the present study, the nuclear DNA values in adenomatous hyperplasia were variable and distributed in a fairly broad range. However, histograms of adenomatous hyperplasia were of different patterns from those of HCC. The mean value of adenomatous hyperplasia was distinctly lower than that of HCC. These findings suggest that adenomatous hyperplasia seems to be far distant from HCC as to their possible precancerous states.

Acknowledgments

This study was supported by Grants-in-Aids for Cancer Research from the Ministry of Education, Science and Culture (001036, 101013, 201031, 301014, 401013). The author is greatly indebted to Prof. Masahiko Okudaira and colleagues at the Department of Pathology, School of Medicine, Kitasato University, for their kind advice and collaboration.

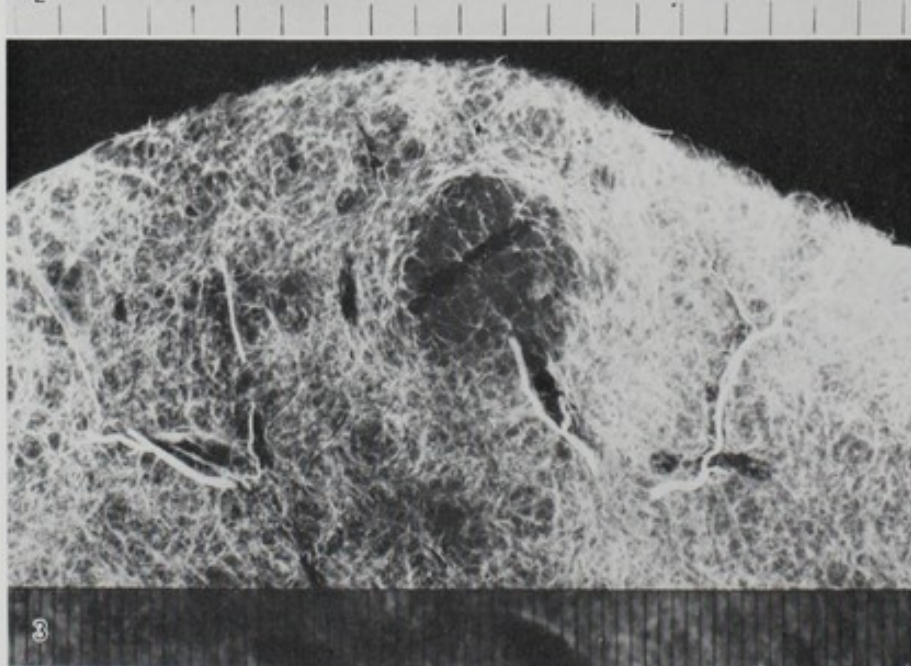
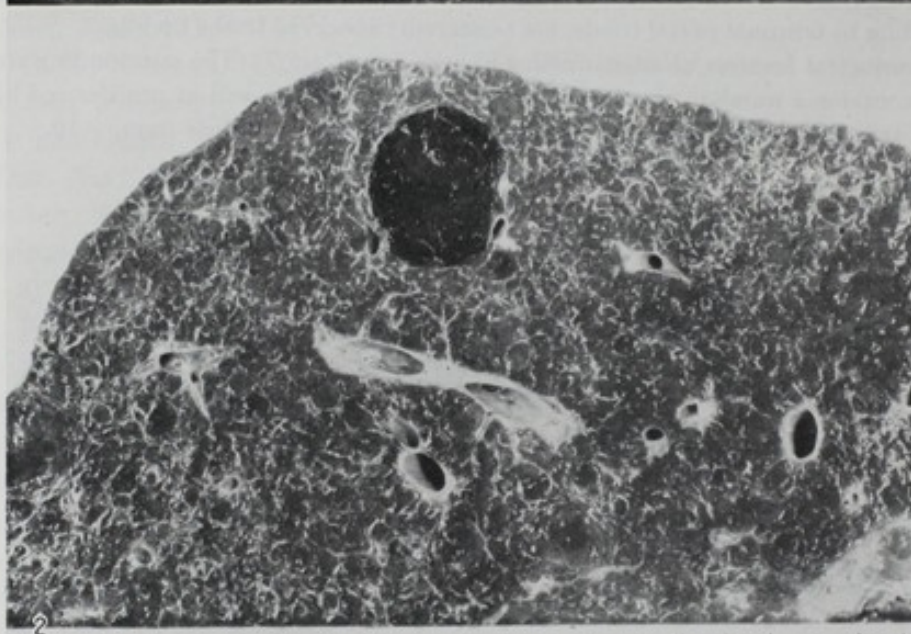
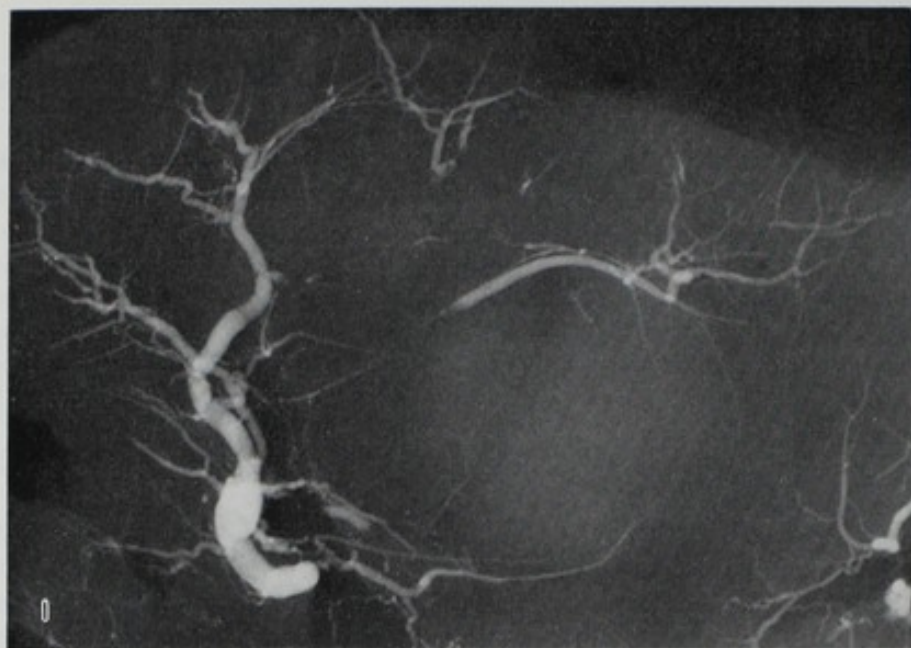
REFERENCES

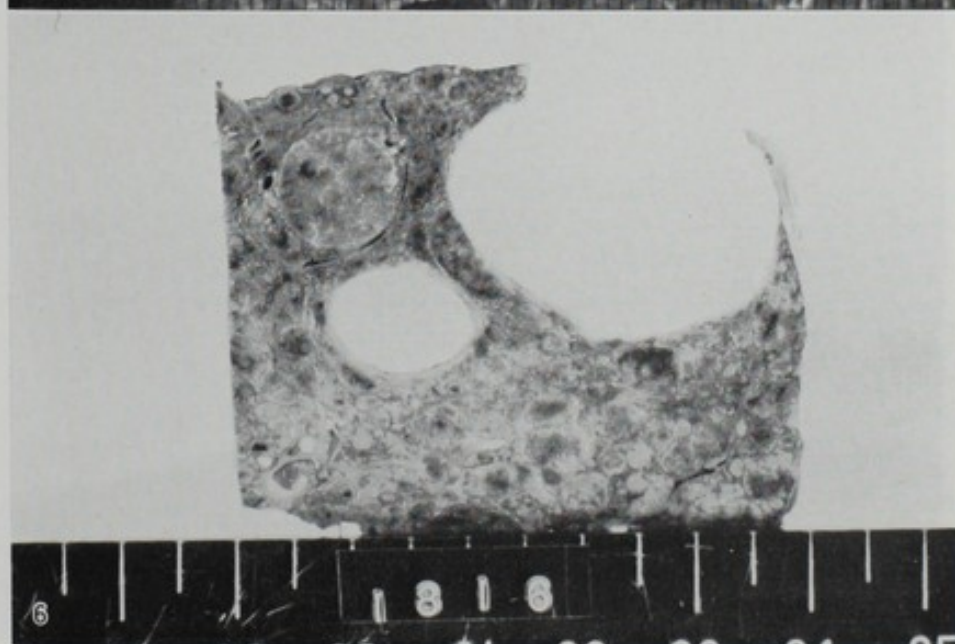
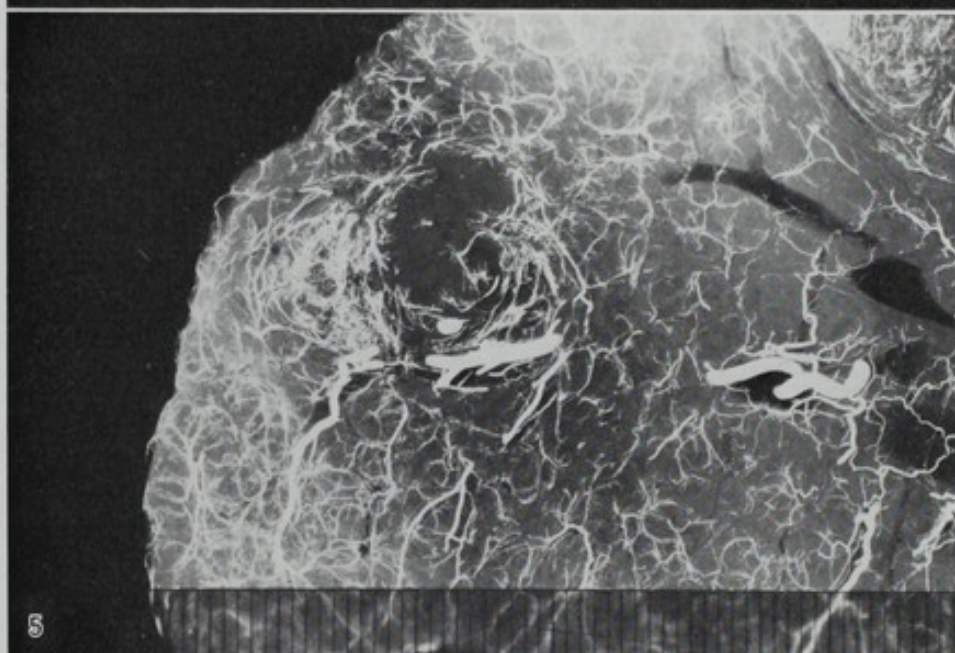
1. Atkin, N. B. and Richards, B. M. Deoxyribonucleic acid in human tumors as measured by microspectrophotometry of Feulgen stain: A comparison of tumor arising at different sites. *Br. J. Cancer*, **10**, 769-786 (1956).
2. Burtley, O., Edrund, Y., and Helander, G. Angiography in primary hepatic carcinoma. *Acta Radiol. (Diag.)*, **6**, 81-91 (1967).
3. Baum, J. K., Holtz, F., and Bookstein, J. J. Possible association between benign hepatomas and oral contraceptives. *Lancet*, **ii**, 926-929 (1973).
4. Beaconsfield, P. Liver tumors and steroid hormones. *Lancet*, **i**, 516-517 (1974).
5. Boehm, N. and Sandritter, W. DNA in human tumors: A cytometric study. *Curr. Topics Pathol.*, **60**, 151-219 (1975).
6. Breedis, C. and Young, G. The blood supply of neoplasms in the liver. *Am. J. Pathol.*, **30**, 969-985 (1954).
7. Edmondson, H. A. Tumor-like lesions. In "Tumor of the Liver and Intrahepatic Bile Ducts," Atlas of Tumor Pathology, Fasc. 25, pp. 191-195 (1958). AFIP, Washington, D.C.
8. Edmondson, H. A. Benign epithelial tumors and tumor-like lesions of the liver. In "Hepatocellular Carcinoma," ed. K. Okuda and R. L. Peters, pp. 309-330 (1976). Wiley, New York.
9. Foster, J. H. and Berman, M. M. The benign hepatic lesions: Adenoma and focal nodular hyperplasia. In "Solid Liver Tumors," pp. 138-178 (1977). W. B. Saunders, Philadelphia.
10. Goldstein, H. M., Neiman, H. L., Mena, E., Bookstein, J. J., and Appelman, H. D. Angiographic findings in benign liver cell tumors. *Radiology*, **110**, 339-343 (1974).
11. Guzman, I. J., Gold, J. H., Rosai, J., Schneider, P. D., Varco, R. L., and Buchwald, H. Benign hepatocellular tumors. *Surgery*, **82**, 495-503 (1977).
12. Johnson, F. L., Feagler, J. R., and Laner, K. G. Association of androgenic anabolic steroid therapy with development of hepatocellular carcinoma. *Lancet*, **ii**, 1273-1276 (1972).
13. Knowles II, D. M. and Wolff, M. Focal nodular hyperplasia of the liver: A clinicopathologic study and review of the literature. *Hum. Pathol.*, **7**, 535-545 (1976).
14. McAvoy, J. M., Tompkins, R. K., and Longmire, W. P. Benign hepatic tumors and their

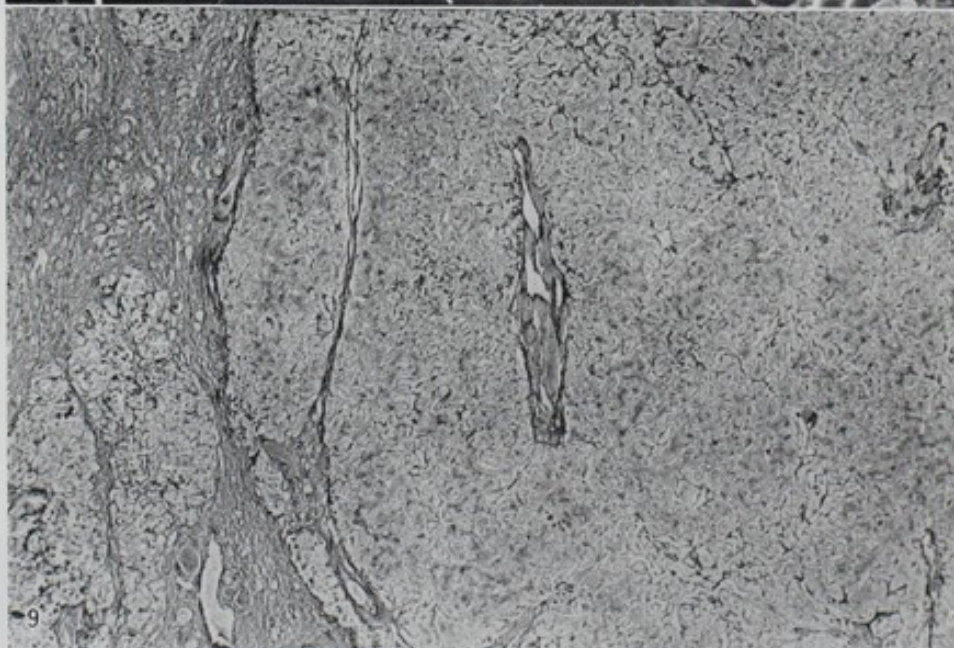
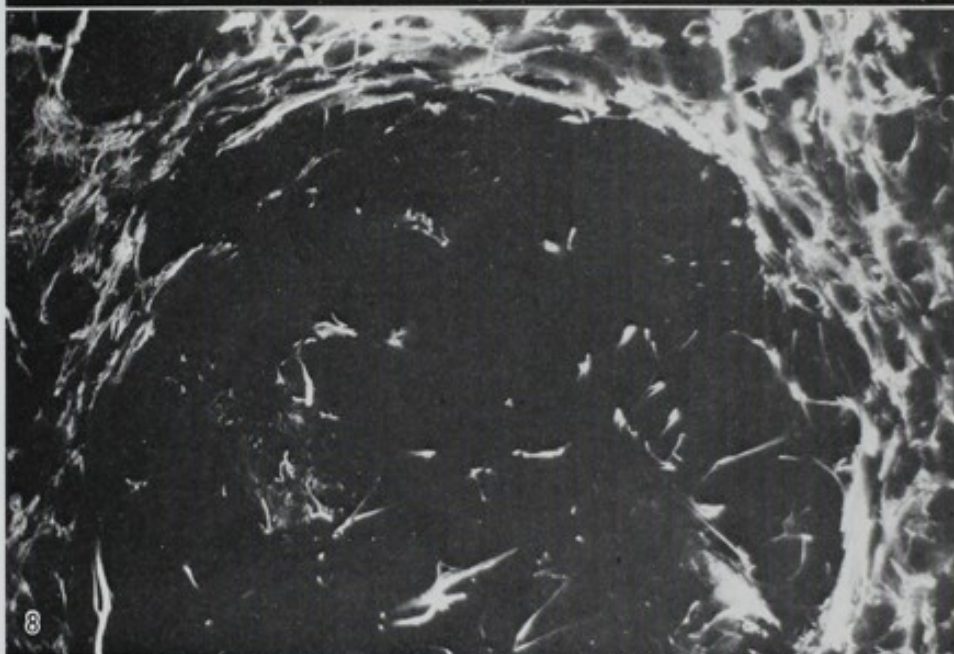
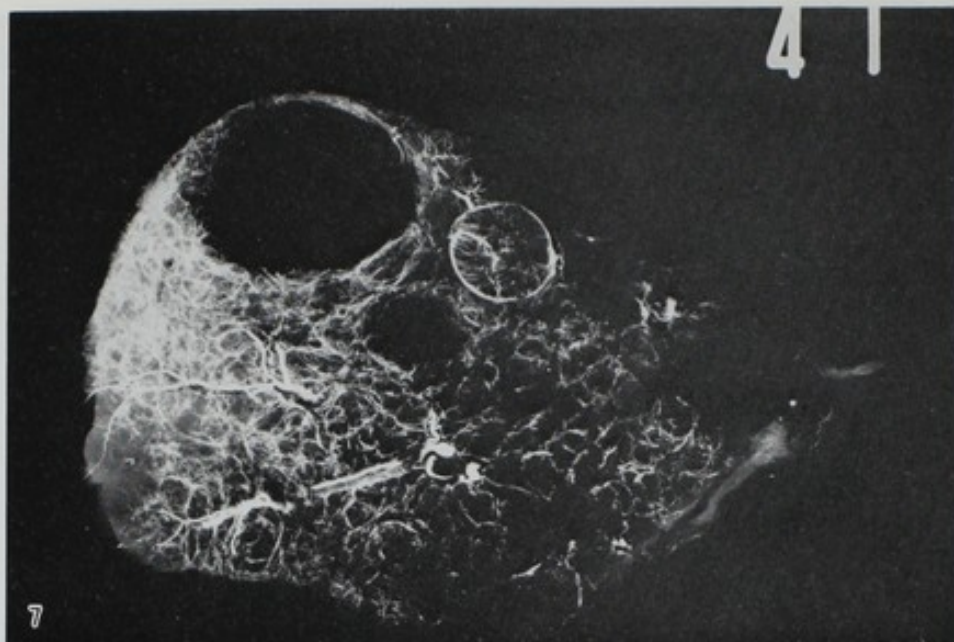
- association with oral contraceptives. Case reports and Survey of the literature. *Arch. Surg.*, **111**, 761-767 (1976).
15. Miyake, M. and Okudaira, M. Pathology of liver diseases from the vascular architectural point of view. *Jpn. J. Gastroenterol.*, **59**, 985-989 (1962).
 16. Miyake, M., Saito, M., and Okudaira, M. Studies on intrahepatic vascular alterations in cirrhosis of the liver. *Jpn. Circ. J.*, **28**, 33-39 (1964).
 17. Nakashima, T. Vascular changes and hemodynamics in hepatocellular carcinoma. In "Hepatocellular Carcinoma," ed. K. Okuda and R. L. Peters, pp. 169-203 (1976). Wiley, New York.
 18. Okudaira, M. Vascular structures of the liver. In "The Liver: Structure, Function and Pathology," 3rd ed., ed. T. Takahashi, pp. 21-49 (1976) (in Japanese). Igakushoin, Tokyo.
 19. Okudaira, M. and Sasaki, K. Pathological investigations on hepatocellular carcinoma. *Kurume Med. J.*, **26**, 215-230 (1979).
 20. Rabinowitz, J. G., Kinkabwala, M., and Ulreich, S. Macroregenerating nodules in the cirrhotic liver. Radiologic features and differential diagnosis. *Am. J. Roentgenol. Rad. Ther. Nucl. Med.*, **121**, 401-411 (1974).
 21. Reuter, S. R., Redman, H. C., and Siders, D. B. The spectrum of angiographic findings in hepatoma. *Radiology*, **94**, 89-94 (1970).
 22. Rossi, P. and Gould, H. R. Angiography and scanning in liver diseases. *Am. J. Roentgenol. Rad. Ther. Nucl. Med.*, **106**, 553-562 (1970).
 23. Sandoritter, W., Carl, M., and Ritter, W. R. Cytophotometric measurements of the DNA content of human malignant tumors by means of the Feulgen reaction. *Acta Cytol.*, **10**, 26-30 (1966).
 24. Sasaki, K., Yajima, M., Okudaira, M., Nemoto, S., Ohmiya, H., Aso, K., Kusano, S., and Shibata, H. Studies on vascular structure of hepatic tumors. 1. On the hepatocellular carcinoma. *Acta Hepatol. Japon.*, **17**, 394 (1976).
 25. Sasaki, K., Atari, H., Saito, Y., Kuwao, S., and Okudaira, M. Pathological studies on vascular alterations in liver diseases. 3. Subacute liver atrophy. *Trans. Soc. Pathol. Japon.*, **66**, 274-275 (1977) (in Japanese).
 26. Sasaki, K., Atari, H., Aida, Y., Kitazume, N., Okudaira, M., and Kusano, S. Studies on vascular structure of hepatic tumors. 4. On adenomatous hyperplasia. *Acta Hepatol. Japon.*, **21**, 376 (1980).

EXPLANATION OF PHOTOS

- PHOTO 1. An arterial microangiograph of adenomatous hyperplasia in Case 4 on sectioned slice. The nodule is notable only by displacement of arterial branches, filled with X-ray contrast meal.
- PHOTO 2. Close-up view of the sectioned slice in Case 7.
- PHOTO 3. A microangiograph of the same slice as in Photo 2. The nodule is hypovascular, but draining vessels are noted in the nodule.
- PHOTO 4. A microangiograph of the sectioned slice in Case 8. A large hypervascular mass is noted in the center. Beside the mass, a hypovascular lesion is also notable in the lateral site of the mass.
- PHOTO 5. Close-up view of the hypovascular lesion in Photo 4. The lesion is hypovascular, but some draining arteries with X-ray contrast meal are noted in the lesion.
- PHOTO 6. A close-up view of Case 9. A well-circumscribed, gray-whitish nodule is observed in the right lobe of Case 9. Several cysts are also noted.
- PHOTO 7. A microangiograph of Case 9. The distinct vascular network is noted, but draining arteries are disclosed by soft X-ray film.
- PHOTO 8. Stereomicroscopical view of cleared slice with methyl salicylate. The adenomatous hyperplasia are hypovascular compared to the surrounding cirrhotic area. A number of arterial branches, corresponding to terminal portal triads, are scatteredly observed in the nodule.
- PHOTO 9. Histological features of adenomatous hyperplasia (Case 7). The surrounding stroma is irregular, and contains a number of arterial and portal branches, as well as proliferated bile ductuli. A number of terminal portal branches are also noted in the nodule. Silver stain, $\times 10$.







ANALYTICAL STUDY OF PRECANCEROUS LESIONS IN RAT STOMACH MUCOSA INDUCED BY N-METHYL- N'-NITRO-N-NITROSOGUANIDINE*¹

Oichiro KOBORI

*First Department of Surgery, Faculty of Medicine, University of Tokyo**²

Sequential morphological changes in N-methyl-N'-nitro-N-nitrosoguanidine (MNNG) carcinogenesis in the glandular stomach of rats were studied.

Eighty inbred Wistar rats were given MNNG solution at a concentration of 80 mg/l and sequentially sacrificed. Twenty-six erosions were found from the 5th to the 31st week, 24 of which were single lesion and exclusively located in the midpoint of the lesser curvature. From the 23rd to the 43rd week, 6 adenomatous epithelia were observed, all of which were single lesion and located in the midpoint of the lesser curvature. Forty-three carcinomas were found from the 23rd to the 61st week. Forty of them were single lesion, all of which were located in the midpoint of the lesser curvature, *i.e.*, exactly that area where the erosions and adenomatous epithelia were found. The fact that these benign and malignant lesions were nearly always located in the same area of the stomach with evident chronological regularity inevitably suggests a definite pathway of development; regenerating epithelium-adenomatous epithelium-carcinoma.

Forty rats of the same strain were divided into 8 subgroups and given the same concentration of MNNG solution for different durations—for 3, 5, 7, 9, 11, 13, 15, and 17 weeks. They were observed for 20–25 weeks after MNNG was stopped and then sacrificed. All the rats which were given MNNG for 3, 5, 7, and 9 weeks showed no remarkable changes in the epithelium of the stomach. Four out of 8 animals which were given MNNG for 11 and 13 weeks showed 3 hyperplastic epithelia and an adenomatous epithelium and eleven out of 12 rats which were given MNNG for 15 and 17 weeks revealed definite adenocarcinomas. All of these changes were singly located in the midpoint of the lesser curvature. This result suggests that: 1) The erosions can be divided into 2 categories, reversible and irreversible; and 2) the crucial period in which the reversible erosion changes to an irreversible one is compatible with the 11th–13th experimental weeks.

In 1967 Sugimura and Fujimura succeeded in inducing adenocarcinoma in the glandular stomach of Wistar rats by oral administration of N-methyl-N'-nitro-N-nitrosoguanidine (MNNG) (9). Their induction procedure was much more simple

*¹ Dedicated to late Professor Herwig Hamperl without whose encouragement and criticism the first part of this experiment could not have been accomplished.

*² Hongo 7-3-1, Bunkyo-ku, Tokyo 113, Japan (小堀 一郎).

and natural than the ones used previously (8), and moreover, showed better organ specificity and a higher frequency of cancer arising, which allowed a great number of successive studies using this carcinogen. Only a few, however, referred to the state of the stomach mucosa before the appearance of full-fledged carcinomas (1, 3, 7, 10).

In the present study, the author wanted to clarify analytically these precancerous states with an inbred strain of Wistar rats expecting that the homogeneity of the animals would show some regularity in the number and position of the precancerous lesions.

An Example of Experimental Tumor Development in the Stomach

All animals used in this experiment were male Wistar rats. They were the offspring of brother-sister matings and were kept for more than 50 years in the Institute of Experimental Gerontology in Basel, Switzerland, from which they were a generous gift to our laboratory. Skin grafts were undertaken on a few rats, and nearly all were retained.

One hundred and twenty 7-week-old male Wistar rats were divided into 3 groups. The 1st and 2nd groups (40 animals each) were allowed to drink only MNNG solution "ad libitum" at a concentration of 80 mg/l for 31 weeks at the longest. From the 32nd week, all the rats were given normal tap water to drink. The 1st group was sacrificed every second week from the 3rd to the 35th weeks. The 2nd group was intended to be observed as long as possible and weighed twice a week and when any rat lost more than 50 g within approximately 2 weeks, it was killed; all animals were sacrificed from the 34th to the 61st week (5). The 3rd group (40 animals) was divided into 8 subgroups and given the same concentration of MNNG solution for different durations—for 3, 5, 7, 9, 11, 13, 15, and 17 weeks. They were observed for 20–25 weeks after MNNG was stopped and then sacrificed.

The stomach was incised along the greater curvature from the pylorus to the cardia and pinned out flat on a cork block, put in fresh 4% formalin solution, embedded in paraffin, and stained with hematoxylin and eosin (HE).

Morphological Changes of the Stomach Mucosa during Carcinogenesis

One hundred and nineteen out of 120 rats were preserved as the effective number at risk. In the 1st and 2nd groups, 26 erosions, 6 adenomatous epithelia, 43 carcinomas and 1 leiomyosarcoma were observed and 3 stomachs of the 1st group which were examined in the 3rd week showed no remarkable change. One rat in the 2nd group which died in the 28th week was discarded without examination (Fig. 1).

Twenty-six erosions were found from the 5th to the 31st week, 24 of which were single lesion and exclusively located in the midpoint of the lesser curvature (Photo 1). These erosions were 2–4.5 mm in diameter, irregularly shaped, but sharply set off against the surrounding mucosa by white fur. On light microscopy, several healing stages of erosions were found: in some cases, the epithelium was completely eroded and the surface of it was covered with a large amount of leucocytes and fibrin (true erosion) (Photo 2); in other cases, it was mostly covered with simple, regenerating epithelium (mostly healed erosion) (Photo 3). A completely healed erosion, however,

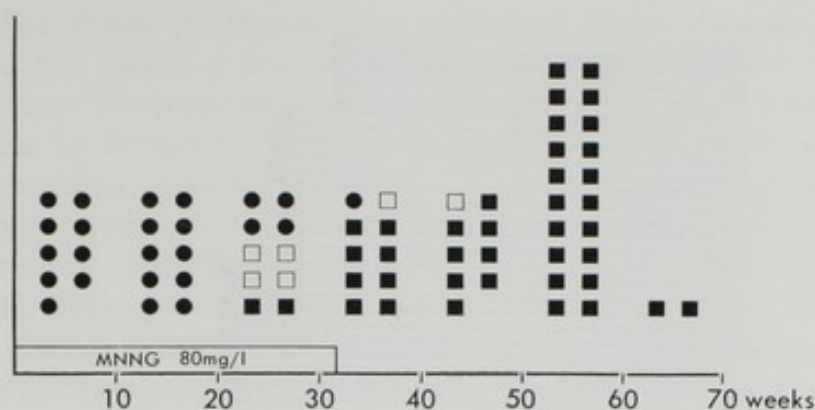


FIG. 1. Chromological relationship of 10 single lesions found in groups 1 and 2. ● erosion; □ adenomatous epithelium; ■ carcinoma.

was never observed. These various stages of erosion were observed randomly through 27 weeks.

From the 23rd to the 43rd week, 6 adenomatous epithelia were observed, all of which were single lesion and located strictly in the midpoint of the lesser curvature. Two cases showed small granular proliferation multifocally distributed in the erosions (Photo 4) and in the remaining 4 cases, the growth extended in the submucosal space showing no structural nor cellular atypia. The latter type of adenomatous epithelium showed a flower-bed-like elevation of the mucosa macroscopically.

Forty out of 43 carcinomas were single lesion, all of which were located in the midpoint of the lesser curvature, *i.e.*, exactly that area where the erosions and adenomatous epithelia were found (Photo 1). They were 6–30 mm in diameter and mostly ulcerated. Histologically, all these tumors were invasive adenocarcinoma with papillary and tubular structure and revealed both structural and cellular atypia (Photo 5). Metastasis to the perigastric lymph nodes was observed in 2 cases.

The results obtained from the studies on the 3rd group are summarized in Fig. 2. All the rats which were given MNNG for 3, 5, 7, and 9 weeks showed no remarkable changes in the epithelium of the stomach on macroscopical and microscopical studies. Four out of 8 animals which were given MNNG for 11 and 13 weeks showed 3 mm-sized protrusions in the midpoint of the lesser curvature (Photos 6 and 7). Microscopically, 3 of these were hyperplastic epithelia, in the center of which the derangement of regenerating tubuli was observed (Photos 6 and 8). Another was an adenomatous epithelium (Photos 7 and 9). The remaining 4 rats showed nonremarkable stomachs. Eleven out of 12 rats which were given MNNG for 15 and 17 weeks revealed definite carcinomas (Photo 10), all of which were located in the midpoint of the lesser curvature.

Comment

It has already been suggested by other authors that the regenerating epithelium in the erosive mucosa and adenomatous epithelium might play an important part as a precancerous lesion (1, 3, 7, 10). A definite pathway of development, regenerating epithelium-adenomatous epithelium-carcinoma, seemed difficult to conclude from their

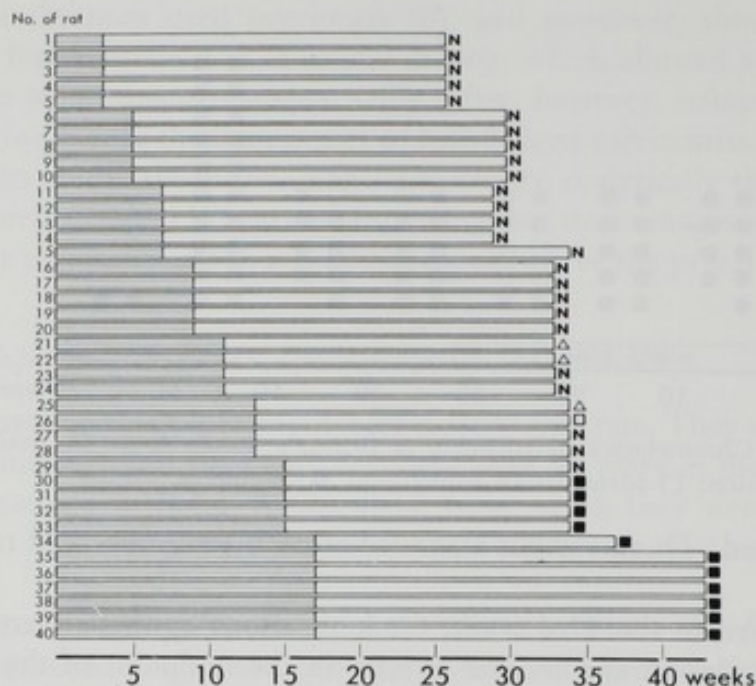


FIG. 2. Data from the experiment in group 3. period on MNNG (80 mg/l); period of observation; N, no change; Δ hyperplastic epithelium; □ adenomatous epithelium; ■ carcinoma.

studies, because: 1) The erosions were mostly observed to be multifocal in a stomach; and 2) they also appeared at a late period of experiment, *i.e.*, during the period in which the adenomatous epithelium and carcinoma were usually observed.

In this experiment, however, out of 80 rats, which were grouped into the 1st and 2nd groups, 70 rats showed singly-occurring lesions, 69 of which were always found in the same point of the stomach mucosa (Photo 1). Moreover, these benign and malignant lesions showed evident chronological regularity; the erosions were observed from the 5th to the 31st week, the adenomatous epithelia from the 23rd to the 43rd week and the carcinomas from the 23rd to the 61st week (Fig. 1). On the other hand, the result of the experiment on group 3 suggested that: 1) The erosions can be divided into 2 categories: reversible and irreversible; and 2) the crucial period in which the reversible erosion changes to an irreversible one is compatible with the 11th–13th experimental week. These results inevitably suggest the following process: The factor initially causing the erosion in approximately the 5th week sustains it by preventing quick healing which otherwise is normal in the stomach of rodents. When the repetition of the erosive process and the regeneration of the epithelium continues for 11–13 weeks, the erosion changes from reversible to irreversible. Between the 25th and 30th week, the small glandular proliferations multifocally arise in the area of the irreversible erosion, which gradually unite to form a growth extended in the submucosal space, and begin to infiltrate deep into the gastric wall from approximately the 30th week.

It is difficult to provide a clear explanation for the fact that nearly all the changes arose in the midpoint of the lesser curvature of the stomach. One possibility is that this area is the one where MNNG-containing water first comes into contact. The determination of ^{14}C -labeled MNNG in various portions in the stomach mucosa may give the answer to this question.

As described above, the regenerating epithelium observed in the early period of the experiment has played a definite part as a precancerous lesion in experimental stomach carcinoma. The same series of experiments, however, at a lower concentration of MNNG must be further undertaken: It is still possible that the carcinoma arises without any preceding erosion if MNNG is given at a lower concentration than 40 mg/l for a longer duration than 25 weeks; Bralow and his coworkers reported the same type of regenerating epithelium induced by MNNG at a concentration of 41.5 mg/l for 25 weeks (1). These possibilities present us with the necessity of careful consideration when we discuss precancerous lesions in experimental carcinoma and, moreover, when we apply our results to humans: Obtained results should be always limited by the dose of the carcinogenic substances given to the animals.

In Fig. 1, the observation period was set from 20 to 26 weeks after stopping the administration of MNNG. The minimum required latent period for the cancer arising is considered to be 10–15% of the lifespan of the animals (4)—3–4 months for rats and 7–10 years for humans. Longer observation, however, may produce different results, *i.e.*, some rats which were given MNNG for only 3 weeks might show carcinomas if they were observed for more than a year (2). This could be supported by the experiment by Tatematsu and his coworkers (11): They gave MNNG to rats at a concentration of 83 mg/l for 8 days and the abnormal isozyme pattern of pepsinogen in the antral mucosa was retained during 455 days.

Only a small number of adenomatous epithelia was observed in this experiment, which suggests that this lesion is of short duration. The study of this change was, therefore, very limited; it was only ascertained by serial sections that they arose multifocally in one erosion. Whether this lesion is precancerous or already cancerous must be studied by its transplantation to isologous rats as in the case of carcinomas (6).

Acknowledgments

A part of this study was undertaken in the Institute of Pathology (Director: Prof. P. Gedigk), University of Bonn, Federal Republic of Germany, sponsored by the Alexander-von-Humboldt Foundation. The gratitude of the author is due to S. Kim Schleipen, R. Speck, E. Brand, M. Kono, R. Miyazawa, and T. Sato for their technical assistance.

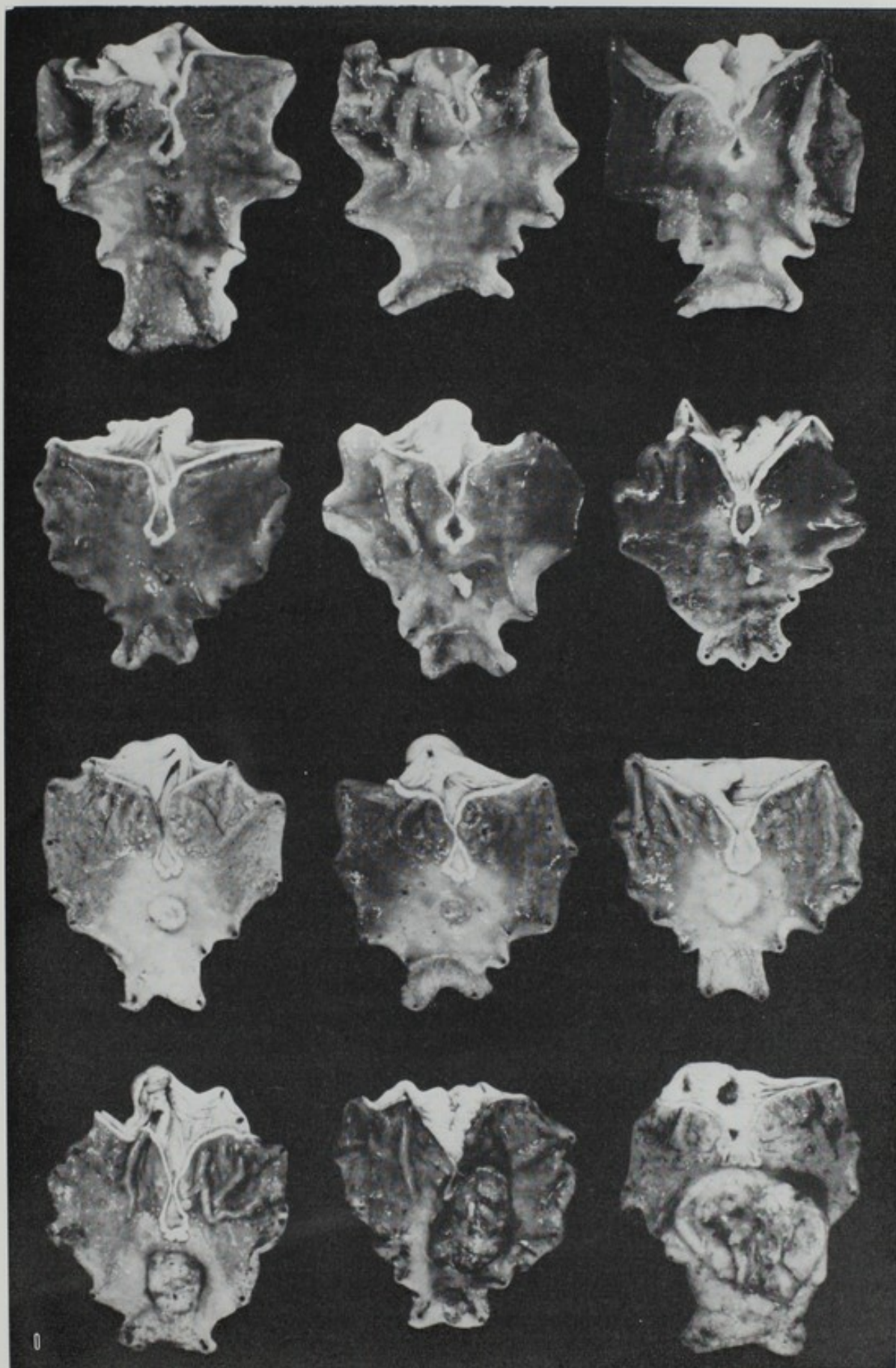
REFERENCES

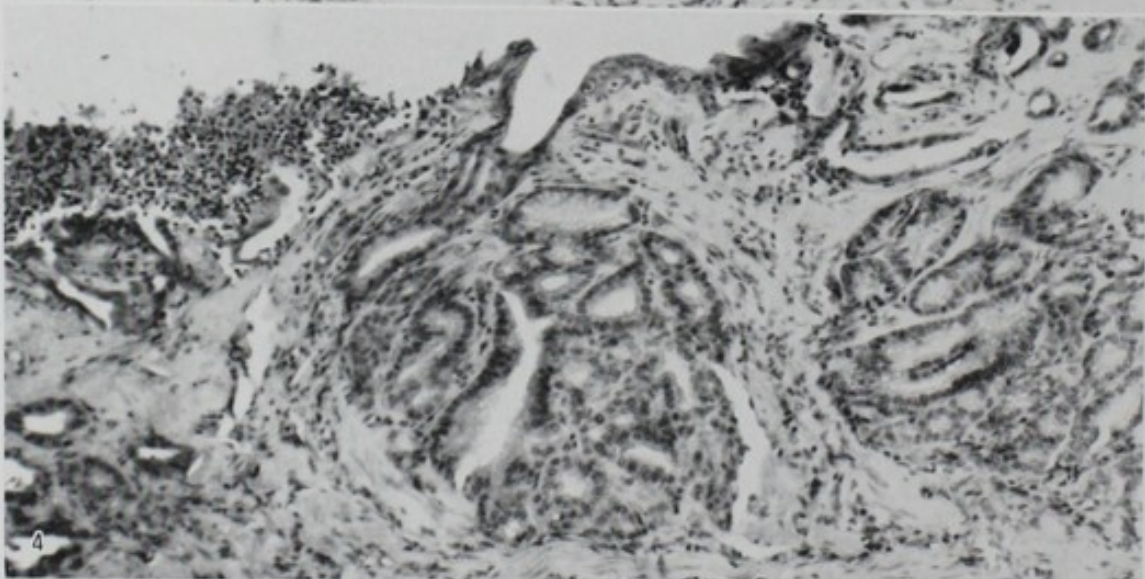
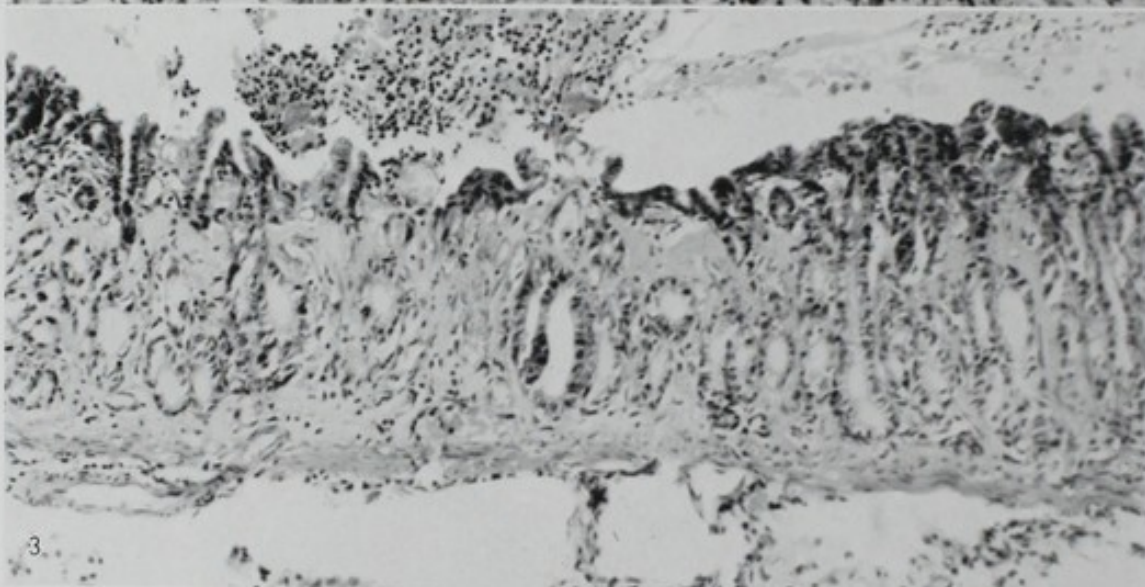
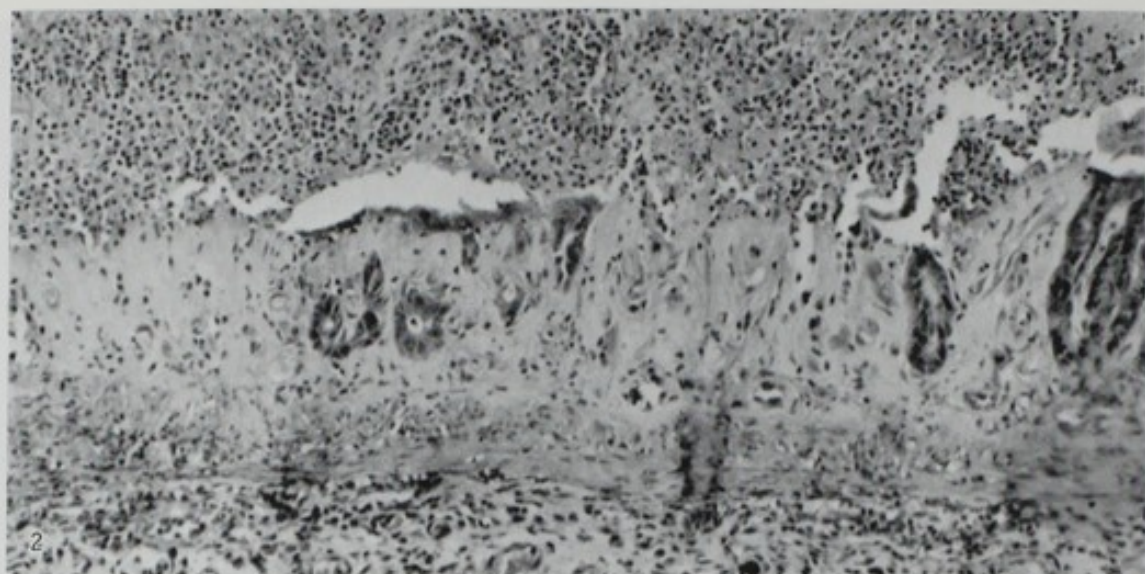
1. Bralow, S. P., Gruenstein, M., and Meranze, D. R. Host resistance to gastric adenocarcinomatosis in three strains of rats ingesting N-methyl-N'-nitro-N-nitrosoguanidine. *Oncology*, **27**, 168–180 (1973).
2. Druckrey, H. Personal communication.
3. Kawachi, T., Kogure, K., Tanaka, N., Tokunaga, A., Fujimura, S., and Sugimura, T. Inductions of the tumors in the stomach and duodenum of hamsters by N-methyl-N'-nitro-N-nitrosoguanidine. *Z. Krebsforsch.*, **81**, 29–36 (1974).
4. Kitagawa, T. Pathology of precancerous lesions. *Saishin-Igaku*, **31**, 1059–1064 (1976) (in Japanese).
5. Kabori, O., Gedigk, P., and Totovic, V. Adenomatous change and adenocarcinoma of glandular stomach in Wistar rats induced by N-methyl-N'-nitro-N-nitrosoguanidine. *Virchows Arch. B Pathol. Anat. Histol.*, **373**, 37–54 (1977).

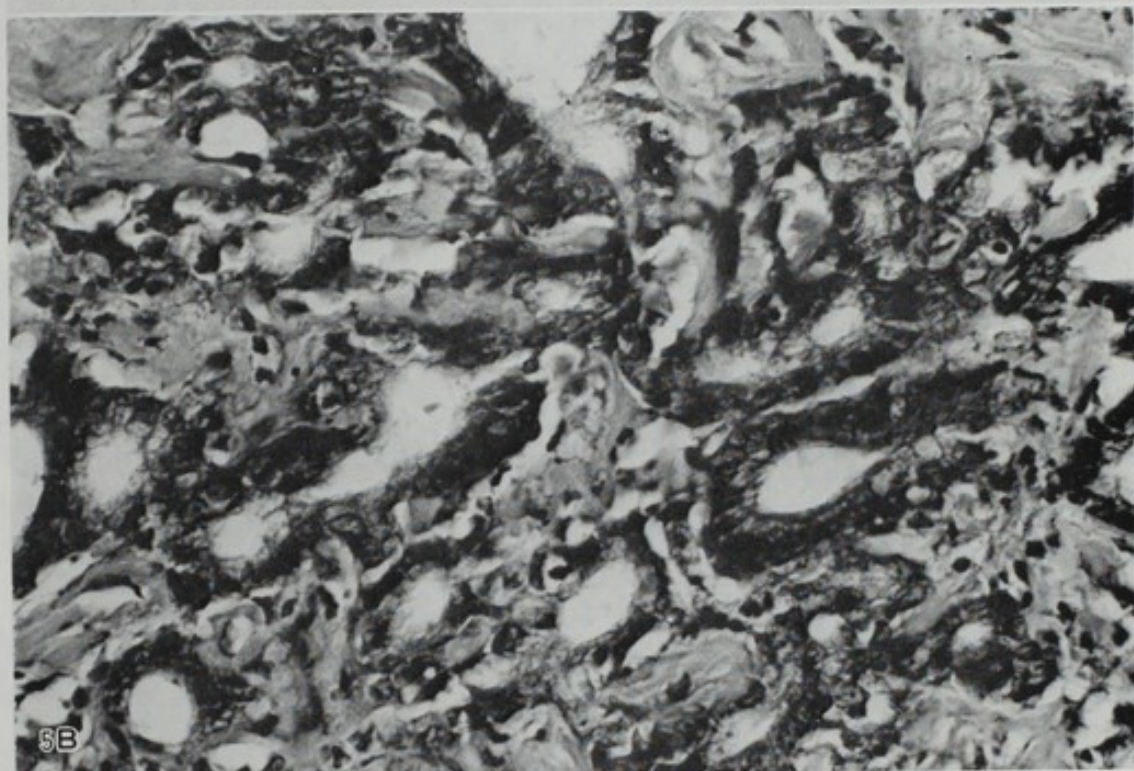
6. Kobori, O. and Oota, K. Neuroendocrine cells in serially passaged rat stomach cancer induced by MNNG. *Int. J. Cancer*, **23**, 536-541 (1979).
7. Saito, T., Inokuchi, K., Takayama, S., and Sugimura, T. Sequential morphological changes in N-methyl-N'-nitro-N-nitrosoguanidine carcinogenesis in the glandular stomach of rats. *J. Natl. Cancer Inst.*, **44**, 769-783 (1970).
8. Stewart, H. L., Snell, K. C., Morris, H. P., Wagner, B. P., and Ray, F. E. Carcinoma of the glandular stomach in rats ingesting N,N'-2,7-fluorenylenebisacetamide. *Natl. Cancer Inst. Monogr.*, **5**, 105-139 (1961).
9. Sugimura, T. and Fujimura, S. Tumor production in glandular stomach of rat by N-methyl-N'-nitro-N-nitrosoguanidine. *Nature*, **216**, 943-944 (1967).
10. Takayama, S., Saito, T., Fujimura, S., and Sugimura, T. Histological findings of gastric tumors induced by N-methyl-N'-nitro-N-nitrosoguanidine in rats. *GANN Monogr.*, **8**, 197-208 (1969).
11. Tatematsu, F., Saito, T., Furihata, C., Miyata, Y., Nakatsuka, T., Ito, N., and Sugimura, T. Initial DNA damage and heritable permanent change in pepsinogen isozyme pattern in the pyloric mucosae of rats after short-term administration of N-methyl-N'-nitro-N-nitrosoguanidine. *J. Natl. Cancer Inst.*, **64**, 775-781 (1980).

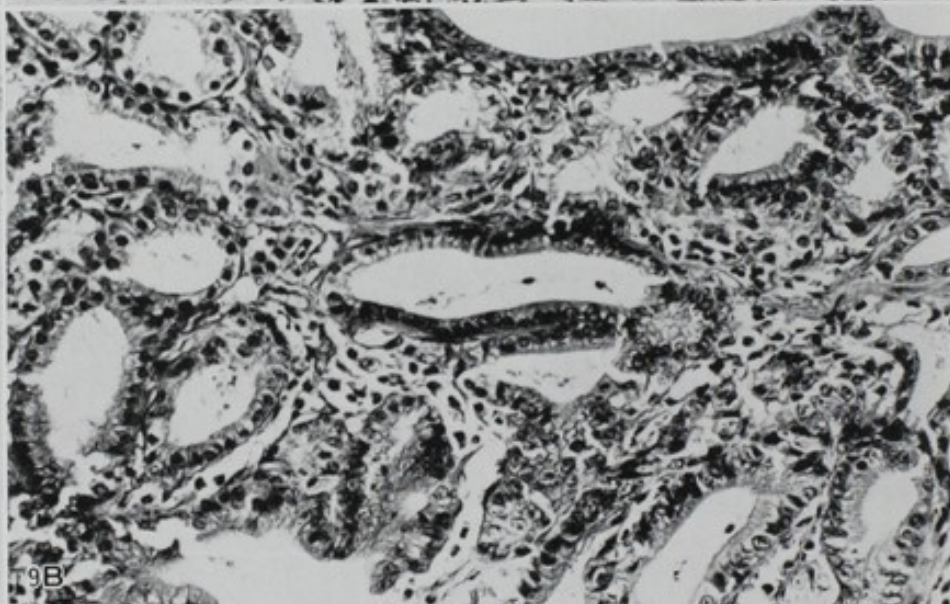
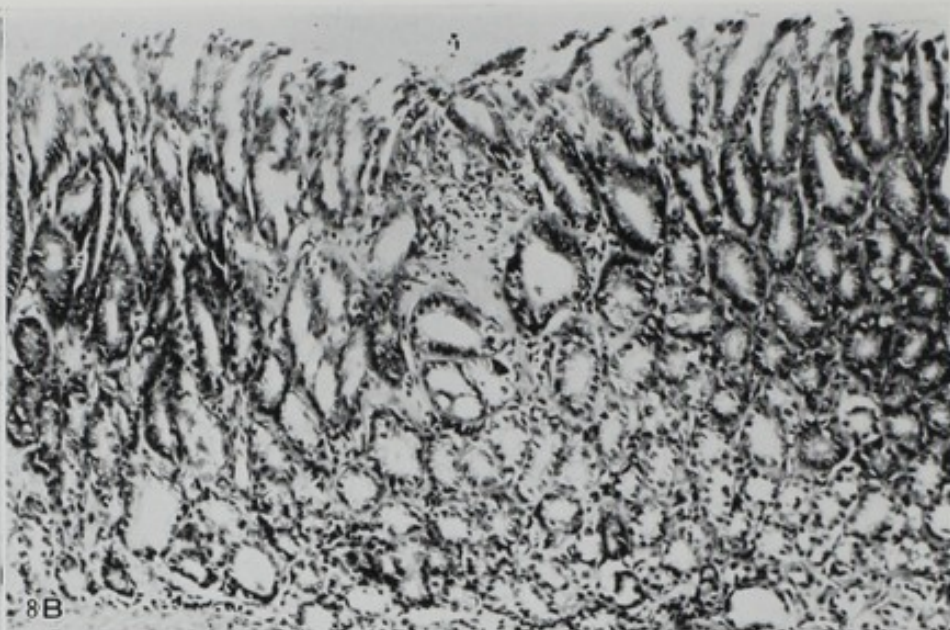
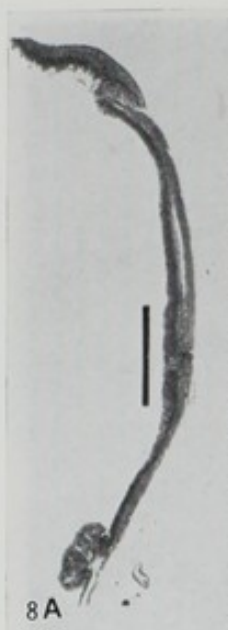
EXPLANATION OF PHOTOS

- PHOTO 1. Macroscopical pictures of 6 erosions and 6 carcinomas observed in the 5th, 7th, 12th, 14th, 15th, 21st, 45th, 34th, 45th, 45th, 61st, and 54th weeks (left to right, top to bottom). Note all the lesions are singly located in the midpoint of the lesser curvature.
- PHOTO 2. Light micrograph of the erosion in the 15th week. Stromal proliferation and inflammatory exudate pouring through breaks in the surface epithelium are observed. HE, $\times 350$.
- PHOTO 3. The mostly healed erosion in the 14th week. The breaks in the epithelium are mostly repaired through the regenerating epithelium. HE, $\times 350$.
- PHOTO 4. Adenomatous change in the 23rd week, which reveals a small glandular proliferation in a part of the erosion. HE, $\times 350$.
- PHOTO 5. Adenocarcinoma penetrating the gastric wall observed in the 53rd week. Note definite structural and cellular atypia. B: HE, $\times 700$.
- PHOTOS 6 and 7. Macroscopical pictures of No. 21 (Photo 6) and No. 26 rat stomach (Photo 7) in Fig. 2. A small mucosal elevation is observed in the midpoint of the lesser curvature of each stomach (arrow).
- PHOTO 8. Light micrograph of the mucosal elevation in Photo 6. Note derangement of the regenerating tubuli in the center of the hyperplastic epithelium. B: HE, $\times 350$.
- PHOTO 9. Light micrograph of the mucosal elevation in Photo 7. Adenomatous epithelium pushing the muscle layer is observed. Note only slight structural and cellular atypia. B: HE, $\times 700$.
- PHOTO 10. Light micrograph of an adenocarcinoma found in the midpoint of the lesser curvature of rat stomach No. 35 in Fig. 2. B: HE, $\times 700$.









RECENT ADVANCES IN MOLECULAR CELL GENETICS A CHRONOLOGICAL REVIEW

Edited by R. G. W. Brown

Department of Cell Biology, University of Cambridge, Cambridge, England

CELL GENETICS OF DISEASES OF HIGH-RISK GROUPS

The discovery of molecular markers for human diseases, the cloning techniques, and the development of the human genome project have revolutionized our understanding of human genetics. In the past few years, the discovery of molecular markers for human diseases has been a major breakthrough. The discovery of molecular markers for human diseases has been a major breakthrough. The discovery of molecular markers for human diseases has been a major breakthrough. The discovery of molecular markers for human diseases has been a major breakthrough.

The present paper reviews the recent developments in the field of molecular cell genetics. The present paper reviews the recent developments in the field of molecular cell genetics. The present paper reviews the recent developments in the field of molecular cell genetics. The present paper reviews the recent developments in the field of molecular cell genetics.

The Human Genome Project

1. Human Genome Project

The human genome project is a major international effort to determine the sequence of the human genome. The human genome project is a major international effort to determine the sequence of the human genome. The human genome project is a major international effort to determine the sequence of the human genome. The human genome project is a major international effort to determine the sequence of the human genome.

The discovery of molecular markers for human diseases has been a major breakthrough. The discovery of molecular markers for human diseases has been a major breakthrough. The discovery of molecular markers for human diseases has been a major breakthrough. The discovery of molecular markers for human diseases has been a major breakthrough.

In the future, the discovery of molecular markers for human diseases will be a major breakthrough. In the future, the discovery of molecular markers for human diseases will be a major breakthrough. In the future, the discovery of molecular markers for human diseases will be a major breakthrough. In the future, the discovery of molecular markers for human diseases will be a major breakthrough.

The Human Genome Project

THE EFFECT OF
THE GROUP

RECENT ADVANCES IN SOMATIC CELL GENETICS: A CHRONOLOGICAL REVIEW

Kazuhiko R. UTSUMI

*Laboratory of Cell Biology, Aichi Cancer Center Research Institute**

The current success of somatic cell genetics seems to be entirely dependent upon the results of improvement in cytological technique. That is, the spreading method of metaphase chromosomes with the use of colchicine and hypotonic pretreatment, the banding method for distinction of individual chromosomes, and the cell-hybridization method that led to the gene mapping. Accidental findings and/or theoretical improvements in cytological technique which played important roles in the cytological revolution and in the genesis of new cytology are reviewed chronologically.

Three discoveries of cytological techniques, hypotonic pretreatment, the banding technique, and somatic cell hybridization, can be considered as turning points in classical cytology, modern human cytogenetics and molecular cell genetics and it was these three techniques that have allowed such rapid progress in this field over the past 30 years. Hypotonic treatment allows us to define the number and clarify the shape of chromosomes, banding techniques make possible the identification of individual chromosomes and the distinction of parts of chromosomes and somatic cell hybridization permits gene assignments to specific chromosomes.

The present paper reviews mainly cytological techniques that had made profound contributions to the rapid progress in cytogenetics. Epoch-making discoveries in cytological techniques and important findings in human cytogenetics are arranged chronologically in Table 1.

The Three Major Milestones in Cytogenetics

1. Hypotonic pretreatment

The spreading effects of hypotonic solutions on metaphasic chromosomes were accidentally discovered independently by three investigators: Makino and Nishimura studying insect testis, Hughes studying plants, and Hsu studying human tissue culture cells. Their publications appeared in the same year, 1952. The dark age or prehypotonic era, as mentioned by Hsu (23), had come to end and a new era began.

The discovery of hypotonic effects and the introduction of hypotonic treatment to chromosome study certainly made profound contributions to the following rapid and surprising development of cytology.

In the prehypotonic era, chromosome studies were exclusively made on histological sections until the squashing method was introduced by Belling (2). In those histological

* Kanokoden 81-1159, Tashiro-cho, Chikusa-ku, Nagoya 464, Japan (内海和彦).

TABLE I. Chronology of Epoch-making Findings in Chromosome Techniques, Tissue Culture, and Human Chromosome Research

Chromosome technique	Tissue culture	Human chromosomes
1907	Frog nerve fiber/Harrison	
1912		F 48, M 47, XX/XO/Winiwarter
1921	Squashing method/Belling	
1923		F 48, M 48, XX/XY/Painter
1937	Colchicine/Blakeslee and Avery	
1943	L-cells/Earle	
1949	Human embryonic tissue/ Enders	
1952	Hypotonic pretreatment/ Hughes ; Makino and Nishimura ; Hsu	
1953	Dry-ice method/Conger and Fairchild	
1956	Plating method/Puck	F 46, M 46, XX/XY/Tjio and Levan
1958	Air-drying method/Rothfels and Siminovitch	
1959		Mongolism : G21 trisomy/ Lejeune
1960	Lymphocytes/Nowell	Ph ¹ /Nowell and Hungerford Denver Conference for Nomenclature
1961	Cell fusion by HVJ/Okada	
1964	Selective system for hybrid cells/Littlefield	
1969	Q-bands/Caspersson/ <i>in situ</i> hybridization/Gall and Pardue	
1970	C-bands/Pardue and Gall	
1971	G-bands/Sumner <i>et al.</i>	
1973		New Haven Conference for Gene Mapping

sections, distortion and/or overlapping of chromosomes was unavoidable, even if metaphase chromosomes were exactly cut at the equatorial plane. Misreadings of the chromosome number was due to technical difficulties which were inevitable at that time.

In contrast to the results obtained by histological sections, squashed metaphase chromosomes after pretreatment with hypotonic solution spread with the least overlapping. Combined with colchicine pretreatment (3), the real figure of chromosomes was disclosed and discrepancy in chromosomal morphology was no longer a question.

2. Banding methods

The flourishing development of cytogenetics these days is certainly based on the use of banding methods, including methods utilizing Q-bands, G-bands, R-bands, C-bands, T-bands, and Cd-bands. For karyotype analyses, both in plant and animal cytology, chromosomes used to be arranged in descending order of length and/or grouping by gross morphology according to the site of the primary constriction. Even in human karyotypes, though they are much more distinct than in other mammals, many chromosomes are indistinguishable by conventional staining. The identification

of chromosomes was the main problem for karyologists, and it required expert work. But in current chromosome research, no detailed analysis is feasible without banding methods or other differential staining techniques.

For the beginning of this prosperous "banding age," the Caspersson group has played an important role. They first discovered differential staining with quinacrine mustard, a synthetic compound of fluorochrome and an alkylating agent, on chromosomes of *Vicia faba* (5) and those of humans (6). The characteristically fluorescent segments of chromosomes of various degrees of brightness are now called Q-bands and they are used as landmarks in distinguishing chromosomes that had been indistinguishable by conventional staining.

Pardue and Gall (41) found that satellite DNA was concentrated in the centromeric areas in mice chromosomes by the *in situ* nucleic acid hybridization technique. In many investigations thereafter it became apparent that highly repetitive or satellite DNA sequences were the principal components of constitutive heterochromatin from which the term C-band was derived. In applying the C-banding method to flame-dried chromosome preparations, new crossbanding was observed on chromosomes: Giemsa banding or simply G-bands (56). G-bands were also obtained by trypsin treatment of chromosomes (55). By heating slides in hot phosphate buffer, Dutrillaux and Lejeune (10) found other chromosome crossbands, just opposite the G-bands. These were called R-bands, meaning reverse bands. Since the appearance of positive G-bands and interbands is exactly complementary to that of R-bands, the application of both banding methods is necessary for confirmation of the precise region of the bands. Dutrillaux (11) also improved a new system, a modification of R-bands, the T-bands where telomeres were stainable by acridine orange or Giemsa. Both the R- and T-banding methods are useful to determine the terminal segment of chromosomes, especially when distinguishing the translocated segment, which is ambiguous by the G-banding method. R-bands were also induced by treatment with olivomycin (51), and with chromomycin A₃ or mitramycin (54).

The Paris Conference (43, 44) for the standardization of human chromosome nomenclature adopted the terms Q-bands, G-bands, and R-bands for identifying human chromosomes. ISCN (26) recommended the use of G-bands and R-bands for confirmation of a certain band, because they were exactly complementary.

The discovery of other staining methods is as follows: the N-banding method (31) and an ammoniacal silver staining method (18) for the nucleolus organizer region and the Cd-banding method for centromeric dots (13).

Sister chromatid differential staining was first reported by Zakharov and Egolina (64) using Giemsa staining, then by Latt (27) using 33258 Hoechst fluorescence and by Perry and Wolff (44) using a combination of 33258 Hoechst staining and Giemsa staining. To obtain such differential staining, the thymidine of DNA has to be substituted for by BrdU. After the incorporation of BrdU into DNA for two cell cycles, chromosomes will consist of one chromatid substituted unifilarly (TB) and another bifilarly substituted chromatid (BB). BB-chromatids fluoresced or stained less intensely than TB-chromatids. However, the staining behavior of TB- and BB-chromatids with Giemsa showed just the opposite behavior depending on staining conditions (53). Differential staining for sister chromatids was useful for the detection of sister chromatid exchange, which is currently being applied for the study of the effects of environmental

TABLE II. The Number of Bands per Unit Length of Chromosome and the Amount of DNA per Nucleus in Humans as Compared with Those in *Drosophila*

	Total length of chromosomes (μm)	Total number of bands	Number of bands per μm	Daltons ^d	Nucleotide pairs ^d
<i>Drosophila melanogaster</i>	1,180 ^a	2,650 ^a	2.2	0.12×10^{12}	0.2×10^9
Human	220.6 ^b	274 ^c	1.2	3.6×10^{12}	5.6×10^9

^a Based on the data of Bridges (7).

^b Average length of five female karyotypes obtained by the present author (unpublished data).

^c Based on the schematic drawings of banded chromosomes which appeared in the Paris Conference (42).

^d Based on the data of McCarthy (32).

mutagens, because the sensitivity of the occurrence of sister chromatid exchange is higher than that of chromosome aberrations occurrence.

The mechanism of chromosome banding caused by various methods has not fully been elucidated. Since it is evident that a different method alters the chromosome structure in different ways, it is important to clarify the mechanism of staining involved in each method to understand the real structure of chromosomes.

G-bands as compared with bands of Drosophila salivary gland chromosomes: It is a well-known fact that the appearance of G-bands in human and any other vertebrate chromosomes is very similar to salivary gland chromosomes of *Drosophila*. To rationalize this impression, some actual data on human and *Drosophila* chromosomes are listed comparatively in Table II. The number of bands per unit length of human chromosomes is about one half that of *Drosophila*. However, if the human G-bands had been examined in the earlier metaphase chromosomes, the bands would have been finer and the number of G-bands would have increased as Yunis (63) commented, and the value would have been closer to that of *Drosophila*. So the impression conceived by cytologists is significant. The total length of chromosomes in humans measures about one fifth that of *Drosophila*, while the amount of DNA per nucleus in humans is 30 times as much as that in *Drosophila*. This means that the unit length of metaphase chromosomes in humans is a result of condensation of 150 unit lengths of prophase chromosomes. Based on these figures, it must be assumed that one band in human chromosomes is loaded with 150–300 genes, according to the one band-one gene theory (34). In other words, since the salivary gland chromosomes are polytenic consisting of some 1,000 DNA strands resulting from nine reduplications, while human G-banded chromosomes consist of 4 DNA strands, one band in humans can be loaded with 250 times as many genes as one band in *Drosophila*.

3. Somatic cell hybridization

The fusion of cells is a phenomenon normally found in osteoclasts and placentas, and is frequently observed in tumors, in granuloma, and in lesions caused by virus. Such a cell fusion is described as polykaryocytosis (PKC) (47). In virological experiments *in vitro*, it is evident that PKC is caused by many viruses, such as mumps, Newcastle disease virus, measles, herpes simplex, vaccinia, and others (47).

Experimental evidence of hybridization between somatic cells was first reported

by Barski *et al.* (1) from the results obtained in a mixed culture of two sarcoma-producing mice cell lines, and was soon confirmed by Ephrussi (15). Cell fusion was possible between cells from different species, and the resultant fused cells were called heterokaryons. The artificial formation of heterokaryons provoked by Sendai virus was first reported by Okada (39), and it was confirmed by Harris and Watkins (19) using UV-inactivated HVJ. Recently, polyethylene glycol has been used for cell fusion, which was introduced by Pontecorvo (45).

In human-mice hybrid cell lines, Weiss and Green (59) reported the elimination of human chromosomes during culture passages; in other words, a few human chromosomes are retained after long-term culture in the hybrid cells. This phenomenon has lately become a powerful tool for gene mapping. By using the hypoxanthine, aminopterin, and thymidine (HAT) medium improved by Szybalski *et al.* (57), Littlefield (29) has successfully selected the hybrid cells.

Gene mapping: Gene assignments to chromosomes were performed by somatic cell hybridization, *in situ* hybridization and/or family study. The most remarkable results recently obtained by somatic cell hybrids in combination with the G-banding technique is human gene mapping. Human genetics is now intensively studied on the cytological level. Previously, there were no other means than family study for human genetics.

In situ nucleic acid hybridization was first attempted by Gall and Pardue (16) in amphibian oöcytes, and then they applied it to mouse satellite DNA (41). This method is now extensively used in direct assignment of genes to chromosomes in cytological preparations. Thus, the first human gene map appeared at the New Haven Conference (35), and then Human Gene Mapping 4 (25) listed a total of 176 mapped loci, including provisional and inconsistent assignments. The progress in human gene mapping is comparable to that in *Drosophila* genetics using salivary gland chromosome bands early in this century.

It is noteworthy that mice gene maps, too, have been finally accomplished. In mice genetics, gene assignment to specific chromosomes was not possible because chromosomes were indistinguishable by conventional staining, and the gene map had long been arranged in the order of linkage group number. But recently, those linkage groups have been assigned to specific chromosomes, and the gene map was rearranged in the order of chromosome number (33).

Other Important Methods Contributing to Chromosome Study

1. Colchicine pretreatment

Colchicine had previously been used to produce polyploid plants in agriculture and in horticulture. For chromosome studies, Blakeslee and Avery (3) first applied it to plant cytology. The usefulness of colchicine resides not only in the metaphase arresting effects which consequently increase the number of metaphasic cells, but also in the inhibiting effects on microtubule formation which disturb the spreading of chromosomes. And besides, since chromosomes stay longer in the metaphase, the condensation of chromosomes advances further, and consequently chromosomes become short and distinct. A derivative of colchicine, colcemid, is ten times as effective as colchicine. A new synthetic microtubule inhibitor, nocodazole (21), is also available for arresting mitotic cells.

2. *Squashing technique and air-drying technique*

Like other pioneering works in the earlier days of cytological chronology, the squashing method was also applied to plant chromosome studies (2). For more than 30 years, this had been the main procedure in preparing chromosomes because of its relative simplicity and reliability as compared to the classical method. Combined with hypotonic pretreatment, the results of the squashing technique were much better than ever. By this method, the fixation and staining of cells were performed simultaneously with acetic acid containing orcein or dahlia, and cells were squashed between a slide glass and a coverslip by pressing with the thumb. Although the chromosomal spreading in this method depended somewhat on the investigators' skillfulness, metaphase figures were so much clearer and flatter than ever that the taking of microphotographs was feasible. Conger and Fairchild (7) converted the squashed preparations from temporary to permanent by putting them on a piece of dry-ice and removing the cover-slips. The squashing technique is still useful in making chromosome preparations from a piece of tissue which is too small to handle by the air-drying method.

The air-drying method was first applied to monkey cells grown on regular microscopic slides *in vitro* by Rothfels and Siminovitch (48). So far as free cells, such as bone marrow cells, lymphocytes, and tissue culture cells, are concerned, this method is excellent in its simplicity and reliability. The tricks to obtain excellent chromosomal spread by this method are thorough fixation with 3:1 methanol-acetic acid by changing it several times, and the use of chemically clean, not optically clean, slides.

3. *Tissue culture*

Harrison (20) was the first one who cultured a frog neural tube in the frog lymph and observed the differentiation of nerve fibers in it. In the early days, like Harrison's experiments, tissue culture was performed in lymph and/or physiologically balanced salt solutions. The biggest problem in tissue culture had been, and still is, the nutrients appropriate for tissue growth. Long-term culture, therefore, became possible after the establishment of chemically defined media as nutrients. Current tissue culture media basically consist of amino acids, essential and non-essential, vitamins, balanced salts, and serum.

The successful proliferation of poliomyelitis virus in tissue cultured cells of human embryos by Enders *et al.* (14) was a milestone for both virology and biology. Since virus proliferation is fully dependent on living cells, the tissue culture method became the best tool for the "virus culture" method instead of inoculation into the brain or chorio-allantoic cavity. The establishment of successful cultures of human embryonic tissues also lead the investigators to human cytology over a broad field. Sanford *et al.* (52) established a single cell clone (L-cells) by isolating cells with capillaries from mice fibroblast cell strains which had been transformed *in vitro* by methylcholanthrene (12). Gey *et al.* (17) also established a cell line from human cervix carcinoma, known as HeLa cells. As seen in the plating method presented by Puck (46), genetically homogeneous cell clones were useful in quantitative analyses of the biological effects of various agents, chemical, physical or virological. Owing to the established method, including nutrients, procedures, and equipment, the tissue culture method is currently a principal tool in the broad field of biological science.

In classical studies of animal chromosomes, materials were limited to the testes

and ovaries, because of their abundance of dividing cells, while in current studies dividing cells may easily be available by culturing even a piece of somatic tissue which normally has very scarce mitotic cells. Since dividing cells are the only material prerequisite to chromosome research, the availability of mitotic cells by tissue culture made a great contribution to chromosome research.

It was in tissue culture cells that the number of human chromosomes was defined as 46 by Tjio and Levan (58). At that time, the number of human chromosomes was believed to be 48 with the sex-determining type of XX/XY presented by Painter (40). Painter revised the findings of Winiwarter (61, 62) who had presented 47 chromosomes in males and 48 in females with an XX/XO type. Oguma and Kihara (38) confirmed Winiwarter's findings. Discrepancy in chromosome number in early cytology must have been due to the ambiguous figures of histological sections. The tissue culture method has thus made a definite contribution to human chromosome study. Analyses of congenital diseases had long been inevitably limited to family studies. But the finding of a trisomy in Down's syndrome by Lejeune *et al.* (28) opened the door to a new field of science: medical cytogenetics.

Lymphocyte culture of human peripheral blood by Nowell (36) who obtained mitotic cells using phytohemagglutinin, further advanced the development of medical cytogenetics. Chromosome examination of blood cultures is now an important tool for diagnosis and a routine procedure in some clinics.

It was prudent that a conference (9) was held in Denver in 1960 for the standardization of the nomenclature for human chromosomes to avoid futile confusion by different observations and assertions. Subsequent conferences, such as the Paris conference (43) and the ISCN Conference (26), adopted new methodology in chromosome techniques and worked out the standardization of terms of human chromosomes. The establishment of standard nomenclature for chromosomes has really rendered human chromosome study more rapidly progressive, precise, and valuable.

Prospective Views in Cancer Chromosome Research

A great many reports on chromosome aberrations in human cancers include gain and loss of individual chromosomes, partial deletion of a certain chromosome, translocations of parts of chromosomes to others, triploid or tetraploid cells appearing in the diploid population, the alteration of ploidy from diploid to polyploid and marker chromosomes transformed by themselves or among different members of chromosomes. These chromosome aberrations inconsistently occurred among different cancers and even in the same cancer in different individuals.

However with the current banding techniques, it has been elucidated that in some cancers the chromosome aberrations are nonrandomly involved in limited members of chromosomes. The most famous case is the Ph¹ chromosome. It had been considered as the deletion of one of No. 21 (37), but was lately revised to a part of No. 22 that translocated to No. 9 (49). Retinoblastoma has a interstitial deletion of No. 13 (60), and in mammary carcinoma, the long-arm of No. 1 is translocated to other chromosomes (8). The nonrandom involvement of chromosomes in human cancers has been shown in Tables by Sandberg (50) based on the data of Lawler, and Mitelman and Levan. In the data of Mitelman and Levan cited by Sandberg (50), it seems clear that chromo-

some aberration is limited to specific chromosomes. The number of chromosomes preferentially involved adds up to 12 out of 23 pairs, and is frequent in Nos. 1, 8, and 14. These three chromosomes hold almost half the total chromosomes involved. Besides, the number of chromosomes involved varies according to the kind of neoplasia. It is interesting, if it is true, that the specific involvement of chromosomes in a specific cancer was reflected by the specific function of the original tissue, and the diversity of manifestation in different cancers was due to specific chromosomal aberrations. It is still ambiguous, however, why normal cells are converted to a cancerous state by those chromosomal aberrations, even if those chromosomal aberrations were consistently accompanied by a specific cancer character.

The characterization of cancer by chromosomal aberration to which the precise gene loci for cancer might be assigned by current techniques of gene mapping is a problem remaining to be elucidated in the future.

REFERENCES

1. Barski, G., Sorieul, S., and Cornfert, Fr. "Hybrid" type cells in combined cultures of two different mammalian cell strains. *J. Natl. Cancer Inst.*, **26**, 1269-1277 (1961).
2. Belling, J. On counting chromosomes in pollen mother cells. *Am. Nat.*, **55**, 573-574 (1921).
3. Blakeslee, A. F. and Avery, A. G. Methods of inducing doubling of chromosomes in plants. *J. Hered.*, **28**, 392-411 (1937).
4. Bridges, C. B. Salivary chromosome maps with a key to the banding of the chromosomes of *Drosophila melanogaster*. *J. Hered.*, **26**, 60-64 (1935).
5. Caspersson, T., Zech, L., Modest, E. J., Foley, G. E., and Wagh, U. Chemical differentiation with fluorescent alkylating agents in *Vicia faba* metaphase chromosomes. *Exp. Cell Res.*, **58**, 128-140 (1969).
6. Caspersson, T., Zech, L., and Johanson, C. Differential banding of alkylating fluorochromes in human chromosomes. *Exp. Cell Res.*, **60**, 315-319 (1970).
7. Conger, A. D. and Fairchild, L. M. A quick freeze method for making smear slides. *Stain Technol.*, **28**, 281-283 (1953).
8. Cruciger, Q. V. J., Pathak, S., and Cailleau, R. Human breast carcinomas: Marker chromosomes involving 1q in seven cases. *Cytogenet. Cell Genet.*, **17**, 231-235 (1976).
9. Denver Report. A proposed standard system of nomenclature of human mitotic chromosomes. *J. Hered.*, **51**, 221-241 (1960).
10. Dutrillaux, B. and Lejeune, J. Sur une nouvelle technique d'analyse du caryotype humaine. *C. R. Acad. Sci. Paris*, **272**, 2638-2640 (1971).
11. Dutrillaux, B. New system of chromosome banding. The T bands. *Chromosoma*, **41**, 395-402 (1973).
12. Earle, W. R. Production of malignancy *in vitro*. IV. The mouse fibroblast cultures and changes seen in the living cells. *J. Natl. Cancer Inst.*, **4**, 165-212 (1943).
13. Eiberg, H. New selective Giemsa technique for human chromosomes, cd staining. *Nature*, **248**, 55 (1974).
14. Enders, J. F., Weller, T. H., and Robbins, F. C. Cultivation of the Lansing strain of poliomyelitis virus in cultures of various human embryonic tissues. *Science*, **109**, 85 (1949).
15. Ephrussi, B. and Sorieul, S. Mating of somatic cells *in vitro*. In "Approaches to the

- Genetic Analysis of Mammalian Cells," ed. D. J. Merchant and J. V. Neel, pp. 81-97 (1962). The University of Michigan Press, Ann Arbor.
16. Gall, J. G. and Pardue, M. L. Formation and detection of RNA-DNA hybrid molecules in cytological preparations. *Proc. Natl. Acad. Sci. U.S.*, **63**, 378-383 (1969).
 17. Gey, G. O., Coffman, W. D., and Kubicek, M. T. Tissue culture studies of the proliferative capacity of cervical carcinoma and normal epithelium (Abstract). *Cancer Res.*, **12**, 264-265 (1952).
 18. Goodpasture, C. and Bloom, S. E. Visualization of nucleolar organizer regions in mammalian chromosomes using silver staining. *Chromosoma*, **53**, 37-50 (1975).
 19. Harris, H. and Watkins, J. F. Hybrid cells derived from mouse and man: artificial heterokaryons of mammalian cells from different species. *Nature*, **205**, 640-646 (1965).
 20. Harrison, R. G. Observations on the living developing nerve fiber. *Proc. Soc. Exp. Biol. Med.*, **4**, 140 (1907).
 21. Hoebeke, J., Van Hijen, G., and DeBrabander, M. Interaction of oncodazole (R 17934), a new antitumoral drug, with rat brain tubulin. *Biochem. Biophys. Res. Commun.*, **69**, 319-324 (1976).
 22. Hsu, T. C. Mammalian chromosomes *in vitro*. I. The karyotype of man. *J. Hered.*, **43**, 172 (1952).
 23. Hsu, T. C. "Human and Mammalian Cytogenetics. An Historical Perspective" (1979). Springer-Verlag, New York.
 24. Hughes, A. Some effects of abnormal tonicity on dividing cells in chick tissue cultures. *Q. J. Microsc. Sci.*, **93**, 207-220 (1952).
 25. Human Gene Mapping 4. Fourth International Workshop on Human Gene Mapping. Birth Defects: Original Article Series, XIV, No. 4. The National Foundation, New York; also in *Cytogenet. Cell Genet.*, **22**, 1-730 (1978).
 26. ISCN. An International System for Human Cytogenetic Nomenclature (1978), Birth Defects: Original Article Series, XIV, No. 8 (1978). The National Foundation, New York; also in *Cytogenet. Cell Genet.*, **21**, 309-404 (1978).
 27. Latt, S. A. Microfluorometric detection of deoxyribonucleic acid replication in human metaphase chromosomes. *Proc. Natl. Acad. Sci. U.S.*, **70**, 3395-3399 (1973).
 28. Lejeune, J., Gautier, M., and Turpin, R. Etude des chromosomes somatiques de neuf enfant mongoliens. *Compt. Rend.*, **248**, 1721-1722 (1959).
 29. Littlefield, J. W. Selection of hybrids from matings of fibroblasts *in vitro* and their presumed recombinants. *Science*, **145**, 709-710 (1964).
 30. Makino, S. and Nishimura, I. Water-pretreatment squash-technic: A new and simple practical method for the chromosome study of animals. *Stain Technol.*, **27**, 1-7 (1952).
 31. Matsui, S. and Sasaki, M. Differential staining of nucleolus organizers in mammalian chromosomes. *Nature*, **246**, 148-150 (1973).
 32. McCarthy, B. J. The evolution of base sequences in nucleic acids. In "Handbook of Molecular Cytology," ed. A. Lima-de-Faria, pp. 3-20 (1969). North-Holland, Amsterdam.
 33. Miller, O. J. The karyotype and chromosome map of the mouse. In "Nobel Symposium 23: Chromosome Identification," ed. T. Caspersson and L. Zech, pp. 132-144 (1973). Academic Press, New York.
 34. Muller, H. J. and Prokofyeva, A. A. The individual gene in relation to the chromomere and chromosome. *Proc. Natl. Acad. Sci. U.S.*, **21**, 16-26 (1935).
 35. New Haven Conference: First International Workshop on Human Gene Mapping. Birth Defects: Original Article Series, X, No. 3 (1974). The National Foundation, New York.

36. Nowell, P. C. Phytohemagglutinin: An initiator of mitosis in cultures of normal human leukocytes. *Cancer Res.*, **20**, 462-466 (1960).
37. Nowell, P. C. and Hungerford, D. A. A minute chromosome in human chronic granulocytic leukemia. *Science*, **132**, 1497 (1960).
38. Oguma, K. and Kihara, H. Etude des chromosomes chez l'homme. *Arch. Biol. (Liege)*, **33**, 493-514 (1923).
39. Okada, Y. Multinucleated giant cell formation by fusion of two different strains of cells. *Biken J.*, **4**, 145-146 (1961).
40. Painter, T. S. Studies in mammalian spermatogenesis. II. The spermatogenesis of man. *J. Exp. Zool.*, **37**, 291-336 (1923).
41. Pardue, M. L. and Gall, J. G. Chromosomal localization of mouse satellite DNA. *Science*, **168**, 1356-1358 (1970).
42. Paris Conference. Standardization in human cytogenetics. Birth Defects: Original Article Series, VIII, No. 7 (1972). The National Foundation—March of Dimes, New York.
43. Paris Conference Supplement. Birth Defects: Original Article Series, XI, No. 9 (1975). The National Foundation—March of Dimes, New York.
44. Perry, P. and Wolff, S. New Giemsa method for the differential staining of sister chromatids. *Nature*, **251**, 156-158 (1974).
45. Pontecorvo, G. Production of mammalian somatic cell hybrids by means of polyethylene glycol treatment. *Somatic Cell Genet.*, **1**, 397-400 (1975).
46. Puck, T. T., Marcus, P. I., and Cieciura, S. J. Clonal growth of mammalian cells *in vitro*. Growth characteristics of colonies from single HeLa cells with and without a "feeder" layer. *J. Exp. Med.*, **108**, 273-284 (1965).
47. Roizman, B. Polykaryocytosis. *Cold Spring Harbor Symp. Quant. Biol.*, **27**, 327-342 (1962).
48. Rothfels, K. H. and Siminovitch, L. An air-drying technique for flattening chromosomes in mammalian cells grown *in vitro*. *Stain Technol.*, **38**, 73-77 (1958).
49. Rowley, J. D. A new consistent chromosomal abnormality in chronic myelogenous leukemia identified by quinacrine fluorescence and Giemsa staining. *Nature*, **243**, 290-293 (1973).
50. Sandberg, A. A. "The Chromosomes in Human Cancer and Leukemia" (1980). Elsevier/North-Holland, Amsterdam.
51. Sande, J. H. van de, Lin, C. C., and Jorgensen, K. F. Reverse banding on chromosomes produced by a guanine-cytosine specific DNA binding antibiotic: Olivomycin. *Science*, **195**, 400-402 (1977).
52. Sanford, K. K., Earle, W. R., and Likely, G. D. The growth *in vitro* of single isolated tissue cells. *J. Natl. Cancer Inst.*, **9**, 229-246 (1948).
53. Scheres, J.M.J.C., Hustinx, Th. W. J., Rutten, F. J., and Merckx, G.F.M. "Reverse" differential staining of sister chromatids. *Exp. Cell Res.*, **109**, 446-468 (1977).
54. Schweizer, D. R-banding produced by DNase I digestion of chromomycin-stained chromosomes. *Chromosoma*, **64**, 117-124 (1977).
55. Seabright, M. A rapid banding technique for human chromosomes. *Lancet*, **ii**, 971-972 (1971).
56. Sumner, A. T., Evans, H. J., and Buckland, R. A. A new technique for distinguishing between human chromosomes. *Nature New Biol.*, **232**, 31-32 (1971).
57. Szybalski, W., Szybalska, E. H., and Ragni, G. Genetic studies with human cell lines. *Natl. Cancer Inst. Monogr.*, **7**, 75-89 (1962).
58. Tjio, J. H. and Levan, A. The chromosome number of man. *Hereditas*, **42**, 1-6 (1956).
59. Weiss, M. C. and Green, H. Human-mouse hybrid cell lines containing partial com-

- plements of human chromosomes and functioning human genes. *Proc. Natl. Acad. Sci. U.S.*, **58**, 1104-1111 (1967).
60. Wilson, M. G., Towner, J. W., and Fujimoto, A. Retinoblastoma and D-chromosome deletions. *Am. J. Hum. Genet.*, **25**, 57-61 (1973).
 61. Winiwarter, H. Von Études sur la spermatogénèse humaine. I. Cellule de Sertoli. *Arch. Biol.*, **27**, 91-127 (1912).
 62. Winiwarter, H. Von Études sur la spermatogénèse humaine. II. L'hétérochromosome et les mitoses de l'épithélium séminal. *Arch. Biol.*, **27**, 128-188 (1912).
 63. Yunis, J. J. High resolution of human chromosomes. *Science*, **191**, 1268-1270 (1976).
 64. Zakharov, A. F. and Egolina, N. A. Differential spiralization along mammalian mitotic chromosomes. I. BUdR-revealed differentiation in Chinese hamster chromosomes. *Chromosoma*, **38**, 341-365 (1972).

1. J. J. O'Brien, 1998: The impact of climate change on the hydrological cycle. *Water Resour. Res.*, **34**, 1151-1161.
2. J. J. O'Brien, 1999: The impact of climate change on the hydrological cycle. *Water Resour. Res.*, **35**, 1151-1161.
3. J. J. O'Brien, 2000: The impact of climate change on the hydrological cycle. *Water Resour. Res.*, **36**, 1151-1161.
4. J. J. O'Brien, 2001: The impact of climate change on the hydrological cycle. *Water Resour. Res.*, **37**, 1151-1161.
5. J. J. O'Brien, 2002: The impact of climate change on the hydrological cycle. *Water Resour. Res.*, **38**, 1151-1161.
6. J. J. O'Brien, 2003: The impact of climate change on the hydrological cycle. *Water Resour. Res.*, **39**, 1151-1161.
7. J. J. O'Brien, 2004: The impact of climate change on the hydrological cycle. *Water Resour. Res.*, **40**, 1151-1161.
8. J. J. O'Brien, 2005: The impact of climate change on the hydrological cycle. *Water Resour. Res.*, **41**, 1151-1161.
9. J. J. O'Brien, 2006: The impact of climate change on the hydrological cycle. *Water Resour. Res.*, **42**, 1151-1161.
10. J. J. O'Brien, 2007: The impact of climate change on the hydrological cycle. *Water Resour. Res.*, **43**, 1151-1161.
11. J. J. O'Brien, 2008: The impact of climate change on the hydrological cycle. *Water Resour. Res.*, **44**, 1151-1161.
12. J. J. O'Brien, 2009: The impact of climate change on the hydrological cycle. *Water Resour. Res.*, **45**, 1151-1161.
13. J. J. O'Brien, 2010: The impact of climate change on the hydrological cycle. *Water Resour. Res.*, **46**, 1151-1161.
14. J. J. O'Brien, 2011: The impact of climate change on the hydrological cycle. *Water Resour. Res.*, **47**, 1151-1161.
15. J. J. O'Brien, 2012: The impact of climate change on the hydrological cycle. *Water Resour. Res.*, **48**, 1151-1161.
16. J. J. O'Brien, 2013: The impact of climate change on the hydrological cycle. *Water Resour. Res.*, **49**, 1151-1161.
17. J. J. O'Brien, 2014: The impact of climate change on the hydrological cycle. *Water Resour. Res.*, **50**, 1151-1161.
18. J. J. O'Brien, 2015: The impact of climate change on the hydrological cycle. *Water Resour. Res.*, **51**, 1151-1161.
19. J. J. O'Brien, 2016: The impact of climate change on the hydrological cycle. *Water Resour. Res.*, **52**, 1151-1161.
20. J. J. O'Brien, 2017: The impact of climate change on the hydrological cycle. *Water Resour. Res.*, **53**, 1151-1161.
21. J. J. O'Brien, 2018: The impact of climate change on the hydrological cycle. *Water Resour. Res.*, **54**, 1151-1161.
22. J. J. O'Brien, 2019: The impact of climate change on the hydrological cycle. *Water Resour. Res.*, **55**, 1151-1161.
23. J. J. O'Brien, 2020: The impact of climate change on the hydrological cycle. *Water Resour. Res.*, **56**, 1151-1161.
24. J. J. O'Brien, 2021: The impact of climate change on the hydrological cycle. *Water Resour. Res.*, **57**, 1151-1161.
25. J. J. O'Brien, 2022: The impact of climate change on the hydrological cycle. *Water Resour. Res.*, **58**, 1151-1161.

INTERSUBSPECIES HYBRID OF MICE AS A TOOL FOR STUDYING GENETIC SYSTEM GOVERN- ING TUMOR DEVELOPMENT

Kazuo MORIWAKI,^{*1} Toshihiko SHIROISHI,^{*1} Nobumoto MIYASHITA,^{*1}
Naotoshi KANDA,^{*2} and Hirotami IMAI^{*1}

*National Institute of Genetics^{*1} and Tokyo Women's Medical College^{*2}*

In intersubspecies hybrids, some disorders of the genetically conservative regulatory system could emerge due to the cross-combinations of the regulator gene and structure gene. In fact, the incidence of lung tumors induced by urethan was remarkably augmented in the intersubspecies hybrids between the ICR strain and Japanese wild mice. But at the chromosomal level, there was no indication of such a "hybrid effect." Probably, biological processes concerning drug metabolism and DNA repair are quite remote from the conservative homeostatic system exhibiting the "hybrid effect."

It was also an interesting finding that the amount of urethan induced chromosome aberrations showed clear strain differences. Furthermore, an inverse relationship between the degree of chromosome aberrations and the susceptibility to lung tumors was revealed, both of them being induced by urethan. Caffeine post-treatment suggested that error-prone DNA repair somewhat contributes to the rejoining of chromosome breaks by urethan.

So far numerous experimental studies on the genetic susceptibility to tumor development have been achieved by using various strains of the laboratory mice. In general, however, genetic characters related to the more important biological functions seem to exhibit the less polymorphic variations. If any regulatory genetic systems could be assumed to be concerned with tumor development, it would be not easy to find out viable mutants of them within a single Mendelian population, a mouse subspecies in this case. The use of hybrid mice between two subspecies which are genetically remote enough to accumulate certain mutations even in the biologically essential characters, possibly be a useful experimental approach to investigate genetically conservative regulatory systems from the view point of tumor research.

Biological Mechanism Suppressing Tumor Development

As it is widely known that most cancer develops after humans reach reproductive age, and, probably develops in the other mammals at the same stage, there should be direct little effect of cancer on the reproduction of species. From a solely evolutionary

^{*1} Yata 1111, Mishima 411, Japan (森脇和郎, 城石俊彦, 宮下信泉, 今井弘民).

^{*2} Kawada-cho, Shinjuku-ku, Tokyo 160, Japan (神田尚俊).

viewpoint, it does not seem to be necessary for mammalian forms to have a genetic mechanism for suppressing tumor development. From another viewpoint, however, there may exist certain mechanism to inhibit the development of tumors during the reproductive period. Recently it has been revealed that xeroderma pigmentosum patients have a tendency to develop skin cancer more frequently than controls. These patients have a heritable retardation of the DNA repair function which is considered to be a major cause of their elevated tumorigenesis. Other than this trait, there are several heritable diseases causing increases in tumor incidence such as Bloom's syndrome, Louis-Bar syndrome and Fankoni syndrome. From these facts, we may imagine that certain genetic mechanisms to repair DNA damage contribute to the suppression of tumor development.

Homeostatic genetic mechanisms to prevent cancer are not limited to the DNA repair function. Burnet proposed the immunological surveillance mechanism which plays an important role in eliminating mutated somatic cells in the body. At one time, this concept was severely criticized because nude mutant mice lacking the thymus did not exhibit a higher incidence of spontaneous tumors. Recently, however, discovery of the higher activities of natural killer cells in nude mice has again supported this hypothesis.

Another hypothesis on the mechanism suppressing carcinogenesis has been presented by Cairns (2). He noticed that the actual incidence of spontaneous tumor development in humans is markedly lower than would be expected from the spontaneous mutation rate and the total number of division in somatic cells. His hypothesis assumes that a DNA strand with a mutation newly synthesized in the dividing stem cell always moves to a daughter cell to differentiate. Thus, an old normal DNA strand can be preserved in the stem cell. By this mechanism, the somatic mutations causing cancer are efficiently eliminated.

As stated above, there seem to be several biological mechanisms that function for blocking tumor development in mammalian forms. But we do not have any definite proof yet which indicates that these mechanisms work solely for the elimination of tumorigenic variant cells. We may also consider that they are essentially directed to govern normal development and differentiation processes. As these processes are quite important not only for the normal growth of individuals but for the prosperity of the species, they should have generated a strong selection pressure to eliminate deleterious variations. So there are a few viable genetic variations in mammalian developmental processes.

A multistep concept for cancer development has recently become popular. If the first step occurs at relatively earlier stage of development, it should have been involved in the regulatory system of normal differentiation which possibly works to eliminate the variation, even if it is tumorigenic or not. Phenotypically this function appears to be solely for blocking tumorigenesis, in spite of the lack of biological necessity to suppress cancer after attainment of reproductive age.

Recent advances in our knowledge of molecular evolution suggest to us that functionally important protein molecules are genetically conservative in general throughout evolutionary processes (5). According to this concept, it is not easy to obtain viable mutants in a developmental stage to use as experimental tools.

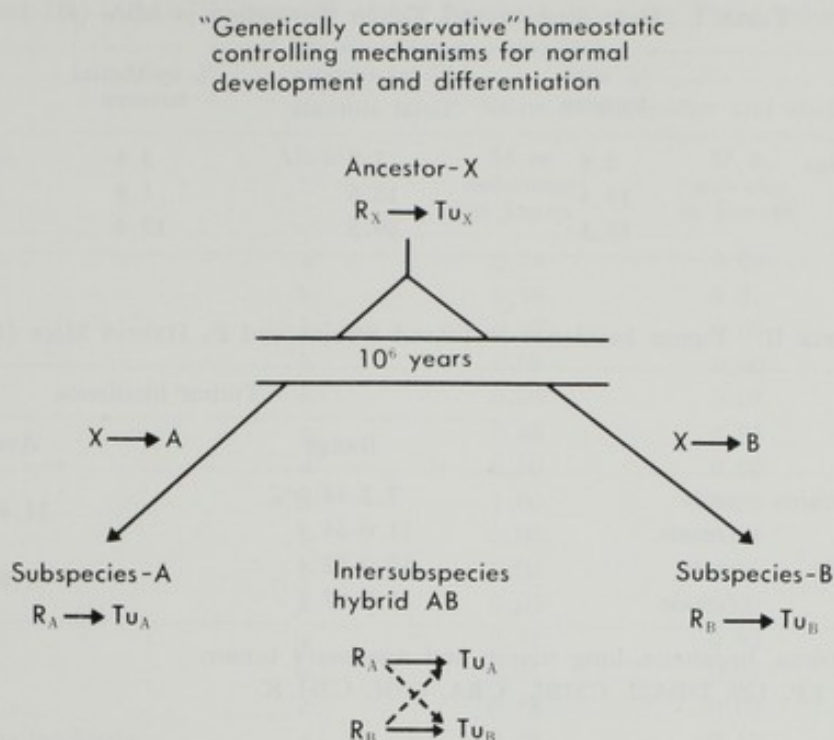


FIG. 1. Evolutionary divergence of R-Tu system. R, repressor gene, no mutation within subspecies; Tu, structural gene which change can lead to tumorigenesis.

Higher Tumor Incidence in Intersubspecies Hybrids

The genetically conservative regulatory system for development and differentiation may contain a tightly coupled combination of a structural gene (Tu) and its regulatory gene (R). Here, we tentatively call it the R-Tu system (see Fig. 1). As both of them are fairly conservative, there may be no genetic polymorphism within a Mendelian population, in this case a subspecies. But during long processes of evolution, this system could accumulate some mutations. Accordingly, two subspecies (A and B) which diverged from a common ancestor (X) a long time ago could have their own R-Tu systems, somewhat different from each other (R_A - Tu_A and R_B - Tu_B). In the intersubspecies F_1 hybrid, neither the R_A - Tu_B nor the R_B - Tu_A system can function properly, which sometimes causes tumor development at a later stage. Thus, intersubspecies hybrids should be useful to investigate the genetically conservative regulatory systems for normal development and differentiation that seem to be relevant to tumor development as well. A notion similar to this has been discussed recently by Stich and Acton (16), but the original concept as such was presented almost 40 years ago by Gordon (See the review article by Anders and Anders (1)).

Gordon demonstrated an extremely higher incidence of melanoma in the interspecies hybrids between two kinds of fresh-water teleosts, the platyfish and swordtail. After laborious efforts in breeding experiments, he found a regulatory gene (SG_1) for a macromelanophore whose structure is coded by the Sd gene in platyfish. As swordtail does not have either of them, and the gene dose of SG_1 was reduced in the F_1 hybrids which causes the higher incidence of melanoma.

The significantly higher incidence of spontaneous tumors in interspecies hybrids has also been found in mice. Little (8) surveyed the incidence of spontaneous tumors in

TABLE I. Hybridization and Tumor Formation in Mice (8)

	% with tumors	Total tumors Total animals	% epithelial tumors	% non-epith. tumors
<i>M. bactrianus</i>	3.8	3.8	3.8	0.0
C57 Black	14.4	15.6	1.8	13.8
F ₁ hybrids	45.5	59.5	17.4	42.1

TABLE II. Tumor Incidence in Inbred Strains and F₁ Hybrid Mice (15)

		Tumor incidence	
		Range	Average
Inbred strains	male	7.3-44.0%	31.4+9.6%
	female	21.0-54.4	
F ₁ hybrids	male	15.0-52.4	41.8+10.3
	female	31.2-67.4	

Tumors: lymphoma, hepatoma, lung tumor, and mammary tumor.

Inbred strains: LP, 129, DBA/2, C57BL, CBA, C3H, C3H. K.

the F₁ hybrids between laboratory mice (DBA strain) and wild mice *Mus bactrianus* (designated *M. m. bactrianus* in our experiments), collected from China. Table I summarizes his data which demonstrates the extremely higher incidence of tumors in the F₁ hybrids.

Such phenomena are not observed in the F₁ hybrids between laboratory mouse strains, though tumor incidences in them increase slightly as compared with the parental strains (Table II). It was also demonstrated in *Drosophila* interspecies hybrids between *D. pseudoobscura* and *D. persimilis* that their lethal and visible mutation rates were much higher than the parental species (17).

Genetic Profile of Mouse (*Mus musculus*) Species

In Little's experiment, two kinds of mouse subspecies were employed. But there is still much controversy in the taxonomy of *Mus musculus* species (13). For our experiments using intersubspecies hybrids, it was desirable to estimate quantitatively the genetic distance between subspecies. The greater the distance between the given two subspecies, the more the regulatory systems in F₁ hybrids exhibit mismatching between R and Tu.

We estimated the genetic distance between mouse subspecies by using two methods. The first one is Nei's method (11) which can estimate the genetic distance between two populations from the differences in allelic frequencies of various biochemical loci. Using the data summarized in Table III, we computed the divergence time between European wild mice (*M. m. domesticus*) and Japanese wild mice (*M. m. molossinus*) to be approximately 1.5×10^6 years (10). Recently we have clearly demonstrated that most of the laboratory mice employed in the world for biomedical research originated from European wild mice, *M. m. domesticus* (18). Thus, one can use the laboratory inbred strains as representatives of *M. m. domesticus*.

TABLE III. Allelic Frequencies of Six Protein Loci in the Three Subspecies of Mouse, *Mus musculus* (10)

Locus	Allele	Name of subspecies and allelic frequencies		
		<i>M. m.</i> <i>molossinus</i> in Japan	<i>M. m.</i> <i>musculus</i> in Europe	<i>M. m.</i> <i>domesticus</i> in Europe
Esterase-1 (Es-1)	a	0.74	0.99	0.00
	b	0.18	0.01	1.00
	c	0.07	0.00	0.00
Esterase-2 (Es-2)	a	0.09	0.00	0.00
	b	0.03	0.07	1.00
	c	0.88	0.93	0.00
Esterase-3 (Es-3)	d	0.00	0.00	0.00
	a	1.00	0.00	0.00
	b	0.00	0.44	0.35
	c	0.00	0.56	0.65
Esterase-5 (Es-5)	d	0.00	0.00	0.00
	a	0.91	0.95	0.74
	b	0.01	0.05	0.26
Isocitrate dehydrogenase (Id-1)	c	0.08	0.00	0.00
	a	0.08	0.12	0.93
	b	0.78	0.88	0.07
	c	0.13	0.00	0.00
Haemoglobin beta-chain (Hbb)	d	0.01	0.00	0.00
	d	0.40	0.33	0.16
	s	0.08	0.67	0.84
	p	0.60	0.00	0.00
Number of samples		194	69	30
Reference		Minezawa <i>et al.</i> , 1977	Selander <i>et al.</i> , 1969	Selander <i>et al.</i> , 1969

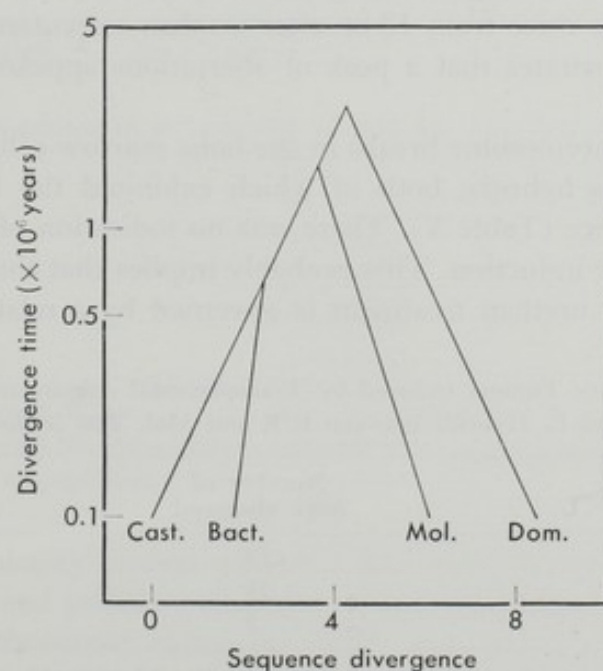


FIG. 2. Divergence points of four mouse subspecies estimated MtDNA analysis.

The second method for estimation of genetic distance is the electrophoretic analysis of mitochondrial DNAs following digestion by restriction endonucleases. Using the electrophoretic differences of the DNA fragments, one can estimate the divergence time of two populations (3). In our case, four mouse subspecies, *M. m. domesticus*, *M. m. bactrianus*, *M. m. castaneus*, and *M. m. molossinus*, were subjected to analyses of their mitochondrial DNA using ten kinds of restriction endonucleases. The results are illustrated in Fig. 2. As shown in this figure, the divergence time between *M. m. domesticus* and *M. m. molossinus* is roughly two million years, which agrees well with the value obtained by Nei's method.

Higher Susceptibility to Urethan-induced Lung Tumors in Intersubspecies Hybrids

We employed urethan induced tumorigenesis in mouse lungs as an experimental system. As it has already been used by many workers, there are plenty of basic data, for instance, the strain difference in tumor susceptibility, dosage effect of urethan, sensitive stages for urethan treatment during development, etc. (See Refs. 4, 9, and 12). In the present study, ICR, BALB/c, C57BL/10 (B10), B10.A (H-2 congenic strain), and *molossinus* stocks Mol. Ten and Mol. Msm were used.

Lung tumor induction was carried out by transplacental administration of urethan (1.5 mg/g B.W.) into ICR, Mol. Ten and their F_1 hybrids at the stage of 17–19 days of gestation. Five months after birth, the number of pulmonary nodules were scored. The result is summarized in Table IV. In the F_1 hybrids, tumor incidence dramatically increased, which allows us to assume a certain disorder of the genetically conservative regulatory systems in the intersubspecies hybrids, although we do not know yet in which stage after administration of urethan such a hybrid specific disorder occurs. To dissolve this problem, we analyzed chromosome changes as a reflection of the urethan effect on DNA within a relatively short period after administration.

Chromosome aberrations including gaps and breaks were scored in the bone marrow cells of BALB/c mice from 12 hr after urethan subcutaneous injection up to 168 hr. Figure 3 demonstrates that a peak of aberrations appears around 24 hr after injection.

Urethan induced chromosome breaks in the bone marrow cells were scored in two kinds of intersubspecies hybrids, both of which exhibited the frequency of breaks between the parental mice (Table V). There was no indication of the "hybrid effect" as shown by lung tumor induction. This probably implies that the DNA repair mechanism functioning after urethan treatment is governed by a relatively simple genetic

TABLE IV. Pulmonary Tumors Induced by Transplacental Administration of Urethan in ICR and F_1 Hybrids between ICR and Mol. Ten (*molossinus*)

Mice strains	Number of mice observed	Pulmonary nodules per mouse
ICR	18	2.7 ± 0.88
(ICR \times Mol. Ten) F_1	25	5.8 ± 2.08
Mol. Ten	7	0.2 ± 0.34

Urethan treatment: subcutaneous injection, 1.0 mg/g B. W., 17–19th day of gestation. Scoring of nodules: 5 months of age.

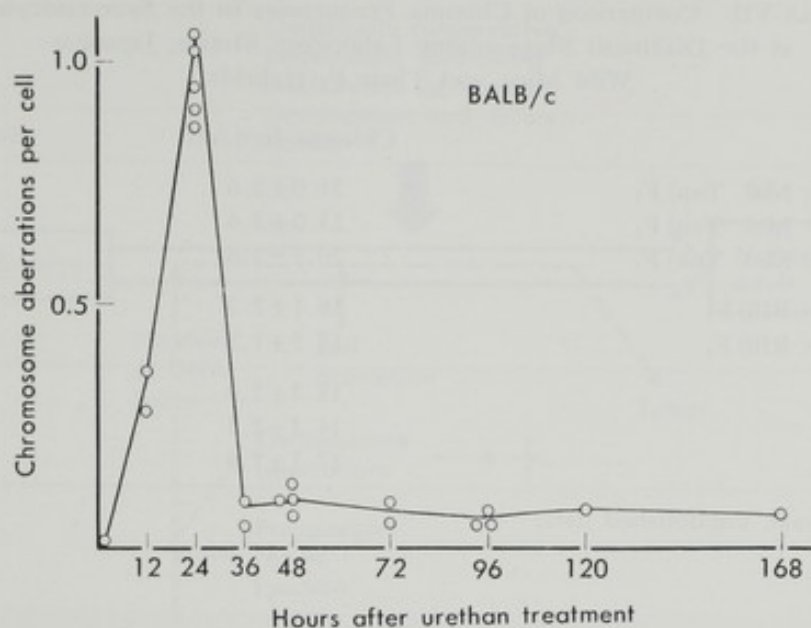


FIG. 3. Chromosome aberrations in the bone marrow cells after urethan administration.

TABLE V. Urethan Induced Chromosome Aberrations in the Bone Marrow Cells of Inter-subspecies Hybrids

Mice strain	Chromosome breaks per cell after urethan treatment				
	0	12	24	36	48 (hr)
BALB/c	0.0	0.10	0.55	0.02	0.06
C. Ten F ₁	0.0	0.20	0.69	0.09	0.04
Mol. Ten	0.0	0.34	1.56	0.72	—
B. Ten F ₁	—	0.20	1.06	0.11	—
C57BL/10	0.0	0.28	0.72	0.11	—

Urethan dose : 1.5 mg/gB. W. Age : 3 weeks.

TABLE VI. Comparison of *in vivo* SCE in BALB/c, Mol. Ten, and Their F₁ Hybrid

Mice strain	Average SCE per cell	
	Control	+MC (0.2 μ g/gB. W.)
BALB/c	1.76 \pm 0.27	3.10 \pm 0.36
C. Ten F ₁	2.45 \pm 0.36	2.57 \pm 0.25
Mol. Ten	2.68 \pm 0.35	3.53 \pm 0.12 ^a

BUDR dose : 2-10 μ g/gB. W./hr.

^a BUDR dose : 10-5- μ g/gB. W. This value is expected to decrease around 2.7 at BUDR dose 2-10 μ g. (Kanda and Moriwaki, unpublished)

system but the regulatory process related to the actual growth of tumors is controlled by a more complex and probably conservative genetic system as mentioned above.

In vivo sister chromatid exchanges (SCE) were also compared between the two subspecies and their F₁ hybrids, indicating no "hybrid effect" in either spontaneous or mitomycin (MC) induced exchange (Table VI). This again suggests that the process

TABLE VII. Comparison of Chiasma Frequencies in the Spermatocytes at the Diakinesis Stage among Laboratory Strains, Japanese Wild Mice, and Their F₁ Hybrids

	Chiasma freq./cell	No. of cells obs.
(BALB/c × Mol. Ten) F ₁	21.0 ± 2.6	13
(BALB/c × Mol. Ten) F ₁	23.0 ± 3.4	9
(BALB/c × Mol. Ynk) F ₁	20.7 ± 2.6	17
(BALB/c × B10) F ₁	16.1 ± 2.3	13
(BALB/c × B10) F ₁	15.5 ± 1.3	20
B10	15.3 ± 2.9	10
BALB/c	14.3 ± 2.1	10
Mol. Ten	17.5 ± 2.0	11

(Imai and Moriwaki, unpublished data)



FIG. 4. Meiotic chiasma in the diakinesis of spermatocytes of the inter-subspecies hybrid (BALB/c × Mol. Ten) F₁. Arrows show the points of crossing-over, and bars terminal association.

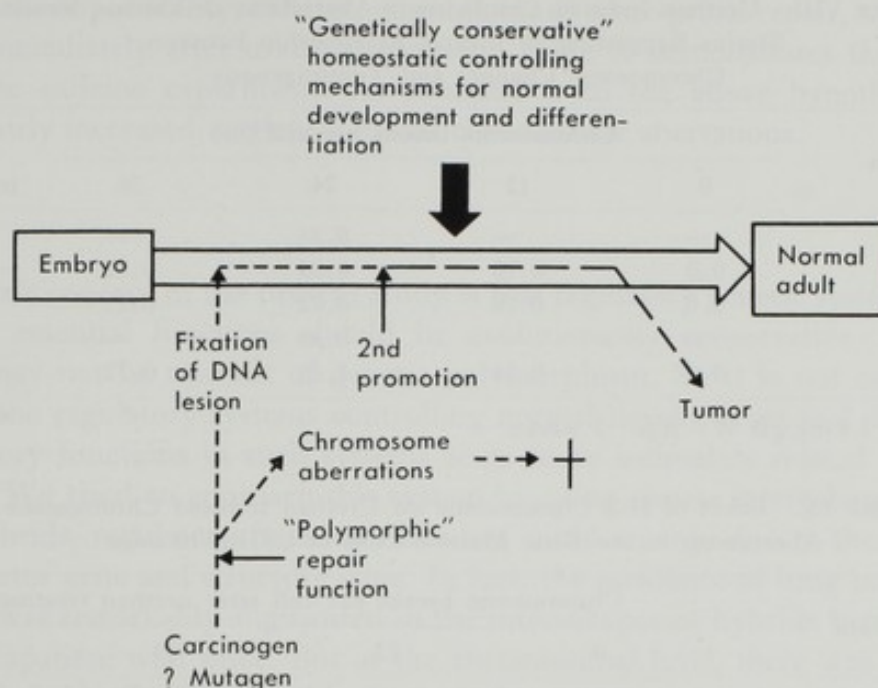


FIG. 5. Genetic systems governing normal development and differentiation and their relation to the genetic control of tumorigenesis.

for DNA strand exchange is not related to the complex and conservative genetic system.

On the other hand, meiotic crossing-over seems to be controlled by more complex mechanisms which exist in the system exhibiting the "hybrid effect." As summarized in Table VII, chiasma frequencies in the spermatocytes at the diakinesis stage are significantly higher in the intersubspecies hybrids than in the parental mice. In this experiment, the number of "terminal chiasma" was not scored (Fig. 4).

Based on the experimental findings demonstrated above, a possible mechanism of the "hybrid effect" on tumor development is assumed as illustrated in Fig. 5. In intersubspecies hybrids, "genetically conservative homeostatic controlling mechanisms for normal development and differentiation" should have a certain leakiness which possibly accelerates tumor growth as compared with that in a single subspecies. Various genetic polymorphisms for tumor development so far reported (See Ref. 7) are mostly related to such processes as metabolism of carcinogens and repair of DNA damage. The first step of tumorigenesis could be settled after passing through these processes. Then the precancerous state (or cell) is subjected to the "conservative controlling mechanisms."

Strain Difference in Urethan Induced Chromosome Aberrations and Error-prone DNA Repair

During the course of the present study, it was observed that the frequencies of chromosome break at 24 hr after urethan treatment vary among mouse strains. Interestingly, the frequency has an inverse relationship with the susceptibility to urethan-induced lung tumors (Table VIII).

We have already developed B10 H-2 congenic strains, B10. MOL-TEN and B10. MOL-YG, which carry H-2 chromosomes originating from Japanese wild mice, *M. m.*

TABLE VIII. Urethan Induced Chromosome Aberrations in Various Mouse Strains Suggesting an Inverse Relationship between Chromosome Changes and Tumorigenesis

Mouse strain	Chromosome breaks per cell (hr)				Urethan-induced tumorigenesis
	0	12	24	36	
A/J	—	—	0.55	—	‡‡
BALB/c	0.0	0.10	0.55	0.02	‡‡
C57BL/10	0.0	0.28	0.72	0.11	+
Mol. Msm	—	—	0.89	—	±
Mol. Ten	0.0	0.34	1.56	0.72	±

Urethan dose: 1.5 mg/gB. W. Age: 3 weeks.

TABLE IX. Effect of H-2 Chromosome on Urethan Induced Chromosome Aberrations in the Bone Marrow Cells of C57BL/10 mice

Mouse strain	Chromosome breaks per cell after urethan treatment (hr)			
	0	12	24	36
C57BL/10 (B10)	0.0	0.28	0.72	0.11
Mol. Ten	0.0	0.34	1.56	0.72
B10. MOL. TEN	0.0	0.40	1.15	—
B10. MOL. YG	0.0	0.16	1.35	0.20
A/J	—	—	0.55	—
B10. A	—	—	0.27	—

Urethan dose: 1.5 mg/gB. W. Age: 3 weeks.

TABLE X. Effect of Caffeine on Urethan Induced Chromosome Aberrations in the Bone Marrow Cells of BALB/c Mice

Treatment	Aberrant cell percentage 24 hr after urethan and caffeine treatment
Control	0.00
Caffeine	0.01
Urethan	19.7 ± 7.9
Urethan + caffeine	23.9 ± 8.3

Urethan dose: 1.5 mg/gB. W. Caffeine dose: 0.1 mg/gB. W. at 0.8, and 16 hr after urethan injection, s.c.

molossinus. Urethan-induced chromosome aberrations in these two strains are considerably higher than in their background strain, C57BL/10 (B10). This data suggests the possible localization of the gene for either urethan metabolism or DNA repair on chromosome 17 (Table IX).

The inverse relationship between urethan induced chromosome aberrations and susceptibility to lung tumors led us to assume a possible commitment of error-prone DNA repair. If this kind of repair system could contribute to the rejoining of chromosome breakages, the frequency of breakage could then be reduced. But in this case tumor incidence will be elevated in a later period. Kondo (6) proposed the possibility that error-prone DNA repair can contribute to tumorigenesis due to somatic mutation.

To test the above possibility, caffeine, an inhibitor of error-prone repair, was introduced for 24 hr immediately after urethan injection. Table X demonstrates the preliminary result of the caffeine experiment. As expected from the above hypothesis, caffeine treatment fairly increased urethan-induced chromosome aberrations.

Conclusion

The basic concept of the present study is that regulatory genetic systems governing biologically essential functions should be evolutionarily conservative. This system, therefore, may not be tolerant of genetic polymorphism. So it is not easy to analyze genetically the regulatory systems controlling normal development and differentiation. But regulatory functions in such systems seem to be intimately related to cancer development. We tried to approach this system by using mouse intersubspecies hybrids. In these hybrids, regulatory function disorders could emerge due to the mismatching of the regulator gene and structure gene. In fact, the incidence of lung tumors induced by urethan was remarkably augmented in the intersubspecies hybrids between the ICR strain and Japanese wild mice. But at the chromosomal level, there was no indication of such a "hybrid effect." Probably, biological processes concerning drug metabolism and DNA repair are quite remote from the conservative homeostatic system exhibiting the "hybrid effect."

It was also an interesting finding that the amount of urethan-induced chromosome aberrations showed clear strain differences. Furthermore, an inverse relationship between the degree of chromosome aberrations and the susceptibility to lung tumors was revealed, both of them being induced by urethan. Caffeine post-treatment suggested that error-prone DNA repair somewhat contributes to the rejoining of chromosome breaks by urethan.

Acknowledgments

We wish to thank Dr. T. Nomura of Osaka University for his kind advice during the course of this study. Technical assistance of Mrs. M. Murofushi is also acknowledged. This work was supported in part by Grants-in-Aid for Special Project Research from the Ministry of Education, Science and Culture of Japan (Nos. 401001 and 401041). Contribution No. 1331 from the National Institute of Genetics, Japan.

REFERENCES

1. Anders, A. and Anders, F. Etiology of cancer as studied in the platyfish-swordtail system. *Biochim. Biophys. Acta*, **516**, 61-95 (1978).
2. Cairns, J. Mutation selection and natural history of cancer. *Nature*, **255**, 197-200 (1975).
3. Gotoh, O., Hayashi, J., Yonekawa, H., and Tagashira, Y. An improved method for estimating sequence divergence between related DNAs from changes in restriction endonuclease cleavage sites. *J. Mol. Evol.*, **14**, 301-310 (1979).
4. Heston, W. E. Genetics of cancer. *J. Hered.*, **65**, 262-272 (1974).
5. Kimura, M. The neural theory of molecular evolution. *Sci. Am.*, **241**, 94-104 (1979).
6. Kondo, S. Misrepair model for mutagenesis and carcinogenesis. In "Fundamentals in Cancer Prevention," ed. P. N. Magee, pp. 417-429 (1976). Japan Scientific Societies Press, Tokyo.

7. Kouri, R. E. and Nebert, D. W. Genetic regulation of susceptibility to polycyclic-hydrocarbon-induced tumors in the mouse. In "Origins of Human Cancer (B)," ed. H. H. Hiatt *et al.*, pp. 811-835 (1977). Cold Spring Harbor Laboratory, Cold Spring Harbor, New York.
8. Little, C. C. Hybridization and tumor formation in mice. *Proc. Natl. Acad. Sci. U.S.*, **25**, 452-455 (1939).
9. Mirvish, S. The carcinogenic action and metabolism of urethan and N-hydroxyurethan. *Adv. Cancer Res.*, **11**, 1-45 (1968).
10. Moriwaki, K., Shiroishi, T., Minezawa, M., Aotsuka, T., and Kondo, K. Frequency distribution of histocompatibility-2 antigenic specificities in the Japanese wild mouse genetically remote from the European subspecies. *J. Immunogenet.*, **6**, 99-113 (1979).
11. Nei, M. Genetic distance between populations. *Am. Nat.*, **106**, 283-292 (1972).
12. Nomura, T. Timing of chemically induced neoplasia in mice revealed by the antineoplastic action of caffeine. *Cancer Res.*, **40**, 1332-1340 (1980).
13. Schwartz, E. and Schwartz, H. K. The wild and commensal stocks of the house mouse, *Mus musculus* Linnæus. *J. Mammal.*, **24**, 59-72 (1943).
14. Selander, R. K., Hant, W. G., and Yang, S. Y. Protein polymorphism and genetic heterozygosity in two European subspecies of the house mouse. *Evolution*, **23**, 379-390 (1969).
15. Smith, G. S., Walford, R. L., and Mickey, M. R. Lifespan and incidence of cancer and other diseases in selected long-lived inbred mice and their F₁ hybrids. *J. Natl. Cancer Inst.*, **50**, 1195-1213 (1973).
16. Stich, H. F. and Acton, A. B. Can mutation theories of carcinogenesis set priorities for carcinogen testing programs? *Can. J. Genet. Cytol.*, **21**, 155-177 (1979).
17. Sturtevant, A. H. High mutation frequency induced by hybridization. *Proc. Natl. Acad. Sci. U.S.*, **25**, 308-310 (1939).
18. Yonekawa, H., Moriwaki, K., Gotoh, O., Watanabe, J., Hayashi, J., Miyashita, N., Petras, M. L., and Tagashira, Y. Relation between laboratory mice and the subspecies *Mus musculus domesticus* based on restriction endonuclease cleavage patterns of mitochondrial DNA. *Jpn. J. Genet.*, **55** 289-296 (1980).

SISTER CHROMATID EXCHANGE AND DNA REPAIR IN BLOOM'S SYNDROME AND HUMAN MALIGNANT DISEASES

Yukimasa SHIRAISHI

*Laboratory of Human Cytogenetics, Department of Anatomy,
Kochi Medical School**

The phenomenon of sister chromatid exchange (SCE) is an interesting genetic event in metaphase chromosomes, even though its exact mechanism remains unknown. The fact that SCE can take place, whether "spontaneously" or induced by various agents, is in itself important, for such an event, involving damage and repair of bilateral loci in chromosomes, presents opportunities for the modification of chromosomal structure and/or function. It is now assumed that under "normal" circumstances SCE does not lead to any change in the functional genome, though this may not apply to abnormal conditions. The latter may be produced by a number of chemical, viral or physical agents which lead to a significantly increased incidence of SCE in normal cells either *in vitro* or *in vivo*. In fact, SCE has now been recognized and advocated as a most sensitive test for potentially mutagenic and/or carcinogenic agents. Thus, the broad field of SCE studies becomes of direct interest to and subject to exploration by those involved with cancer causation and biology.

"Spontaneous" SCE in Human Chromosomes

The incidence of sister chromatid exchange (SCE) in human lymphocytes is relatively constant among individuals and independent of their age and sex (7), though a notable exception is the high SCE incidence in lymphocytes of Bloom's syndrome (BS), which exhibits a 10-fold higher SCE frequency than that in the cells of normal subjects (3, 25). SCE detection procedures that employ 5-bromo-2-deoxyuridine (BrdU) are now commonly used, despite the potential problem of effects due to exposure to BrdU. It is known that BrdU can cause chromosome aberrations in cultured mammalian cells (4, 10). Thus, it is possible that it may also cause SCE. Actually, the incidence of SCE was found to increase with increasing concentrations of BrdU (18, 34). However, this does not necessarily mean that SCE detected by the BrdU-labeling method have been all induced by this compound. At low concentrations of BrdU, ranging from 0.1 to 2.5 $\mu\text{g/ml}$, the SCE frequency in Chinese hamster chromosomes remains at a constant level. In human chromosomes the frequency of SCE also tends to level off at low BrdU concentrations (18). These results suggest that a fraction of SCE arises independently of the BrdU effect. Therefore, it is important to know whether

* Oko-machi, Nangoku 781-51, Japan (白石行正).

the SCE increase in BS is a BrdU-associated effect only or whether it is demonstrable when other methods of differentiating sister chromatids are used and whether cultured cells other than blood lymphocytes exhibit increased SCE. An increased SCE frequency has been demonstrated by us in BS lymphocytes, skin fibroblasts and bone marrow cells using two techniques, *i.e.*, one based on BrdU incorporation and another on labeling with ^3H -deoxycytidine (25, 26). The marrow cells and lymphocytes of BS were shown to have a dramatic increase in SCE (average 81.5 *vs.* 5.3 in normal cells) at all concentrations of BrdU used (Photos 1–5). The SCE frequency in chromosome #1 at a BrdU concentration of 0.05 $\mu\text{g/ml}$ was 4.31 in lymphocytes and 4.21 in bone marrow cells and remained constant up to 3.0 $\mu\text{g/ml}$ BrdU (4.35 SCE per chromosome #1). Raising the concentration of BrdU had little effect on the SCE frequency. No SCE was observed when the concentration of BrdU was raised to 6.0 $\mu\text{g/ml}$, since under these conditions mitosis ceased. Since BrdU labeling at concentrations lower than 0.05 $\mu\text{g/ml}$ did not permit unequivocal demarcation of sister chromatids, it was uncertain as to whether the rather constant SCE frequency reflected spontaneous exchanges or would fall at lower concentrations of BrdU. Therefore, the SCE frequency obtained by the BrdU method was compared with that based on an autoradiographic method utilizing ^3H -deoxycytidine. Of course, it might be argued that the labeled deoxycytidine, like BrdU, is capable of inducing SCE at any concentration of the deoxyriboside. One study (4) indicates that low levels of β -radiation do not cause an increase in SCE in human lymphocytes and that a number, if not all, the SCE observed at low levels of β -radiation (0.001–0.01 μCi of ^3H -uridine) with autoradiography may be spontaneous events. At a high level of β -radiation (0.2 μCi of ^3H -uridine) an increase in SCE was observed. BS lymphocytes exhibited a high frequency of SCE when ^3H -deoxycytidine rather than BrdU was used to differentiate sister chromatids; a many-fold increase in SCE was observed in comparison to the number of SCE in lymphocytes of controls (Photos 1–5). The SCE frequency was scored only in the largest chromosomes, *i.e.*, #1, since the poor resolution of multiple exchanges with the autoradiographic technique made an accurate estimation of the SCE frequency in shorter chromosomes difficult. The SCE frequency in cells labeled with two different concentrations of ^3H -deoxycytidine (0.5 and 2.0 $\mu\text{Ci/ml}$) was compared with that observed with BrdU in chromosome #1; no statistically significant difference was observed. SCE was not detected in cells labeled with less than 0.5 $\mu\text{Ci/ml}$ of ^3H -deoxycytidine because of rare grains on the chromosomes. There was no statistically significant difference in the SCE number between the ^3H -deoxycytidine and BrdU methods (25). These observations constitute evidence against the increased SCE being due to an unusual cellular reaction to BrdU; thus, the increased SCE in BS is probably not due to a BrdU effect and points to the existence of a chromosomal instability *in vivo* in BS syndrome patients. An increased *in vivo* frequency of SCE is most characteristic of BS, in contrast to other chromosome breakage syndromes. This increased SCE frequency occurs in various types of cells besides blood lymphocytes. Though some results (18, 34) presumably account for BrdU-induced SCE, it is not at all clear why only a very small fraction of the events associated with BrdU incorporation are interpreted as DNA lesions and as such result in SCE. The discrepancy between “spontaneous” SCE and BrdU-induced effects remains unexplained. In order to truly compare “spontaneous” SCE frequencies

in different cells, it may be necessary to generate linear dose response curves and then extrapolate to zero BrdU substitution.

The Effects of Radiation and Chemical Agents on SCE

The incidence of SCE can readily be elevated beyond the basal level by treatment of cells with various exogenous agents. X-rays cause only a slight increment in SCE frequency, in contrast to its remarkable ability to produce chromosome aberrations (20, 22), whereas UV light can evoke a significant increase in SCE frequency and chromosome aberrations (12, 13). Various chemical agents can cause an increase in the incidence of SCE in mammalian and plant cells (15, 19, 22). The mode of action, however, differs considerably from agent to agent. On the basis of their efficiency in inducing SCE and chromosomal aberrations, chemical agents may fall into one of two or three categories. They may exert their effects in a manner similar to that of X-rays, *i.e.*, a minimal increase in SCE frequency in spite of their remarkable ability to produce chromosome aberrations. For this reason, they are tentatively designated as X-ray type agents. Among the chemical agents so far reported, caffeine, 8-ethoxycaffeine, nitrosoguanidine, and bleomycin belong to this group. Agents in the second group, the UV-type group, are able to induce SCE very efficiently as well as chromosome aberrations. This group includes most alkylating agents and some DNA intercalating agents, such as proflavine and acridine orange. Bifunctional alkylating agents, such as mitomycin C (MC), nitrogen mustard, and chlorambucil, are extremely potent inducers of SCE, whereas monofunctional alkylating agents are less effective inducers (22). This is consistent with the finding that monofunctional agents are usually less efficient in inducing chromosome aberrations than their bifunctional analogs (14). Methyl methanesulfonate (MMS) and ethyl methanesulfonate (EMS) are monofunctional alkylating agents, and yet, the former is a more potent inducer of SCE than the latter, and this is also true in the production of chromosome aberrations (22). In mammalian cells caffeine is known to inhibit post-replication repair of DNA lesions (16), by preventing the gap filling in the daughter strand when the damaged DNA template is replicated. The details of the biological effects of caffeine on mammalian cells are unclear. Conflicting results have been reported concerning the effect of caffeine on SCE. In Chinese hamster cells the induction of SCE by MC, 4-nitroso-quinoline-oxide (4NQO), and UV is inhibited to a certain extent by caffeine treatment (13), whereas in human cells (16, 24, 29) caffeine enhances the induction of SCE by UV, MC, and 4NQO. Caffeine has no effect on the induction of SCE by thiotepa in *Vicia faba* cells (15). However, recent evidence has been accumulating that caffeine did not significantly decrease the SCE frequency and, if anything, increased or had almost no effect on the SCE incidence following exposure of the cells to alkylating agents (29). The enhancement of SCE by caffeine does not support the idea that the process of SCE is a manifestation of caffeine-sensitive post-replication repair of DNA damage. However, the molecular processes underlying the induction of SCE by chemical agents are largely unknown. A model based on a replication mechanism to bypass DNA crosslinks produced by chemicals (or other agents) has also been proposed (23); however, the validity of this model has been questioned on the grounds that it cannot explain SCE induction by non-crosslinking chemical

agents and the observation of twin SCE in tetraploid cells (30). Further screening of chemicals with regard to their potency in inducing SCE may allow a more illuminating grouping of chemical agents on a functional basis.

SCE in Human Genetic Conditions Associated with High Risk of Cancer and DNA Abnormalities (Bloom's Syndrome, Fanconi's Anemia, Ataxia Telangiectasia, Xeroderma Pigmentosum)

Three human genetic diseases (BS, Fanconi's anemia (FA), and ataxia telangiectasia (AT)), are characterized by a high incidence of chromosome aberrations and an increased susceptibility to cancer. In cells from patients with two of these disease, *i.e.*, FA (2, 3) and AT (3, 7), the frequency of SCE in untreated cells is normal. But in cells from patients with BS there are about 10 times more SCE than in normal cells (3, 25). The number of spontaneous SCE is normal in the DNA-repair-deficient human disease xeroderma pigmentosum (XP) (33), as well as in cells from patients with Werner's syndrome (33). Normal numbers of SCE also occur in untreated cells from patients with leukemia (chronic myelogenous leukemia (CML) and acute myeloblastic leukemia (AML)), regardless of the existence of marker chromosomes and karyotypic instability (12, 21).

Based on the finding that the number of SCE in cells from XP patients is identical to that in normal cells, Wolff *et al.* (31) concluded that hypotheses involving known DNA repair processes to account for the induction of SCE are inadequate. It should be noted here that comparison of the susceptibility to SCE of these repair-deficient cells has been made only in terms of the number of spontaneous SCE. In these cells, the deficiency in DNA repair is manifested as the result of an insult to DNA by exogenous agents. A crucial issue, therefore, is whether they would still show the same level of SCE frequency as normal cells if exposed to DNA-damaging agents. XP cells and lymphoid cell lines, derived from cells of patients with chronic lymphocytic leukemia, seem to be remarkably sensitive to the induction of SCE by N-methyl-N'-nitro-N-nitrosoguanidine (MNNG) (31) and MC (27), respectively; this is in contrast to the low incidence of chromosome aberrations in the same cells induced by these chemicals. Latt *et al.* (19) have reported that, even though the frequency of SCE in phytohemagglutinin (PHA)-stimulated lymphocytes from FA patients does not differ from that of normal lymphocytes, treatment of these cells with MC causes less than half as great an increase in SCE as that occurring in identically treated normal lymphocytes. This seems to indicate that the mechanism of spontaneous SCE may be different from that involved in the genesis of induced SCE. Many of the MC-induced SCE in FA cells are incomplete and, thus, contain chromatid breaks at the point of SCE. In FA cells the induction of SCE by MC may be affected greatly by their deficiency in certain steps in the repair process of the DNA crosslink, whereas the mechanism for spontaneous SCE may not be related to this defect. In AT rejoining of radiation-induced single- and double-strand breaks in DNA is normal and the only abnormality, so far identified, is defective excision of some products of anoxic radiation (7): The SCE frequencies after treatment with X-rays or chemical mutagens were equivalent to those of normal cells (6). In BS cells, which exhibit a very high level of spontaneous SCE (3, 25), no repair defect has been identified so far, but DNA replication itself may be

abnormal (9). However, the finding (9) that in BS cells bifunctional-(MC) and monofunctional-(MC, 4NQO) alkylating agents easily induce a "saturation" level (almost two times higher than the spontaneous level) of SCE, suggests that such cells are probably characterized by an easily induced lesion leading to SCE. Considering the possibility that SCE formation is not due to single-strand exchanges between the double DNA helices of sister chromatids and most likely involves double-strand exchanges (14, 16, 28), a feasible process which may induce SCE is one requiring as an initial event (possibly in the first S period) breaks in the template strand (parental strand) permitting double-strand exchange to occur. Possibly, there is a condition present in the BS cells which permits easy occurrence of double-strand exchanges. However, the molecular processes underlying the induction of spontaneous SCE in BS are still unknown.

Evaluation of SCE and DNA repair

The exact mechanism of SCE is not known and some models involving both single- and double-strand exchanges have been proposed (14-16, 26), though the latter form of exchanges appears to be more likely. The formation of SCE has been postulated to be associated with the action of a DNA repair enzyme, possibly being related to processes such as excision (1) or post-replication repair (13, 32). SCE formation has also been attributed to a hypothetical single polynucleotide strand-exchange involving DNA repair enzymes (1), and thought to be followed by DNA strand migration (8). However, Kihlman's (15) and our findings (16) indicate that the single-strand exchanges between the double DNA helices in sister chromatids are not detected at the chromosomal level. If SCE were derived from single-strand exchanges, gaps or unlabeled segments along the chromatids at the second, as well as the first, mitosis should

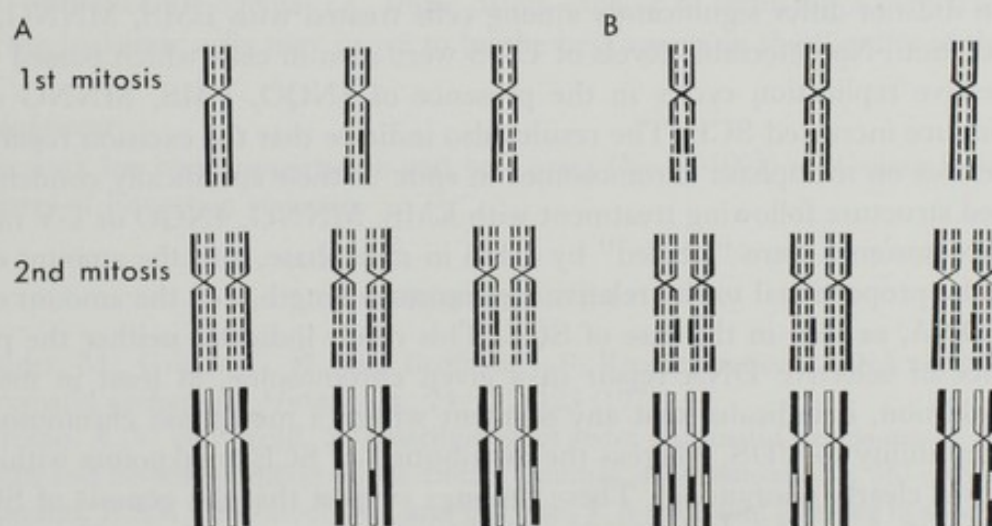


FIG. 1. Schematic presentations of expected BrdU labeling patterns and Giemsa staining of sister chromatids and SCE of single-strand (A) or double-strand (B) exchanges based on the semiconservative replication pattern of DNA. Unbroken lines represent original strands of DNA and broken lines indicate BrdU labeling. Isolabeling of broken lines exhibits staining gaps; the latter would be observed in single-strand but not in double-strand exchanges.

have been seen (Fig. 1). No such gaps were observed, even though a many-fold increase in SCE was seen in the chromosomes of BS. The data suggest that both strands of the DNA double helix are involved in SCE (Fig. 1). Since the exchanges connected with post-replication repair of DNA damage involve single strands of DNA, a relationship between SCE and post-replication repair seems doubtful.

In mammalian cells caffeine is known to inhibit post-replication repair of DNA lesions, though a caffeine-sensitive pre-replication repair system, presumably an excision mechanism, capable of repairing a fraction of MC-induced DNA lesions has been described (11). Evidence was presented that, whereas caffeine alone exerted no effect on the SCE frequency in untreated cells, it increased the SCE frequency in MC- or chemically-treated chromosomes in all specimens observed so far (29). If SCE is derived from single-strand exchanges, these should be inhibited by caffeine and the SCE frequency reduced. However, caffeine did not significantly decrease the SCE frequency in human cells and, if anything, increased or had almost no effect on the SCE incidence following exposure of cells to alkylating agents. The increased occurrence of SCE after caffeine treatment reported recently (5, 16, 24) indicates that post-replication repair is probably not important in SCE formation. It is, therefore, of importance to inquire further into the possible association of SCE with cellular DNA-excision repair processes. We undertook a comparative study (27) on the excision repairability (unscheduled DNA synthesis) in relation to the yields of SCE induced by chemicals (MC, EMS, 4NQO, MMS), with the view that it might be effective in elucidating the mechanism of increased SCE formation. Unscheduled DNA synthesis (UDS) (non-semiconservative DNA synthesis) was examined in normal lymphoid cell lines treated with 4NQO, EMS, MNNG, MC, and UV radiation and was compared with the SCE frequency, inasmuch as unscheduled DNA synthesis is a reliable index of repair replication (27). Significantly, we found that MC induced almost no detectable levels of UDS, even though it induced a high frequency of SCE. The amount of repair replication did not differ significantly among cells treated with EMS, MNNG, 4NQO or UV radiation. No detectable levels of UDS were seen in cells which passed through two successive replication cycles in the presence of 4NQO, EMS, MNNG or MC; MC did induce increased SCE. The results also indicate that the excision repair mechanism operates on metaphase chromosomes in spite of their specifically condensed and multifolded structure following treatment with EMS, MNNG, 4NQO or UV radiation. All the chromosomes were "labeled" by UDS in metaphase, and the amount of UDS seemed to be proportional to the relative chromosome length, *i.e.*, the amount of chromosomal DNA, as seen in the case of SCE. This result indicates neither the presence nor absence of selective DNA repair in a given chromosome, at least in metaphase cells. In addition, it indicates that any segment within a metaphase chromosome had equal susceptibility to UDS, whereas the distribution of SCE breakpoints within chromosomes was clearly nonrandom. These findings suggest that the genesis of SCE was independent of the excision and post replication repair mechanisms. The SCE frequency does not correlate consistently with the rate of cell survival following treatment with alkylating agents (27, 35). SCE may, thus, be the result of fundamentally different cellular events rather than being a reflection of a DNA repair system. In this respect, there is a report (9) pointing to a reduced rate of DNA synthesis as a consequence of an inherently low rate of DNA chain growth in BS cells, which have an increased SCE

frequency. The significance of this DNA-replication defect in relation to SCE formation in chemically treated cells, as well as in BS cells, certainly warrants further study.

SCE in Human Neoplasia

To date the cells of no human tumor or leukemia have been shown to be consistently associated with an increased incidence of SCE. Thus, examination of the leukemic marrow cells in acute and chronic leukemias has revealed a normal range of SCE in the leukemic cells (12). The latter can be often identified on the basis of the aneuploidy present, or, in the case of CML, by the presence of the Ph¹ chromosome. Furthermore, when acute leukemia is treated, the SCE incidence is increased, but this seems to involve primarily the normal (nonleukemic) cells present in the marrow and blood rather than the leukemic ones. When CML transforms to the blastic phase, SCE values above normal are observed, but whether these changes are due to the biologic progression of the disease or are a result of previous chemotherapy is at the moment unknown. The increased incidence of SCE in circulating lymphocytes in most forms of leukemia appears to be due to chemotherapy, with an increased SCE incidence persisting for varying periods of time, depending on the type of chemotherapeutic agents used. Thus, it appears that leukemic cells are not characterized by an inherently high incidence of SCE, regardless of the type of leukemia (12, 21). The higher than normal SCE frequency in the circulating lymphocytes of some patients with lymphoma or leukemia may be related to the presence of infection (particularly viral) and/or the effects of the neoplasia (17), since the high incidence tends to disappear when the patients are treated for their disease.

The fact that some antileukemic drugs are capable of inducing a high frequency of SCE, whereas others do not, might be related to the mechanism of action of such chemotherapeutic agents. It is possible that SCE may find a usefulness in screening potential antileukemic agents, *i.e.*, those drugs capable of inducing a high frequency of SCE in the leukemic cells may prove to be the best agents in the therapy of the disease.

Acknowledgment

This work has been supported in part by a grant (No. 401001) for Cancer Research from the Ministry of Education of Japan.

REFERENCES

1. Bender, M., Griggs, G. H., and Bedford, J. S. Recombinational DNA repair and sister chromatid exchanges. *Mutat. Res.*, **24**, 117-123 (1974).
2. Carrano, A. V. and Wolff, S. Distribution of sister chromatid exchanges in the euchromatin and heterochromatin of the Indian muntjac. *Chromosoma*, **53**, 361-369 (1975).
3. Chaganti, R.S.K., Schonberg, S., and German, J. A manyfold increase in sister chromatid exchanges in Bloom's syndrome lymphocytes. *Proc. Natl. Acad. Sci. U.S.A.*, **71**, 4508-4512 (1974).
4. Dewey, W. C. and Humphrey, R. M. Increase in radiosensitivity to ionizing radiation related to replacement of thymidine in mammalian cells with 5-bromodeoxyuridine. *Radiat. Res.*, **26**, 538-553 (1965).
5. Faed, M.J.W. and Mourelatos, D. Enhancement by caffeine of sister chromatid ex-

- changes frequency in lymphocytes from normal subject after treatment by mutagens. *Mutat. Res.*, **49**, 437-440 (1978).
6. Galloway, S. M. Ataxia telangiectasia: The effects of chemical mutagens and X-rays on sister chromatid exchanges in blood lymphocytes. *Mutat. Res.*, **45**, 343-349 (1977).
 7. Galloway, S. M. and Evans, H. J. Sister chromatid exchange in human chromosomes from normal individuals and patients with ataxia telangiectasia. *Cytogenet. Cell Genet.*, **15**, 17-29 (1975).
 8. Gatti, M. and Olivieri, G. The effect of X-rays on labelling pattern of M_1 and M_2 chromosomes in Chinese hamster cells. *Mutat. Res.*, **17**, 101-112 (1973).
 9. Hand, R. and German, J. A retarded rate on DNA chain growth in Bloom's syndrome. *Proc. Natl. Acad. Sci. U.S.A.*, **72**, 758-762 (1975).
 10. Hsu, T. C. and Somers, C. E. Properties of L cells resistant to 5-bromodeoxyuridine. *Exp. Cell Res.*, **26**, 404-410 (1962).
 11. Ishii, Y. and Bender, M. A. Caffeine inhibition of prereplication repair of mitomycin C-induced DNA damage in human peripheral lymphocytes. *Mutat. Res.*, **51**, 419-425 (1978).
 12. Kakati, S., Abe, S., and Sandberg, A. A. Sister chromatid exchange in Philadelphia chromosome (Ph^1)-positive leukemia. *Cancer Res.*, **38**, 2918-2921 (1979).
 13. Kato, H. Induction of sister chromatid exchanges by UV light and its inhibition by caffeine. *Exp. Cell Res.*, **82**, 383-390 (1973).
 14. Kato, H. In "International Review of Cytology," Vol. 49, ed. G. H. Bourne and J. F. Danielli, p. 55 (1977). Academic Press, New York.
 15. Kihlman, B. A. Sister chromatid exchanges in *Vicia faba*. II. Effects of thiotepa, caffeine and 8 ethoxycaffeine on the frequency of SCEs. *Chromosoma*, **51**, 11-18 (1975).
 16. Kihlman, B. A., Sturelid, S., Hartley-Asp, B., and Nilsson, K. The enhancement by caffeine of the frequencies of chromosomal aberrations induced in plant and animal cells by chemical and physical agents. *Mutat. Res.*, **26**, 105-122 (1974).
 17. Kurvink, K., Bloomfield, C. D., Keenen, K. M., Levitt, S., and Cervenka, J. Sister chromatid exchange in lymphocytes from patients with malignant lymphoma. *Hum. Genet.*, **44**, 137-144 (1978).
 18. Latt, S. A. Microfluorometric detection of deoxyribonucleic acid replication in human metaphase chromosomes. *Proc. Natl. Acad. Sci. U.S.A.*, **70**, 3395-3399 (1973).
 19. Latt, S. A., Stetten, G., Juergens, L. A., Buchman, G. R., and Gerald, P. S. Induction by alkylating agents of sister chromatid exchanges and chromatid breaks in Fanconi's anemia. *Proc. Natl. Acad. Sci. U.S.A.*, **72**, 4066-4070 (1975).
 20. Marin, G. and Prescott, D. M. The frequency of sister chromatid exchanges following exposure to varying doses of 3H thymidine or X-rays. *J. Cell Biol.*, **21**, 159-167 (1964).
 21. Michalová, K., Málková, J., Cinátl, J., and Placerová, J. Chromosomal characteristics and non-random distribution of sister chromatid exchanges in lymphoblastoid cell lines isolated from acute leukemias. *Neoplasma*, **24**, 537-545 (1977).
 22. Perry, P. and Evans, H. J. Cytological detection of mutagen-carcinogen exposure by sister chromatid exchange. *Nature*, **258**, 121-125 (1975).
 23. Shafer, D. A. Replication bypass model of sister chromatid exchanges and implications for Bloom's syndrome and Fanconi's anemia. *Hum. Genet.*, **39**, 177-190 (1977).
 24. Shiraishi, Y. Some critical studies on the sister chromatid exchange in human chromosomes. *Proc. Jpn. Acad.*, **53**, 272-275 (1977).
 25. Shiraishi, Y., Freeman, A. I., and Sandberg, A. A. Increased sister chromatid exchanges in bone marrow and blood cells from Bloom's syndrome. *Cytogenet. Cell Genet.*, **17**, 162-173 (1976).

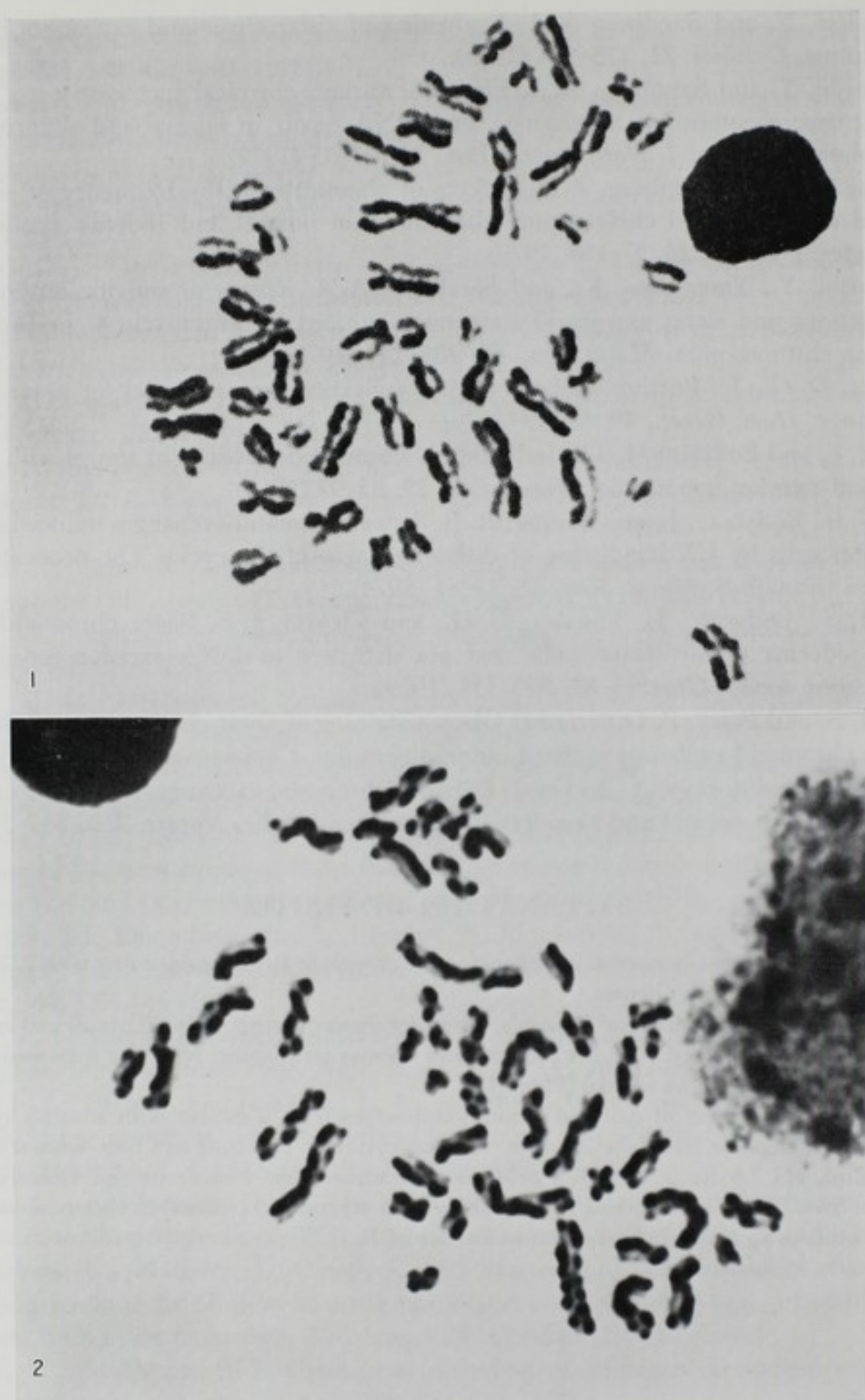
26. Shiraishi, Y. and Sandberg A. A. Evaluation of sister chromatid exchanges in Bloom's syndrome. *Cytobios*, **21**, 175-184 (1978).
27. Shiraishi, Y. and Sandberg, A. A. Effects of various chemical agents on sister chromatic exchanges, chromosome aberrations, and DNA repair in normal and abnormal human lymphoid cell lines. *J. Natl. Cancer Inst.*, **62**, 27-35 (1979).
28. Shiraishi, Y. and Sanberg, A. A. Effects of chemicals on the frequency of sister chromatid exchanges and chromosome aberrations in normal and Bloom's syndrome lymphocytes. *Cytobios*, **26**, 97-108 (1979).
29. Shiraishi, Y., Yamamoto, K., and Sandberg, A. A. Effects of caffeine on chromosome aberrations and sister chromatid exchanges induced by mitomycin C in BrdU-labeled human chromosomes. *Mutat. Res.*, **62**, 139-149 (1979).
30. Stetka, D. G., Jr. Further analysis of the replication bypass model for sister chromatid exchange. *Hum. Genet.*, **49**, 63-69 (1979).
31. Wolff, S. and Bodycote, J. The induction of chromatid deletions in accord with the breakage-and-reunion hypothesis. *Mutat. Res.*, **29**, 85-91 (1975).
32. Wolff, S., Bodycote, J., and Painter, R. B. Sister chromatid exchanges induced in Chinese hamster cells by UV irradiation of different stages of the cycle: The necessity for cells to pass through S. *Mutat. Res.*, **25**, 73-81 (1974).
33. Wolff, S., Bodycote, J., Thomas, G. H., and Cleaver, J. E. Sister chromatid exchange in xeroderma pigmentosum cells that are defective in DNA excision-repair or post-replication repair. *Genetics*, **81**, 349-355 (1975).
34. Wolff, S. and Perry, P. Differential Giemsa staining of sister chromatids and the study of sister chromatid exchange without autoradiography. *Chromosoma*, **48**, 341-353 (1974).
35. Wolff, S., Rodin, B., and Cleaver, J. E. Sister chromatid exchanges induced by mutagenic carcinogens in normal and xeroderma pigmentosum cells. *Nature*, **265**, 347-349 (1977).

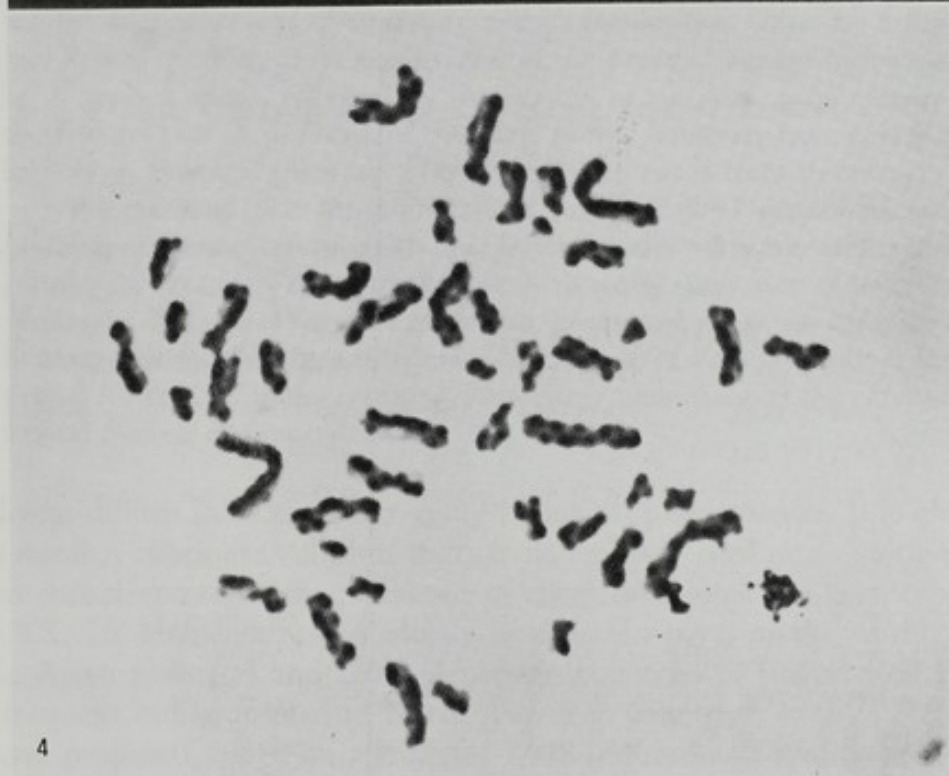
EXPLANATION OF PHOTOS

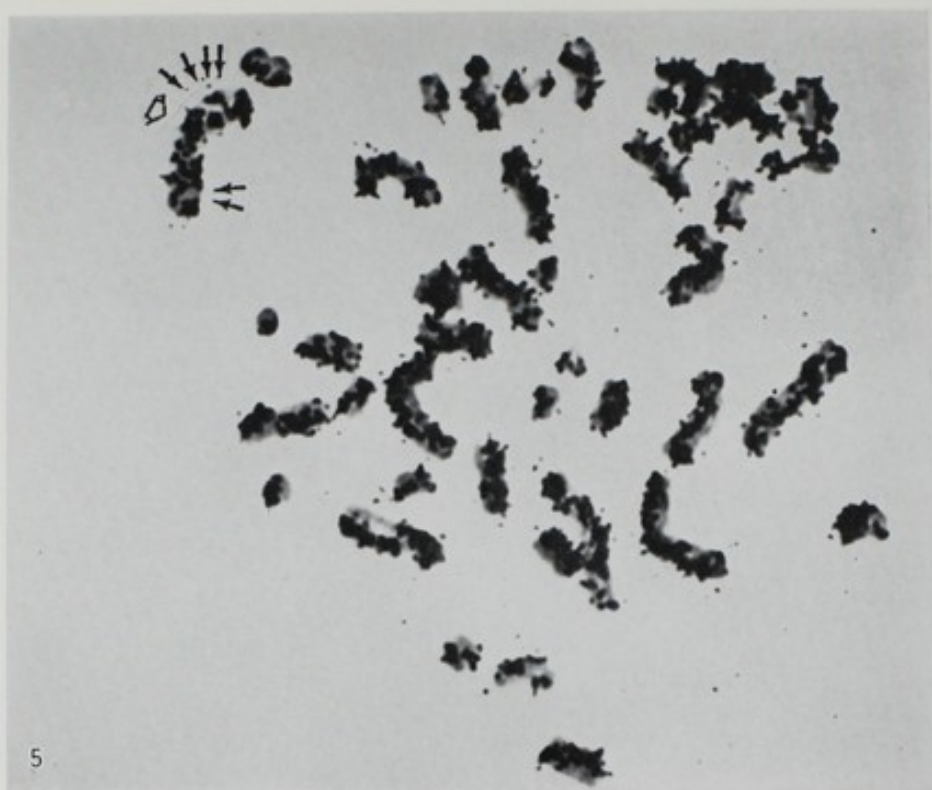
PHOTO 1. Chromosomes of a normal lymphocyte after growth in BrdU, stained first with 33258 Hoechst dye and a day later with Giemsa.

PHOTOS 2-4. The chromosomes of Bloom's syndrome bone marrow cells (Photo 2) and lymphocytes (Photos 4 and 5), stained with the Hoechst and Giemsa techniques. Note the increased number of SCE in comparison to the normal (Photo 1).

PHOTO 5. Autoradiography of cultured blood lymphocytes from a patient with Bloom's syndrome at the second metaphase after labeling with ^3H -deoxycytidine. The slide had been treated with RNase (100 $\mu\text{g}/\text{ml}$, pH 7.4 for 2 hr at 37°) prior to autoradiography. Numerous and extensive SCE are present. Switches of silver grains (SCEs) are seen at several loci (arrows) in chromosome #1. Wide arrow points to an isolabeled area with numerous SCE.







ANDROGENETIC ORIGIN OF HYDATIDIFORM MOLES: ITS BEARING ON CARCINOGENESIS

Tadashi KAJII

*Department of Pediatrics, Yamaguchi University School of Medicine**

Moles can be classified into complete moles and partial moles. The two entities can be distinguished from one another by either macroscopic or histological observation. Only complete moles undergo malignant transformation to become invasive moles or choriocarcinoma. In view of the difference in the prognosis and treatment of the two entities, it is urged that every possible molar specimen is checked, under a dissecting microscope, for the mode of swelling of the villi, the presence or absence of an embryo, amniotic membrane or chorionic membrane.

The majority of complete moles have a 46,XX karyotype. They result from diploid androgenesis involving enucleation or inactivation of the female pronucleus of an ovum, and its fertilization either by a diploid sperm resulting from nondivision at the paternal second meiosis or by a haploid sperm followed by duplication of the male pronucleus at the first mitosis. A minority of complete moles, however, have a 46,XY karyotype. Some of them have been verified to result from dispermy.

We reasoned that the high rate of malignancy of gestational trophoblastic disease results from the homozygosity of a mutation of a gene(s) that controls cell growth. The high malignancy rate of possibly dispermic, XY moles suggests otherwise. Dispermic moles are only 50% homozygous for their genes, while a higher rate of homozygosity is expected for the XX moles resulting from either nondivision at the paternal second meiosis or first mitosis.

The hydatidiform mole is an intriguing biological phenomenon. It is characterized by grossly swollen chorionic villi, but there is no embryo, cord or amniotic membrane. It has been considered to be the precursor of choriocarcinoma. Its karyotype is almost always 46,XX. Its incidence varies greatly in different parts of the world. It is most frequent in Asian countries and Latin American countries of the tropical zone, while it is least frequent in European and North American countries.

We have proposed, based on a study of 1,918 induced and spontaneous abortuses, that moles can be classified into two clinically and histologically distinct categories (17): Classic or complete moles, in which all chorionic villi are hydropic and in which neither amniotic membrane, cord nor fetus is present, have a 46,XX karyotype. Partial moles, in which hydatid and normal villi are mixed and which may contain an amniotic membrane, cord or even a fetus, have various karyotypes, predominantly triploidy. Only the complete, classic mole gives rise to choriocarcinoma. Complete and partial moles are not different stages of one disease, but distinct entities with different origins.

* Kogushi 1144, Ube 755, Japan (梶井 正).

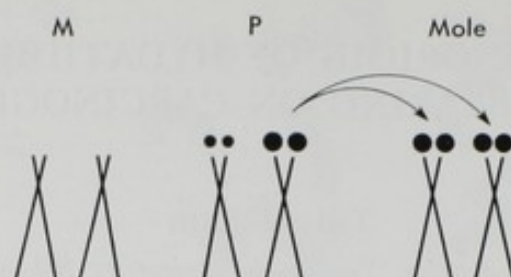


FIG. 1. Analysis of chromosomal heteromorphisms indicates no contribution of the maternal chromosomes, while a paternal chromosome was transmitted in duplicate to the mole.

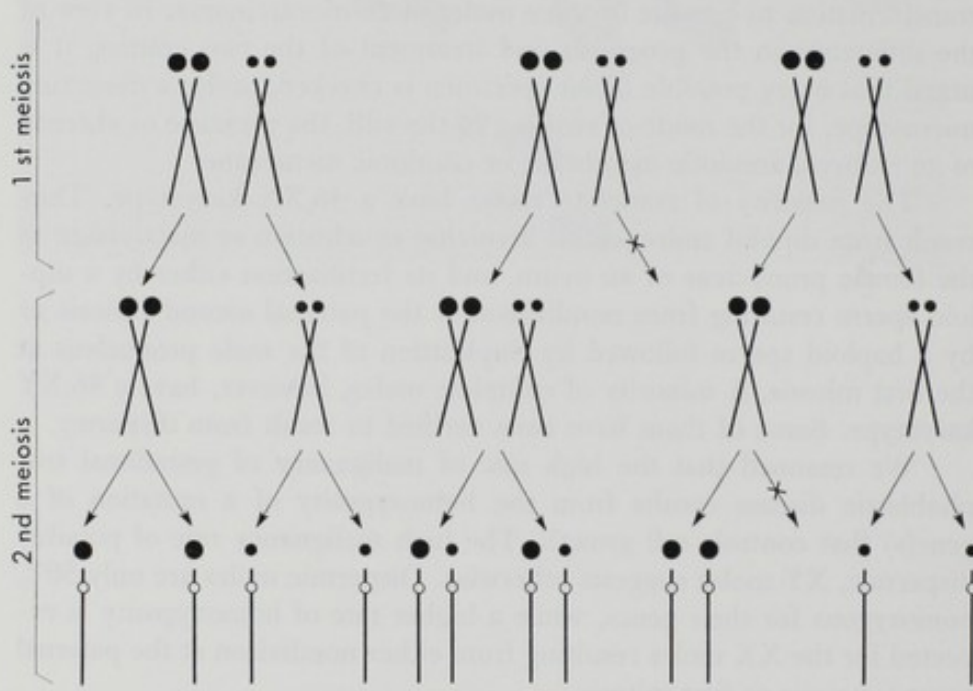


FIG. 2. Segregation of a pair of homologous chromosomes during the first and second meioses. Normal meiosis (left), nondivision at first meiosis (center), and nondivision at second meiosis (right). Nondivision at first meiosis results in transmission of both homologous chromosomes, while that at second meiosis results in transmission of a homologue in duplicate. Nondivision at first meiosis is indistinguishable from that at second meiosis.

This classification gained support from our finding that complete moles are androgenetic in origin (4). Chromosomes from seven complete moles, five Japanese and two Caucasian, were stained so as to show fluorescent bands on the chromosomes. When the chromosomal bands of the moles were compared with those of normal cells of the parents, each of the 26 chromosome pairs that could be assigned was found to derive from a chromosome in duplicate in the father (Fig. 1). This implies that complete moles originate in diploid androgenesis, in which the egg nucleus is either absent or inactivated and the spermatozoan nucleus contributed all the genetic material, either as a diploid sperm or as a haploid sperm followed by duplication of its chromosomes

(Fig. 2). The former mechanism involves take over of an ovum by a diploid XX sperm resulting from a failure of the second meiotic division. The theoretically possible YY counterparts are assumed to be lost, the YY karyotype being highly lethal.

We have proposed that choriocarcinoma results from a recessive mutation in a paternal gene(s). The presence in the mole of genetic material from only one parent, with a possibility that only one homolog from that parent is inherited, implies that the mole is essentially homozygous. Thus, any mutation in the father's gene(s) affecting growth control would have a 50% chance of being passed to the mole, where it would be expressed in the absence of the normal gene. This may explain the high rate (around 10%) of progression from the classic mole to choriocarcinoma.

Gestational trophoblastic diseases, including classic moles, invasive moles and choriocarcinoma, are ideal tools in the test of the recessive mutation hypothesis in the genesis of malignant tumors. This review will examine whether the recessive mutation hypothesis has stood the test of time, although the time elapsed since the inception of the theory in 1977 is rather short.

Androgenetic Origin of Complete Mole

Since our report in 1977 on seven complete moles of diploid androgenetic origin, at least 100 complete moles have been studied for their origin. They included moles from Japan, Switzerland, Hawaii, England and mainland U.S.A. (3, 5-8, 10, 15, 16, 18, 20). Various polymorphisms were used for tracing the origin of the moles including chromosomal (Q-, C-, and R-banding) heteromorphisms, human lymphocyte antigen (HLA), and various isozymes. Some of the isozymes employed were those in which the locations of their gene loci have been determined. They included phosphoglucomutase-1 (its gene locus is located at the short arm of chromosome 1), esterase D (long arm chromosome 13), and glucose-6-phosphate dehydrogenase (G6PD) (X chromosome). The HLA loci are on the short arm of chromosome 6.

Of the 100 moles studied, 67 were informative. 1) Fifty-four moles resulted from either nondivision at the paternal first meiotic division or duplication of the male pronucleus at the first mitotic division. 2) Nine moles were androgenetic in origin, but the exact stage of nondivision was not determined. 3) A mole resulted from either nondivision at the paternal first meiosis or dispermy. 4) Three moles were proven to originate in dispermy. The last category will be discussed in more detail later. In conclusion, the results of these studies support our conclusion that complete moles are androgenetic in origin. The mechanisms leading to androgenesis, however, are not uniform.

Dispermic Moles and Malignant Transformation

We reasoned in our previous paper (4) that the presence in the mole of only one homolog of paternal origin in duplicate implies that the mole is essentially homozygous except for the genes exchanged through crossing over. Thus, any recessive mutation in the paternal gene(s) controlling cell growth, transmitted to the mole, would be fully expressed in the absence of normal gene(s). This may explain the high malignancy rate in the mole. The recessive mutation may be inherited from the father, or, more likely,

may occur at any point of germ cell production down to the midpoint of meiosis I, when the chromosomes duplicate to have two chromatids.

It is now known that the majority of moles result from either nondivision at the paternal first meiosis or from duplication of the male pronucleus. The former mechanism results in homozygosity of the genes except for those exchanged through crossing over at meiosis I, while the latter mechanism implies complete homozygosity of homologous chromosomes. Thus, the recessive mutation hypothesis can explain the situation of the majority of moles. However, recent studies on the origin of the mole revealed the presence of 46,XY moles, some of which were proven to originate in dispermy. The impact of this discovery on the recessive mutation hypothesis will be discussed in the following.

At least four moles have been proven to have a 46,XY karyotype (6, 10). In addition, we have seen a mole with a negative X-chromatin and positive Y-chromatin test. Thus, this mole could have had a 46,XY karyotype. Three more moles have been reported to be Y-chromatin positive (1, 19). Altogether, eight proven or probable XY moles are known to us. Of these, three (6, 10, 19) underwent malignant transformation as evidenced by pulmonary metastasis. It seems from the limited data that the malignancy rate is high among XY moles.

XY moles could result from the conception of an enucleated or inactivated ovum by either a diploid sperm, resulting from nondivision at paternal meiosis I, or by two spermatozoa (dispermy). As mentioned earlier, at least three of the eight known XY moles have been proven to originate in dispermy (6). Dispermic moles are 50% homozygous and 50% heterozygous for their genes on the homologous chromosomes. Taking the 50% homozygosity rate and the high malignancy rate in the XY moles into consideration, the recessive mutation hypothesis encounters the following difficulties. 1) If it is assumed that the recessive mutation occurs during the paternal germ cell production, it is unlikely that both of the two spermatozoa that take part in dispermy carry the same fresh mutation. Therefore, if the recessive mutation hypothesis is to hold, the mutant gene must be carried by the father and transmitted to the mole. A paternal recessive mutant gene has a 50% chance of being transmitted to the mole. Therefore, the rate of men carrying the mutant gene must be very high. This is most unlikely. 2) XX moles usually originate in either nondivision at meiosis II, or duplication at mitosis I. In the former, genes on homologous chromosomes become homozygous except for the segments exchanged through crossing over. In the latter, complete homozygosity is expected. In the dispermic mole, on the other hand, a 50% homozygosity rate is expected. According to the recessive mutation hypothesis, the malignancy rate of moles is proportional to the homozygosity rate of their genes. Yet, XX moles with a high homozygosity rate have a relatively low malignancy rate, around 10%, while the XY moles, with a 50% homozygosity rate, have a malignancy rate of 40%. In conclusion, the discovery of dispermic moles and their high malignancy rate virtually killed the recessive mutation hypothesis. The reason for the high rate of malignancy in hydatidiform moles may have to be sought elsewhere. We have already initiated such a study.

Geographic Distribution and Maternal Age Effect

Complete moles are more frequent in Asian countries as well as Latin American

countries of the tropical zone than in European and North American countries. The difference is as much as 10-fold. The reason for this marked geographic variation is unknown. The frequently cited factors such as parity, nutritional state and race, cannot explain such a wide variation. Living standards and nutritional conditions have greatly improved in Japan during the past 20-year period. Yet, the incidence of gestational trophoblastic diseases, including complete moles, invasive moles, and choriocarcinoma, has not changed in proportion to these social changes. The maternal age distribution of livebirths drastically shifted to the younger age side. Gestational trophoblastic diseases are maternal age dependent (21). Therefore, a decline in the incidence of the diseases in recent years is to be expected. Their incidence in Japan in 1955–1956 was estimated at one in 281 births (2), while that in 1974–1975 was one in 300 births (14). A better ascertainment rate in recent surveys may in part explain the unexpected high incidence of trophoblastic diseases, but it alone cannot account for the phenomenon.

Can Partial Moles Undergo Malignant Transformation?

Our classification of hydatidiform moles into two entities—partial and complete moles—was criticized by several groups on various grounds. The criticisms include: 1) At least two cases of partial mole required chemotherapy after evacuation (9, 13), 2) A mole with both swollen and nonswollen villi was androgenetic in origin (3); 3) The term “partial mole” should be used exclusively for triploid specimens which are usually accompanied by slight to moderate hyperplasia of the trophoblast of the chorionic villi (11, 12).

The evidence for malignant transformation of partial moles is not conclusive. No choriocarcinoma with a triploid karyotype has been reported. Thus, we do not believe that a partial mole could undergo malignant changes. As for the classification of moles, the presence or absence of a fetus, amniotic membrane or cord overrides the appearance of the chorionic villi. Thus, there could be a complete mole specimen without a fetus, cord or amniotic membrane, but with a mixture of swollen and nonswollen chorionic villi. We have seen partial mole specimens with karyotypes other than triploidy. They are accompanied by hyperplasia of the trophoblast. Therefore, we do not see a reason for restricting the term partial mole to triploidy.

Acknowledgment

This study was supported in part by Grants-in-Aid for Cancer Research from the Ministry of Education of Japan.

REFERENCES

1. Akaeda, T. The value of Y chromatin in the human placenta and trophoblastic tumors. *Bull. Tokyo Med. Sch.*, **36**, 281–294 (1978) (in Japanese).
2. Hasegawa, T. Statistical investigations of hydatid mole and chorioepithelioma in Japan. *Asiatic Congr. Obstet. Gynecol.*, Tokyo (1957).
3. Jacobs, P. A., Hassold, T. J., Matsuyama, A. M., and Newlands, I. M. Chromosome constitution of gestational trophoblastic disease. *Lancet*, **i**, 49 (1978).
4. Kajii, T. and Ohama, K. Androgenetic origin of hydatidiform mole. *Nature*, **268**, 633–634 (1977).

5. Lawler, S. D., Pickthall, V. J., Fisher, R. A., Povey, S., Evans, M. W., and Szulman, A. E. Genetic studies of complete and partial hydatidiform moles. *Lancet*, **ii**, 580 (1979).
6. Ohama, K. Personal communication.
7. Ohama, K., Fujiwara, A., and Fukuda, Y. HLA in hydatidiform mole. *Igaku-no-Ayumi*, **108**, 297-298 (1979) (in Japanese).
8. Shokier, M.H.K. and Lawler, S. Genetic studies of hydatidiform mole. *Lancet*, **ii**, 1296 (1979).
9. Stone, M. and Bagshawe, K. D. Hydatidiform mole: Two entities. *Lancet*, **i**, 535-536 (1976).
10. Surti, U., Szulman, A. E., and O'Brien, S. Complete (classic) hydatidiform mole with 46,XY karyotype of paternal origin. *Hum. Genet.*, **51**, 153-155 (1979).
11. Szulman, A. E. and Surti, U. The syndrome of hydatidiform mole I. Cytogenetic and morphologic considerations. *Am. J. Obstet. Gynecol.*, **131**, 665-671 (1978).
12. Szulman, A. E. and Surti, U. The syndrome of hydatidiform mole II. Morphologic evolution of the complete and partial mole. *Am. J. Obstet. Gynecol.*, **132**, 20-27 (1978).
13. Szulman, A. E., Surti, U., and Berman, M. Patient with partial mole requiring chemotherapy. *Lancet*, **ii**, 1099 (1978).
14. Takeuchi, S. Report of committee on trophoblastic tumors in Japan. *Acta Obstet. Gynecol. Japon.*, **31**, 525-530 (1979) (in Japanese).
15. Tsuji, Y., Matsuda, S., Hirai, T., Fujiwara, H., and Hamaoka, T. Selective expression of paternal human major histocompatibility antigens of the tissue surface of hydatidiform mole cells. *Gann*, **69**, 849-853 (1978).
16. Vassilakos, P., Riotton, G., and Kajii, T. Hydatidiform mole: Two entities. A morphologic and cytogenetic study with some clinical considerations. *Am. J. Obstet. Gynecol.*, **127**, 167-170 (1977).
17. Wake, N., Takagi, N., and Sasaki, M. Androgenesis as a cause of hydatidiform moles. *J. Natl. Cancer Inst.*, **60**, 51-57 (1978).
18. Wake, N., Shiina, Y., and Ichinoe, K. A further cytogenetic study of hydatidiform mole, with reference to its androgenetic origin. *Proc. Jpn. Acad.*, **54**, 533-537 (1978).
19. Yagi, S. and Ichinoe, K. The sex of hydatidiform mole. *Acta Obstet. Gynecol. Japon.*, **30**, 529-532 (1978) (in Japanese).
20. Yamashita, K., Wake, N., Araki, T., Ichinoe, K., and Kuroki, M. Human lymphocyte antigen expression in hydatidiform mole: Androgenesis following fertilization by a haploid sperm. *Am. J. Obstet. Gynecol.*, **135**, 597-600 (1979).
21. Yen, S. and MacMahon, B. Epidemiologic features of trophoblastic disease. *Am. J. Obstet. Gynecol.*, **101**, 126-132 (1968).

SUBJECT INDEX

- Actinomycin D, inhibition of RNA synthesis 14
- Actual growth rate 68
- Adenomatosis coli 115
 - cell transformation by murine sarcoma virus 119
 - morphology of cell colonies 123
 - 4NQO-reductase activity 116
 - plating efficiency of cells 123
 - sensitivity to chemical carcinogen 116
 - sensitivity to mitomycin 116
 - susceptibility to 4NQO 116
- Adenomatous epithelium 141
- Adenomatous hyperplasia, liver 127
- Adhesive factor
 - cell surface-associated 14
 - separation 11
 - serum-associated 14
 - synthesis (or regeneration) 17
- Androgenesis 189
- Ataxia telangiectasia 180

- Banding age 155
- Banding method 154
- Birth rate, cell production rate 68,69
- Bloom's syndrome 177
- Bone marrow cell 178
- 5-Bromo-2-deoxyuridine 177

- Carcinoembryonal proteins 19
- Carcinogenicity test 177
- Cell adhesion 3
- Cell electrophoresis 41
- Cell loss 58, 60
 - rate 68
- Cell proliferation 41
- Cell surface 29
- Cellular recognition 3
- Chemical mutagen 180
- Chiasma 173
- Chondroitin sulfate 41
- Choriocarcinoma 189
- Chromosome 177
 - aberrations 170, 179
- Chronology of chromosome studies 154

- Dark age 153
- Decycling 67, 74
- Desmosome 10
- DMBA (di-methyl-benz-anthracene) 57, 60-62
- DNA repair 177
 - error-prone 174
- DNA scission by 4NQO 116
- Duodenal cancer 89

- ENNG, N-ethyl-N''-nitro-N-nitrosoguanidine 89
- Esterase histochemistry, nonspecific 105

- Fanconi's anemia 180
- Feulgen's reaction 129
- Fibroblast 178
 - chick embryo 29
 - skin 115
- Focal nodular hyperplasia (FNH) 134

- Gap junction 5
- Gardner's syndrome 119

- Gelatine injection 128
- Gene mapping 157
- Generation times 58, 61, 64
- Genetically conservative regulatory systems 170
- Genetic distance 168
- Glucosamine 32
- Glucose 64
 - 6-phosphatase histochemistry 103
- γ -Glutamyl transpeptidase, histochemistry 104
- Glycopeptide 37
- Glycosaminoglycans 41
- Growth 29
 - density-dependent inhibition 29
 - fraction 70, 74
 - inhibitor 29
 - rate equation 71, 77
 - tumors 61
- Heparan sulfate 33, 41
- Hepatocellular carcinoma 127
- Hepatocarcinogenesis, chemical 103
- Histogram, nuclear DNA 132
- Hormone-dependent tumors 62, 63
- Human tumors, growth 58
- Hyaluronic acid 41
- Hybrid effect 171
- Hydatidiform mole 189
- Hyperplastic areas 103
- Hyperplastic epithelia 143
- Hyperplastic nodules 103
- Hypotonic pretreatment 153
- Intermediate junction 5, 10
- International System for Human Cytogenetic Nomenclature (ISCN) 155
- Intersubspecies hybrids 166
- Irreversible erosion 144
- Junctional complex, development 10
- Leukemia 41
- Liver cancer 103
- Lung tumor 170
- Lymphocyte 177
- Macrophage chemotactic lymphokine 20
- 3'-Me-DAB (3'-methyl-4-(dimethyl-amino) azobenzene) 104
- Microangiography 131
- Microspectrophotometry 135
- Mitochondrial DNAs 170
- MNNG, N-methyl-N'-nitro-N-nitrosoguanidine 141
- Morphological transformation, MSV (MLV), effect of pepstatin and leupeptin 121
- Mucopolysaccharide 33
- Multiple-phase birth- and -death process 67
- Mutagenicity test 177
- N-ethyl-N''-nitro-N-nitrosoguanidine (ENNG) 89
- N-methyl-N'-nitro-N-nitrosoguanidine (MNNG) 141
- Nocodazole 157
- Partial pressure of oxygen 64
- Peutz-Jeghers' syndrome 115
 - cell transformation by murine sarcoma virus 119
 - plating efficiency of cells 123
 - sensitivity to chemical carcinogens 116
- Ph¹ (chromosome) 159
- Phytohemagglutinin (PHA) 41
- Potential doubling time 69, 74
- Precancerous lesions 141
 - in liver 107
 - remodeling 104
- Primordial germ cell
 - extended proliferative period 83
 - proliferative activity in developing testes 80

- reduced number (or sparc) 83
Proliferative cell loss rate 68, 74

Quiescent cell loss rate 68, 74

R-Tu system (regulatory gene-structural gene system) 167
Radiation effect 178
Rat ascites hepatoma
 free tumor cells 11
 island-forming tumor cells 11
Rat stomach 141
Rate-limiting factor 57, 60, 63
Rate-limiting process 64
Recessive mutation 191
Regenerating epithelium 141
Reproductive coefficient 71, 72
Reversible erosion 144

Salivary gland chromosome 156
Sister chromatid exchange 171, 177
Soft X-ray 128
Somatic cell hybridization 156
Stroma 59-64

T-lymphocyte 41
Teratocarcinogenesis
 critical period 80
 susceptibility 80, 83
Teratoma incidence 80, 83
 testicular teratomas, congenital (spontaneous) 80
Tight junctions 10
Transformation by MSV(MLV), effect of TPA 122
Tritiated thymidine 59, 63, 64
 autoradiography 57, 60, 62
Trypsin 4
Tumor growth 60
 aggregation and adhesiveness 11

Ultraviolet light 179
Urethan 170

Virtual growth rate 72, 77
Volume doubling time 58, 61, 62, 64

Wild mouse 168

Xeroderma pigmentosum 180

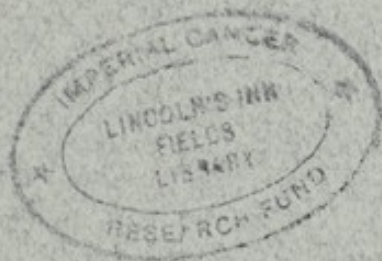








1984-1



¥7000